Asymmetric Hydrogenation of Esters and Efforts Towards Photohydrogenation

by

Riley Thomas Endean

A thesis submitted in partial fulfillment of the requirements for the degree of

Doctor of Philosophy

Department of Chemistry
University of Alberta

Abstract

A thorough overview of esters and their reductions is presented. A large focus was placed on reductions via homogeneous catalytic hydrogenation. Although several ester hydrogenation systems have been developed, the production of highly enantioenriched alcohols has generally relied upon the usage of enantioenriched esters.

A system for homogeneous asymmetric hydrogenation of esters to enantioenriched alcohols was discovered and optimized via an in-house screening method. The optimal system uses an in situ formed Ru-based catalyst made from [Ru(1-3:5,6-η^5-C$_8$H$_{11}$)(η^6-anthracene)]BF$_4$, the chiral ligand (1R,2R)-N,N'-bis{2-[bis(3,5-dimethylphenyl)phosphino]benzyl}cyclohexane-1,2-diamine, and H$_2$. This catalyst is highly active and enantioselective towards hydrogenating α-phenoxy esters to β-chiral primary alcohols under mild conditions. The system operates via dynamic kinetic resolution (DKR), where the esters undergo base-assisted racemization and the catalyst preferentially reacts with one enantiomer. Specifically, NaO^{i}Pr in THF and NaOEt in DME were optimal base and solvent combinations for the DKR. The alkoxide bases participate in transesterification and catalyst activation. Under 4 atm H$_2$ and at room temperature, the catalyst provides quantitative conversion (50 turnovers) over 1 h for α-phenoxy propionate and butyrate esters (2 mol% catalyst, 50 mol% base). The enantiomeric excesses of the resulting β-chiral alcohols ranged from 79 to 93%. The hydrogenation of (±)-ethyl 2-phenoxypropionate at 0 °C resulted in a 95% enantiomeric excess (ee). Under 15 atm H$_2$ and at room temperature, the catalyst performed 950 turnovers of (±)-ethyl 2-phenoxypropionate over 9 h and resulted in a 91% ee towards (R)-2-phenoxypropan-1-ol (0.1 mol% catalyst, 20 mol% NaOEt, DME). Hydrogenation of the potential intermediate aldehyde (±)-2-phenoxypropionaldehyde and

deuteration of (±)-ethyl 2-phenoxypropionate were performed to experimentally investigate the mechanism.

Three Ru(II)–polypyridyl complexes were prepared for the underexplored area of photohydrogenation. [Ru(bipy)$_2$(1,10-phenanthroline-5,6-diamine)](OTf)$_2$ (bipy = 2,2′-bipyridine) was synthesized in 56% yield from [Ru(MeCN)$_2$(bipy)$_2$](OTf)$_2$ and the bis-bidentate ligand 1,10-phenanthroline-5,6-diamine in MeOH at 70 °C. The dinuclear complex was not the major product. The imidazolium ligand 1-benzyl-3-(propan-2-yl)-1*H*-imidazol[4,5-*f*][1,10]phenanthroline-3-ium (bpip) was prepared in 55% yield over three steps from 1,10-phenanthroline-5,6-diamine. The complexation of bpip to the Ru–dichloride precursors *cis*-[Ru(Cl)$_2$(bipy)$_2$] and *cis*-[Ru(Cl)$_2$(dmbipy)$_2$] (dmbipy = 4,4′-dimethyl-2,2′-bipyridine) proceeded smoothly in MeOH at 70 °C. [Ru(bpip)(bipy)$_2$](OTf)$_3$ and [Ru(bpip)(dmbipy)$_2$](OTf)$_3$ were prepared from their respective dichloride precursors, over two steps, in 87 and 73% yields, respectively. Crystals suitable for X-ray diffraction were obtained for [Ru(bpip)(bipy)$_2$](BF$_4$)$_3$.

The [Ru(bipy)$_2$(1,10-phenanthroline-5,6-diamine)](OTf)$_2$ and [Ru(bpip)(dmbipy)$_2$](OTf)$_3$ were incorporated into two separate known hydrogenation systems. The photohydrogenation of acetophenone was attempted with in situ catalyst formation from [Ru(bipy)$_2$(1,10-phenanthroline-5,6-diamine)](OTf)$_2$ and *fac*-[Ru((*R*)-BINAP)(H)(^{i}PrOH)$_3$]BF$_4$ (BINAP = 2,2′-bis(diphenylphosphino)-1,1′-binaphthyl). Only ~2% of the acetophenone was converted (~10 turnovers) over 45 min (0.2 mol% catalyst, 10 mol% KO^{t}Bu, ^{i}PrOH, ~1 atm H$_2$, rt, 15 min 400–700 nm *hv*). The photohydrogenation of styrene was attempted with in situ catalyst formation from [Ru(bpip)(dmbipy)$_2$](OTf)$_3$ and [Co(TMEDA)(CH$_2$SiMe$_3$)] (TMEDA = *N,N,N′,N′*-tetramethylethylenediamine). No detectable reaction occurred under the conditions examined (0.2 mol% catalyst, 0.2 mol% KO^{t}Bu, MeOH, ~1 atm H$_2$, 450 nm *hv*, 10.5 h).

Preface

A portion of the data presented in this dissertation was acquired in collaboration with other researchers within the Department of Chemistry at the University of Alberta. All HRMS analyses were performed by staff members in the Mass Spectrometry Laboratory. All elemental analyses were performed by staff members in the Analytical and Instrumentation Laboratory.

Chapter 1 is an introductory chapter that presents a significant amount of data involving esters. The data presented is that of the respective referenced authors. Reaction and mechanistic schemes were drawn or redrawn by Riley Endean. Copyright permissions were obtained for redrawn tables and mechanistic schemes.

Chapter 2 has been adapted and expanded upon from the following publication: Endean R. T.; Rasu L.; Bergens S. H. Enantioselective Hydrogenations of Esters with Dynamic Kinetic Resolution. *ACS Catal.* **2019**, *9* (7), 6111–6117. Riley Endean performed most of the reactions and data collection. Dr. Loorthuraja Rasu participated in the development of the screening method and initial ligand screenings. Dr. Rasu also synthesized (±)-ethyl 2-phenoxypropionate and (±)-butan-2-yl-phenoxypropionate. The reported syntheses of (±)-ethyl 2-phenoxypropionate are that performed by Riley Endean. Steven H. Bergens was the supervisory author. The NMR spectra from the ester deuteration study were acquired with the aid of Mark Miskolzie from the NMR Laboratory at the University of Alberta.

Chapter 3 is unpublished work that was performed in collaboration with James Pearson. Specifically, James Pearson assisted with the development of the imidazolium salts. All syntheses reported are those performed by Riley Endean. The NMR data were collected by Riley Endean. The X-ray crystallographic study was performed by Dr. Michael Ferguson from the X-ray Crystallography Laboratory. The crystal and refinement data were collected by Dr. Ferguson.

Chapter 4 is unpublished and independent work by Riley Endean.

Chapter 5 is a summary and possible future research directions.

Acknowledgements

There are many people that deserve recognition for supporting me while at the University of Alberta.

Several professors have contributed to my development as a scientist. First and foremost, my supervisor Prof. Steven Bergens has been an invaluable source of knowledge, guidance, and enthusiasm. I am grateful for his positive and humorous attitude. To my supervisory committee members Prof. Eric Rivard and Prof. Jonathan Veinot, I sincerely appreciate your various involvement and advice. I would also like to thank Prof. Arthur Mar for being part of my candidacy examination committee and Prof. Rylan Lundgren for serving on both my candidacy and final examination committees. I am also appreciative of my non-examining committee members Prof. Josef Takats and Prof. Robert Jordan. I am greatly appreciative of Prof. Jennifer Love for serving as my external examiner. I am extremely appreciative of the time and effort that each professor put into reviewing this dissertation.

To past and present Bergens group members, your advice, support, and friendship has been incredibly important to me. A special thanks to Dr. Loorthuraja Rasu who has served as a mentor, trainer, and friend. I would also like to specifically express gratitude towards Dr. Mona Amiri, Dr. Chao Wang, Dr. Shuai Xu, Suneth Kalapugama, Prabin Nepal, Octavio Martinez Perez, James Pearson, Jinkun Liu, Benjamin Rennie, and Emily Majaesic for their years of friendship.

There are various staff that also deserve recognition. Thank you to my teaching assistant coordinators Dr. Yoram Apelblat, Dr. Norman Gee, and Dr. Alexandra Faucher. I thoroughly enjoyed my teaching assistant experience and learnt a lot. I would like to acknowledge Mark Miskolzie for his exceptional NMR services, knowledge, and his unique friendliness. I also appreciate Dr. Ryan McKay and Nupur Dabral for their NMR services. I would like to thank Dr. Michael Ferguson from the X-ray Crystallography Laboratory. I would like to express gratitude towards everyone from the Mass Spectrometry Laboratory and the Analytical and Instrumentation Laboratory. I would also like to thank all of the support staff members. A particular thank you goes to Anuar Rivero and Scott Stelck for dealing with my various purchases throughout the years. I would like to thank Ryan Lewis, Michael Barteski, Matthew

Table of Contents

Chapter 4: Preliminary Photohydrogenation Trials with Ru(II) Complexes

Chapter 5: Summary and Possible Future Directions

List of Tables

List of Figures

List of Schemes

xv

Rights and Permissions Obtained

Chapter 2. Contents have been reprinted or adapted with permission from my following publication: Endean R. T.; Rasu L.; Bergens S. H. Enantioselective Hydrogenations of Esters with Dynamic Kinetic Resolution. *ACS Catal.* **2019**, *9* (7), 6111–6117. Copyright 2019 American Chemical Society.

Table 1-1. Adapted with permission from Adkins, H.; Folkers, K. The Catalytic Hydrogenation of Esters to Alcohols. *J. Am. Chem. Soc.* **1931**, *53* (3), 1095–1097. Copyright 1931 American Chemical Society.

Scheme 1-40. Adapted with permission from Nomura, K.; Ogura, H.; Imanishi, Y. Ruthenium Catalyzed Hydrogenation of Methyl Phenylacetate Under Low Hydrogen Pressure. *J. Mol. Catal. A: Chem.* **2002**, *178* (1), 105–114. Copyright 2002 Elsevier.

Scheme 1-43. Adapted with permission from Zhang, J.; Leitus, G.; Ben-David, Y.; Milstein, D. Efficient Homogeneous Catalytic Hydrogenation of Esters to Alcohols. *Angew. Chem. Int. Ed.* **2006**, *45* (7), 1113–1115. Copyright 2006 John Wiley and Sons.

Scheme 1-57. Adapted with permission from O, W. W. N.; Morris, R. H. Ester Hydrogenation Catalyzed by a Ruthenium(II) Complex Bearing an N-Heterocyclic Carbene Tethered with an "NH$_2$" Group and a DFT Study of the Proposed Bifunctional Mechanism. *ACS Catal.* **2013**, *3* (1), 32–40. Copyright 2013 American Chemical Society.

Scheme 4-2. Adapted with permission from Enachi, A.; Baabe, D.; Zaretzke, M.-K.; Schweyen, P.; Freytag, M.; Raeder, J.; Walter, M. D. [(NHC)CoR$_2$]: Pre-Catalysts for Homogeneous Olefin and Alkyne Hydrogenation. *Chem. Commun.* **2018**, *54* (98), 13798–13801. Copyright 2018 The Royal Society of Chemistry.

List of Abbreviations and Symbols

atm	Atmosphere(s)
acac	Acetylacetonate
aq	Aqueous
Ad	Adamantyl
Anal.	Combustion analysis
Ar	Argon; Aryl
Å	Angstrom(s)
*	Denoting an enriched chiral centre
bipy	2,2′-Bipyridine
br	Broad
Bn	Benzyl
Boc	*tert*-Butyloxycarbonyl
$BAr^F_4{}^-$	Tetrakis[3,5-bis(trifluoromethyl)phenyl]borate anion
BINAP	2,2′-Bis(diphenylphosphino)-1,1′-binaphthyl
[]	Encloses coordination complexes, transition states, ligands, and concentrations
$[M]^+$	Parent molecular ion
c	Centi
conv	Conversion
C	Carbon; Celsius
Calcd	Calculated
Cp*	1,2,3,4,5-Pentamethylcyclopentadienyl
Cy	Cyclohexyl
CAS	Chemical abstracts service
COD	1,5-Cyclooctadiene
d	Doublet
dd	Doublet of doublets
dr	Diastereomeric ratio
dt	Doublet of triplets
ddd	Doublet of doublets of doublets

dmbipy	4,4′-Dimethyl-2,2′-bipyridine
dpen	1,2-Diphenylethylenediamine
dppp	1,3-Bis(diphenylphosphino)propane
dtb	3,5-Di-*tert*-butylphenyl
dtbm	3,5-Di-*tert*-butyl-4-methoxyphenyl
Diglyme	Diethylene glycol dimethyl ether
Dipp	2,6-Diisopropylphenyl
DACH	1,2-Diaminocyclohexane
DCM	Dichloromethane
DFT	Density functional theory
DIBAL-H	Diisobutylaluminum hydride
DKR	Dynamic kinetic resolution
DME	1,2-Dimethoxyethane
DMF	*N*,*N*-Dimethylformamide
°	Degree(s)
δ	Delta; Chemical shift
Δ	Denoting a change; heat
‡	Denoting a transition state
ee	Enantiomeric excess
en	Ethylenediamine
eq	Equation(s)
equiv	Equivalent(s)
Et	Ethyl
EtO	Ethoxy
EI	Electron impact
ESI	Electrospray ionization
e^-	Electron
FLB	Fluorescent light bulb
g	Gram(s)
Gen.	Generation
GC–MS	Gas chromatography mass spectroscopy

G	Gibbs free energy
h	Hour(s)
Hz	Hertz
HFP	1,1,1,3,3,3-Hexafluoro-2-propanol
HPLC	High-performance liquid chromatography
HRMS	High-resolution mass spectrometry
hv	Indicates light energy
^{i}Pr	Isopropyl
^{i}PrO	Isopropoxy
J	Joule(s)
J	Coupling constant
k	Kilo
K	Kelvin(s)
KR	Kinetic resolution
L	Litre(s)
LMCT	Ligand-to-metal charge transfer
LRMS	Low-resolution mass spectrometry
m	Metre(s); Milli; Multiplet
min	Minute(s)
mol	Mole(s)
M	Mega; Molar
Me	Methyl
MeO	Methoxy
Mes	Mesitylene
2-MeTHF	2-Methyltetrahydrofuran
MLCT	Metal-to-ligand charge transfer
MOM	Methoxymethyl
MTBE	Methyl *tert*-butyl ether
m/z	Mass to charge ratio
μ	Micro
^{n}Bu	*n*-Butyl

^{n}Pr	*n*-Propyl
N/A	Not available
NBD	Norbornadiene
ND	Not determined
NHC(s)	N-Heterocyclic carbene(s)
NMR	Nuclear magnetic resonance
NNNP	Triamine–monophosphine ligand
NNP	Diamine–monophosphine ligand
NN	Diamine ligand
NP	Monoamine–monophosphine ligand
n	Integer value
OAc	Acetate
OTf	Trifluoromethanesulfonate anion
ppm	Parts per million
py	Pyridine
Ph	Phenyl
PhO	Phenoxy
PAP	Pyridine–aminophosphine ligand
PNNP	Diamine–diphosphine ligand
PP	Diphosphine ligand
%	Percent
±	Denoting a racemic mixture
q	Quartet
qd	Quartet of doublets
rt	Room temperature
Ref.	Reference
RBF	Round-bottom flask
ROMP	Ring-opening metathesis polymerization
R_f	Retention factor
s	Singlet
sat.	Saturated

^{s}BuO	*sec*-Butoxy
sept	Septet
sepd	Septet of doublets
sext	Sextet
skewphos	2,4-Bis(diphenylphosphino)pentane
solv	Solvent
SET	Single-electron transfer
SPINOL	1,1′-Spirobiindane-7,7′-diol
SPS	Solvent purification system
t	Triplet
^{t}Bu	*tert*-Butyl
td	Triplet of doublets
tol	Methylphenyl
tpphz	Tetrapyrido[3,2-*a*:2′,3′-*c*:3″,2″-*h*:2‴,3‴-*j*]phenazine
tt	Triplet of triplets
Tetraglyme	Tetraethylene glycol dimethyl ether
Triphos	1,1,1-Tris(diphenylphosphinomethyl)ethane
TBDMS	*tert*-Butyldimethylsilyl
THF	Tetrahydrofuran
TMEDA	*N*,*N*,*N*′,*N*′-Tetramethylethylenediamine
TOF	Turnover frequency
TON	Turnover number
t_R	Retention time
vs	Versus
wt	Weight
xyl	3,5-Dimethylphenyl
xyl-BINAP	2,2′-Bis[di(3,5-xylyl)phosphino]-1,1′-binaphthyl
X$^-$	Represents any counter anion

Chapter 1:

Introduction

1.1 Esters

Esters are ubiquitous and important chemical compounds that are used for a wide variety of functions.[1] Industries use esters as anesthetics, insecticides, flavouring agents, solvents, and fragrances.[1] Esters are most commonly related to fragrances, as they are widely known for their pleasant aromas. For example, methyl dihydrojasmonate (Figure 1-1), an ester first synthesized in 1958, is a jasmine smelling fragrance in perfumes.[2-4] The different odours of esters, and even their isomers, are the result of unique binding to chemoreceptors of olfactory systems. For instance, *cis*- and *trans*-methyl dihydrojasmonate smell differently, and varying mixtures of these isomers have been trademarked.[4]
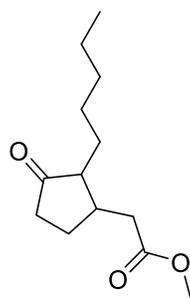
Figure 1-1. Chemical structure of methyl dihydrojasmonate.

Esters are more volatile than their respective carboxylic acids from which they are classically made (Scheme 1-1).[5] The lower boiling points and higher vapour pressures of esters, in comparison to their respective carboxylic acids, are due to weaker intermolecular forces. Esters have both dipole–dipole and van der Waals forces but are not hydrogen bond donors like carboxylic acids. The chemical structure of esters also affects their reactivity.
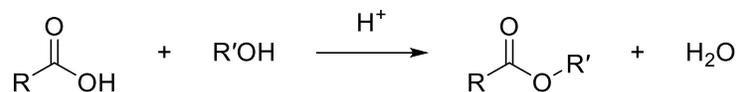
Scheme 1-1. Classical method for ester synthesis from carboxylic acids (i.e., Fischer esterification).

Esters are less reactive towards nucleophilic acyl substitutions than acid chlorides, anhydrides, aldehydes, and ketones. Their greater stability is primarily due to π-electron delocalization (Figure 1-2). The alkoxy group's (O–R′) oxygen's lone pairs donate electron density towards the acyl group (R–C=O). This results in a partial double-bond character for the carbon–oxygen single (C–O) bond between the acyl carbon (sp^2) and the alkoxy oxygen (sp^3). For example, methyl acetate's calculated C–O (sp^2–sp^3) bond lengths are 1.353 and 1.345 Å for its E and Z isomers, respectively.[6] These bond lengths are shorter than the C–O bond in methyl acetate's respective alcohol, methanol (MeOH), which has a C–O (sp^3–sp^3) bond length of 1.427(7) Å.[7] Although esters tend to be planar, due to the delocalization, the alkoxy group is not rotationally restricted and allows for conformational isomers.
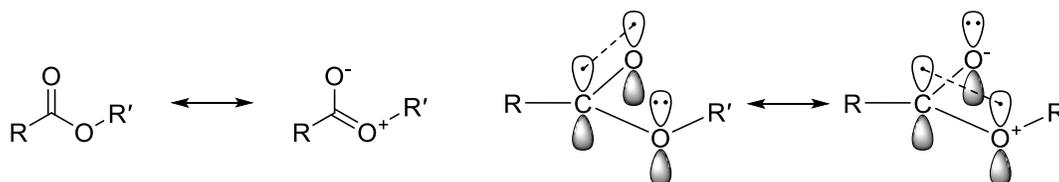
Figure 1-2. Ester resonance structures illustrating the delocalization of electrons.

Acyclic esters exist as both E and Z conformers about their C–O (sp^2–sp^3) bond with partial double-bond character. Despite the steric consequences of alkyl substituents oriented towards the acyl oxygen, the Z conformer is generally lower in energy.[8-10] This stabilization is normally explained by anomeric effects, which include dipole minimization and negative hyperconjugation (Figure 1-3). When esters are E oriented the dipoles are partially aligned and the oxygens' lone pairs are situated closer. This results in destabilization via dipole–dipole repulsion and lone pair–lone pair repulsions. In comparison, the Z orientation results in a

2

dipole–dipole attraction and minimizes lone pair repulsions. The *Z* conformer is also stabilized

by negative hyperconjugation, which involves the alkoxy oxygen's *anti*-periplanar lone pair

donating electron density towards the σ* orbital of the C=O bond.[8]
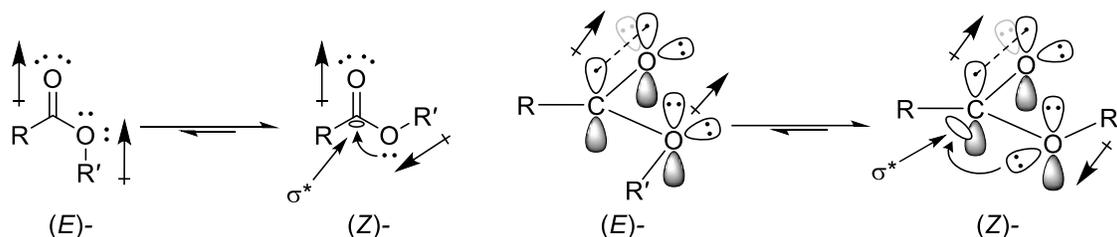
Figure 1-3. *E* and *Z* conformational isomers of esters and their anomeric effects.

The preference for the *Z* conformation of esters is exemplified by bulky alkoxy

substituents and formate esters. For example, the *E* conformer of *tert*-butyl acetate is 46 kJ/mol

higher in potential energy than its *Z* conformer.[11] Even when the acyl group is formate the *Z*

isomer is still the major conformer.[12, 13] For instance, *tert*-butyl formate was found in a *E* to *Z*

ratio of 9 to 91 at -113.8 °C.[14] The *E* and *Z* conformers of butyl acetate and butyl formate are

shown in Figure 1-4. Although acyclic esters prefer the *Z* conformation, cyclic esters, known as

lactones, are structurally *E* oriented.

(*E*)-*tert*-butyl acetate   (*Z*)-*tert*-butyl acetate   (*E*)-*tert*-butyl formate   (*Z*)-*tert*-butyl formate
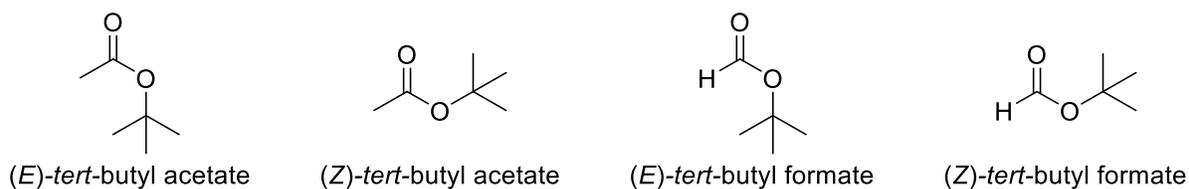
Figure 1-4. *E* and *Z* conformational isomers of *tert*-butyl acetate and *tert*-butyl formate.

Lactones are more reactive than acyclic esters towards nucleophilic acyl substitutions.

The increased reactivity of lactones is a result of their inherent destabilization and ring strain.

Lactones are *E* oriented esters; therefore, they experience destabilization due to their

dipole–dipole repulsions and weaker orbital overlaps. Lactones come in a variety of different

sizes (Figure 1-5). The five- and six-membered lactones are the most common due to their lower ring strain energies. The five-membered lactone, γ-butyrolactone, and the six-membered lactone, δ-valerolactone, have strain energies of 32.6 and 42.7 kJ/mol, respectively.[15] In comparison, the smaller lactones α-acetolactone and β-propiolactone have strain energies of 181 and 95.0 kJ/mol, respectively.[15] All lactones experience strain energy due to the presence of an sp^2 carbon that causes the bonds to differ from ideal angles. Therefore, the lower strain energy of γ-butyrolactone, in comparison to the other unsubstituted lactones, is due to the bond angles being closer to ideal. When lactones undergo nucleophilic attack, these strain energies are released by forming an sp^3 carbon. This combination of strain energy and electronic destabilization makes lactones more reactive to reduction than acyclic esters.
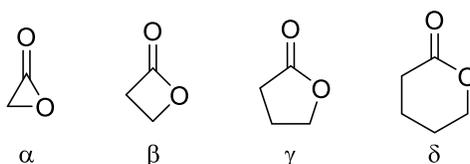
Figure 1-5. Chemical structures of selected unsubstituted lactones and their respective Greek symbols.

1.2 Stoichiometric Ester Reductions

The reduction of carbonyl compounds to alcohols is a fundamental chemical transformation. Traditional methods used stoichiometric amounts of boron or aluminum hydrides. The reactivity and selectivity of hydride reagents are well established.[16] The most familiar and commercially available hydride reagents are sodium borohydride ($NaBH_4$), lithium borohydride ($LiBH_4$), and lithium aluminum hydride ($LiAlH_4$). The discovery and synthetic development of $NaBH_4$ occurred during the World War II era.[17] Brown, under the doctoral supervision of Prof. Schlesinger, was attempting to isolate a solid with acetone when a vigorous

reaction occurred.[17] The solid, $NaBH_4$, produced from sodium hydride and trimethyl borate (eq 1-1), had reacted with the acetone and then water (eq 1-2 and 1-3).[17]

$$4 \; NaH \quad + \quad B(OCH_3)_3 \quad \longrightarrow \quad NaBH_4 \quad + \quad 3 \; NaOCH_3 \qquad \textbf{(1-1)}$$

$$NaBH_4 \quad + \quad (CH_3)_2CO \quad \longrightarrow \quad NaOCH(CH_3)_2 \quad + \quad BH_3 \qquad \textbf{(1-2)}$$

$$NaOCH(CH_3)_2 \quad + \quad H_2O \quad \longrightarrow \quad (CH_3)_2CHOH \quad + \quad Na^+ \quad + \quad {}^-OH \qquad \textbf{(1-3)}$$

The Brown–Schlesinger process, for $NaBH_4$ synthesis, was published in 1953[18] and implemented into industrial production in 1954.[16] The same process is still utilized and the annual consumption of $NaBH_4$ was estimated at several millions of kilograms in 2016.[16]

Although $NaBH_4$ is an important reducing agent, it is unable to reduce esters without an additive or forced reaction conditions. The first reported $NaBH_4$ ester reduction was in 1954.[19] Gábor and co-workers reported the reduction of ethyl 4-nitrobenzoate with stoichiometric amounts of $NaBH_4$ and LiI in THF.[19] Gábor stated that catalytic amounts of LiI hindered the reaction and that it could not be substituted with LiCl or LiBr.[19] In 1955, Brown et al. reported the reduction of ethyl esters with $NaBH_4$ and LiBr in diglyme (Scheme 1-2).[20]
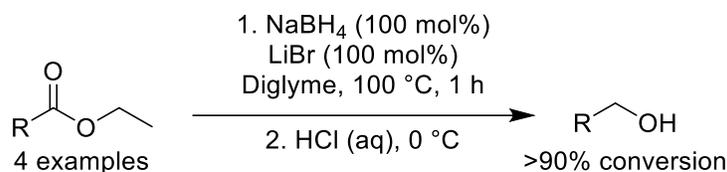
Scheme 1-2. Brown's reduction of ethyl esters with $NaBH_4$ and LiBr in diglyme.[20]

Brown stated that LiBr could be substituted with $MgCl_2$ or $MgBr_2$, but that the solubility of the Mg salts in diglyme affected the reductions.[20] In the same year, Gábor and co-workers reported the usage of Ca, Sr, and Ba salts with $NaBH_4$ for ester reductions.[21] In 1956, Brown reported the addition of $AlCl_3$ to $NaBH_4$ for ester reductions at 25 °C.[22] The addition of specific metal salts

activates the carbonyl carbon, by polarization of the C=O bond, making it more susceptible to nucleophilic attack (Figure 1-6).
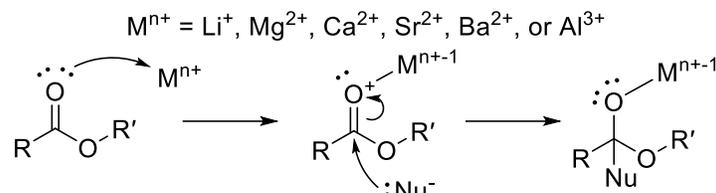
Figure 1-6. Activation of an ester's C=O bond by polarization and subsequent nucleophilic attack.

Cationic sodium is unable to sufficiently activate the carbonyl ester C=O bond due to its weaker Lewis acidity. It is likely that the respective metal borohydrides are forming in situ through the metathesis reaction with $NaBH_4$ (eq 1-4).

$$n\ NaBH_4\ +\ MX_n\ \longrightarrow\ M(BH_4)_n\ +\ n\ NaX\qquad \textbf{(1-4)}$$

$LiBH_4$ is a stronger reducing agent than $NaBH_4$ and is particularly useful for ester reductions.[23] Importantly, $LiBH_4$ is chemoselective and able to reduce esters in the presence of nitro groups, halides, nitriles, alkenes, alkynes, amides, and even carboxylic acids.[16, 23-25] For instance, Laïb and Zhu selectively reduced the methyl ester of **1** with $LiBH_4$ in the presence of its amides, halide, and nitro group (Scheme 1-3).[26] An 83% yield of **2** was obtained in 10 min.[26]
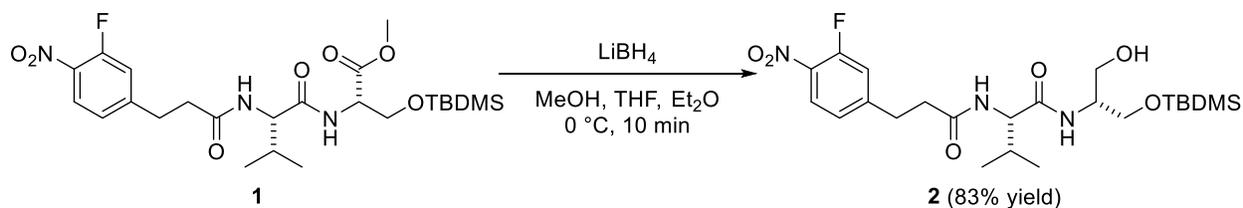
Scheme 1-3. Laïb and Zhu's selective ester reduction of **1** with $LiBH_4$.[26]

The selective reduction of an ester with $LiBH_4$ can even be applied on a large scale in the presence of a carboxylic acid and still result in a quantitative yield. This is demonstrated with the reduction of butylmalonic acid monoethyl ester (**3**) to (±)-2-butyl-3-hydroxypropionic acid (**4**),

by Hu et al. (Scheme 1-4).[27] When selective ester reduction is required, LiBH$_4$ is an excellent reducing agent. If selectivity is not necessary, LiAlH$_4$ is a more attractive reducing agent due to its greater reactivity.
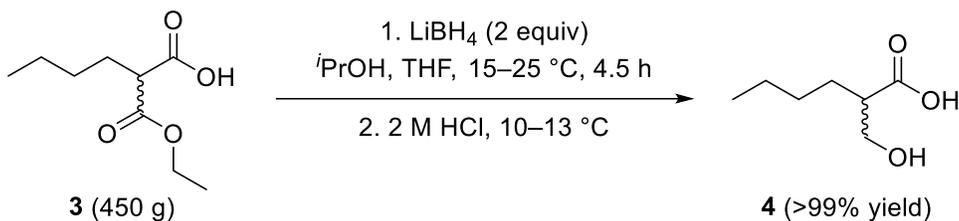
Scheme 1-4. Selective ester reduction of butylmalonic acid monoethyl ester (**3**) with LiBH$_4$.[27]

LiAlH$_4$ is a strong, non-selective reducing agent that was discovered by Finholt, Bond, and Schlesinger in 1947.[28] LiAlH$_4$ is industrially prepared from LiH and AlCl$_3$ (eq 1-5).[16]

$$4 \text{ LiH} \quad + \quad \text{AlCl}_3 \quad \longrightarrow \quad \text{LiAlH}_4 \quad + \quad 3 \text{ LiCl} \quad \textbf{(1-5)}$$

The greater reducing strength of LiAlH$_4$, compared to LiBH$_4$, is due to the hydride bonding. The aluminum hydride (Al–H) bonds and borohydride (B–H) bonds have Pauling electronegativity differences of 0.59 and 0.16, respectively.[29] The polar covalent nature of the Al–H bonds result in more electron density being present on the hydrides. Thus, making the aluminum's hydrides more nucleophilic, in comparison to the hydrides of the covalent B–H bonds. LiAlH$_4$ has been used for ester reductions since its discovery.[28] The reaction and mechanism are well established (Scheme 1-5). An ester reduction requires two equivalents of hydride, as it proceeds via reduction to the aldehyde and then subsequent reduction to the alkoxide. The alkoxide is then converted to alcohol with a protic work-up. The aldehyde, produced from the first reduction, is more susceptible to reduction than the ester. Therefore, any hydride source will preferentially react with the aldehyde. Notably, the reduction of an ester can be stopped at the aldehyde by using another aluminum hydride, diisobutylaluminum hydride (DIBAL-H).
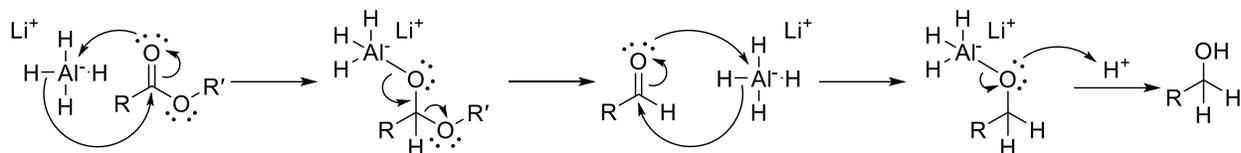
Scheme 1-5. General mechanism for ester reduction with LiAlH$_4$.

Unlike other hydride reducing agents, which act as nucleophilic reductants, DIBAL-H is an electrophilic reductant. The general mechanism is shown in Scheme 1-6. An ester's acyl oxygen's lone pair bonds to the Lewis acidic aluminum centre in DIBAL-H. The resulting compound then undergoes hydride addition to form a hemiacetal intermediate that is stable at low temperatures. Generally, DIBAL-H reactions are performed at -78 °C.[30] The stable hemiacetal intermediate stops a second reduction from proceeding. The hemiacetal is then slowly quenched, with protic solvent, to form an aldehyde. This method is an effective alternative to an ester being reduced to an alcohol and then oxidized to an aldehyde in a secondary reaction.
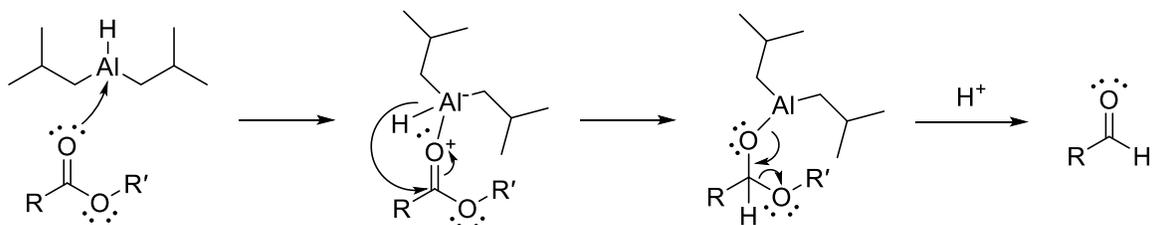
Scheme 1-6. General mechanism for ester reduction to aldehyde with DIBAL-H.

Esters are reduced by a variety of stoichiometric reducing agents, including the aforementioned, and others, such as lithium triethylborohydride and sodium bis(2-methoxyethoxy)aluminum hydride.[16] The use of these hydrides for ester reduction produces two desirable organic products, either an aldehyde and primary alcohol or two primary alcohols. The aldehydes and alcohols, produced from ester reductions, can be used in a variety of chemical industries, including fragrance and pharmaceutical.[31, 32] For example, the aforementioned alcohol **4**, produced from the LiBH$_4$ reduction of **3** (Scheme 1-4), was used by

8

Novartis in the preparation of the peptide deformylase inhibitor **5**.[27] Racemic **4** is resolved with

(*R*)-α-methylbenzylamine (**6**) and then acidified to form (*R*)-2-butyl-3-hydroxypropionic acid

(**7**), which is used to produce **5** (Scheme 1-7).[27]
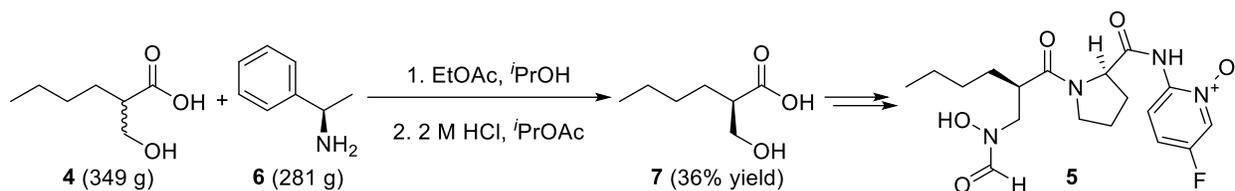
Scheme 1-7. Chiral resolution of **4** and Novartis' peptide deformylase inhibitor **5**.[27]

Another example is the incorporation of DIBAL-H into the synthetic route of Telcagepant (**8**),

which is a discontinued migraine-related drug developed by Merck.[33] Burgey and co-workers

reported the synthesis of **9**, a key intermediate to **8**, which includes the reduction of the methyl

ester of **10** to the aldehyde **11** using DIBAL-H (Scheme 1-8).[33]
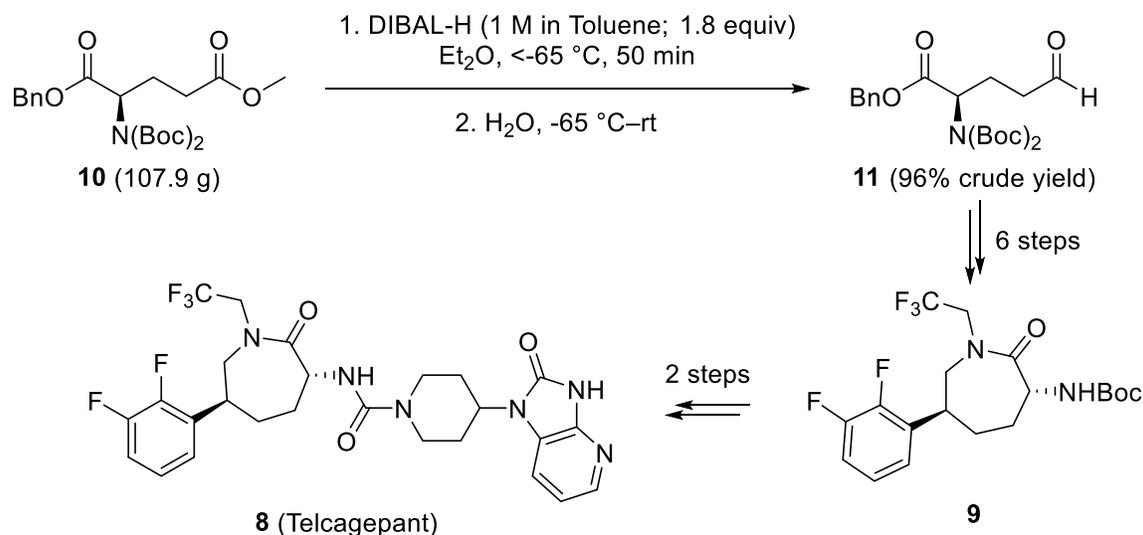
Scheme 1-8. Usage of DIBAL-H in Merck's preparation of Telcagepant (**8**).[33]

Notably, the reaction proceeds with selective reduction of the methyl ester of **10** and not the

benzyl ester. This selectivity was probably induced by the steric interactions of the larger benzyl

group and the proximity of the bulky *tert*-butyloxycarbonyl (Boc) groups.

9

The stoichiometric reduction of esters also produces stoichiometric by-products. Due to the aqueous or alcohol solvent work-up, inorganic hydroxide or alkoxides species form, respectively. Any excess hydride reagent is also oxidized into waste products. The aqueous oxidations of $LiBH_4$ and $LiAlH_4$ are shown in eq 1-6 and 1-7, respectively.[16]

$$LiBH_4 \quad + \quad 2\,H_2O \quad \longrightarrow \quad LiBO_2 \quad + \quad 4\,H_2 \quad \textbf{(1-6)}$$

$$LiAlH_4 \quad + \quad 4\,H_2O \quad \longrightarrow \quad LiAl(OH)_4 \quad + \quad 4\,H_2 \quad \textbf{(1-7)}$$

Therefore, the reduction of esters with stoichiometric amounts of reducing agents is not an atom-economical process. The quenching is also exothermic and produces H_2, which is extremely flammable. The flammability limit of H_2 is 4 to 74% by volume in air.[34] H_2 is also known to be explosive with finely divided metals and halogens.[34] Generally, the production of H_2 is not problematic if the quenching is performed slowly, at a low temperature, and under an inert atmosphere. Although H_2 is considered dangerous, controls have been developed for its safe production and usage. In fact, H_2 has been used in catalysis for over a century.[35]

Catalytic hydrogenation can be an advantageous and greener alternative to stoichiometric reduction. H_2 is a readily available non-toxic raw material[34, 35] and its use with a catalyst circumvents the production of stoichiometric inorganic by-products from the tedious work-up procedures involved with stoichiometric reducing agents. Hydrogenations are generally 100% atom-economic processes[35] and can be either homogeneous or heterogeneous. The first reported catalytic hydrogenation of esters was with a heterogeneous system.[36]

1.3 Heterogeneous Hydrogenation of Esters to Alcohols

1.3.1 Adkins Era

The first published heterogeneous hydrogenation of esters was in 1931.[36] Homer B. Adkins and Karl A. Folkers reported a system that used copper chromite to hydrogenate seven ethyl esters at 250 °C and under 220 atm H_2 (Table 1-1).[36]

Table 1-1. Adkins and Folkers' ethyl ester hydrogenations over $Cu_2Cr_2O_5$.[36,a]

$$R-C(=O)-O-Et \xrightarrow[\text{H}_2\ (220\ \text{atm}),\ 250\ °\text{C}]{Cu_2Cr_2O_5} R-CH_2-OH\ +\ EtOH$$

entry	ester	grams	catalyst (g)	time (h)	non-EtOH product	yield (%)
1	(ethyl pentanoate)	35	5	13	(1-pentanol)	94
2	$CH_3(CH_2)_{11}CH_2$–C(=O)–O–Et	38	5	2.0	$CH_3(CH_2)_{11}CH_2$–OH	99
3	(ethyl pivalate)	30	5	1.5	(neopentyl alcohol)	88
4	(diethyl succinate)	77	7	6.5	HO–(CH2)4–OH	81
5	(ethyl cinnamate)	37	3	9.0	(3-phenyl-1-propanol)	83
6	(ethyl 3-hydroxy-2,2-dimethylbutanoate)	34	4	0.1	(isobutyl alcohol derivative)	98

[a]Adapted with permission from Adkins, H.; Folkers, K. The Catalytic Hydrogenation of Esters to Alcohols. *J. Am. Chem. Soc.* **1931**, *53* (3), 1095–1097. Copyright 1931 American Chemical Society. (Ref. 36).

Copper chromite's chemical formula was later established as $Cu_2Cr_2O_5$.[37] The authors reported varying loadings and reaction times to obtain high yields (81–99%).[36] Saturated aliphatic esters (entries 1–4) produced their expected alcohol products. $Cu_2Cr_2O_5$ was not chemoselective, as the

hydrogenation of ethyl cinnamate (entry 5) resulted in reduction of both the olefin and the ester.

The hydrogenation of ethyl 2,2-dimethyl-3-hydroxybutyrate (12, entry 6) did not result in the

expected product.[36] The ester 12 underwent β-cleavage during the hydrogenation to produce two

equivalents of EtOH and one equivalent of 2-methylpropan-1-ol.[36]

In the following year, Adkins and Folkers reported the hydrogenation of over thirty

different esters with their heterogeneous Cu–Cr oxide catalysts.[38] Similar to their previous report,

the authors used varying loadings and reaction times. Unlike their previous report, a wide

pressure range (177–300 atm H_2) and two temperatures (225 and 250 °C) were used.[38] Only 10

esters were hydrogenated to their respective alcohol products in yields greater than 80%.[38]

Several reactions resulted in side-products. For example, the attempted hydrogenation of methyl

salicylate (13) over $Cu_2Cr_2O_5$ resulted in two cleavage products, *ortho*-cresol (14), and the arene

reduced product, 2-methyl cyclohexanol (15) (Scheme 1-9).[38]
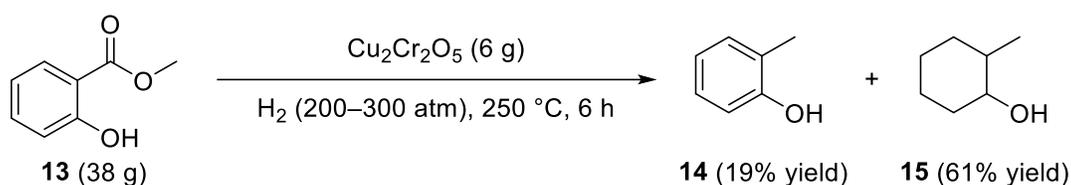
Scheme 1-9. Adkins and Folkers' attempted hydrogenation of methyl salicylate (13) over $Cu_2Cr_2O_5$.[38]

Cleavage occurred even when the arene was on the α-carbon of the ester. For instance, ethyl

phenylacetate (16) underwent cleavage, within 1 h over $Cu_2Cr_2O_5$, to yield ethylbenzene (17)

(Scheme 1-10).[38] A small portion of 16 was converted to the desired phenethyl alcohol (18).
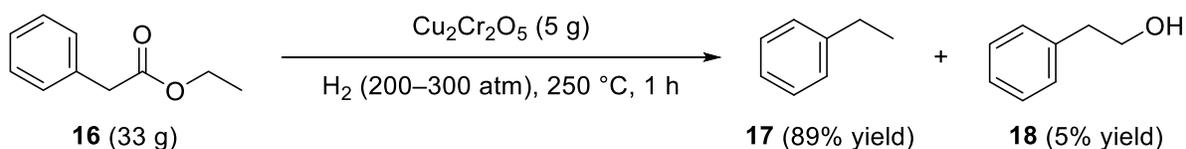
Scheme 1-10. Adkins and Folkers' attempted hydrogenation of ethyl phenylacetate (16) over $Cu_2Cr_2O_5$.[38]

These hydrogenations further demonstrate the chemoselectivity issues with $Cu_2Cr_2O_5$.

In the interest of selectively hydrogenating unsaturated esters to unsaturated alcohols, Sauer and Adkins examined six catalysts containing Zn or Cu with Cr, V, or Mo.[39] Zn–Cr oxide gave optimal selectively. For example, *n*-butyl oleate (**19**) was mostly hydrogenated to *cis*-9-octadecen-1-ol (**20**) over 11 h at 300 °C and 200 atm H_2 (Scheme 1-11).[39] Only 13% of the saturated alcohol product was obtained.[39] The Zn–Cr oxide catalyst did not result in good activity, as high pressure, temperature, and catalyst loading were required to achieve a fair yield. The hydrogenation is also questionably catalytic, as the catalyst loadings are extreme (≤ 2 to 1 weight ratio of ester to Zn–Cr oxide). Despite the extreme conditions, a system for selective hydrogenation of unsaturated esters to unsaturated alcohols was discovered.
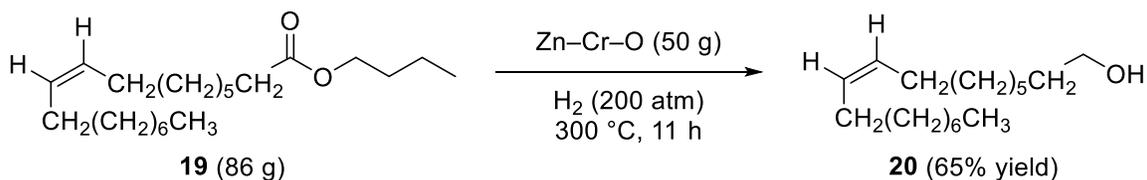
Scheme 1-11. Sauer and Adkins' selective unsaturated ester hydrogenation of **19** over Zn–Cr–O.[39]

Reports of ester hydrogenations over Raney® nickel (Raney Ni) began in the 1940s. In March 1940, Levene and co-workers reported the hydrogenation of methyl leucinate (**21**) over Raney Ni at 150 atm H_2.[40] The authors varied reaction temperatures between 70 to 200 °C. The most successful hydrogenation of **21** to leucinol hydrochloride (**22**) is shown in Scheme 1-12.[40] Notably, the Raney Ni system operated well below 200 °C. In fact, temperatures higher than 135 °C did not result in the formation of **22**.[40] Although their optimal run, the authors did not include the amount of Raney Ni used. Therefore, it cannot be concluded that the reaction was catalytic.
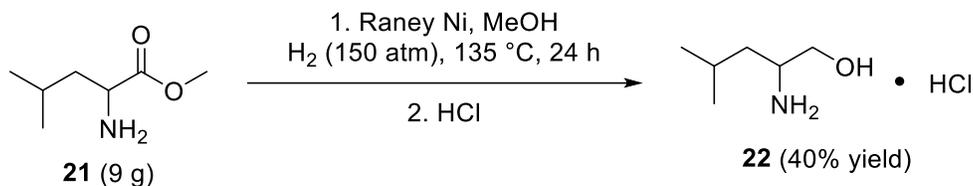
Scheme 1-12. Levene's hydrogenation of methyl leucinate (**21**) over Raney Ni at 135 °C.[40]

In May 1940, Levene and co-workers published their hydrogenation of ethyl 2-phenyl-2-aminoacetate (**23**) over Raney Ni at varying temperatures and 150 atm H$_2$.[41] The authors discovered that 40 °C and a 9 h reaction time over Raney Ni resulted in the desired product, 2-amino-2-phenylethanol (**24**) (Scheme 1-13).[41] Longer reaction times and higher temperatures resulted in the phenyl reduced product and other non-desired products. Levene and co-workers used 31 g of Raney Ni for the hydrogenation of **23**.[41] Therefore, the heterogeneous Raney Ni hydrogenations of **23** and **21**, from Levene's prior publication, are probably more stoichiometric than catalytic.
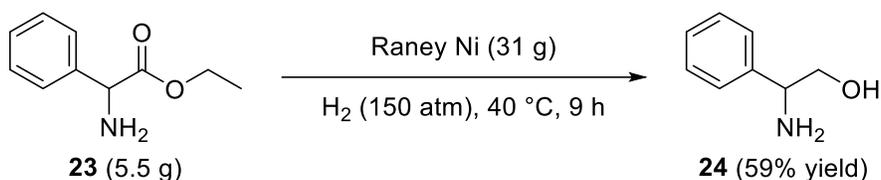
Scheme 1-13. Levene's hydrogenation of ethyl 2-phenyl-2-aminoacetate (**23**) over Raney Ni at 40 °C.[41]

In the late 1940s, Adkins and co-workers developed several variations of Raney Ni[42, 43] and applied them towards ester hydrogenations.[44, 45] Specifically, W-4 and W-6 Raney Ni were active towards the hydrogenation of esters. For example, W-4 Raney Ni was used to hydrogenate **23** at 50 °C and 150 to 200 atm H$_2$ (Scheme 1-14).[44] In comparison to Levene's Raney Ni system, significantly less Raney Ni was required to obtain a higher yield (93%) of **24** over less time (7 h).[44] The increased activity may be attributed to the 10 °C higher temperature and possible higher pressure, but Adkins demonstrated that the preparation of the Raney Ni

14

significantly alters its activity. Notably, W-6 Raney Ni can hydrogenate esters at 25 °C, albeit at 340 atm H_2 with a 3 to 2 weight ratio of Raney Ni to ester.[45] Although W-6 Raney Ni can be used for room-temperature hydrogenation, it can also react explosively.[45] Overall, Raney Ni systems can operate at lower temperatures, but their preparations, high loadings, and dangerous reactivity make them less appealing than Cu–Cr oxide systems.
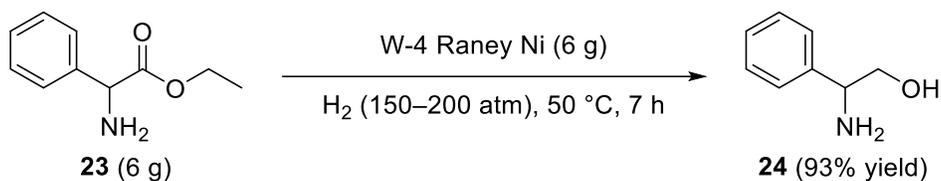
Scheme 1-14. Adkins' hydrogenation of ethyl 2-phenyl-2-aminoacetate (**23**) over W-4 Raney Ni at 50 °C.[44]

In 1948, Mozingo and Folkers published two articles for ester hydrogenations over Cu–Cr oxides below 200 °C.[46, 47] The first article examined the hydrogenation of ethyl β-oxy esters to glycols.[46] The authors hydrogenated seven β-oxy esters over Cu–Cr–Ba oxide, at temperatures ranging from 160 to 180 °C.[46] Their hydrogenation of ethyl acetoacetate (**25**) to 1,3-butanediol (**26**) is shown in Scheme 1-15.[46] The hydrogenation of **25** resulted in a 30% yield of **26**.
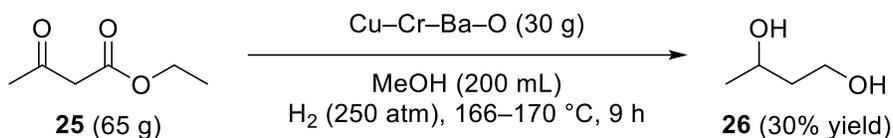
Scheme 1-15. Mozingo and Folkers' hydrogenation of ethyl acetoacetate (**25**) over Cu–Cr–Ba–O.[46]

The average yield of the hydrogenations reported is only 33%. Although the yields are low, the reactions are significant as they did not result in the β-cleavage products, which occurred for the hydrogenation of the β-oxy ester **12** at 250 °C (Table 1-1, entry 6).[36] Based on this success, Mozingo and Folkers decided to investigate the hydrogenation of aromatic esters at lower temperatures.[47] As discussed previously, esters with arenes, such as **13** and **16** (Schemes 1-9 and

1-10, respectively), underwent cleavage over $Cu_2Cr_2O_5$ at 250 °C.[38] Mozingo and Folkers

reported the hydrogenation of nine α-phenyl esters over Cu–Cr–Ba oxide at 125 to 165 °C.[47] For

example, ethyl benzoate (**27**) was hydrogenated to benzyl alcohol (**28**) at 155 to 160 °C (Scheme

1-16).[47] The 3 h and 15 min hydrogenation of 50 g of **27** over 7 g of Cu–Cr–Ba oxide, at a

pressure somewhere between 300 and 400 atm H_2, resulted in a 63% yield of **28**.[47] The yields of

the other α-phenyl ester hydrogenations ranged from 49 to 89%.[47] Mozingo and Folkers' catalyst

to ester loadings and yields are respectable, but the pressure reported is both enormous and

imprecise. Although the authors used enormous and imprecise H_2 pressure, it is notable that the

desired products, without cleavage or arene reduction, were acquired.

27 (50 g) → Cu–Cr–Ba–O (7 g), MeOH (75 mL), H_2 (300–400 atm), 155–160 °C, 3.25 h → **28** (63% yield)
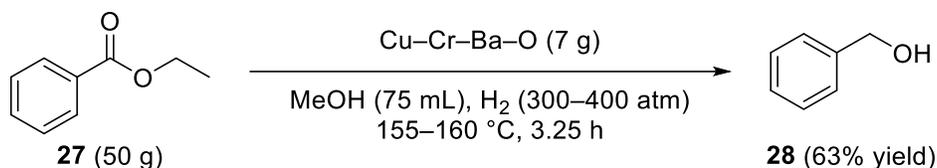
Scheme 1-16. Mozingo and Folkers' hydrogenation of ethyl benzoate (**27**) over Cu–Cr–Ba–O.[47]

There are many publications involving the hydrogenation of esters over Cu– and Zn–Cr

oxides, and Raney Ni.[48] An unsurprising lapse of literature involving these species occurred with

the untimely death of Homer B. Adkins in 1949, and the discoveries of $LiBH_4$ and $LiAlH_4$.

1.3.2 Post-Adkins Era

The development of heterogeneous ester hydrogenation systems resurged in the 1980s,

due to the discovery of homogeneous ester hydrogenations. Focus was placed on developing

Cr-free Cu systems, due to the high toxicity of some Cr compounds.

Many gas- and vapour-phase reactions of H_2 and esters over Cu catalysts have been

reported.[49-58] In 1984, Wainwright and co-workers reported the gas-phase addition of H_2 to

aliphatic esters over Raney® Cu at 210 to 280 °C.[49] The reactions proceeded at approximately

atmospheric pressure. Significantly, the authors suggested that the hydrogenation mechanism between formates and acetates were different.[49] This mechanistic difference was later supported in a comparative gas-phase kinetic study on the rate of formate and acetate hydrogenation over SiO_2-supported Cu (Cu/SiO_2).[50] Agarwal and co-workers study focused on methyl and ethyl esters of formate and acetate (Figure 1-7).[50] The formate esters were found to react over 1,000 times faster than acetates at 180 °C and 0.5 atm H_2.[50] The authors attribute this activity difference to two different mechanisms. The acetates were believed to undergo dissociative adsorption with cleavage at the acyl–alkoxide bond prior to addition of H_2 across the C=O bonds.[50] While the formate C=O bonds were hydrogenated directly.[50]
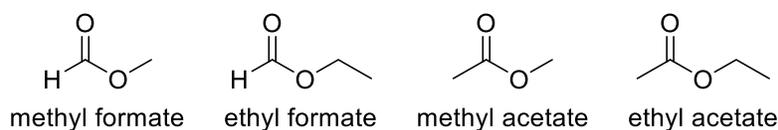
Figure 1-7. Methyl and ethyl esters of formate and acetate.

This mechanistic difference began separating the literature into two reaction types: hydrogenation and hydrogenolysis. Hydrogenation is defined as the addition of H_2 across double and triple bonds, while hydrogenolysis is defined as the cleavage or breakdown of carbon–carbon or carbon–heteroatom single bonds by H_2. The hydrogenation and hydrogenolysis of esters can result in the same products. This happens when the hydrogenolysis only occurs between the acyl carbon and alkoxy oxygen. The adsorbed acyl C=O bond is then hydrogenated to an aldehyde. Many, if not all, of the aforementioned heterogeneous ester hydrogenations may in fact be hydrogenolysis reactions. These reactions can still be considered hydrogenations, as the aldehyde produced is still hydrogenated. Therefore, it is acceptable for an ester hydrogenolysis to be called an ester hydrogenation. A large review of the catalytic hydrogenolysis of esters to alcohols has been published.[59]

The effects of promoters on Cu/SiO$_2$ ester hydrogenations have been reported.[52-55, 60, 61] Cu supported on oxides other than SiO$_2$ have also been investigated for ester hydrogenation, including ZnO,[62] ZrO$_2$,[63-65] Al$_2$O$_3$,[66, 67] and TiO$_2$.[68] The effects of promoters, supports, and their Cu ester hydrogenation systems will not be elaborate on, as they deserve their own focused review. Although Cu systems are viable, they generally require harsher reaction conditions than other developed heterogeneous systems.

In 2017, Pidko and co-workers examined methyl ester hydrogenations with a series of Ni–Re catalysts supported on Al$_2$O$_3$, C, CeO$_2$, SiO$_2$, and TiO$_2$.[69] Ni–Re, in a 1 to 2 ratio, supported on TiO$_2$ gave optimal results for the hydrogenation of methyl hexanoate (**29**) to hexan-1-ol (**30**) in octane (Scheme 1-17).[69] The hydrogenation of **29** proceeded with 0.75 wt% catalyst loading, 49 atm H$_2$, and 180 °C.[69] Only a modest conversion (70%) and selectivity for **30** (76%) were achieved over 8 h.[69] Significantly, the catalyst was recycled and only a minor activity decrease occurred for the second hydrogenation of **29** (67% conv).[69]
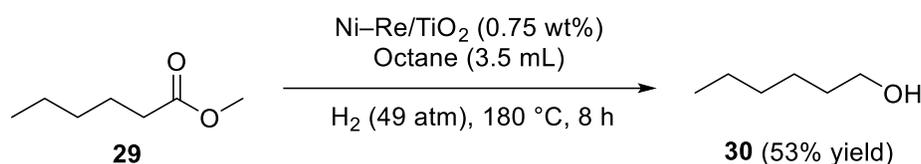
Scheme 1-17. Pidko's hydrogenation of methyl hexanoate (**29**) over Ni–Re/TiO$_2$.[69]

Pidko's system demonstrates a significant problem with a lot of the heterogeneous ester hydrogenations. The problem, which is likely caused by hydrogenolysis, is a lack of selectivity. When the selectivity is not 100% towards the alcohol, the esters are converted to unwanted side-products and this results in diminished yields of the desired alcohol product.

Heterogeneous ester hydrogenations also suffer from several other drawbacks. These drawbacks can include harsh reaction conditions, such as high pressure, temperature, catalyst

loading, and/or long reaction times. The systems may also suffer from low activity and/or limited substrate scope. Heterogeneous systems are also difficult to compare as most authors only provide the mass or wt% of catalyst. Although sometimes difficult to obtain for heterogeneous catalysts, the mol% is a more appropriate value for comparisons. Specifically, the mol% of catalyst allows for the determination of the turnover number (TON). The TON is the moles of substrate converted to product per mole of catalyst. This number provides insight into the catalyst's stability under the observed reaction conditions. If reaction times are given, the number of turnovers a catalyst makes in a given time frame can be determined. This value, known as the turnover frequency (TOF), can be useful for comparing catalysts' activities.

Homogeneous catalyst systems generally endure less drawbacks but are not as easily recovered and recycled. In the interest of limiting drawbacks, researchers are examining the immobilization of homogeneous catalysts to solid supports. These anchored homogeneous catalysts become heterogeneous catalyst systems.

In 2016, Kamer and co-workers reported their immobilized Ru-based catalyst system for ester hydrogenation.[70] The authors used their diphosphine (PP) supports **31** and **32** (Figure 1-8) for their initial investigation.
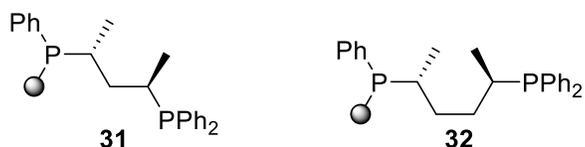
Figure 1-8. Kamer's diphosphine (PP) supports for immobilization of catalysts.[71]

These PP supports were made by a five-step procedure from *Janda*Jel™-Cl resin, a cross-linked polystyrene resin.[71] The resin (illustrated as a grey ball) contains several sites where a Cl has been substituted with a PP. These PP sites act as ligands and immobilize metals to the resin. The

PP supports were screened with Ru precursors and diamine ligands for the hydrogenation of

methyl benzoate (**33**).[70] The best screening result is shown in Scheme 1-18.[70]
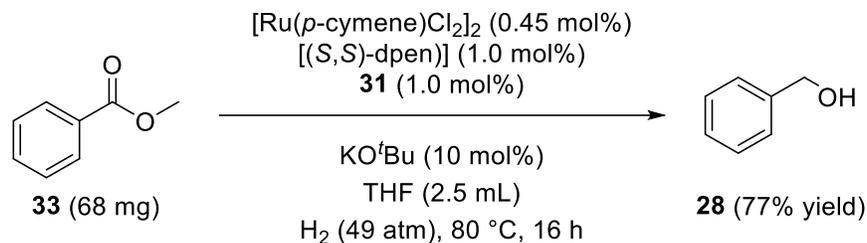
Scheme 1-18. Kamer's best screening result for **33** hydrogenation with in situ immobilization on **31**.[70]

The best immobilized catalyst system performed ~89 turnovers of **33**. Unfortunately, the catalyst

only had a 96% selectivity for **28**.[70] Therefore, 77% of the 80% conversion was **28**. The authors

also developed supports **34** and **35** (Figure 1-9)[70] based upon prior activity studies.[72-74]
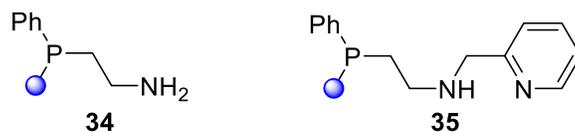
Figure 1-9. Kamer's PN and PNN supports for immobilization of catalysts.[70]

These supports were made from a different cross-linked polystyrene resin, called a Merrifield

resin (illustrated as a blue ball), and were also examined for the hydrogenation of **33**. With 1

mol% **35** and 0.9 mol% [RuCl$_2$(PPh$_3$)$_3$], ~110 turnovers were obtained for the hydrogenation of

33 (Scheme 1-19). This immobilized catalyst had greater than 99% selectivity.[70]
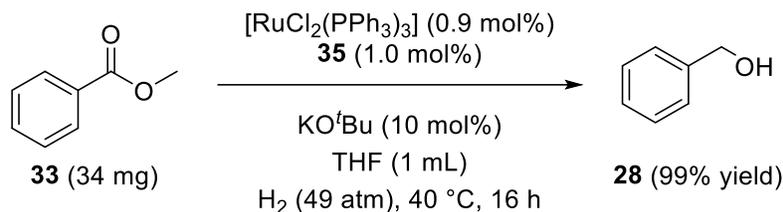
Scheme 1-19. Kamer's hydrogenation of methyl benzoate (**33**) with in situ immobilization on **35**.[70]

Notably, the hydrogenation was performed under 49 atm H_2 at 40 °C. These are the mildest reaction conditions for a heterogeneous ester hydrogenation system presented thus far. Although the reaction conditions are desirable, the reaction required 10 mol% KO^{t}Bu and 16 h.[70] The reusability of the system was examined with four 2 h runs.[70] The conversion and selectivity decreased over the four runs and resulted in 265 turnovers of **33** to **28**. The hydrogenation of seven other esters, including aliphatic, were also examined with **35**. Great conversions (>90%) and selectivities (>95%) for five of the other esters were obtained.[70]

Kamer and co-workers reported their second system for the hydrogenation of esters over heterogenized homogeneous catalysts in 2019.[75] The authors developed non-symmetrical PNP pincer supports from their Merrifield[71] and polystyrene[76] resins.[75] Their resin-bound ligands were reacted with [RuHCl(PPh$_3$)$_3$CO] at 60 °C to prepare their heterogeneous catalysts.[75] A total of 14 different heterogeneous catalysts were prepared and screened for the hydrogenation of **33**.[75] Out of the 14 heterogeneous catalysts, only two had excellent activity (≥98%) and selectivity (≥99%) for hydrogenation of **33** to **28** (1.0 mol% catalyst, 10 mol% KO^{t}Bu, 1 mL THF, 49 atm H_2, 80 °C, 16 h).[75] These two catalysts, attached to a Merrifield resin, are shown in Figure 1-10.
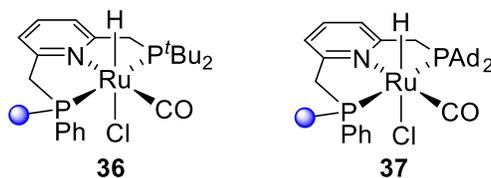
Figure 1-10. Kamer's two most active and selective immobilized Ru–PNP catalysts for ester hydrogenation.[75]

Of these, **36** was more active towards a wider variety of esters than **37**. Twelve esters were hydrogenated with **36** (1.0 mol% catalyst, 10 mol% KO^{t}Bu, 1 mL THF, 49 atm H_2, 80 °C, 24 h).[75] The conversions and selectivities varied significantly, but **36** was highly selective (>97%)

for the hydrogenation of α-aryl esters and lactones.[75] The recyclability of **36** was also examined

over five hydrogenations of **33** (Scheme 1-20).[75]
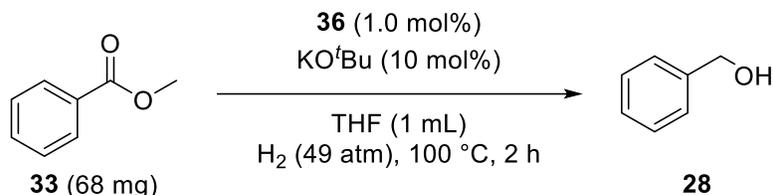
Scheme 1-20. Kamer's methyl benzoate (**33**) hydrogenation conditions for testing recyclability of **36**.[75]

The activity and selectivity decreased over the five runs by only 11 and 9%, respectively.[75] The

TON and TOF of **33** to **28** over the five runs are ~141 and 14.1 h^{-1}, respectively. These numbers

are low compared to those obtained by modern homogeneous systems.

Instead of synthesizing a support with a ligand and then immobilizing the metal for

catalysis, Bergens and co-workers used a different approach. In 2019, Bergens and co-workers

reported their heterogeneous precatalyst for the hydrogenation of **33**.[77] Bergens and co-workers

used alternating ring-opening metathesis polymerization (ROMP) to integrate **38** into a

cross-linked organic framework supported on BaSO₄ (Scheme 1-21).[77]
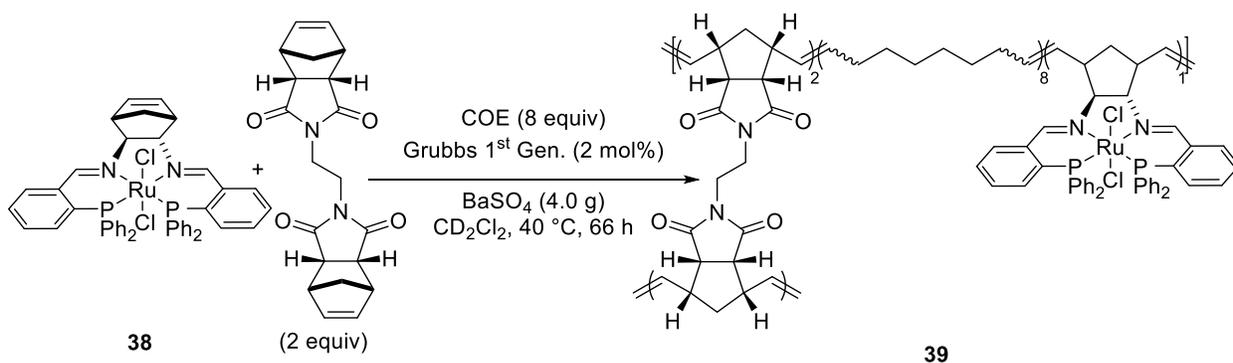
Scheme 1-21. Bergens' alternating ROMP immobilization of **38** to give the supported catalyst **39**.[77]

Their polymerized precatalyst **39** was used for the hydrogenation of **33** under mild heterogenous

conditions (Scheme 1-22).[77]
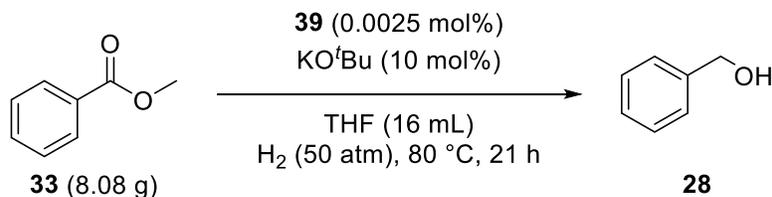
Scheme 1-22. Bergens' methyl benzoate (**33**) hydrogenation conditions for testing recyclability of **39**.[77]

The reusability of **39** was examined over five runs and resulted in 121,680 turnovers of **33**.[77] The total TON is remarkable, but the activity of the catalyst dropped significantly between runs. The catalyst initially performed 32,960 turnovers (TOF = 1,570 h⁻¹), but by its fifth run only 14,760 turnovers were obtained (TOF = 703 h⁻¹).[77] This averages out to be an 11% activity drop per run. Notably, even after the activity drops, the catalyst was still providing a far superior TON and TOF than Kamer and co-workers' catalyst. Bergens and co-workers compared their heterogeneous system with the homogeneous hydrogenation of **33** with **38**, under slightly greater catalyst loading and temperature (0.004 mol% **38**, 10 mol% KO^{t}Bu, 16 mL THF, 50 atm H$_2$, 90 °C, 3 h).[77] The homogeneous catalyst reached 18,000 turnovers over 3 h, which is a TOF of 6,000 h⁻¹.[77] Unlike the heterogeneous system, the homogeneous catalyst was not able to be recycled for further runs. This lack of recyclability demonstrates the importance of heterogenizing homogeneous catalysts. In summary, Bergens an co-workers' system used mild heterogeneous hydrogenation conditions to obtain a remarkably high TON of **33**. In fact, to the best of my knowledge, this is the highest TON of **33** across both heterogeneous and homogeneous literature.

Although heterogeneous catalysts are more easily recovered and recycled than homogeneous catalysts, they suffer from several drawbacks. It can simply be more efficient to use a homogeneous catalyst for ester hydrogenation.

1.4 Homogeneous Hydrogenation of Esters with Ru-Based Catalysts

1.4.1 Non-Bifunctional Catalysts

The first catalytic homogeneous hydrogenation of acyclic esters was reported by Grey

and Pez in 1980.[78] The anionic dihydride $K[RuH_2(PPh_3)_2(PPh_2C_6H_4)]$ (**40**) was used in catalytic

hydrogenation of reactive esters.[78] The hydrogenation of methyl trifluoroacetate (**41**) to

2,2,2-trifluoroethanol (**42**) under low pressure and catalyst loading (Scheme 1-23) only resulted

in ~14 turnovers to **42** (10% yield) over 20 h (TOF = 0.70 h^{-1}).[78]
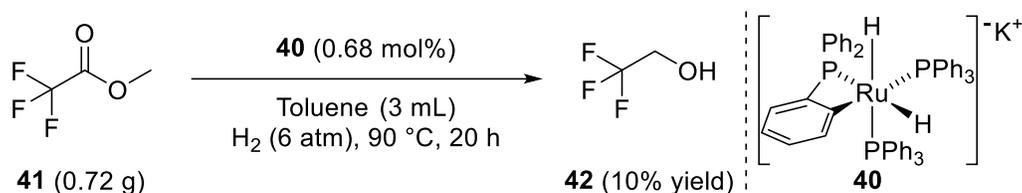
Scheme 1-23. Grey and Pez's homogeneous hydrogenation of methyl trifluoroacetate (**41**) with **40**.[78]

While, the more reactive ester 2,2,2-trifluoroethyl trifluoroacetate (**43**) underwent ~112 turnovers

to **42** (76% yield) over 20 h (TOF = ~5.6 h^{-1}) under the same conditions (Scheme 1-24).[78]
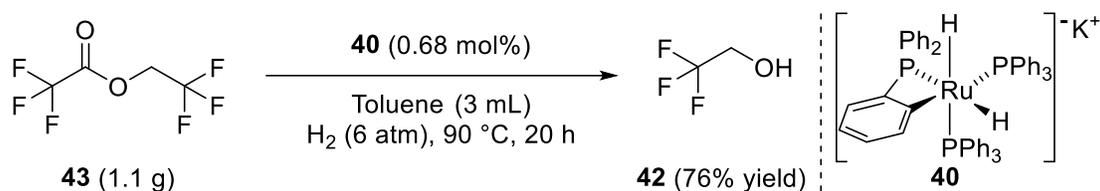
Scheme 1-24. Grey and Pez's hydrogenation of 2,2,2-trifluoroethyl trifluoroacetate (**43**) with **40**.[78]

The hydrogenation of dimethyl oxalate (**44**) produced a small amount of methyl glycolate (**45**)

(Scheme 1-25),[78] with no evidence of hydrogenation of **45** to ethylene glycol (**46**).
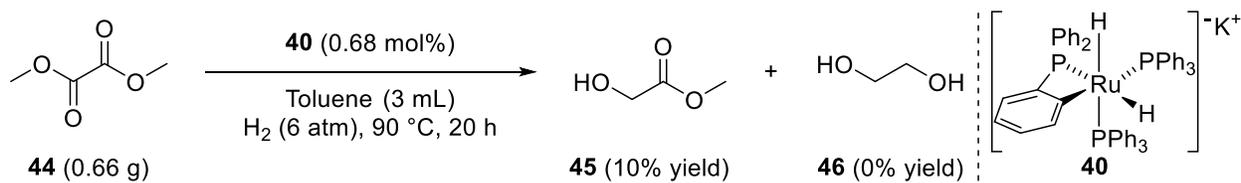
Scheme 1-25. Grey and Pez's hydrogenation of dimethyl oxalate (**44**) to methyl glycolate (**45**) with **40**.[78]

24

Although reactive esters were required, this was the first demonstration of a catalytic

homogeneous ester hydrogenation.

Grey and co-workers reported a second Ru-based catalyst that hydrogenated both reactive

and less reactive aliphatic esters in 1980.[79] The proposed catalyst, $K_2[Ru_2H_4(PPh_2)(PPh_3)] \bullet$

(diglyme)$_2$ (structure not given, **47**), hydrogenated the fluorinated esters **41** and **43** with excellent

conversions (Scheme 1-26).[79] This result demonstrates that **47** was a more effective catalyst than

40, with ~274 and ~312 turnovers of **41** and **43**, respectively. The hydrogenation of methyl

acetate (**48**), ethyl acetate (**49**), and methyl propionate (**50**) with **47**, under the same conditions

(20 h), occurred in 22, 8, and 5% conversions, respectively.[79] Notably, the hydrogenation of **48**

was hindered by addition of 18-crown-6.[79] This observation supports the theory that K^+ was

necessary to activate the carbonyl C=O bond towards hydride attack.[79] The hydrogenation did

not proceed without solvent.[79] Although the conversions were low for unreactive esters, the

system used mild pressure (6 atm) and was the first catalytic example of a homogeneous

aliphatic ester hydrogenation.

47 (0.32 mol%)

Toluene (3 mL)
H$_2$ (6 atm), 90 °C

41 (R=CH$_3$, 0.68 g)
43 (R=CH$_2$CF$_3$, 1.0 g)

42 (20 h, 88% conv)
42 (4 h, >99% conv)

Scheme 1-26. Grey's homogeneous hydrogenations of trifluoroacetate esters **41** and **43** with **47**.[79]

Matteoli et al. reported the hydrogenation of dimethyl oxalate (**44**) to **45** with the Ru

cluster [Ru$_4$H$_4$(CO)$_8$(P^{n}Bu$_3$)$_4$] (**51**) under harsh conditions (Scheme 1-27).[80]

51 (0.40 mol%)

Benzene (15 mL)
H$_2$ (130 atm at 20 °C)
180 °C, 144 h

44 (1.3 g)   **45** (51% yield)   **46** (0% yield)

+   HO   OH

HO   O

Scheme 1-27. Matteoli's hydrogenation of dimethyl oxalate (**44**) to methyl glycolate (**45**) with the Ru cluster **51**.[80]

Like Grey's hydrogenation, the relatively unreactive ester **45** did not undergo further

hydrogenation. Only ~128 turnovers of **44** occurred over 144 h (6 days) with 0.40 mol% **51**.[80]

Full conversion of **44** to **45** (TON = 125) was obtained over 36 h by doubling **51** (0.80 mol%).

This supports that the limiting TON of the catalyst is ~128.[80] The hydrogenation of dimethyl

succinate (**52**), catalyzed by **51**, resulted in lactonization to form γ-butyrolactone (**53**) (Scheme

1-28).[80] The hydrogenation of **52** occurred at an extremely low rate under harsh conditions.[80]

51 (0.05 mol%)

H$_2$ (130 atm at 20 °C)
180 °C, 144 h

52 (6 g)   **53** (7% yield)   **54** (0% yield)

+   HO   OH
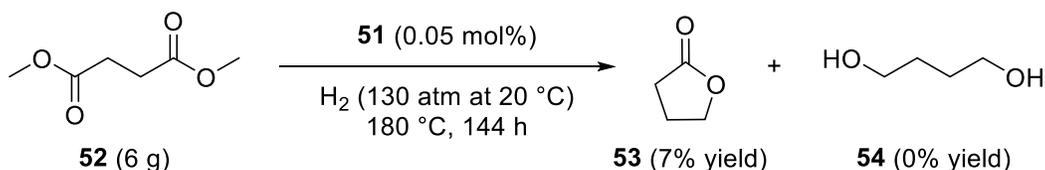
Scheme 1-28. Matteoli's hydrogenation of dimethyl succinate (**52**) to γ-butyrolactone (**53**) with the Ru cluster **51**.[80]

1,4-Butanediol (**54**) was not detected.[80] Diesters with longer connecting alkyl chains were

inactive.

In 1985 and 1986, Matteoli et al. reported their screenings of Ru–carbonyl complexes as

catalysts for the hydrogenation of **44**.[81, 82] Of the eight precursors examined, the Ru–carbonyl

[Ru(CO)$_2$(OAc)$_2$(P^{n}Bu$_3$)$_2$] (**55**) gave the best result, albeit under harsh conditions (Scheme

1-29).[81, 82] The mono-alcohol **45** and the diol **46** were obtained in 73 and 27% yield,

respectively.[81, 82] These correspond to ~130 turnovers over 144 h (TOF = ~0.9 h^{-1}). The nature of

the solvent had significant influence on the product distribution.[81, 82] The use of coordinating

solvents, such as 1,4-dioxane and THF, resulted in exclusive reduction to **45** over 144 h.[81, 82]

While 93% **45** and 7% **46** formed in benzene.[81, 82] The highest yield of **46** was obtained in MeOH (Scheme 1-29). The authors also reported that the addition of **45** and **46** enhanced the reaction.[82, 83] The diol **46** was obtained in 95% yield by increasing the pressure, catalyst loading, and pretreating **55** with an equivalent of **46** in benzene (1.6 mol% **55**, 200 atm H_2 at 20 °C, 180 °C, 144 h).[83] The mechanism of catalyst activation by the addition of alcohol is unknown.
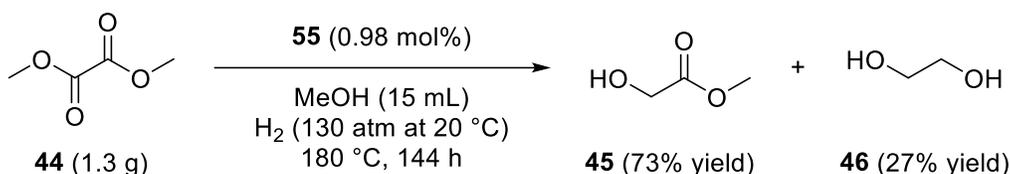
Scheme 1-29. Matteoli's hydrogenation of dimethyl oxalate (**44**) to **45** and ethylene glycol (**46**) with **55**.[81, 82]

In 1992, Hara et al. reported the hydrogenation of lactones to diols in tetraethylene glycol dimethyl ether (tetraglyme) with in situ formed Ru–trialkylphosphine catalysts.[84] The catalysts were prepared from [Ru(acac)$_3$] (**56**) and 10 equivalents of a trialkylphosphine.[84] The alkyl phosphine P($^nC_8H_{17}$)$_3$ formed the most active catalyst, which NMR studies supported as a mixture of *cis*- and *trans*-[RuH$_2$(P($^nC_8H_{17}$)$_3$)].[84] The catalyst resulted in ~250 turnovers of **53** to **54** over 3 h (TOF = ~83.3 h^{-1}) at 200 °C and 49 atm H_2 (Scheme 1-30).[84]
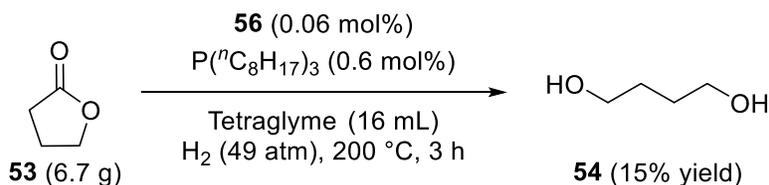
Scheme 1-30. Hara's hydrogenation of γ-butyrolactone (**53**) with in situ formed [RuH$_2$(P($^nC_8H_{17}$)$_3$)].[84]

Hara et al. discovered that the addition of acids promoted the reaction. Specifically, the addition of NH$_4$PF$_6$ (0.3 mol%) nearly doubled the reaction rate (28% yield of **54**).[84] The hydrogenation of δ-valerolactone (**57**) to 1,5-pentanediol (**58**) was also examined (Scheme 1-31).[84]

56 (0.08 mol%)
P(^{n}C$_8$H$_{17}$)$_3$ (0.8 mol%)
NH$_4$PF$_6$ (0.4 mol%)

Tetraglyme (16 mL)
H$_2$ (49 atm), 200 °C, 3 h

HO⌒⌒⌒⌒OH

57 (6.5 g)   **58** (24% yield)
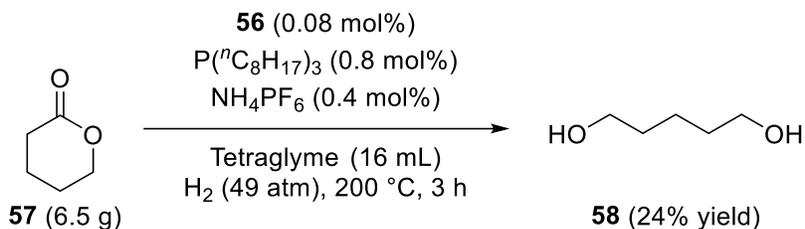
Scheme 1-31. Hara's hydrogenation of δ-valerolactone (**57**) with NH$_4$PF$_6$ and in situ formed [RuH$_2$(P(^{n}C$_8$H$_{17}$)$_3$)].[84]

The diol **58** formed in 24% yield.[84] Although **57** should be more reactive than **53** due to its higher ring strain energy, the catalyst is more reactive towards **53**. This may be caused by a larger steric hindrance of **57**.

In 1997, Elsevier and Teunissen reported the hydrogenation of **44** under milder conditions than Matteoli's system.[85] The hydrogenation of **44** was screened with **56**, Zn, and 10 ligands. Notably, the combination of **56** and 1,1,1-tris(diphenylphosphinomethyl)ethane (Triphos, **59**) with a small amount of Zn metal gave the highest yield of **46** (Scheme 1-32).[85]

56 (1.2 mol%)
59 (1.4 mol%)
Zn (0.3 mol%)

MeOH (12 mL)
H$_2$ (69 atm)
100 °C, 16 h

44 (209 mg)   **45** (1% yield)   **46** (95% yield)
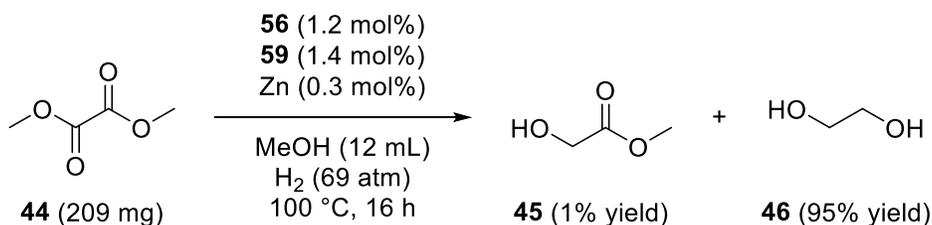
Scheme 1-32. Elsevier's hydrogenation of **44** to **46** with Zn and an in situ formed Ru–Triphos catalyst (**56+59**).[85]

Under 69 atm H$_2$ and 100 °C, the catalyst system performed 159 turnovers over 16 h (TOF = ~9.9 h^{-1}).[85] It was speculated that Zn accelerated the formation of precatalyst species by reducing **56** from a Ru(III) species to a Ru(II) species.[85] The ligand screening also supported that a facial coordination was important for the hydrogenation of **44**.[85] The activity was further increased by using dried MeOH. The hydrogenation with dried MeOH resulted in 857 turnovers of **44** over 16 h (TOF = 53.6 h^{-1}) without modification of the temperature or pressure (Scheme 1-33).[85]

28
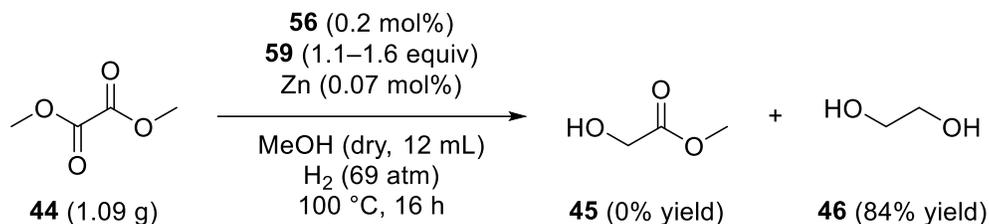
Scheme 1-33. Elsevier's higher TON hydrogenation of **44** with a Ru–Triphos catalyst (**56**+**59**) and Zn.[85]

This greater activity may have resulted by removing the side-reaction between Zn and trace H_2O (eq 1-8). It is also possible that trace H_2O interferes with the formation of the catalyst. Specifically, the ligand **59** is insoluble in H_2O.

$$Zn \ + \ H_2O \ \longrightarrow \ ZnO \ + \ H_2 \quad \textbf{(1-8)}$$

Elsevier and Teunissen examined the hydrogenation of dimethyl phthalate (**60**) to phthalide (**61**) and 1,2-benzenedimethanol (**62**) with their Zn system (Scheme 1-34).[86]
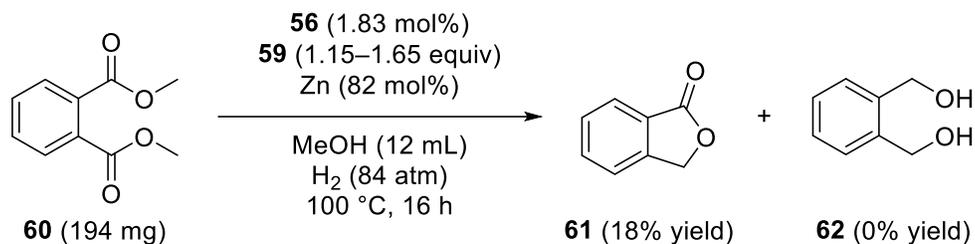
Scheme 1-34. Elsevier's hydrogenation of dimethyl phthalate (**60**) with a Ru–Triphos catalyst (**56**+**59**) and Zn.[86]

The hydrogenation of **60** proceeded with a poor yield of **61** and no **62**.[86] NEt_3 and HBF_4 were screened as promoters for the hydrogenation. Addition of HBF_4 in 2-propanol (*i*PrOH) resulted in complete conversion of **60** to **61** and **62** (Scheme 1-35).[86]
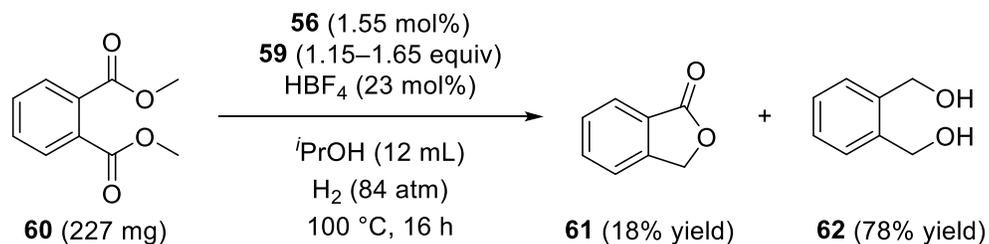
Scheme 1-35. Elsevier's hydrogenation of dimethyl phthalate (**60**) with a Ru–Triphos catalyst (**56**+**59**) and HBF_4.[86]

The highest activity for hydrogenation of benzyl benzoate (**63**) was obtained with NEt$_3$ as additive in 1,1,1,3,3,3-hexafluoro-2-propanol (HFP) (Scheme 1-36).[86]
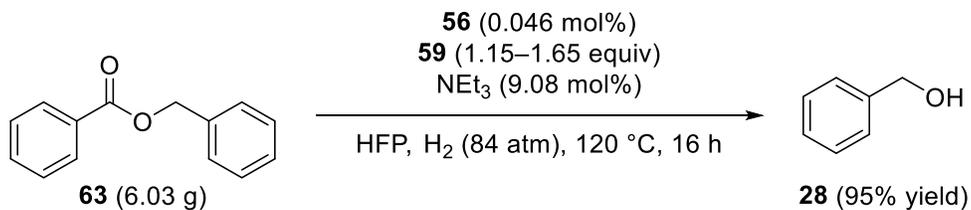
Scheme 1-36. Elsevier's hydrogenation of benzyl benzoate (**63**) with a Ru–Triphos catalyst (**56+59**) and NEt$_3$.[86]

An incredible 2,070 turnovers of **63** was obtained over 16 h (TOF = ~129 h^{-1}).[86] The transesterification of **63** to 1,1,1,3,3,3-hexafluoropropan-2-yl benzoate (**64**) (Scheme 1-37) was not attributed to the remarkable acitivity.[86]
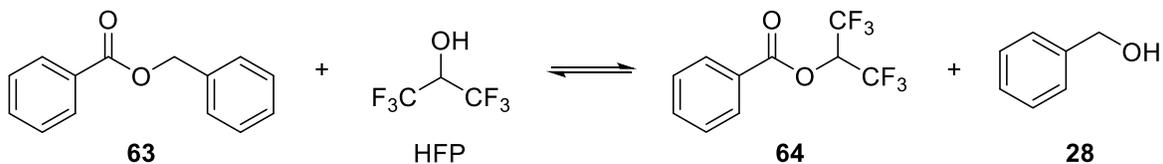
Scheme 1-37. Transesterification reaction of benzyl benzoate (**63**) with 1,1,1,3,3,3-hexafluoro-2-propanol (HFP).

The authors concluded that the high activity was the result of HFP activating the C=O bond by polarization through hydrogen bonding (Figure 1-11).[86] The rates of transesterification were not studied, and the activity is likely the result of both transesterification and polarization.
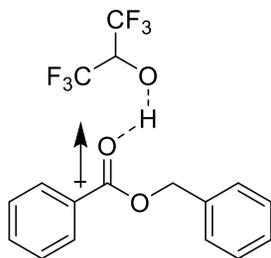
Figure 1-11. Hydrogen bonding between benzyl benzoate (**63**) and 1,1,1,3,3,3-hexafluoro-2-propanol (HFP).

In 2001 and 2002, Nomura and co-workers reported their 10 atm hydrogenations of methyl phenylacetate (**65**).[87, 88] Features of from both Hara's and Elsevier's reports were

investigated. Elsevier's HFP system was the least active (<1 turnover) for the hydrogenation of

65 (2 mol% **56**, 4 mol% **59**, 20 mol% NEt₃, 3 mL HFP, 10 atm H₂, 200 °C).[87] While Hara's

tetraglyme system with Zn was the most active (Scheme 1-38).[87]
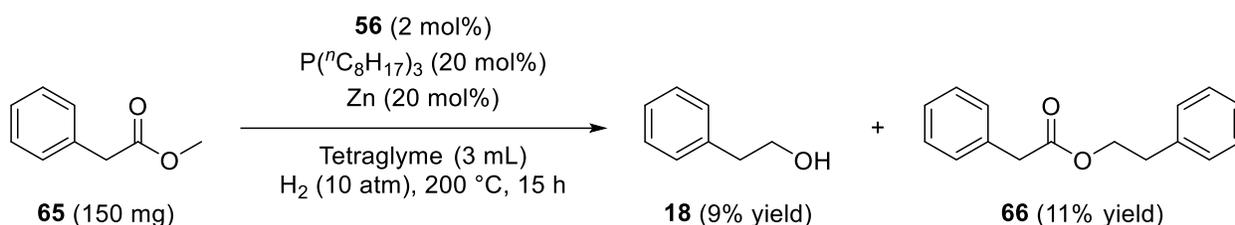
Scheme 1-38. Nomura's 10 atm hydrogenation of methyl phenylacetate (**65**) with a modified Hara's system.[87]

The hydrogenation of **65** yielded **18** (~10 turnovers) and the transesterification product, 2-

phenethyl phenylacetate (**66**). The TON improved to ~24 in xylene at higher concentration of **56**

and with less Zn (2 mol% **56**, 20 mol% P(^{n}C₈H₁₇)₃, 5 mol% Zn, 0.5 mL xylene, 10 atm H₂, 200

°C, 15 h).[87] In their follow-up report, chelating solvents such as 1,2-dimethoxyethane (DME) and

diethylene glycol dimethyl ether (diglyme) gave more favourable results.[88] The hydrogenation in

DME (Scheme 1-39) proceeded with ~67 turnovers over 15 h (TOF = ~4.5 h⁻¹).[88]
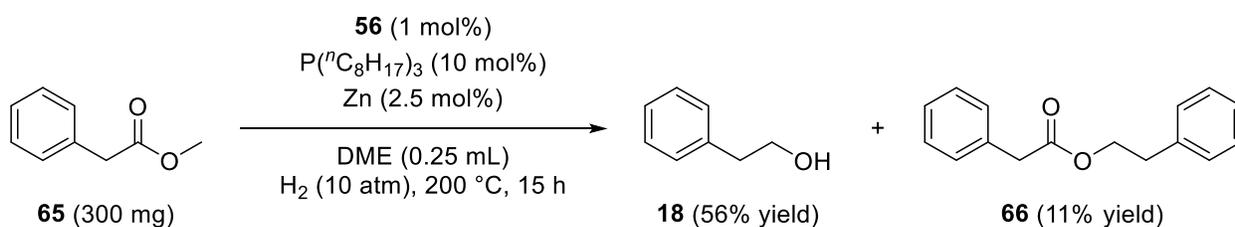
Scheme 1-39. Nomura's 10 atm hydrogenation of **65** with a modified Hara's system in DME.[88]

While in diglyme, the reaction proceeded with ~74 turnovers (60% yield of **18** and 14% yield of

66) in 15 h (TOF = ~4.9 h⁻¹).[88] These results demonstrated for the first time that less reactive

esters could be hydrogenated at 10 atm in fair yield, albeit at 200 °C with an activating additive.

In their 2002 report, Nomura and co-workers considered the mechanism of ester hydrogenations. Based on prior literature,[84] the following catalytic cycle was proposed (Scheme 1-40).[88] The cycle begins with the formation of the Ru–dihydride species **67**. These active catalysts hydrogenate **65** to phenylacetaldehyde (**68**) and then **68** to **18** via hydride transfers.[88] Albeit not discussed or illustrated, **65** likely associates to **67** and then undergoes hydride transfer to form a Ru–hemiacetalate species. This hemiacetalate species undergoes dissociation and the hemiacetal forms **68** and methoxide. The methoxide then fills the open coordination site to form the Ru–methoxide compound **69**. Phenylacetaldehyde (**68**) then undergoes addition with **67** to form the second Ru–alkoxide species **70**. Both **69** and **70** are believed to undergo reductive elimination with ligand association to their respective alcohols and **71**. The oxidative addition of H_2 to **71** reforms the active dihydride species. The authors suggested that the rate-limiting step was the addition of hydride to ester and that the Zn activates the ester via weak coordination.[88] This mechanism, albeit likely the first proposed, is vague as it does not specify whether the ester and aldehyde coordinate to the Ru prior to hydride transfer (inner-sphere mechanism). The hydride transfer may occur without coordination of the ester and aldehyde to the Ru (outer-sphere mechanism), but the former, inner-sphere mechanism, is more probable.

$[Ru(acac)_3]$ + n $P(^nC_8H_{17})_3$ + H_2

56

-3 acac | Δ

L

RuH_2L_n

L = $P(^nC_8H_{17})_3$

n = 3 or 4

67

H_2

RuL_{n+1}

71

MeOH

L

$RuH(OMe)L_n$

69

Ph — (methyl phenylacetate) O / O

65

Ph, O, O $H—RuL_n$ H

Ph, O, H $H—RuL_n$ H

Ph $\diagup$ O H

68

$RuH(OCH_2CH_2Ph)L_n$

70

L

Ph

OH

18

RuL_{n+1}

71

H_2

L

RuH_2L_n

67
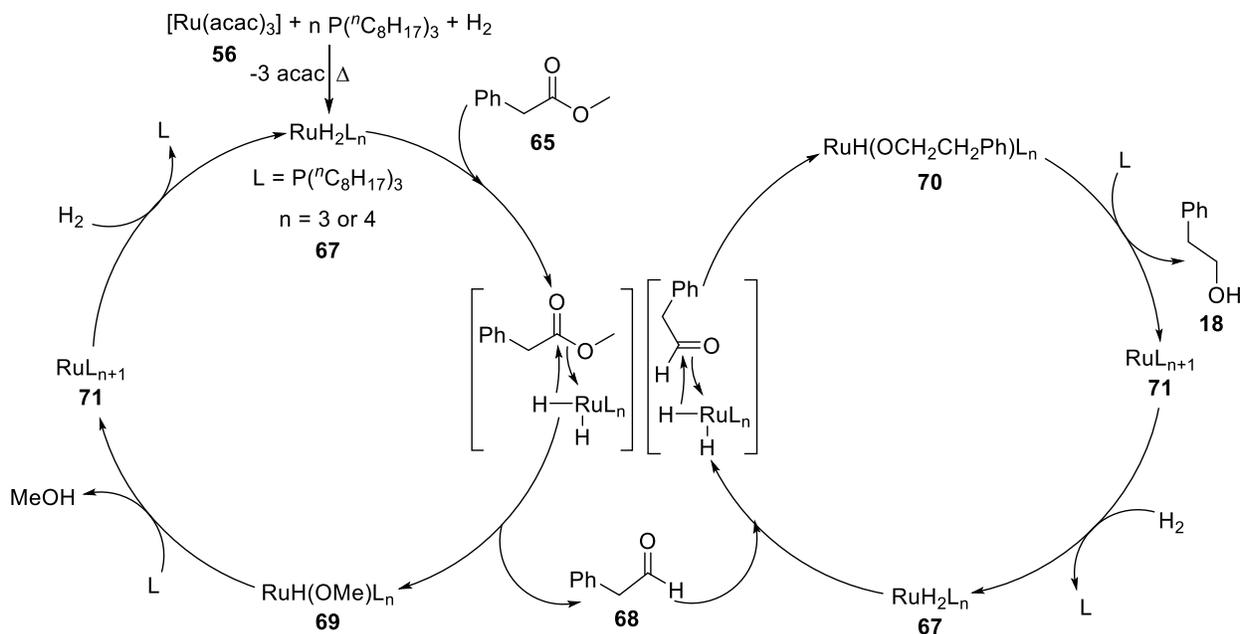
Scheme 1-40. Nomura's proposed mechanism for the catalytic hydrogenation of methyl phenylacetate (**65**).[88]

These early homogeneous systems required either very reactive ester substrates or additives for their activation. Many of the systems also required pressures ≥50 atm H_2 and temperatures ≥100 °C to obtain low to high yields. Although these homogeneous systems generally operated under milder reaction conditions than their heterogeneous counterparts, they did not result in a paradigm shift in ester hydrogenation. A paradigm shift occurred with the introduction of bifunctional ester hydrogenation catalysts.

1.4.2 Bifunctional Catalysts

There are two general types of bifunctional catalysts used for ester hydrogenations. The first type was introduced when Milstein and co-workers reported the hydrogenation of esters with the Ru–NNP pincer complex **72** in 2006. Complex **72** undergoes aromatization–dearomatization processes (Milstein-type) and activates H_2 to generate the *trans*-dihydride **73** (Scheme 1-41).[89]
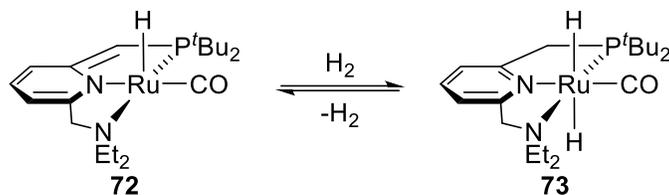
Scheme 1-41. Milstein's Ru–NNP catalyst (**72**) and its reversible reaction with H$_2$.[89]

The strong *trans*-effect of mutually *trans*-positioned hydrides renders them highly nucleophilic.

Several esters were hydrogenated under low pressure and neutral conditions (Scheme 1-42).[89]
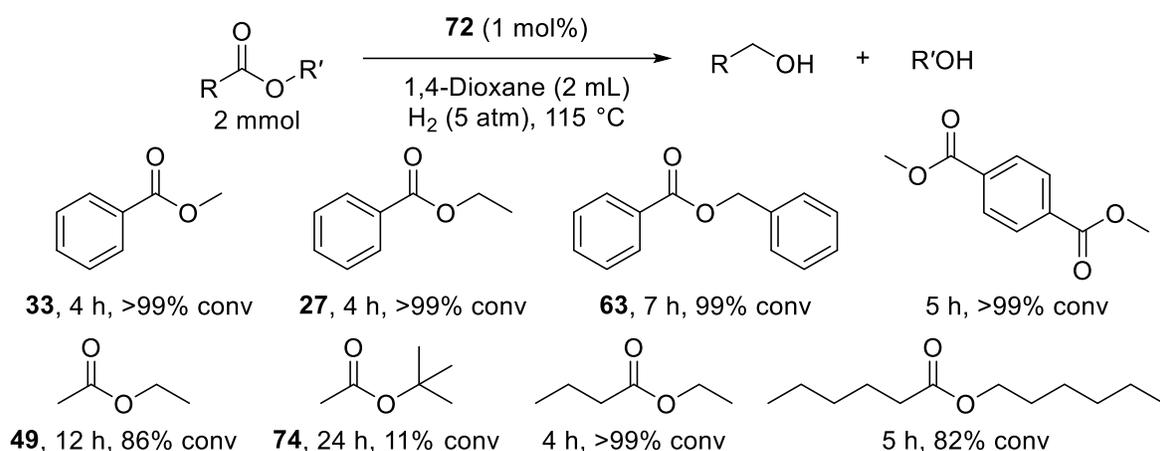
Scheme 1-42. Milstein's hydrogenation of esters under low pressure and neutral conditions with **72**.[89]

The products were the expected primary alcohols, and the yields were only slightly lower (≤3%)

than the conversions.[89] The catalyst provided ~100 turnovers for most esters and the highest TOF

was ~25 h^{-1}. The relatively low conversion of *tert*-butyl acetate (**74**) was attributed to steric

hindrance.[89] Although low pressure and no additives were used, the hydrogenation required 115

°C. Milstein and co-workers proposed mechanism (Scheme 1-43) involves the heterolytic

cleavage of H$_2$ by **72** to form **73**.[89] Complex **73** undergoes dissociative substitution of the

diethylamino group for the ester carbonyl oxygen to form **75**. The coordination of the carbonyl

activates it towards the hydridic ligands on the Ru. The activated carbonyl carbon is attacked by

an adjacent hydride to form the Ru–hemiacetalate complex **76**. The hemiacetalate then

undergoes intramolecular proton transfer to generate **72** and a free hemiacetal that forms the

aldehyde and alcohol. The aldehyde is then hydrogenated via similar process with **73**.
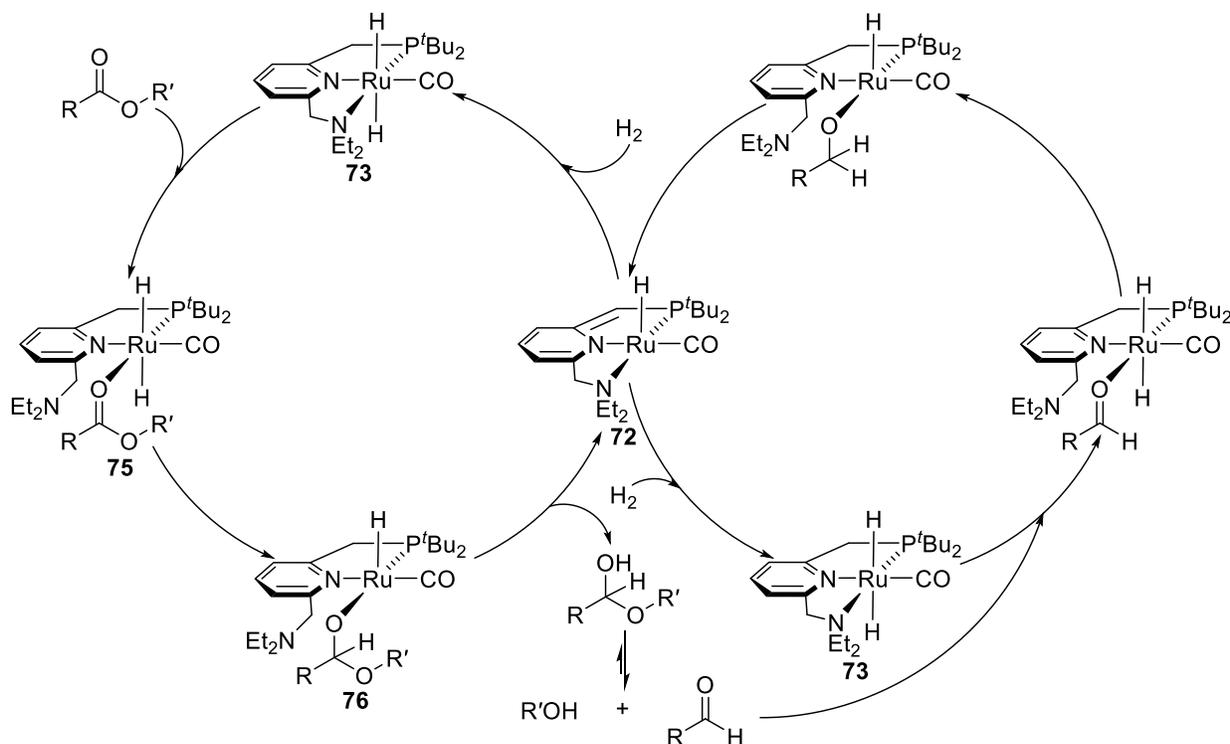
Scheme 1-43. Milstein's proposed mechanism for hydrogenation of esters with **72**.[89]

In the following year Saudan and co-workers, at Firmenich SA, reported three Ru-based

precatalysts for ester hydrogenations (Figure 1-12).[72]
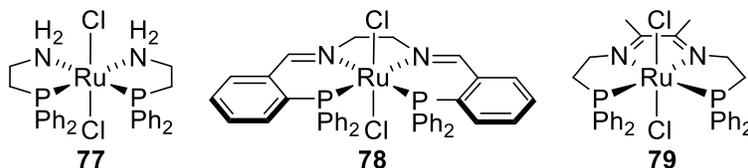
Figure 1-12. Saudan's Ru precatalysts for homogeneous ester hydrogenations.[72]

These precatalysts react with base and H_2 to form *trans*-dihydride catalysts with metal-bound

N–H functionalities (Noyori-type).[72] These catalysts gave significantly higher TONs and TOFs

than all previously published catalysts. For example, the hydrogenation of **33** with **77**, **78** and **79**

provided remarkable results (Scheme 1-44).
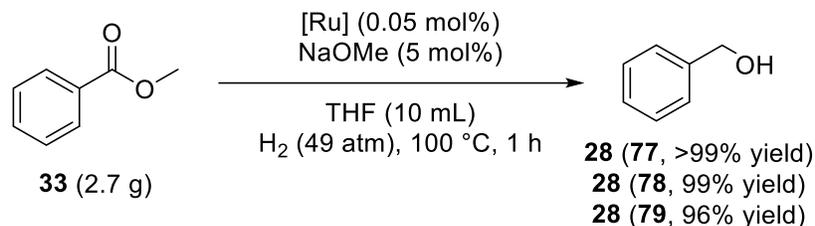
Scheme 1-44. Saudan's highly reactive hydrogenations of methyl benzoate (**33**) with three Ru precatalysts.[72]

Complex **77** was the most active and provided 2,000 turnovers over 1 h (TOF = 2,000 h^{-1}).

Several other alkyl benzoates were examined with **77** and each resulted in 2,000 turnovers over 1

h (TOF = 2,000 h^{-1}).[72] It is possible that all of the alkyl benzoate hydrogenations partially

proceeded through the respective methoxide transesterification product, **33**. Incredibly, the

hydrogenation of isopropyl benzoate (**80**) to **28** proceeded with 10,000 turnovers over 4 h (TOF

= 2,500 h^{-1}).[72]

The chemoselectivities of **77**, **78**, and **79** towards esters with an alkene group (i.e.,

unsaturated esters) were examined. Complex **78** was the most chemoselective, hydrogenating

five unsaturated esters with ≥98% ester selectivity.[72] However, the selectivity of **78** was

significantly lower towards α,β-unsaturated esters (≤12% unsaturated alcohol) and esters with a

terminal alkene (≤35% unsaturated alcohol).[72]

Saudan and co-workers proposed that the ester hydrogenation mechanism was similar to

the classical outer-sphere proton–hydride transfer for ketone hydrogenation.[72] As shown in

Scheme 1-45, the proposed transition state involves hydrogen bonding between the acyl oxygen

of **80** and the protic N–H group of **81**. This renders the acyl carbon susceptible to hydride attack.

After the hydride attack and proton transfer, the classical mechanism proposes that the Ru–amido

complex **82** and the hemiacetal product **83** form. The N-methyl analog **84** did not hydrogenate

esters, supporting an outer-sphere mechanism with an N–H functionality for carbonyl activation.[72]
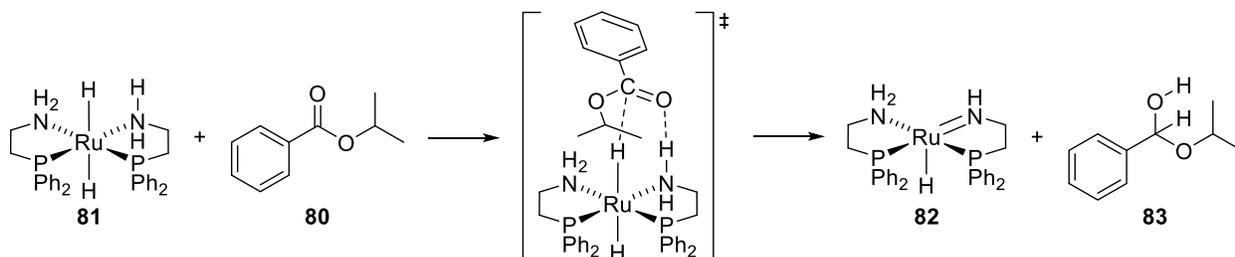
Scheme 1-45. Outer-sphere proton–hydride transfer from **81** to isopropyl benzoate (**80**).

The first intermediates in homogeneous ester hydrogenation were reported by Takebayashi and Bergens.[90] The authors used the Noyori ketone hydrogenation catalyst *trans*-[Ru((R)-BINAP)(H)$_2$((R,R)-dpen)] (**85**) under low pressures and temperatures for their investigation. The activity of **85** with esters was first confirmed with ethyl hexanoate (**86**). The hydrogenation of **86** with **85** was 23% complete (TON = ~14) after 4 h (TOF = ~3.5 h^{-1}) under only 4 atm H$_2$ at -20 °C (60 equiv **86**, 4 equiv K[N(Si(CH$_3$)$_3$)$_2$], THF).[90] The authors then carried out the addition of γ-butyrolactone (**53**) to **85** at -80 °C (Scheme 1-46).[90]
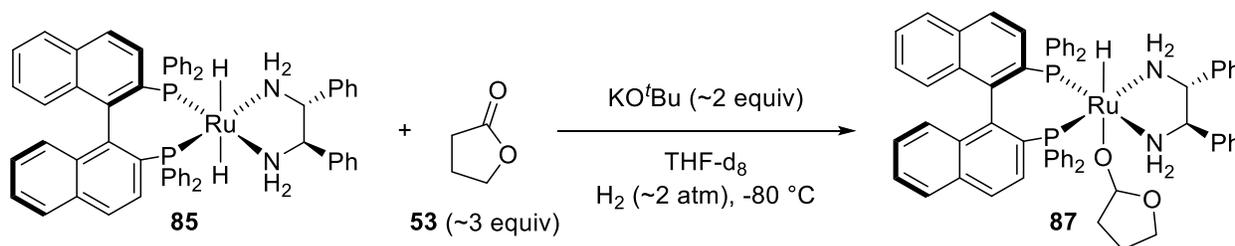
Scheme 1-46. Formation of the Ru–hemiacetaloxide **87** from **85** and γ-butyrolactone (**53**) at -80 °C.[90]

The addition formed the Ru–hemiacetaloxide **87**. Observation of this putative intermediate at -80 °C supports that the bifunctional addition of esters is stepwise. Takebayashi and Bergens also observed that the Ru–amido complex **88** reacts quickly with 2-hydroxytetrahydrofuran (**89**) at -80 °C to also form **87** (Scheme 1-47).[90]

37
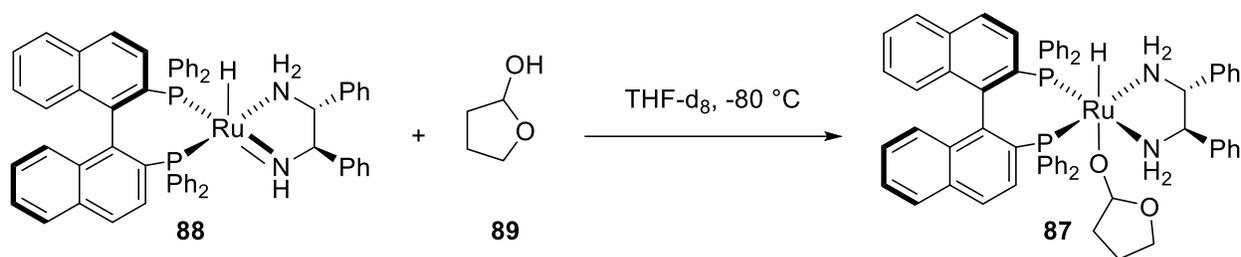
Scheme 1-47. Formation of **87** from Ru–amido complex **88** and 2-hydroxytetrahydrofuran (**89**) at -80 °C.[90]

Based on these observations, the authors proposed that Noyori's catalyst is intrinsically very active towards ester hydrogenation, and that ester hydrogenations are inhibited by alcohol products forming Ru– hemiacetaloxide and alkoxide species.[90] The authors emphasized the importance of base in eliminating these species to regenerate the Ru–amido **88**, which reacts readily with H_2 to form the dihydride **85**.[90, 91] This process is illustrated in Scheme 1-48.
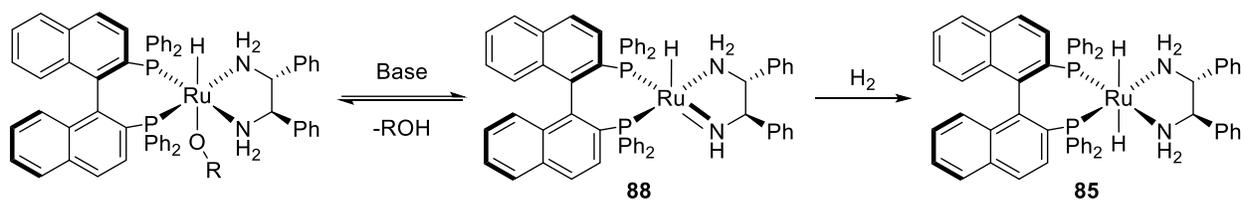
Scheme 1-48. Roles of base and H_2 in reforming the active Ru–dihydride catalyst **85**.[91]

Notably, Takebayashi and Bergens also reported the hydrogenation of eight esters with *trans*-[Ru((*R*)-BINAP)(en)(H)$_2$] (**90**) under very mild reaction conditions.[90] For example, 100 equivalents of **33** were hydrogenated by **90** at 4 atm H_2, 50 °C, over 3 h (9 equiv KO^{t}Bu, 1 mL THF).[90]

Kuriyama and co-workers from Takasago International Corporation, reported their first homogeneous ester hydrogenations in 2009.[92] The authors screened several RuCl$_2$ complexes containing one diamine and one diphosphine ligand for the hydrogenation of **33**. Of the precatalysts examined [RuCl$_2$((*S,S*)-dpen)(dppp)] (**91**) was the most active, giving 485 turnovers of **33** over 3 h (TOF = ~162 h^{-1}) under moderate reaction conditions (Scheme 1-49).[92]
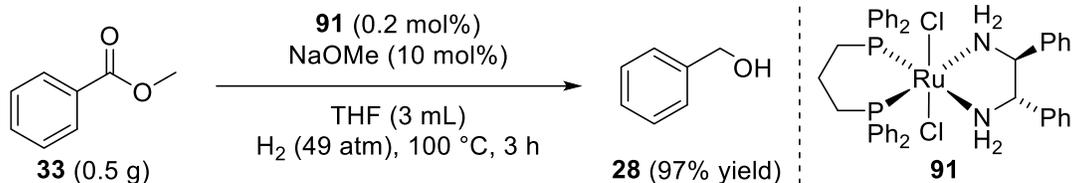
Scheme 1-49. Takasago's hydrogenation of methyl benzoate (**33**) with [RuCl₂((*S*,*S*)-dpen)(dppp)] (**91**).[92]

Kuriyama and co-workers' main interest was not the hydrogenation of **33**, but the hydrogenation of chiral esters to chiral primary alcohols. To avoid base-assisted racemization of their ester substrates, [RuH(η¹-BH₄)((*S*,*S*)-dpen)(dppp)] (**92**) was prepared from **91**.[92] Notably, complex **92** was used to hydrogenate nine chiral esters in excellent yields (≥89%) and with negligible drops in enantiomeric excess (<2% Δee) (Scheme 1-50).[92] Although the yields were excellent and the enantiomeric excesses maintained, the hydrogenations required significantly more catalyst and a longer reaction time (1 mol % **92**, 49 atm H₂, 80 °C, 16 h).[92]
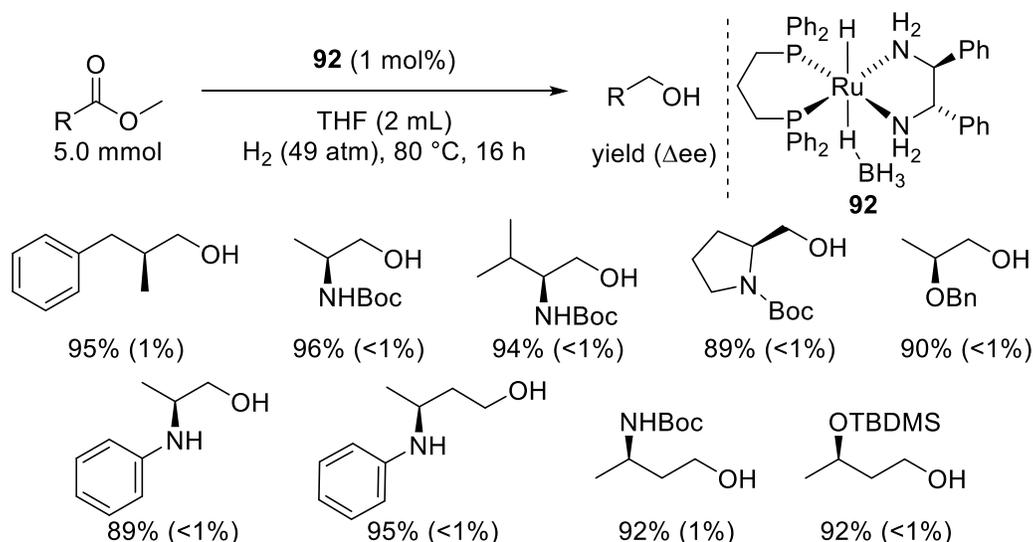
Scheme 1-50. Takasago's base-free hydrogenation of chiral esters to chiral alcohols with **92**.[92]

In the interest of finding a more effective catalyst, Kuriyama and co-workers developed [RuHCl(CO)(HN(CH₂CH₂PPh₂)₂)], which they trademarked as Ru-MACHO® (**93**).[93] Importantly, **93** is less prone to alcohol inhibition and carbonylation.[93] For example, **33** was

hydrogenated to **28** in MeOH (Scheme 1-51). The MeOH solvent did not hinder the reaction, which proceeded in 980 turnovers (98% conv) over 16 h (TOF = ~61.3 h^{-1}). This process is industrially relevant as the MeOH produced from the ester can be recovered with the solvent.[93] Similar to Kuriyama and co-workers previous work, the hydrogenation of **33** was not their main interest.
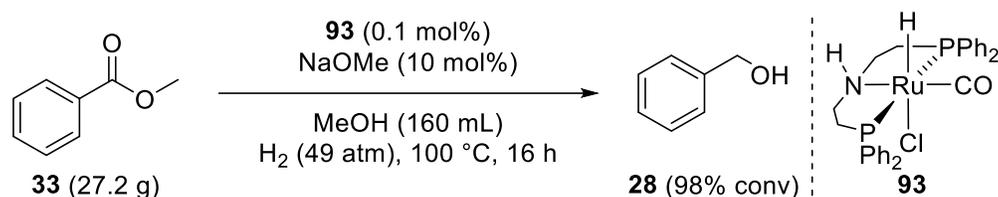
Scheme 1-51. Takasago's hydrogenation of methyl benzoate (**33**) with Ru-MACHO® in MeOH.[93]

Takasago's primary focus was to replace their syntheses of (*R*)-(-)-1,2-propanediol (**94**) and 2-(L-menthoxy)ethanol (**95**). Previously, the synthesis of highly enantioenriched (≥99% ee) **94** involved the asymmetric hydrogenation of hydroxyacetone (**96**), functionalization with *para*-nitrobenzoate (**97**), recrystallization, and work-up (Scheme 1-52).[93]
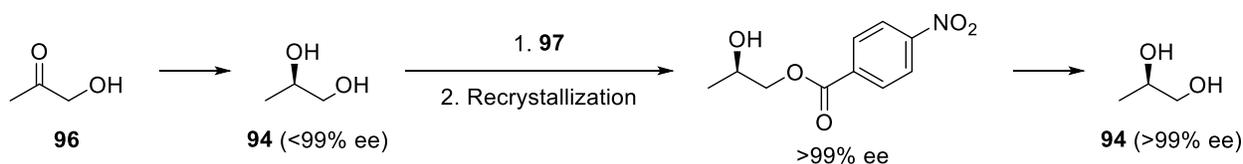
Scheme 1-52. Takasago's recrystallization method for enriching ee of (*R*)-(-)-1,2-propanediol (**94**).[93]

This tedious method was replaced with the hydrogenation of (*R*)-methyl lactate (**98**) to **94** on a megagram scale with **93** (Scheme 1-53).
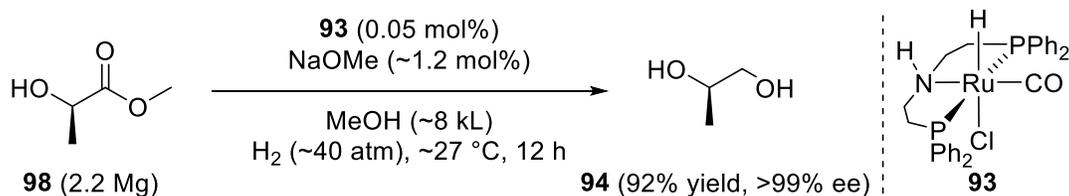
Scheme 1-53. Takasago's megagram-scale hydrogenation of (*R*)-methyl lactate (**98**) with Ru-MACHO®.[93]

40

Remarkably, **93** resulted in 2,000 turnovers over 12 h (TOF = ~166.7 h^{-1}) with only a 0.4%

decrease in ee.[93] The isolated yield of **94** was also excellent at 92% (1,477 kg).[93] The synthesis of

95 previously required a stoichiometric amount of LiAlH₄ and a tedious work-up procedure. This

was replaced by the hydrogenation of methyl L-menthoxyacetate with **93** (0.05 mol% **93**, 20

mol% NaOMe, MeOH, 44 atm H₂, 80 °C, 5 h).[93] Both reactions with **93** demonstrate its

applicability in industry. One notable drawback of this system is its inability to convert a racemic

ester into an enantioenrich product. For example, it would be more advantageous to convert

racemic methyl lactate to enantioenriched **94**.

Clarke and co-workers began reporting homogeneous ester hydrogenations in 2007.[94]

The Ru–NNP complex **99**, which was mainly active towards ketones and aldehydes, was used to

hydrogenate two activated esters under forcing reaction conditions.[94] With this early success,

Clarke and co-workers began screening Ru precatalysts for the hydrogenation of methyl

4-fluorobenzoate (**100**) to 4-fluorobenzylic alcohol (**101**) (Scheme 1-54).[95]
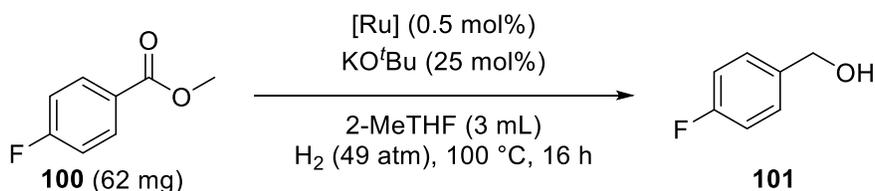
Scheme 1-54. Clarke's precatalyst screening conditions for the hydrogenation of methyl 4-fluorobenzoate (**100**).[95]

The five most active precatalysts, which included **99** and **91**, are shown in Figure 1-13.[95]
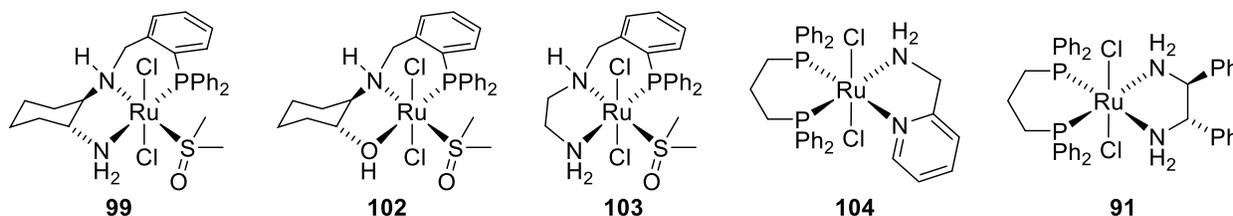
Figure 1-13. Clarke's examined Ru precatalysts that were active towards **100** hydrogenation.[95]

Of these precatalysts, **103**, **104**, and **91** were examined with other α-aryl methyl esters.[95] All three resulted in ~200 turnovers over 16 h (TOF = ~12.5 h^{-1}) under moderate reaction conditions (0.05 mol% precatalyst, 25 mol% KO^{t}Bu, 2-MeTHF, 49 atm H$_2$, 50 °C).[95] This example demonstrates that most modern (post-2006) bifunctional catalysts are gauged by hydrogenation of α-aryl esters. Specifically, α-phenyl esters **27** and **33** are commonly examined as model substrates due to their product **28** having a high boiling point.

Hydrogenations that lead to products with lower boiling points are more difficult to accurately analyze due to product losses during work-up (e.g., solvent removal). For example, shorter straight-chain (<4 carbons) aliphatic esters are not ideal model substrates due to their products' lower boiling points. These losses are also the reason that the product from the ester's alkoxy moiety is generally not shown in reaction schemes.

In 2008, Ito and Ikariya reported that [Cp*RuCl(Ph$_2$PCH$_2$CH$_2$NH$_2$)] (**105**) hydrogenated six esters under moderate reaction conditions (1 mol% **105**, 25 mol% NaOMe, ^{i}PrOH, 50 atm H$_2$, 100 °C).[96] Although good to excellent yields (78–99%) were obtained, the reaction times were not included.[96] In 2011, Ikariya and co-workers reported their screening of bidentate diamine (NN) ligands with [Cp*RuCl(isoprene)] (**106**) for the hydrogenation of phthalide (**61**) to **62** (Scheme 1-55).[97] Out of the ligands examined, the NN ligand 2-picolylamine was the most active (89% yield).[97] The precatalyst [Cp*RuCl(2-picolylamine)] (**107**) hydrogenated 11 lactones to their respective diols (TON = 100) over 18 h (TOF = 5.55 h^{-1}) under moderate reaction conditions (1 mol% **107**, 25 mol% KO^{t}Bu, ^{i}PrOH, 49 atm H$_2$, 100 °C).[97] Ikariya and co-workers also reported the first asymmetric hydrogenation of a lactone via dynamic kinetic resolution (DKR). This DKR will be discussed in the introduction of Chapter 2.
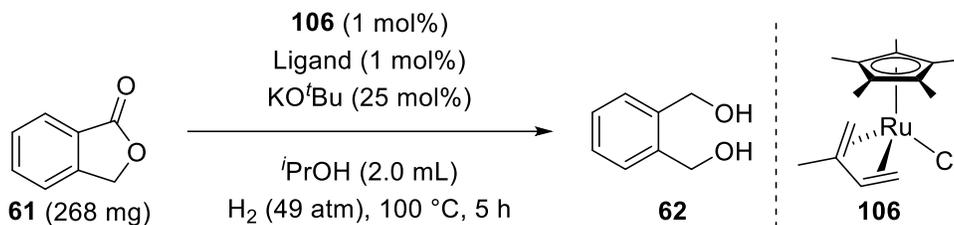
Scheme 1-55. Ikariya's ligand screening conditions for the hydrogenation of phthalide (**61**).[97]

The use of a N-heterocyclic carbene (NHC) ligand in ester hydrogenation was first reported by Morris and co-workers in 2010.[98] The NHC complex [Cp*Ru(NHC-NH$_2$)(py)]PF$_6$ (**108**) catalyzed the hydrogenation of **33** to **28** under mild reaction conditions (Scheme 1-56).[98] Notably, complex **108** resulted in ~345 turnovers (23% conv) over 3 h (TOF = ~115 h^{-1}) under 8 atm H$_2$ at 25 °C.[98] The TON and TOF of **33** to **28** increased (TON = 1,170, TOF = 585 h^{-1}) at higher pressure and temperature (25 atm H$_2$, 50 °C, 2 h).[98]
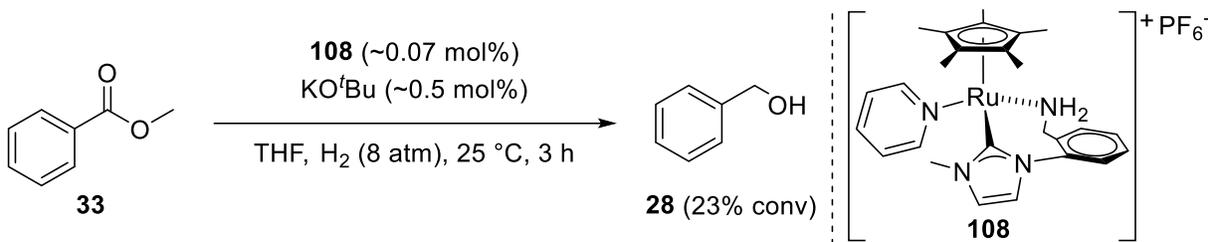
Scheme 1-56. Morris' hydrogenation of methyl benzoate (**33**) under mild reaction conditions with Ru–NHC **108**.[98]

In 2013, O and Morris reported the hydrogenation of 10 esters with **108** and conversions ranged from 6 to 98%.[99] Notably, methyl pivalate (**109**) and **61** were converted to 2,2-dimethyl-1-propanol (**110**) and **62** in 98 and 96% conversions, respectively (50 °C, 4 h).[99] Importantly, the authors also investigated the mechanism using density functional theory (DFT). Their proposed mechanism is illustrated in Scheme 1-57.
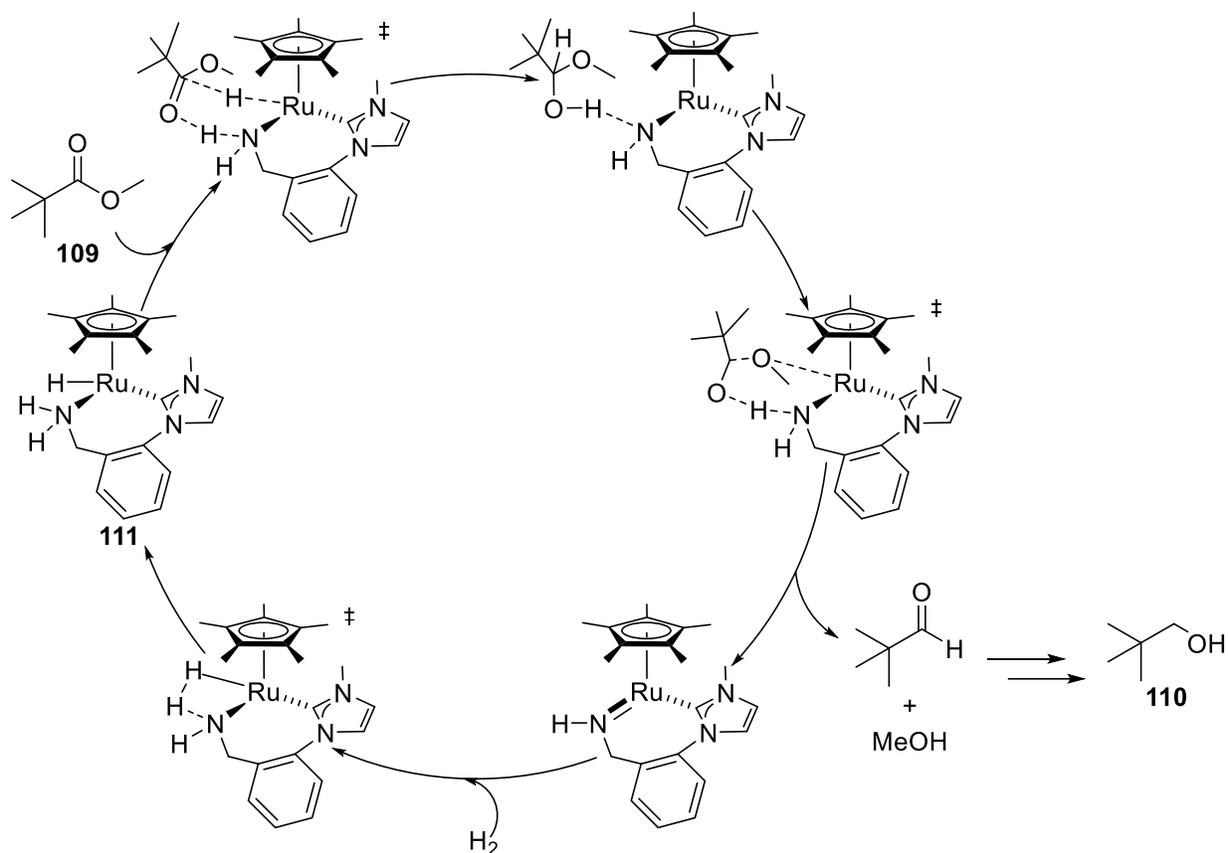
Scheme 1-57. Morris' proposed hydrogenation mechanism with Ru–NHC catalyst **111** and **109** as ester.[99]

The hydrido complex **111** reacts in a bifunctional manner to form a six-membered transition state

with **109** hydrogen bonding with a protic N–H. The hydride and proton are transferred to form a

hemiacetal that is hydrogen bonded to the nitrogen. This hemiacetal then forms a six-membered

transition state with the alkoxy oxygen partially bonded with Ru. The alkoxy C–O bond cleaves,

and a proton is transferred from the amine ligand to give the aldehyde, MeOH, and the

Ru–amido complex. The Ru–amido complex activates H_2 to reform **111** and the aldehyde

undergoes hydrogenation to give the alcohol **110**. In this mechanism, the strong σ-donation by

the NHC ligand presumably renders the *trans*-positioned hydride nucleophilic.

Song and co-workers reported two tridentate Ru–NHC pincer complexes for ester

hydrogenation in 2011.[100] Complex **112** was used to hydrogenate seven esters in excellent

conversions (90 to >99%).[100] For instance, **27** was hydrogenated to **28** in >99% conversion (Scheme 1-58).[100] Although a low pressure (~5 atm) was used, the temperature was high (≥100 °C) and only ~100 turnovers were obtained over 2 h (TOF = 50 h^{-1}). Stoichiometric NMR studies indicated that steps similar to those proposed by Milstein operate during these hydrogenations (Scheme 1-41).[100]
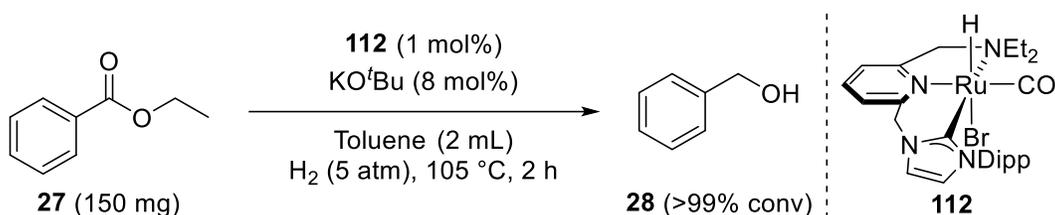
Scheme 1-58. Song's low-pressure hydrogenation of ethyl benzoate (**27**) with Ru–NHC complex **112**.[100]

In the same year, Milstein and co-workers reported their Ru–NHC–bipyridine complex **113** that was used to hydrogenate four less reactive esters under mild pressure.[101] This system used a stoichiometric amount of base to catalyst to obtain a similar conversion (97%) as Song did for the hydrogenation of **27** (Scheme 1-59).[101] Similar to Song's hydrogenation, a low pressure and high temperature were used to obtain 97 turnovers over 2 h (TOF = 48.5 h^{-1}). Notably, a high TON hydrogenation of **27** proceeded with 2,880 turnovers (72% conv) over 12 h (TOF = 240 h^{-1}) under moderate conditions (0.025 mol% **113**, 0.025 mol% KO^{t}Bu, 5 mL toluene, 50 atm H$_2$, 110 °C).[101]
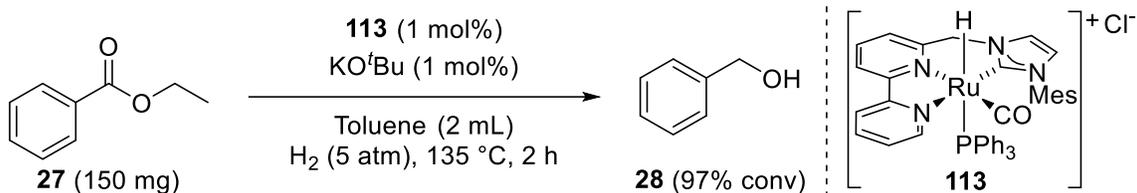
Scheme 1-59. Milstein's hydrogenation of ethyl benzoate (**27**) with Ru–NHC–bipyridine complex **113**.[101]

Milstein and co-workers reported base-free systems with Ru-based PNP **114** and NNP **115** pincer catalysts in 2011 (Figure 1-14).[102]

Figure 1-14. Milstein's Ru-based complexes for base-free ester hydrogenation.[102]

Complex **114** was weakly active towards aliphatic and aromatic esters. For example, the hydrogenation of **63** with **114** resulted in 34 turnovers to **28** (0.5 mol% **114**, 2 mL THF, 10 atm H₂, 110 °C, 12 h).[102] While, the hydrogenation of **63** with **115** (Scheme 1-60) was quantitative (TON = ~200) over 12 h (TOF = ~17 h⁻¹).[102]

Scheme 1-60. Milstein's base-free hydrogenation of benzyl benzoate (**63**) with Ru–NNP complex **115**.[102]

Milstein and co-workers attributed the higher activity of **115** to the greater hemilability of the diethylamino group, which creates a vacant side for ester coordination.[102]

In 2014, Milstein and co-workers synthesized three Ru–NNP complexes that could hydrogenate esters through either the aromatization–dearomatization process (Scheme 1-43) or the N–H activation/transfer process (Scheme 1-45).[103] Of the three precatalysts, the benzyl substituted N–H Ru–NNP precatalyst **116** was the most active, quantitatively hydrogenating aliphatic esters under low pressure (5 atm H₂) and room temperature.[103] For example, the

Milstein and co-workers reported base-free systems with Ru-based PNP **114** and NNP **115** pincer catalysts in 2011 (Figure 1-14).[102]

Figure 1-14. Milstein's Ru-based complexes for base-free ester hydrogenation.[102]

Complex **114** was weakly active towards aliphatic and aromatic esters. For example, the hydrogenation of **63** with **114** resulted in 34 turnovers to **28** (0.5 mol% **114**, 2 mL THF, 10 atm H_2, 110 °C, 12 h).[102] While, the hydrogenation of **63** with **115** (Scheme 1-60) was quantitative (TON = ~200) over 12 h (TOF = ~17 h^{-1}).[102]

Scheme 1-60. Milstein's base-free hydrogenation of benzyl benzoate (**63**) with Ru–NNP complex **115**.[102]

Milstein and co-workers attributed the higher activity of **115** to the greater hemilability of the diethylamino group, which creates a vacant side for ester coordination.[102]

In 2014, Milstein and co-workers synthesized three Ru–NNP complexes that could hydrogenate esters through either the aromatization–dearomatization process (Scheme 1-43) or the N–H activation/transfer process (Scheme 1-45).[103] Of the three precatalysts, the benzyl substituted N–H Ru–NNP precatalyst **116** was the most active, quantitatively hydrogenating aliphatic esters under low pressure (5 atm H_2) and room temperature.[103] For example, the

hydrogenation of methyl hexanoate (**29**) was quantitative (Scheme 1-61). Although active at very

low pressure and room temperature, only ~200 turnovers occurred over 24 h (TOF = ~8.3 h^{-1}).
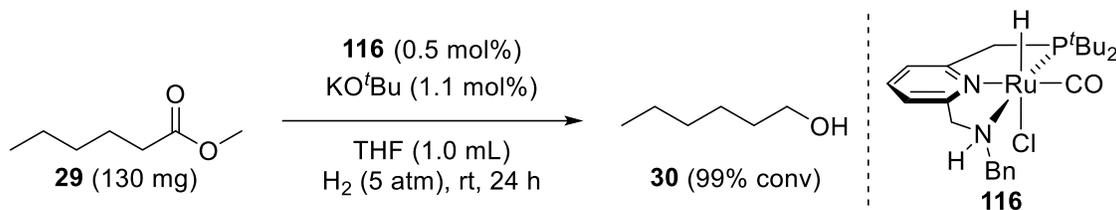
Scheme 1-61. Milstein's low-pressure and room-temperature hydrogenation of methyl hexanoate (**29**) with **116**.[103]

Gusev and co-workers began contributing to the Ru-based homogeneous ester

hydrogenation literature in 2012.[73] The Ru–NNP complex **117** was reacted with base to prepare

the dimeric Ru complex **118** (Scheme 1-62).
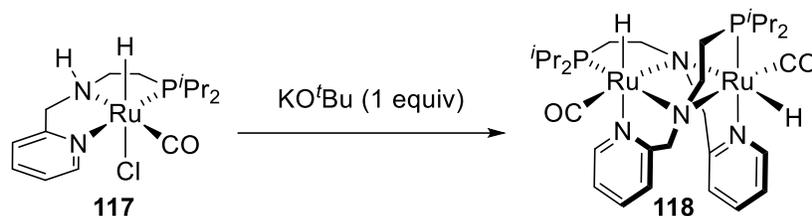
Scheme 1-62. Synthesis of Gusev's dimeric Ru-based ester hydrogenation complex **118**.[73]

Both complexes were active towards the hydrogenation of **33**, but the authors focused on

optimizing with **118** as it did not require added base for hydrogenation.[73] Under optimized

conditions, 18,000 turnovers were obtained over 17 h (TOF = 1,059 h^{-1}) for the hydrogenation of

33 (Scheme 1-63).[73]
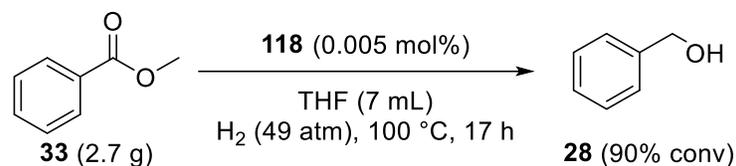
Scheme 1-63. Gusev's optimized hydrogenation of methyl benzoate (**33**) with dimeric Ru complex **118**.[73]

The hydrogenation of the aliphatic ester **29** (Scheme 1-64) resulted in 7,100 turnovers (71% conv) over 18 h (TOF = 394 h^{-1}).[73] Therefore, **118** was highly active for both aromatic and aliphatic esters under neutral conditions. These TONs were substantially higher than previously reported for **29** and **33**.
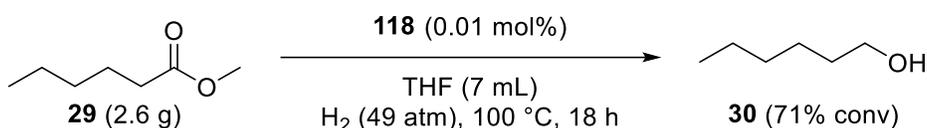
Scheme 1-64. Gusev's optimized hydrogenation of methyl hexanoate (**29**) with dimeric Ru complex **118**.[73]

Gusev and co-workers reported the air-stable Ru–NNP complex **119** in 2012.[74] Complex **119** was used for the hydrogenation of five esters. For example, the hydrogenation of **33** (Scheme 1-65) proceeded with 3,920 turnovers (98% conv) over 16 h (TOF = 245 h^{-1}) under 49 atm H$_2$ at 40 °C [74] Notably, the hydrogenation of the aliphatic ester **29** proceeded with 18,800 turnovers (94% conv) over 18 h (TOF = 1,044 h^{-1}) with a 0.005 mol% loading of **119**.[74] The drawbacks to these reactions are the moderate pressure, added base, and reaction times.
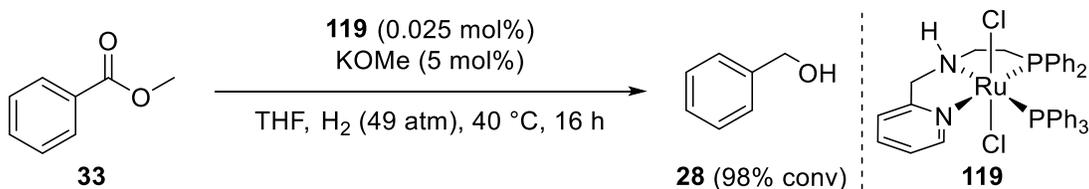
Scheme 1-65. Gusev's hydrogenation of methyl benzoate (**33**) with air-stable Ru–NNP complex **119**.[74]

In 2013, Gusev and co-workers reported four Ru–SNS complexes for ester hydrogenation (Figure 1-15).[104]
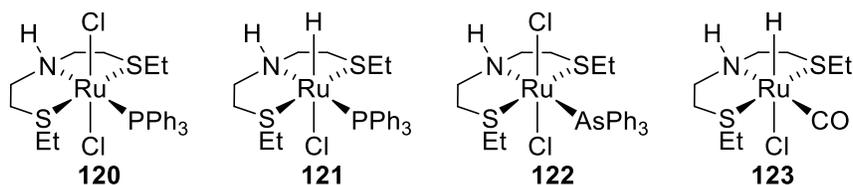
Figure 1-15. Gusev's Ru–SNS complexes for ester hydrogenation.[104]

Complexes **120** and **121** were more active than **72**, **77**, and **93** for the hydrogenations of **29** and **33**.[104] A variety of esters were effectively hydrogenated with **120**. For example, the hydrogenation of **29** resulted in 9,800 turnovers over 2 h (TOF = 4,900 h^{-1}) under 49 atm H_2 at 100 °C (Scheme 1-66).[104]
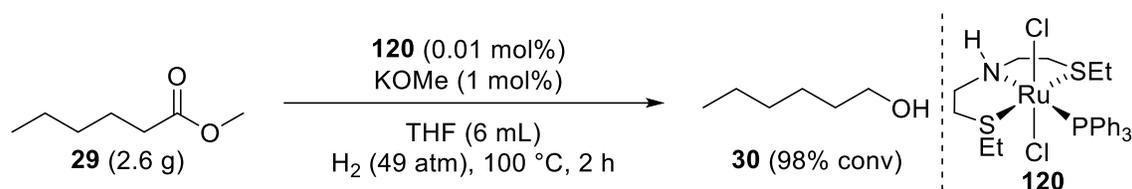
Scheme 1-66. Gusev's highly active hydrogenation of methyl hexanoate (**29**) with Ru–SNS complex **120**.[104]

Gusev and co-workers discovered that when **121** reacts with NaOEt in EtOH and the resulting complex **124** is heated in toluene the *cis*-dihydride **125** forms (Scheme 1-67).[104]
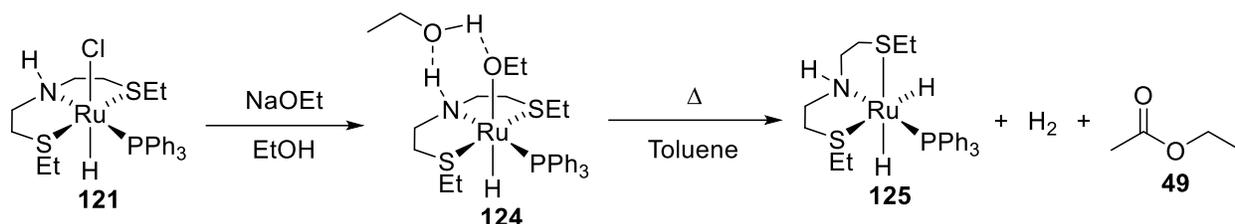
Scheme 1-67. Gusev's synthesis of the *cis*-dihydride–Ru–SNS complex **125**.[104]

The other products formed are ethyl acetate (**49**) and H_2. Based on microscopic reversibility, the *cis*-dihydride species **125** is believed to be the active ester hydrogenation catalyst in these systems.[104]

In 2016, Gusev reported the Ru–NNP complex **126** that was active (95% conv) and chemoselective (97% selectivity) towards the hydrogenation of methyl 10-undecenoate (**127**) to 10-undecen-1-ol (**128**) (Scheme 1-68).[105] This reaction is notable, as the terminal olefin was not significantly hydrogenated (2% saturated alcohol) by the catalyst.

49
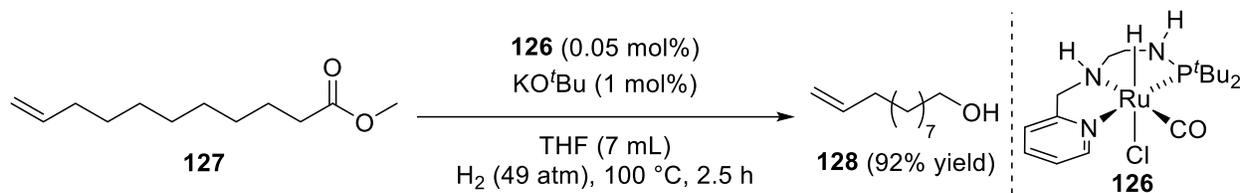
Scheme 1-68. Gusev's chemoselective hydrogenation of the ester of methyl 10-undecenoate (**127**) with **126**.[105]

In 2014, Zhou and co-workers reported three tetradentate bipyridine–Ru precatalysts for ester hydrogenation.[106] Complex **129** was an incredibly efficient precatalyst for the hydrogenation of γ-valerolactone (**130**) to 1,4-pentanediol (**131**) (Scheme 1-69). Under optimized conditions, 91,000 turnovers was obtained over 48 h (TOF = ~1,900 h^{-1}).[106] Complex **129** also hydrogenated 18 other esters with excellent results. For instance, 91,000 turnovers were obtained for the hydrogenation of **33** over 64 h (TOF = 1,400 h^{-1}) under 100 atm H$_2$ at 25 °C (0.001 mol% **129**, 10 mol% NaOMe, 20.0 mL ^{i}PrOH, 64 h).[106] To the best of my knowledge, this is the highest TON for a homogeneous hydrogenation of **33** in the literature, albeit with a large excess of base and under 100 atm H$_2$.
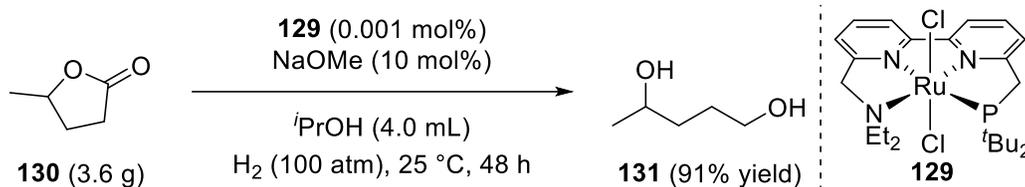
Scheme 1-69. Zhou's high TON and TOF hydrogenation of γ-valerolactone (**130**) with Ru–NNNP complex **129**.[106]

In the same year, Pidko and co-workers reported their bis-NHC Ru–CNC complexes that were modestly active towards ester hydrogenation.[107] For example, the bis-NHC Ru–CNC complex **132** hydrogenated **33** with 194 turnovers over 4 h (TOF = 48.5 h^{-1}) under 49 atm H$_2$ at 70 °C (Scheme 1-70).[107] Although not incredibly active, these are among the very few examples of phosphorus-free ester hydrogenation catalysts.
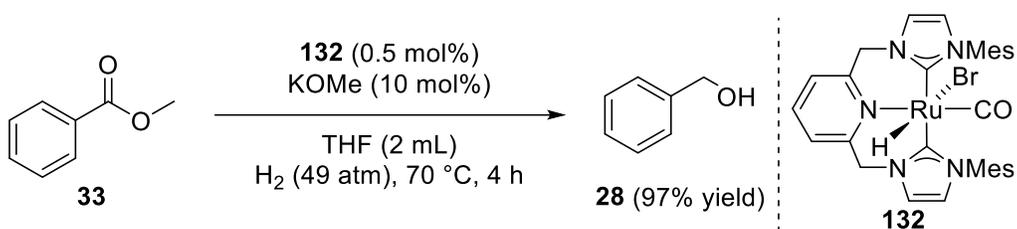
Scheme 1-70. Pidko's hydrogenation of methyl benzoate (**33**) with bis-NHC Ru–CNC complex **132**.[107]

In the following year, Pidko and co-workers reported the active Ru–CNC dimer **133** for

ester hydrogenation.[108] For instance, complex **133** hydrogenated the aliphatic ester **86** with

79,680 turnovers over 16 h (TOF = 4,980 h^{-1}) under 49 atm H$_2$ at 70 °C (Scheme 1-71).[108]

Complex **133** is less active towards aromatic esters, with 9,370 turnovers for the hydrogenation

of ethyl benzoate (**27**) over 16 h (TOF = ~586 h^{-1}).[108] Complex **133** was a significant

improvement to Ru–CNC precursors for ester hydrogenation. This improvement is likely due to

the bis-NHCs and the N–H functionality.
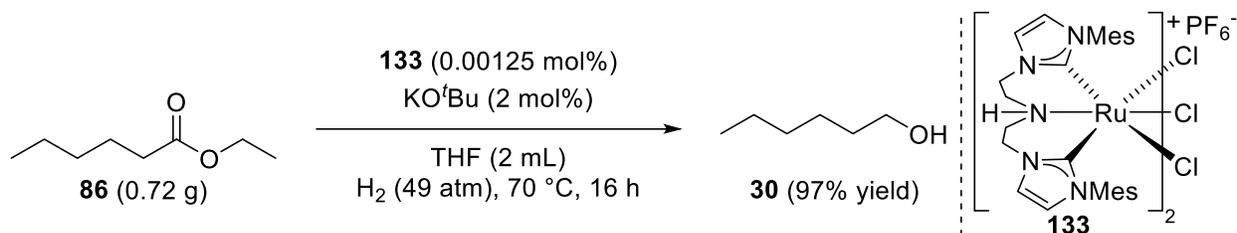
Scheme 1-71. Pidko's high TON and TOF hydrogenation of ethyl hexanoate (**86**) with Ru–CNC dimer **133**.[108]

An exceptionally stable and active Ru-based ester hydrogenation catalyst was reported by

Zhang and co-workers in 2015.[109] The authors devised and used a tetradentate PNNP ligand that

contained both Milstein's aromatization–dearomatization functionality (Scheme 1-41) and

Firmenich's PPh$_2$–N–H functionality (Figure 1-12).[109] The Ru–PNNP complex **134** hydrogenates

a wide variety of aliphatic and aromatic esters in high yields (>80%).[109] The hydrogenation of **33**

(Scheme 1-72) proceeded in 49,000 turnovers over 5 h (TOF = 9,800 h^{-1}).[109]
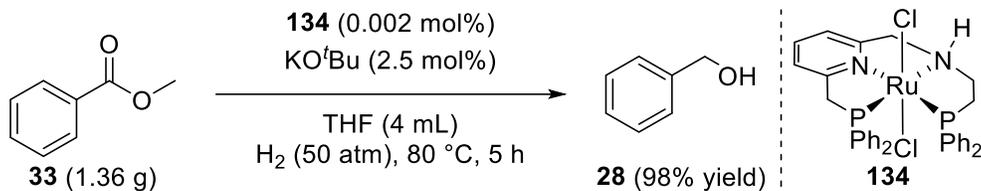
Scheme 1-72. Zhang's high TON and TOF hydrogenation of methyl benzoate (**33**) with Ru–PNNP complex **134**.[109]

Although moderate pressure (50 atm H₂) and temperature (80 °C) were used, this is, to the best

of my knowledge, the highest TOF for the homogeneous hydrogenation of **33** in the literature.[109]

Complex **134** was also highly active towards the hydrogenation of fatty acid methyl esters. For

example, 54.1 g of methyl palmitate (**135**) was hydrogenated to cetyl alcohol (**136**) with 6.9 mg

of **134** (Scheme 1-73).[109] Notably, 20,000 turnovers of **135** occurred over 5 h (TOF = 4,000 h⁻¹).
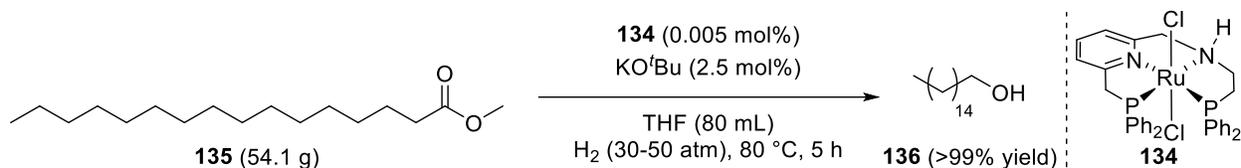
Scheme 1-73. Zhang's high TON and TOF hydrogenation of methyl palmitate (**135**) with **134**.[109]

In 2017, Sun and co-workers reported their Ru–NNP precatalyst **137**.[110] The

hydrogenation of **33** with **137** (Scheme 1-74) proceeded with 1,980 turnovers of **33** over 4 h

(TOF = 495 h⁻¹).[110] Although this system is not as active as aforementioned systems, it is notable

that NaBH₄ gave higher activity than alkoxide bases. It was found that **137** reacts with NaBH₄ to

form an η¹-BH₄ complex that helps form the active catalytic *trans*-dihydride species.[110]
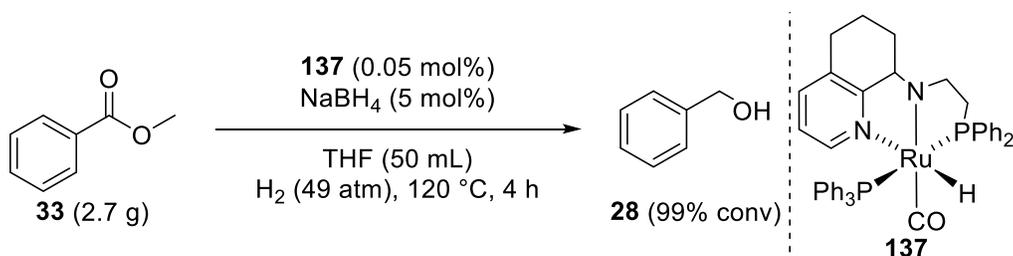
Scheme 1-74. Sun's hydrogenation of methyl benzoate (**33**) with Ru–NNP precatalyst **137** and NaBH₄.[110]

In 2016, Chianese and co-workers reported two Ru–CNN pincer complexes that did not contain a methylene linker between the pyridine and NHC functionalities (Figure 1-16).[111]
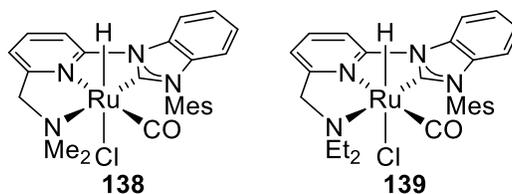
Figure 1-16. Chianese's Ru–CNN pincer complexes for ester hydrogenation.[111]

The ethyl substituted complex **139** was more active than **138** towards **27** (Scheme 1-75).[111]
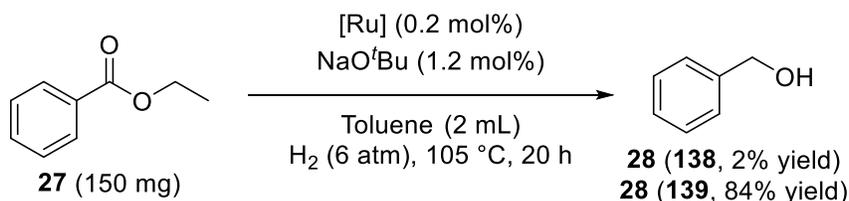
Scheme 1-75. Chianese's hydrogenation of ethyl benzoate (**27**) with Ru–CNN complexes **138** and **139**.[111]

Chianese and co-workers attributed the activity difference to the dissociation of the alkyl amino groups.[111] Complex **139** was examined for the hydrogenation of several other esters. Complex **139** was relatively inactive towards methyl esters, but MeOH did not poison the catalyst.[111]

Chianese and co-workers have since synthesized a library of similar Ru–CNN complexes and found that the 2,6-diisopropylphenyl (Dipp) complex **140** was the most active.[112] Complex **140** gave good results for the hydrogenation of both aliphatic and aromatic esters.[112] For instance, **27** was hydrogenated (Scheme 1-76) in 1,960 turnovers over 20 h (TOF = 98 h^{-1}) at low pressure (6 atm) and high temperature (105 °C).[112] It is unclear why the Dipp group of **140** results in higher catalyst activity than the mesitylene (Mes) group in **139**.
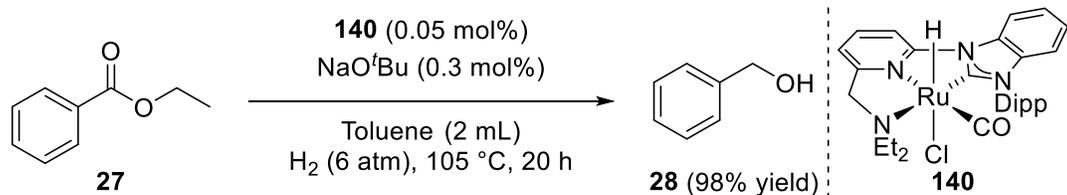
Scheme 1-76. Chianese's hydrogenation of ethyl benzoate (**27**) with Ru–CNN–Dipp complex **140**.[112]

In 2019, Chianese and co-workers eliminated the need for added base by reacting their Ru–CNN precatalysts with base and monodentate phosphines to produce Ru–CC precursors.[113] For example, complex **141** is prepared from **140**, tricyclohexylphosphine (**142**), and NaO^{t}Bu (Scheme 1-77).[113]
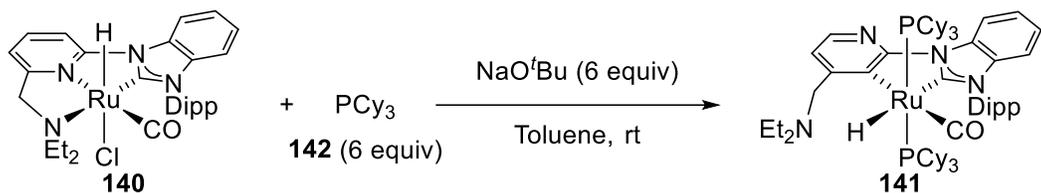
Scheme 1-77. Chianese's synthesis of Ru–CC precursor **141** from Ru–CNN precursor **140**.[113]

Complex **141** was the most active Ru–CC precursor and provided 990 turnovers of **27** over 20 h (TOF = 49.5 h^{-1}) without base (Scheme 1-78).[113]

Scheme 1-78. Chianese's base-free hydrogenation of ethyl benzoate (**27**) with Ru–CC–Dipp complex **141**.[113]

Although not as active as the Ru–CNN complexes, enantioenriched esters were hydrogenated without significant losses in enantiomeric excess (ee). For example, (*S*)-ethyl ibuprofen (**143**) was hydrogenated to (*S*)-2-(4-isobutylphenyl)propan-1-ol (**144**) with less than 2% loss in ee (Scheme 1-79).[113]
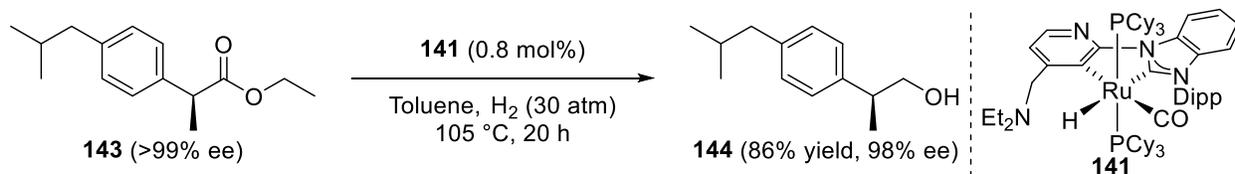
Scheme 1-79. Chianese's base-free hydrogenation of (*S*)-ethyl ibuprofen (**143**) with Ru–CC–Dipp complex **141**.[113]

Chianese and co-workers also synthesized five-coordinate Ru(0)–imine complexes that are extremely active for ester hydrogenation (Figure 1-17).[114]
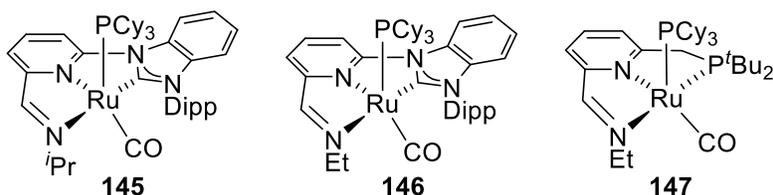
Figure 1-17. Chianese's Ru(0)–imine complexes for ester hydrogenation.[114]

The complexes' Ru(0) is presumably stabilized by their tridentate ligands, a tricyclohexylphosphine, and carbonyl group. Complex **147**, derived from Milstein's **72**, was the most active. For example, the hydrogenation of **33** with **147** resulted in 15,520 turnovers over 16 h (TOF = 970 h^{-1}) under base-free conditions at room temperature (0.00625 mol% **147**, ^{i}PrOH, 30 atm H$_2$).[114] This is a massive improvement to the 100 turnovers obtained with **72** over 4 h (Scheme 1-42). The chiral ester **143** was hydrogenated with less than 2% loss in ee (Scheme 1-80).[114] This remarkable discovery, of active Ru(0) complexes, could possibly be applied to other similar pincer-type complexes, such as **112**, **116**, and **129**.
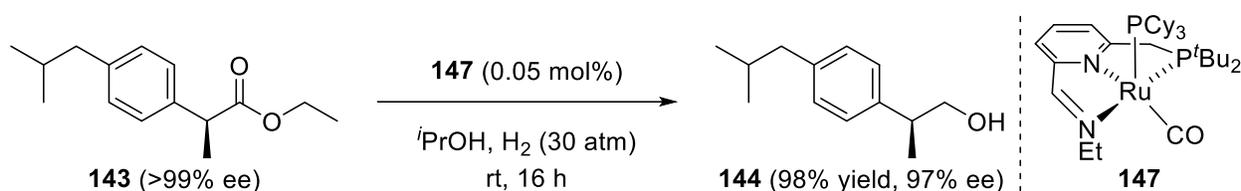
Scheme 1-80. Chianese's active and base-free hydrogenation of (*S*)-ethyl ibuprofen (**143**) with complex **147**.[114]

Overall, the homogeneous hydrogenation of esters with Ru-based complexes has developed substantially since the seminal papers by Milstein and Saudan. A wide variety of esters can be hydrogenated with high TON, TOF, and chemoselectivity with the homogeneous bifunctional catalysts. Several of these active Ru-based systems (e.g., Firmenich SA's catalysts from Figure 1-12) are used in industrial productions. The hydrogenation of esters with other metals has received far less attention and will now be shortly discussed.

1.5 Homogeneous Hydrogenation of Esters with Non-Ru-Based Catalysts

The homogeneous hydrogenation of esters has been reported with precious metal complexes other than Ru, such as Os,[73, 115, 116] and Ir[117-121] (Figure 1-18). The Os-based complexes generally give good TON (>1,000) and can be uniquely chemoselective for ester hydrogenations. Specifically, Gusev's 2015 Os-based complex gives excellent chemoselectivity for ester hydrogenation over alkene hydrogenation (18 examples with >95% selectivity).[116] The Ir-based complexes give far less activity (TON = ≤500), but can operate without base[118] and hydrogenate lactones enantioselectively.[119-121]
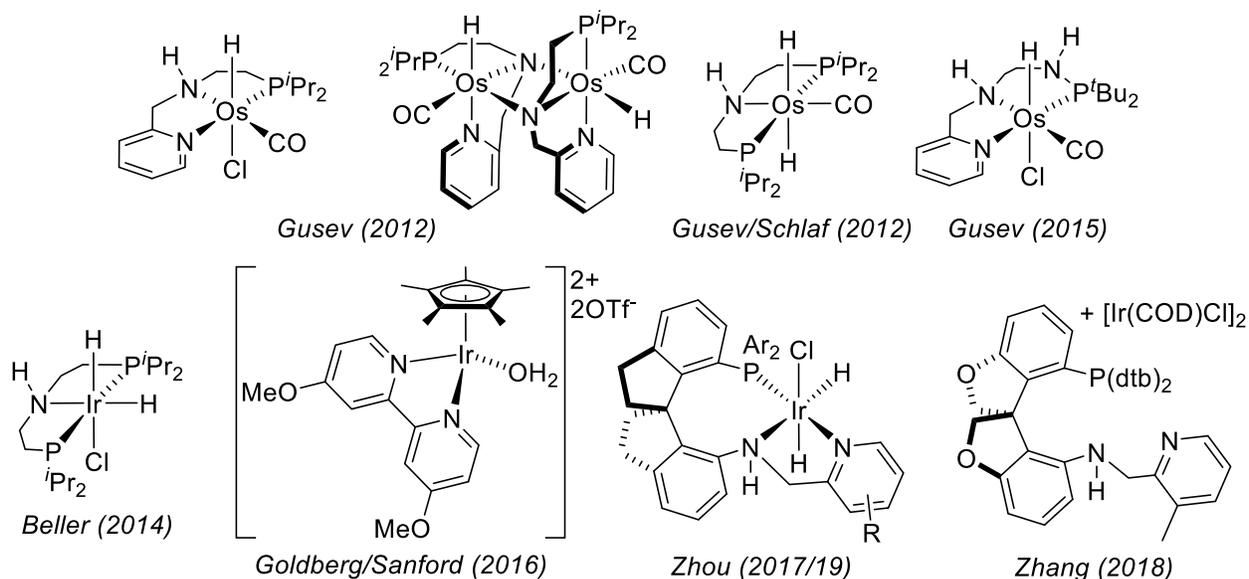
Figure 1-18. Non-Ru precious metal complexes for ester hydrogenation.

56

Non-precious metal complexes containing Mn,[122-127] Fe,[128-132] or Co[133-137] have also been reported for ester hydrogenation (Figure 1-19). These systems use earth-abundant metals but are generally less active than the precious metal systems. The Mn-based complexes usually give low TON (<100) even with long reaction times (≥16 h). Clarke's Mn-based complex is the exception as it gives up to 1,000 turnovers and is used to produce β-chiral alcohols from α-chiral esters.[126] The Fe-based systems also typically give low activity (TON = <100). The exception being Milstein's Fe-based system giving 1,280 turnovers of the fluorinated ester **43**.[128] Notably, Guan and Beller's Fe-based systems hydrogenate esters without added base.[129-131] Most of the Co-based complexes are less active (TON = <50). Notably, a Co-based system by Jones and co-workers operates without added base and gives ~4,000 turnovers for the hydrogenation of the lactone **130** over three days.[135]
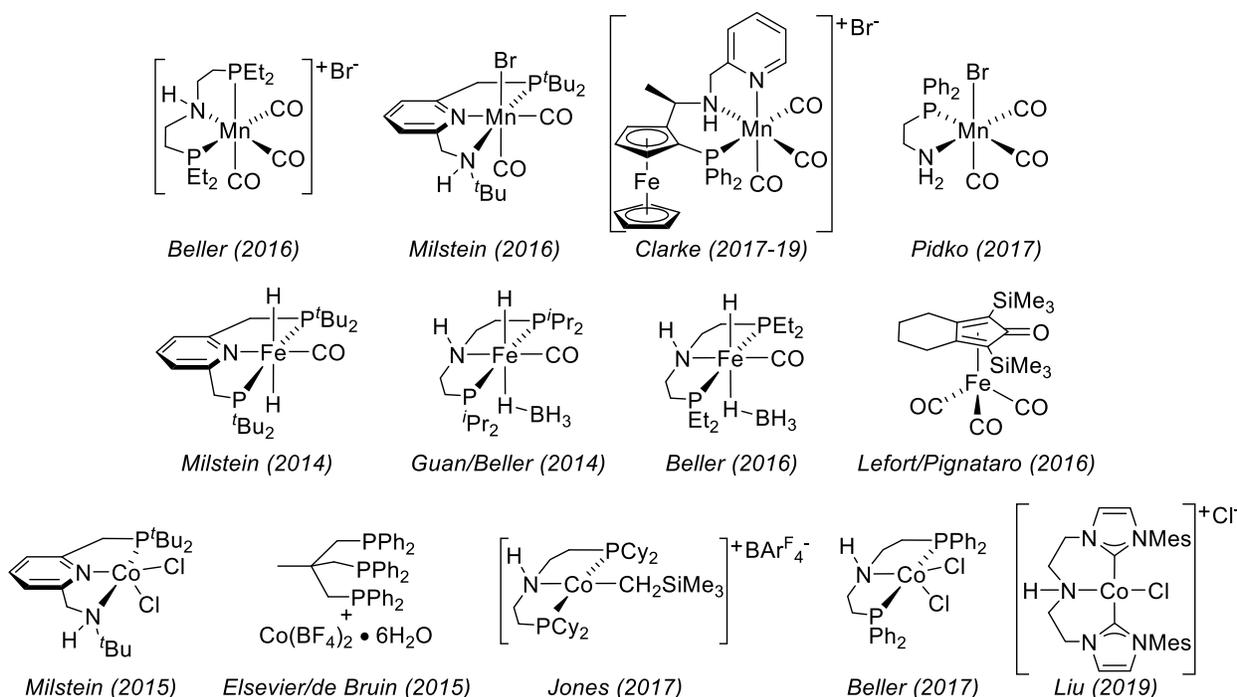
Figure 1-19. Non-precious metal complexes for ester hydrogenation.

Non-Ru-based homogeneous systems are currently less than a decade old and the area is still rather underdeveloped. In time earth-abundant systems may reach the activity and chemoselectivity of Ru-based systems. For further information on ester hydrogenations please consult the publications cited and the relatively recent reviews by Beller[138] and Pidko.[139]

1.6 Research Objectives

The introduction has covered the activity of esters, their stoichiometric reductions, and hydrogenations. Although several ester hydrogenation systems have been developed, the production of highly enantioenriched alcohols has relied on the usage of enantioenriched esters, as demonstrated by Kuriyama,[92, 93] Chianese,[113, 114] and Clarke.[126] Inspired by the Bergens group's recent success for the asymmetric hydrogenation of amides,[140] I speculated that a system could be discovered for the asymmetric hydrogenation of racemic esters to highly enantioenriched alcohols.

The discovery and development of hydrogenation systems is a time-consuming process, as it is limited by the number of pressure vessels available for reactions. To expedite this process, the Bergens group previously used a high-throughput screening facility. Although effective, this method was expensive.

For my primary project, I was tasked with discovering and developing a system for asymmetric hydrogenation of acyclic esters without the use of a high-throughput screening facility. To facilitate discovery and development, an in-house screening method for multiple simultaneous hydrogenations was created. Chapter 2 presents my in-house hydrogenation screening method and its application in the discovery of an asymmetric hydrogenation of acyclic esters.

Following this discovery, I was given another challenging project. The integration of photocatalysis with catalytic hydrogenation is underexplored. Encouraged by the Bergens group's recent work with polypyridyl complexes[141] and hydrogenation systems,[140, 142-144] I hypothesized that a dual-catalytic photohydrogenation system could be created. Chapter 3 introduces the ideology of these systems and syntheses for this project. Chapter 4 presents the preliminary photohydrogenation trials.

Chapter 2:

Asymmetric Hydrogenation of Esters via Dynamic Kinetic Resolution[*][145]

2.1 Introduction

The catalytic hydrogenation of esters is an excellent alternative to stoichiometric reductions, as demonstrated in Chapter 1. The production of highly enantioenriched alcohols from ester hydrogenations has relied on converting enantioenriched esters without significant loss of enantiomeric excess (ee).[92, 93, 113, 114, 126] A more efficient approach is a system that utilizes asymmetric hydrogenation via dynamic kinetic resolution (DKR) to give high yields of enantioenriched alcohols from racemic esters.

Asymmetric hydrogenation is the stereoselective addition of H_2 across an unsaturated bond. The stereoselectivity is driven by a chiral feature in the system (i.e., substrate, reagent, catalyst, or solvent). When a stereoselective addition occurs on a racemic mixture (1:1) of enantiomers the process is known as kinetic resolution (KR). A Gibbs free energy diagram of an exergonic KR favouring the S isomer is shown in Figure 2-1. In KR, the substrate (S) exists as two enantiomers (R and S) of equal energy. The reaction rate for each substrate (S_R, S_S) is dependent on its respective activation energy ($\Delta G_R^{\ddagger}$, $\Delta G_S^{\ddagger}$) to form a diastereomeric transition state (TS). The difference in activation energy between the diastereomeric transition states ($\Delta\Delta G^{\ddagger}$) is therefore related to the difference in reaction rates. In Figure 2-1, the activation energy for the R isomer is higher ($\Delta G_S^{\ddagger} < \Delta G_R^{\ddagger}$) and thus the S isomer reacts faster. Although an

enantioenriched mixture can be produced from KR, the maximum theoretical yield of a perfectly

stereoselectivity reaction is only 50%. On the other hand, DKR can provide enantioenriched

mixtures with yields greater than 50%.
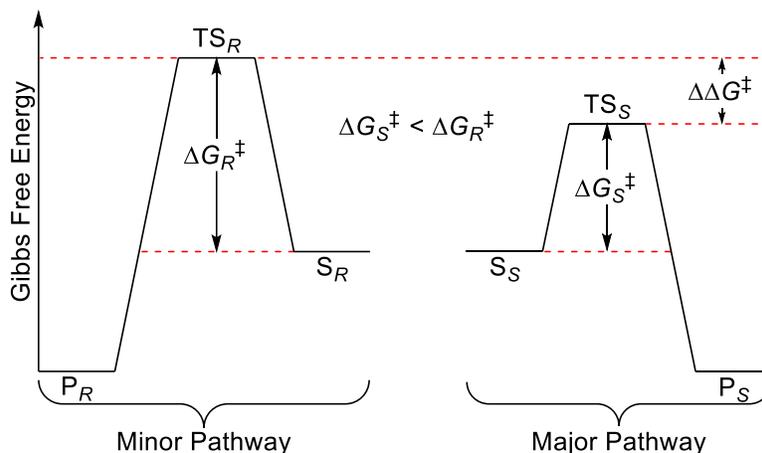
Figure 2-1. Gibbs free energy diagram of an exergonic kinetic resolution favouring the *S* enantiomer.

DKR is analogous to KR but includes relatively rapid racemization between the substrate

enantiomers. A Gibbs free energy diagram of an exergonic DKR favouring the *S* isomer is shown

in Figure 2-2. Racemization, the dynamic portion of DKR, is the conversion of an

enantioenriched mixture to a racemic one. This conversion constantly replenishes the consumed

substrate during KR and therefore yields greater than 50% of one enantiomer can be obtained.

Importantly, racemization only occurs between the substrate enantiomers and not the product

enantiomers. If racemization occurred between product enantiomers, the ee would be diminished

or absent. It is also important that the energy of substrate racemization ($\Delta G_{rac}^{\ddagger}$) is less than the

activation energies ($\Delta G_R^{\ddagger}$, $\Delta G_S^{\ddagger}$), as this allows for rapid racemization and higher product ee to

be obtained. In Figure 2-2, the *S* isomer reacts faster and is replenished by racemization until

both enantiomers of substrate are consumed. If the equilibration between substrate enantiomers

is rapid and product formation is irreversible, then the DKR occurs under Curtin–Hammett
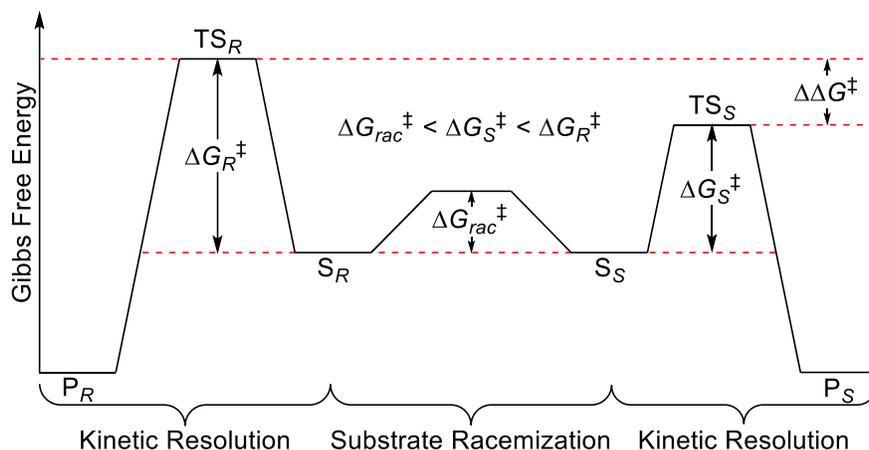
conditions.

Figure 2-2. Gibbs free energy diagram of an exergonic dynamic kinetic resolution favouring the *S* enantiomer.

Under Curtin–Hammett conditions, the ratio of products and ee can be calculated from $\Delta\Delta G^{\ddagger}$.[146] In the following equations (eq 2-1, 2-2, and 2-3) and Table 2-1 the *S* isomer is

$$\frac{[P_R]}{[P_S]} = e^{\frac{-\Delta\Delta G^{\ddagger}}{RT}} \text{ (2-1)} \qquad ee\ (\%) = \frac{[P_S]-[P_R]}{[P_S]+[P_R]} \times 100 \text{ (2-2)} \qquad ee\ (\%) = \frac{1-e^{\frac{-\Delta\Delta G^{\ddagger}}{RT}}}{1+e^{\frac{-\Delta\Delta G^{\ddagger}}{RT}}} \times 100 \text{ (2-3)}$$

considered the major product. The product ratio is calculated by eq 2-1. Usually, ee is expressed as a percentage and determined by the amount of excess enantiomer divided by the total of both enantiomers (eq 2-2). Instead, by normalizing the [P_s] to one the ee can be directly determined with eq 2-3. Table 2-1 shows the effect of different $\Delta\Delta G^{\ddagger}$ on product ratios and ees at 298.2 K.

Table 2-1. Curtin–Hammett principle applied to calculate product ratios and ees at 298.2 K.

$\Delta\Delta G^{\ddagger}$ (kJ/mol)	RT at 298.2 K (kJ/mol)	$\Delta\Delta G^{\ddagger}$ / RT	[P_R]/[P_S]	ee (%)[a]
1.00	2.48	0.403	0.668	19.9
2.50	2.48	1.01	0.36	47
5.00	2.48	2.02	0.13	77
10.00	2.479	4.034	0.0177	96.5
20.00	2.479	8.068	0.000313	99.9

[a]Towards the *S* isomer.

The first homogeneous asymmetric hydrogenation of a carbonyl group via DKR was reported by Noyori and co-workers.[147] The authors reported three Ru–BINAP precatalysts for the asymmetric hydrogenation of five α-branched β-keto esters via DKR. For example, with [RuCl(C$_6$H$_6$)((R)-BINAP)]Cl (148) as precatalyst the asymmetric hydrogenation of methyl 2-oxocyclopentanecarboxylate (149) gave 1,112 turnovers (95% yield) towards (R,R)-methyl-2-hydroxycyclopentanecarboxylate (150) (92% ee) via DKR (Scheme 2-1).[147] The remaining products were the enantiomer of 150 (4% yield) and its diastereomers (1% yield).
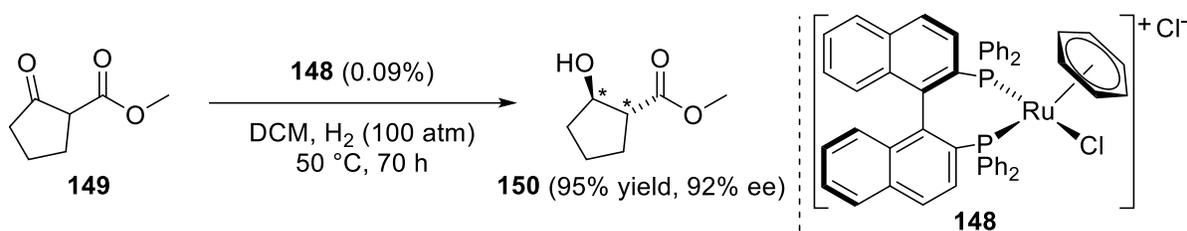
Scheme 2-1. Noyori's asymmetric hydrogenation of 2-oxocyclopentanecarboxylate (149) via DKR.[147]

Since this seminal work by Noyori and co-workers a large number of asymmetric carbonyl hydrogenations via DKR have been designed. The asymmetric hydrogenation of ketones via DKR is well established, and recent developments have been reviewed within the last five years.[148] However, the asymmetric hydrogenations of racemic α-chiral aldehydes,[149-152] amides,[140] and lactones[97, 119-121] via DKR have significantly fewer publications. As lactones are cyclic esters these publications will be presented here.

As mentioned in Chapter 1, Ikariya and co-workers reported the first catalytic asymmetric hydrogenation of a lactone via DKR.[97] The authors screened four chiral diamine precatalysts, derived from 106, for the hydrogenation of (±)-α-phenyl-γ-butyrolactone (151) under moderate DKR conditions (Scheme 2-2).
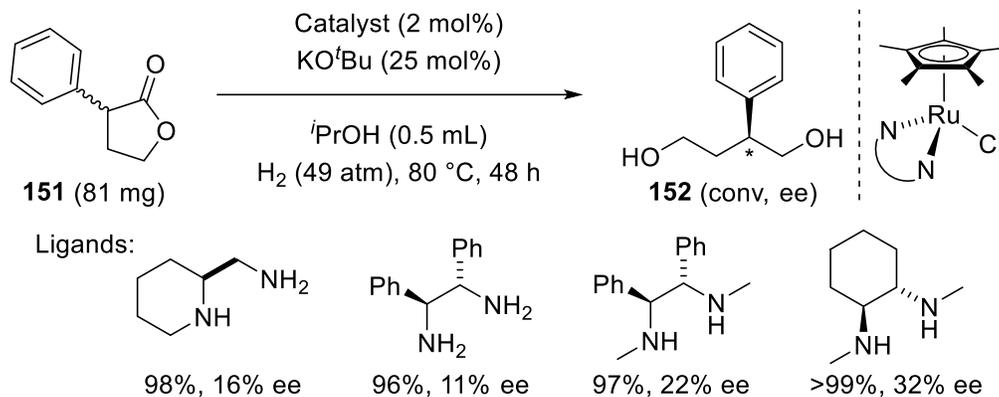
Scheme 2-2. Ikariya's asymmetric hydrogenations of (±)-α-phenyl-γ-butyrolactone (**151**) via DKR.[97]

The hydrogenations of **151** proceeded with 48 to 50 turnovers (≥96% conv) over 48 h (TOF = 1 h^{-1}) and ees ranged from 11 to 32% towards (*S*)-2-phenyl-1,4-butanediol (**152**).[97] The 25 mol% loading of KO^{t}Bu per **151** was used to promote the hydrogenation and racemization of **151**. The racemization of **151** is base-assisted and occurs through the enolate ion (Scheme 2-3).
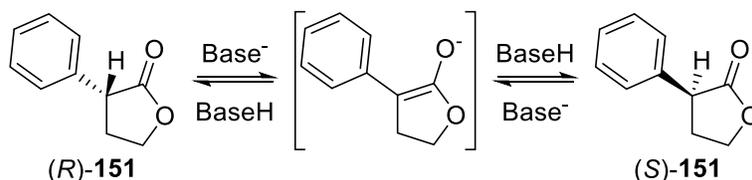
Scheme 2-3. Base-assisted racemization of (±)-α-phenyl-γ-butyrolactone (**151**) through its enolate.

Although the hydrogenations were not highly enantioselective, this was the first example of a catalytic asymmetric lactone hydrogenation via DKR. The second publication of an asymmetric lactone hydrogenation via DKR occurred six years later.

In 2017, Zhou and co-workers reported their Ir-based system for asymmetric lactone hydrogenation via DKR.[119] The authors screened Ir–SpiroPAP complexes, solvents, and bases for the asymmetric hydrogenation of (±)-α-phenyl-δ-valerolactone (**153**) to (*R*)-2-phenyl-1,5-pentanediol (**154**).[119] The most enantioselective catalyst [Ir-(*R*)-dtb-SpiroPAP-3-Me] (**155**) gave ~500 turnovers (92% yield) over 10 h (TOF = 50 h^{-1}) and 93% ee (Scheme 2-4).[119] Notably, this

hydrogenation occurred under only 10 atm H_2 at 25–30 °C.[119] Complex **155** provided ~500 turnover (80–95% yield) over 7 to 36 h (TOF = 71–14 h^{-1}) and 69 to 95% ee for 17 other lactones.[119] The major drawback to this DKR is the full equivalent of KO^{t}Bu required per lactone.
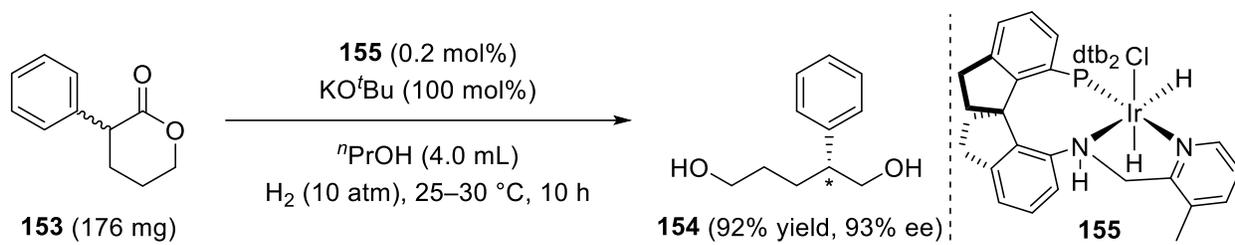
Scheme 2-4. Zhou's optimized asymmetric hydrogenation of (±)-α-phenyl-δ-valerolactone (**153**) via DKR.[119]

Zhou and co-workers also examined the asymmetric hydrogenation of the acyclic ester propyl 5-hydroxy-2-phenylpentanoate (**156**) with their Ir system (Scheme 2-5).[119] The hydrogenation gave ~500 turnovers (93% yield) and 93% ee.[119] Although the acyclic ester hydrogenation worked, it proceeded through the in situ formed lactone **153**.[119] The authors supported this by protecting the hydroxy group of **156** with methoxymethyl (MOM).[119] Once protected the hydrogenation did not proceed, thus supporting that **155** was only active towards asymmetric lactone hydrogenations.
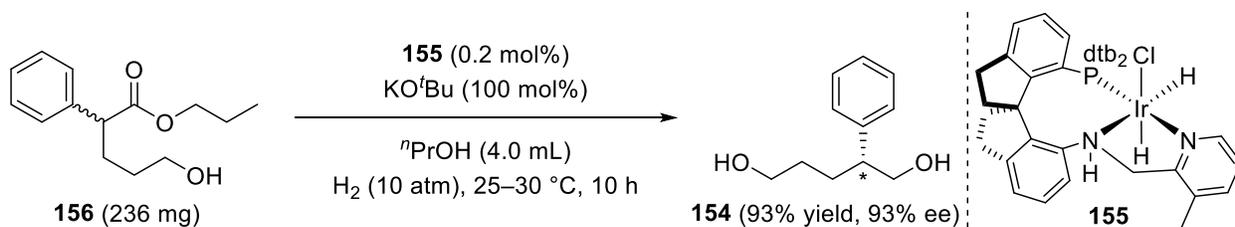
Scheme 2-5. Zhou's asymmetric hydrogenation of propyl 5-hydroxy-2-phenylpentanoate (**156**) via DKR.[119]

In 2019, Zhou and co-workers reported their asymmetric hydrogenation of α-arylamino lactones via DKR.[121] The authors synthesized and screened 18 variations of (*R*)-Ir–SpiroPAP for

the asymmetric hydrogenation of (±)-α-phenylamino-γ-butyrolactone (**157**).[121] All

(*R*)–Ir–SpiroPAP catalysts produced (*S*)-2-(phenylamino)butane-1,4-diol (**158**). The best catalyst

159 gave ~500 turnovers (92% yield) over 6 h (TOF = 83.3 h^{-1}) and 90% ee under 10 atm H$_2$ at

25–30 °C (Scheme 2-6).[121]
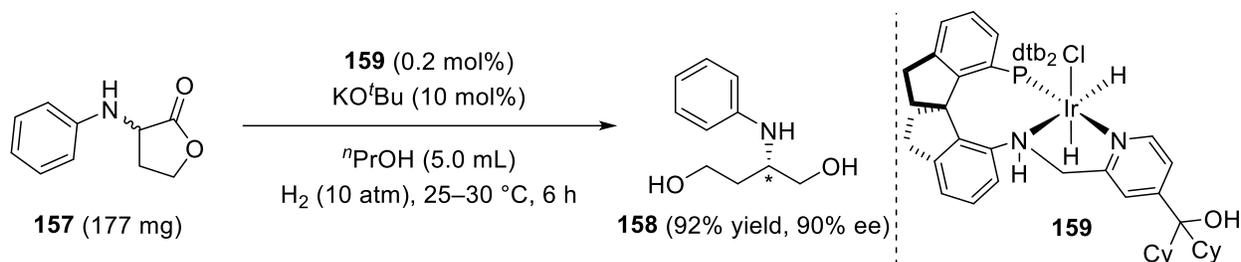
Scheme 2-6. Zhou's optimized asymmetric hydrogenation of (±)-α-phenylamino-γ-butyrolactone (**157**) via DKR.[121]

Notably, complex **159** was used for the asymmetric hydrogenation of 15 other α-arylamino-γ-

butyrolactones and 16 α-arylamino-δ-valerolactone via DKR. Complex **159** provided ~500

turnovers (≥85% yield) over 6 to 24 h (TOF = 83–21 h^{-1}) and 88 to 98% ee.[121] Notably, complex

159 hydrogenated **160** with ~2,000 turnovers over 16 h (TOF = 125 h^{-1}) and in 97% ee towards

161 under higher pressure (Scheme 2-7).[121]
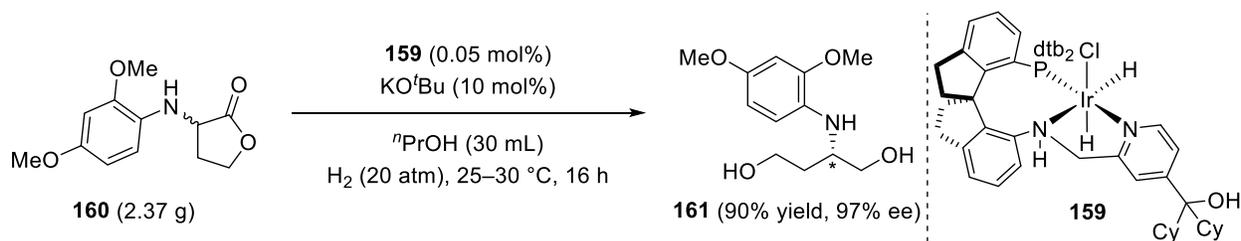
Scheme 2-7. Zhou's high TON asymmetric hydrogenation of **160** via DKR with Ir complex **159**.[121]

In 2018, Zhang and co-workers reported their synthesis of a SPINOL derivative and its

application in asymmetric hydrogenation of biaryl lactones.[120] The authors reacted (*S*)-*O*-

SPINOL (**162**), to form a similar NNP ligand (**163**) to Zhou's SpiroPAP ligands (Scheme 2-8).
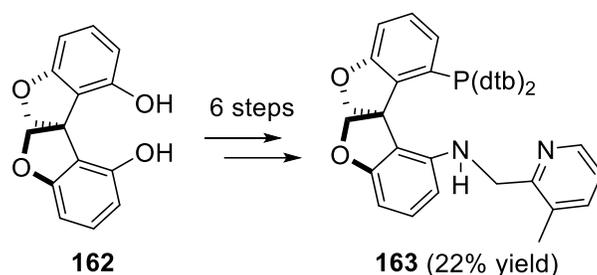
Scheme 2-8. Zhang's (*S*)-*O*-SPINOL and (*S*)-*O*-SpiroPAP derivative.

The (*S*)-*O*-SpiroPAP derivative **163** was used in situ with [Ir(COD)Cl]$_2$ for the asymmetric

hydrogenation of (±)-1,3-dimethyl-6*H*-benzo[*b*]naphtho[1,2-*d*]pyranone (**164**) to the

(*S*)-atropisomer of its respective diol **165** (Scheme 2-9).[120]
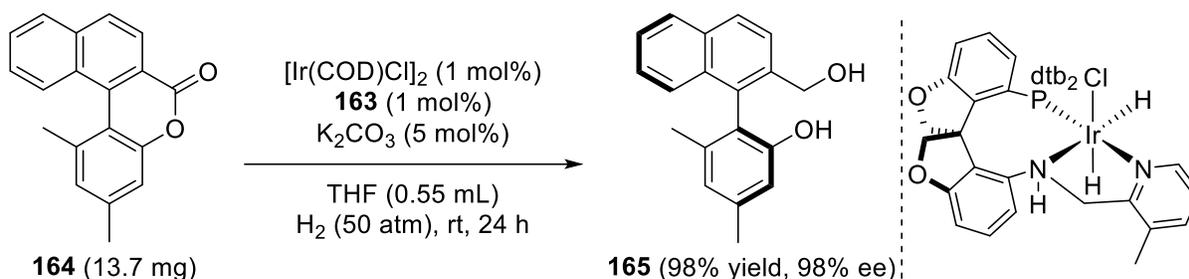
Scheme 2-9. Zhang's optimized asymmetric hydrogenation of biaryl lactone **164** via DKR.[120]

The system provided ~100 turnovers (98% yield) over 24 h (TOF = ~4.2 h^{-1}) and 98% ee. Zhou's

(*S*)-SpiroPAP ligand ((*S*)-dtb-SpiroPAP-3-Me) gave similar results (98% yield, 97% ee) for the

same reaction.[120] Therefore, **163** is not an obvious improvement to Zhou's commercially

available ligand. Notably, the system with **163** provided ~100 turnovers (83–99% yield) with ees

ranging from 79 to >99% for 16 other biaryl lactones.[120] This system undergoes DKR as the

biaryl lactones of this type (i.e., Bringmann's lactones) rapidly racemize due to configurational

instability.[153] The major drawback of this system is the activity, as only 100 turnovers are

obtained over 24 h (TOF = ~4.2 h^{-1}) under 50 atm H$_2$.[120] Although the activity is low, the biaryl

lactones are challenging substrates, and the chiral biaryl diols are valuable as they can possibly

be used as chiral ligands.

To the best of my knowledge, prior to my publication from this chapter, there is only one brief mention of an asymmetric acyclic ester hydrogenation via DKR in the literature. In a chapter written by Saudan, preliminary screening results were reported for the asymmetric hydrogenation of 2-phenylpropionate esters.[32] Saudan screened [RuCl$_2$((R)-BINAP)(DMF)$_2$] and [RuCl$_2$((R)-xyl-BINAP)(DMF)$_2$] with three diamine ligands (six combinations) for the hydrogenation of methyl 2-phenylpropionate (**166**).[32] Based on the initial screening, [RuCl$_2$((R)- xyl-BINAP)(S,S)-dpen)] (**167**) was the most active and enantioselective. Synthesized **164** was used to hydrogenate methyl (**166**), isobutyl (**168**), and isopropyl (**169**) 2-phenylpropionates (Scheme 2-10). The asymmetric hydrogenations of **166**, **168**, and **169** proceeded with ~380 to 396 turnovers (≥95% conv) over 20 h (TOF = 19.0–19.8 h^{-1}) and the ees ranged from 46 to 60% towards (R)-2-phenylpropan-1-ol (**170**).[32] The H$_2$ pressure of these hydrogenations was not reported. Although the H$_2$ pressure was not indicated, this was the first example of acyclic esters being hydrogenated to an enantioenriched β-chiral primary alcohol.
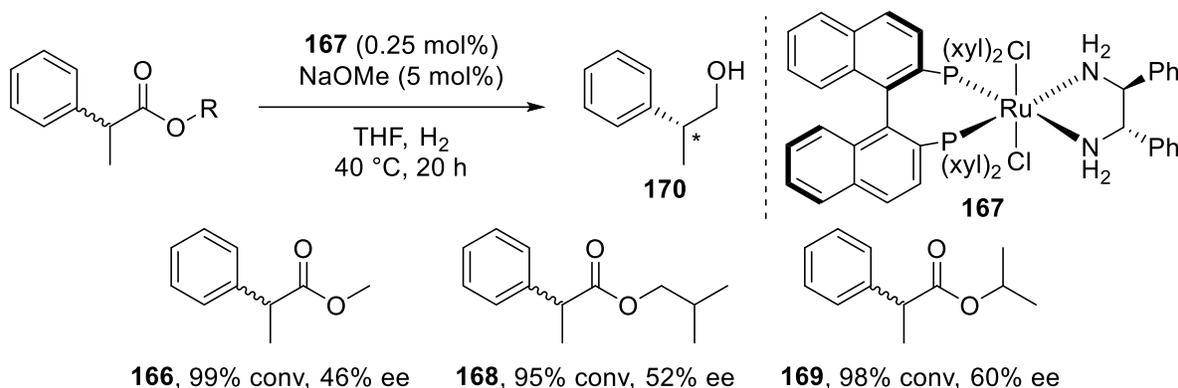
Scheme 2-10. Saudan's asymmetric hydrogenation of 2-phenylpropionates via DKR with **167** as precatalyst.[32]

The lack of asymmetric acyclic ester hydrogenations via DKR is likely related to their inherent difficulty being hydrogenated, as discussed in Chapter 1 (Section 1.1). The enantioenriched β-chiral primary alcohols produced from asymmetric hydrogenations on acyclic

esters can be useful synthetic intermediates. For example, the (R)-2-(4-fluorophenoxy)propan-1-ol in this chapter is used to synthesize (2R)-methyl sorbinil, which is an aldose reductase inhibitor in a topical treatment for dog cataracts.[154]

Herein this chapter, I report the discovery and development of a Ru-based asymmetric ester hydrogenation system that operates under mild DKR conditions to give β-chiral primary alcohols in high yields and ees.

2.2 Results and Discussion

2.2.1 Catalyst Screening and Optimization of Conditions

Racemic (±)-ethyl 2-phenoxypropionate (**171**) was used as substrate to screen on-hand chiral ligands for asymmetric hydrogenation via DKR. To accelerate the screening process, a Parr™ pressure vessel was adapted to setup and perform eight simultaneous hydrogenations in the absence of air. The chiral ligands were reacted with the Bergens group's standard Ru precursor, *cis*-[Ru(MeCN)$_2$(η^3-C$_3$H$_5$)(COD)]BF$_4$ (**172**), to form cationic Ru–allyl-type complexes.[143] These complexes react with H$_2$ and base to form dihydride complexes that are typically air-sensitive. The ligand screening (2 mol% **172**, 2 mol% ligand(s), 50 mol% KO^{t}Bu) was carried out under extremely mild pressure (4 atm H$_2$) and at room temperature for 3 h (Scheme 2-11).
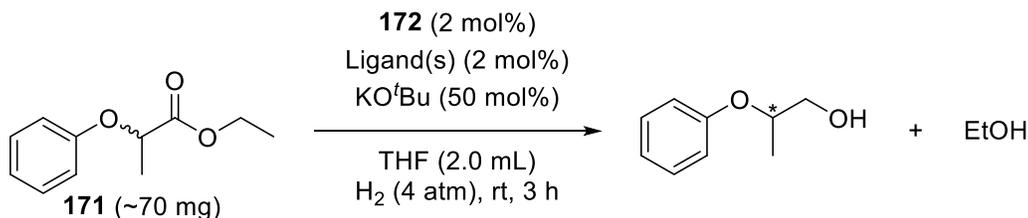
Scheme 2-11. Ligand screening conditions for the asymmetric hydrogenation of **171** via DKR.

Chiral diphosphine (PP, 1 equiv to **172**) ligands were screened with one equivalent of

(*R*,*R*)-(+)-dpen to include N–H functionalities into the dihydride catalysts. Chiral

monoamine–monophosphine (NP, 2 equiv to **172**) and chiral diamine–diphosphine (PNNP, 1

equiv to **172**) ligands were also examined. The ligand screening results were categorized into

four groups (I, II, III, IV) based on activity and enantioselectivity for the hydrogenation of **171**.

Group I ligands had low (≤10% conv) or no activity (Figure 2-3). Group II ligands had good

(61–74% conv) to moderate (11–60% conv) activity with moderate (11–60% ee) to low (≤10%

ee) or no enantioselectivity (Figure 2-4). Group III ligands had high (≥75% conv) activity but

low (≤10% ee) enantioselectivity (Figure 2-5). Group IV ligands had high (≥75% conv) activity

and moderate enantioselectivity (Figure 2-6).
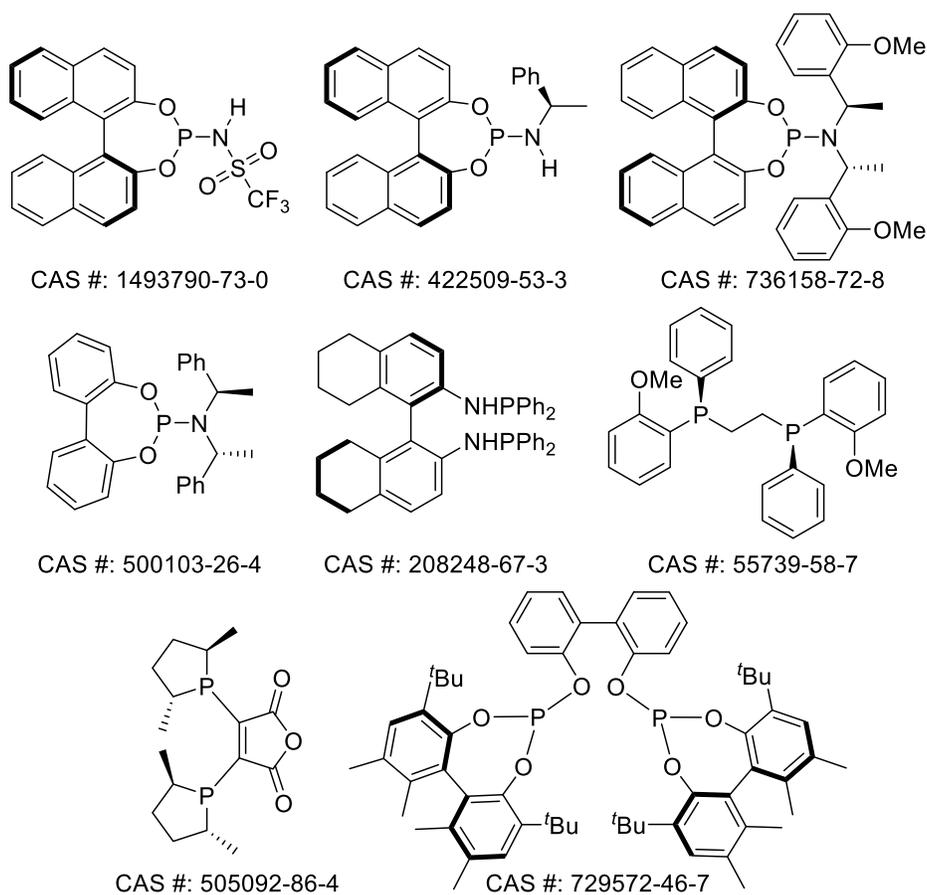
Figure 2-3. Chemical structures of ligands in Group I and their respective CAS Registry Numbers®.

70

43% conv, 0% ee
CAS #: 443965-14-8

35% conv, 0% ee
CAS #: 494227-35-9

51% conv, 3% ee
CAS #: 136705-64-1

45% conv, 6% ee
CAS #: 164858-78-0

65% conv, 11% ee
CAS #: 1400149-69-0

45% conv, 13% ee
CAS #: 1091606-68-6

57% conv, 24% ee
CAS #: 256390-47-3
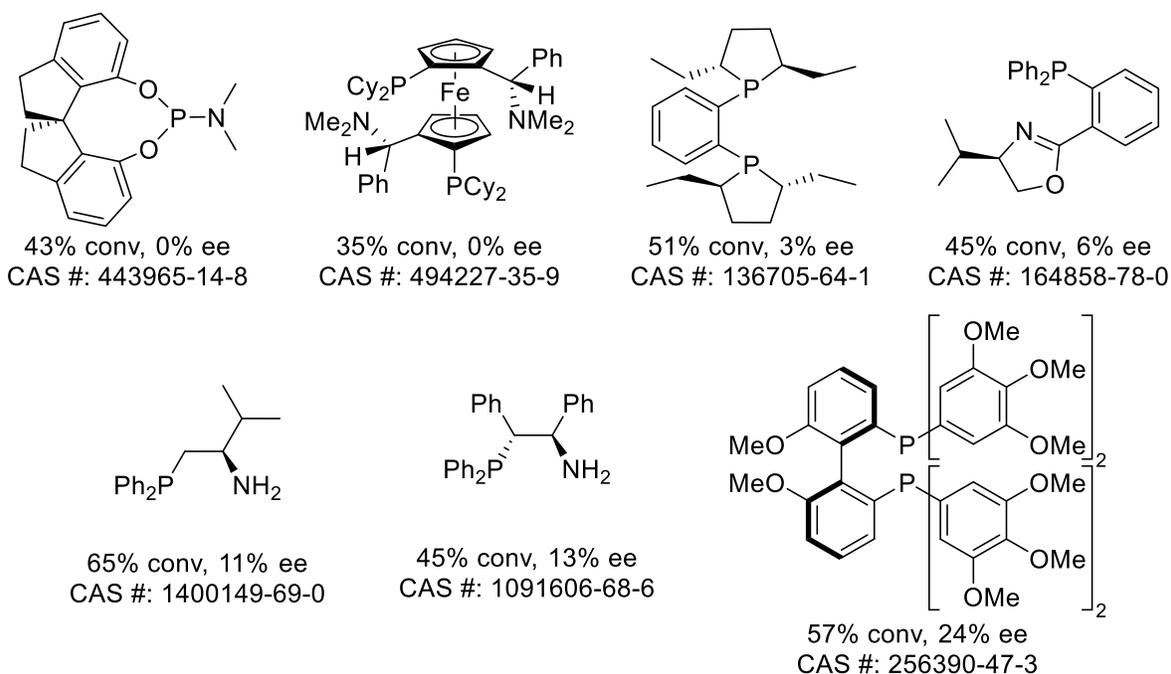
Figure 2-4. Chemical structures of ligands in Group II and their respective results and CAS Registry Numbers®.

83% conv, 2% ee
CAS #: 192057-60-6

86% conv, 3% ee
CAS #: 325168-88-5

85% conv, 4% ee
CAS #: 799297-44-2

81% conv, 5% ee
CAS #: 960128-64-7

78% conv, 8% ee
CAS #: 607389-84-4

88% conv, 10% ee
CAS #: 452304-59-5
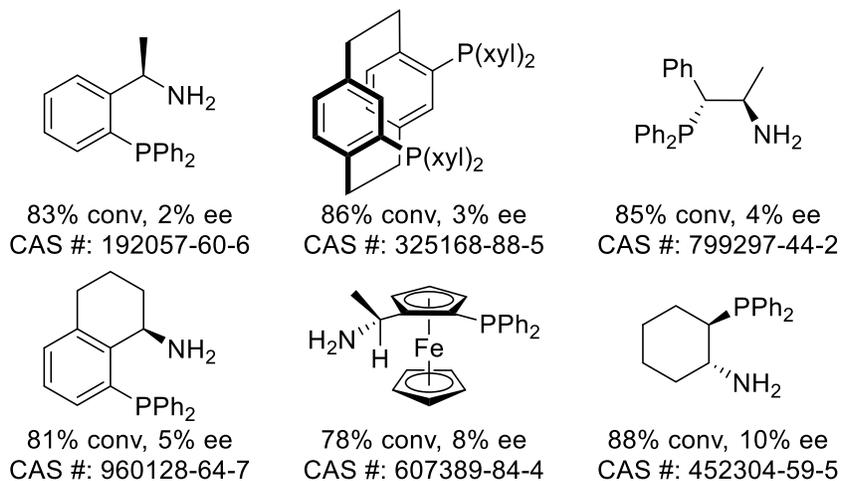
Figure 2-5. Chemical structures of ligands in Group III and their respective results and CAS Registry Numbers®.

>99% conv, 57% ee
CAS #: 174758-63-5

>99% conv, 60% ee
CAS #: 1150113-66-8
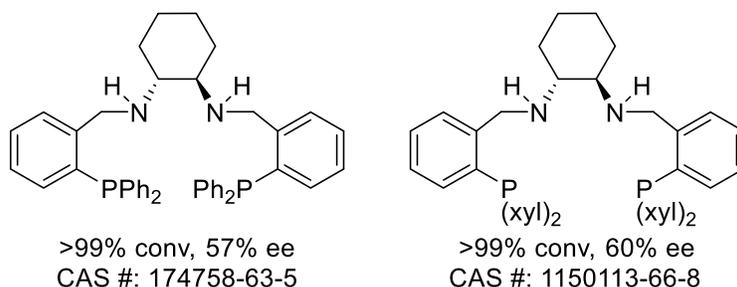
Figure 2-6. Chemical structures of ligands in Group IV and their respective results and CAS Registry Numbers®.

A smaller ligand screening was performed on (±)-ethyl 2-phenoxybutyrate (**173**) under the same conditions (Scheme 2-12).
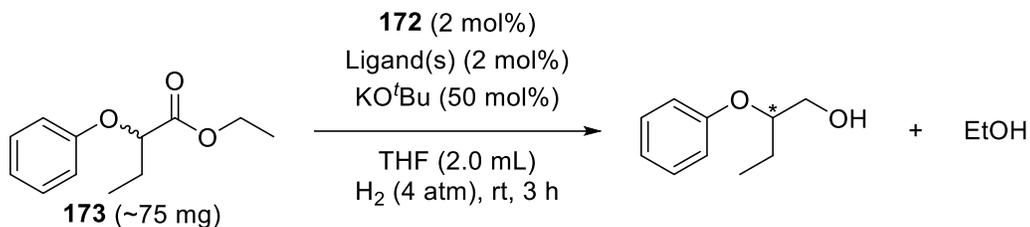
Scheme 2-12. Ligand screening conditions for the asymmetric hydrogenation of **173** via DKR.

This was done to support the ligand screening results with **171** and investigate a few more on-hand ligands. The results of this screening were also categorized into four groups (V, VI, VII, VIII) based on the activity and enantioselectivity for the hydrogenation of **173**. Group V ligands had low (≤10% conv) or no activity (Figure 2-7). Group VI ligands had good (61–74% conv) to moderate (11–60% conv) activity with moderate (11–60% ee) to low (≤10% ee) or no enantioselectivity (Figure 2-8). Group VII ligands had high (≥75% conv) activity but low (≤10% ee) enantioselectivity (Figure 2-9). Group VIII ligands had high (≥75% conv) activity and moderate enantioselectivity (Figure 2-10).
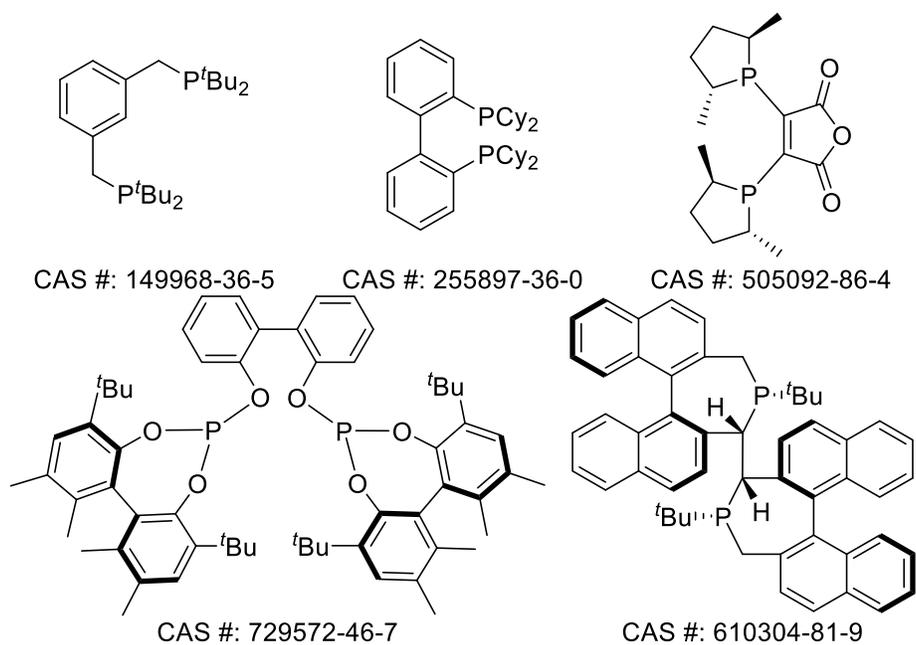
Figure 2-7. Chemical structures of ligands in Group V and their respective CAS Registry Numbers®.

CAS #: 149968-36-5   CAS #: 255897-36-0   CAS #: 505092-86-4

CAS #: 729572-46-7   CAS #: 610304-81-9

66% conv, 8% ee
CAS #: 147253-67-6

65% conv, 10% ee
CAS #: 917377-74-3

45% conv, 13% ee
CAS #: 256390-47-3

54% conv, 18% ee
CAS #: 1020670-88-5

66% conv, 39% ee
CAS #: 133545-24-1
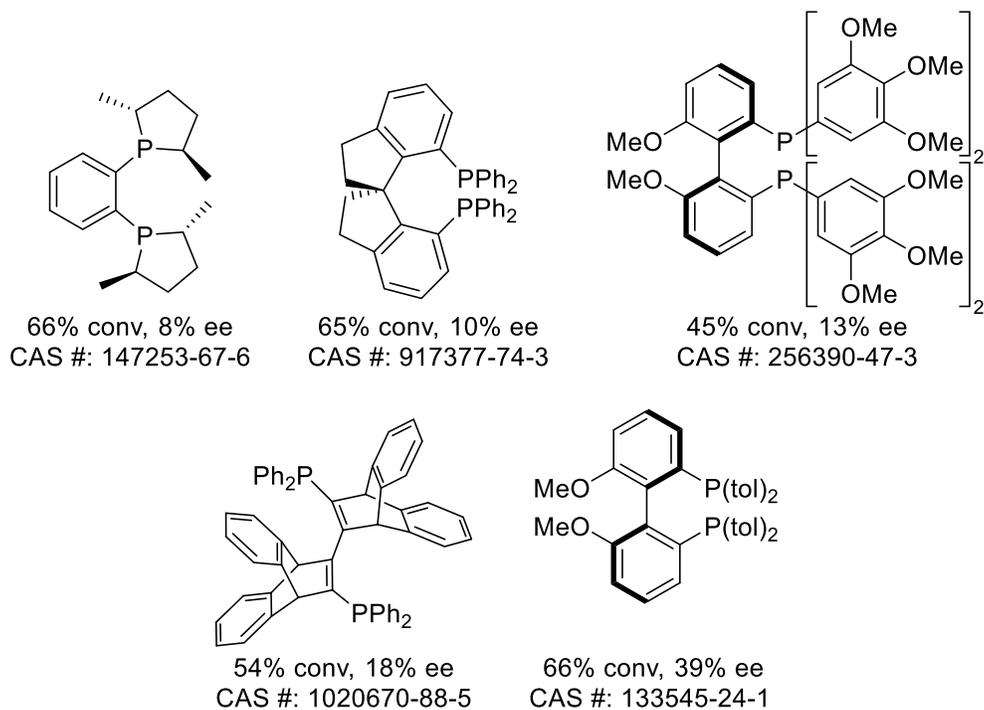
Figure 2-8. Chemical structures of ligands in Group VI and their respective results and CAS Registry Numbers®.
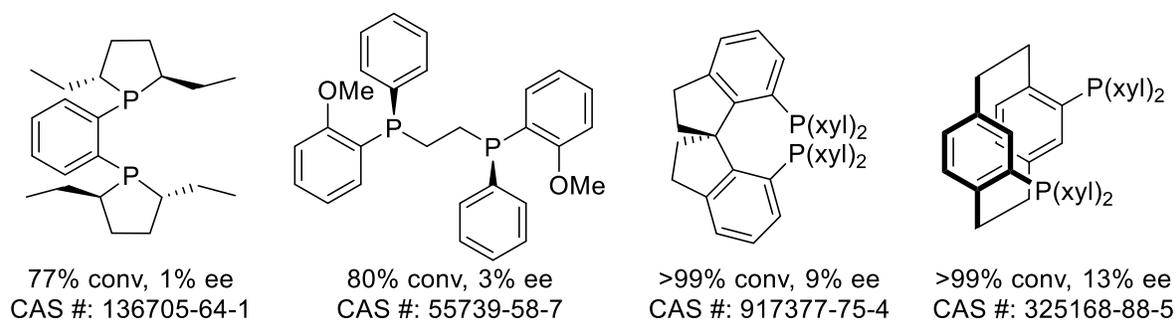
Figure 2-9. Chemical structures of ligands in Group VII and their respective results and CAS Registry Numbers®.

77% conv, 1% ee	80% conv, 3% ee	>99% conv, 9% ee	>99% conv, 13% ee
CAS #: 136705-64-1	CAS #: 55739-58-7	CAS #: 917377-75-4	CAS #: 325168-88-5

80% conv, 20% ee	90% conv, 31% ee	93% conv, 33% ee
CAS #: 71042-55-2	CAS #: 37002-48-5	CAS #: 868851-47-2
78% conv, 46% ee	>99% conv, 50% ee	>99% conv, 74% ee
CAS #: 244261-66-3	CAS #: 503538-69-0	CAS #: 1150113-66-8
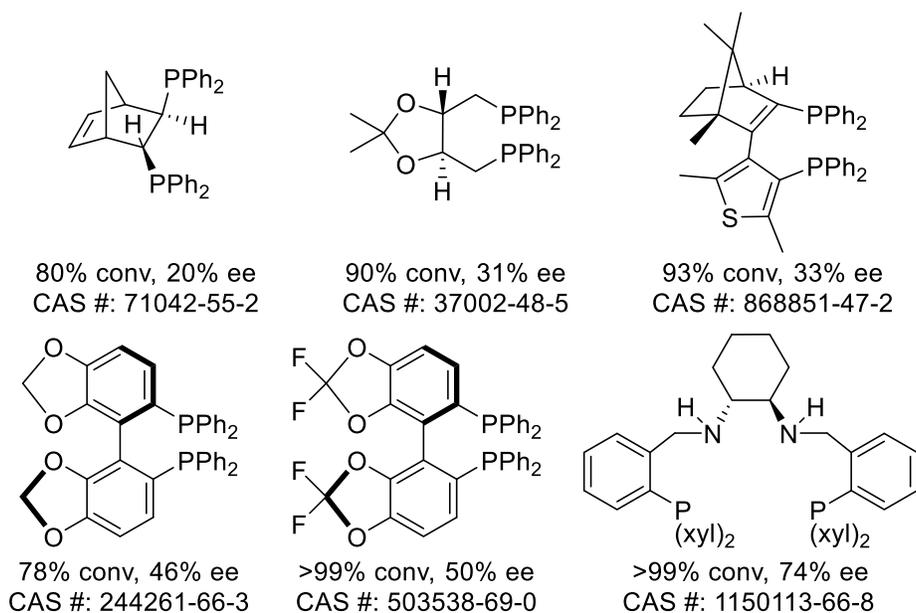
Figure 2-10. Chemical structures of ligands in Group VIII and their respective results and CAS Registry Numbers®.

The remaining **171** and **173** was racemic for all reactions that did not go to completion and had an enantioenriched product. Therefore, the base-assisted racemization of **171** (Scheme 2-13) and **173** was sufficient for DKR under the ligand screening conditions. The most active and enantioselective system used the tetradentate PNNP ligand (1*R*,2*R*)-*N*,*N*′-bis{2-[bis(3,5-dimethylphenyl)phosphino]benzyl}cyclohexane-1,2-diamine (**174**). Therefore, **174** became my optimal ligand for further investigations.

74
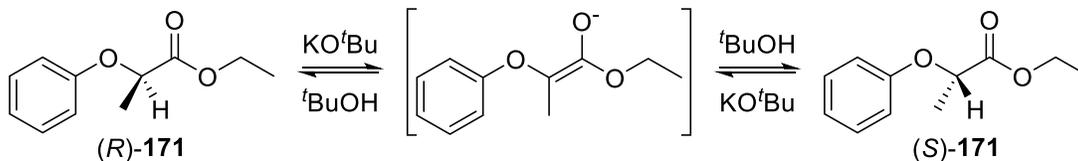
Scheme 2-13. Racemization of (±)-ethyl 2-phenoxypropionate (**171**) with KO^{t}Bu as base.

In a recent investigation by the Bergens group on the asymmetric hydrogenation of α-chiral amides[140], the isolated dichloride precursor, *trans*-RuCl$_2$((*S,S*)-skewphos)((*R,R*)-dpen), resulted in similar yields and higher enantioselectivity than the in situ prepared cationic catalyst.

In the interest of synthesizing a well-defined precatalyst and increasing ee, **174** was reacted with the standard dichloride precursor *trans*-[RuCl$_2$(NBD)(py)$_2$] (**175**) in boiling DCM for 18 h (Scheme 2-14). The reaction produced **176** as a mixture of *cis*- and *trans*-dichloride products (57% *cis*-**176** and 43% *trans*-**176** by ^{31}P NMR spectroscopy). Prior literature that examined [RuCl$_2$(PNNP)] synthesis, with the opposite-handed diphenyl derivative (1*S*,2*S*)-*N,N′*-bis[2-(diphenylphosphino)benzyl]cyclohexane-1,2-diamine, calculated the relative energies of the four possible *cis*-isomers and the *trans*-isomer using molecular modelling.[155] Based on this literature, the speculated lowest energy *cis*-dichloride Λ-β-*cis*-**176** and *trans*-**176** are illustrated in Scheme 2-14. The *trans*-product can be isolated via chromatography but resulted in low yield (23% yield). Isolation of *trans*-**176** was deemed unproductive due to the low yield, possible low-energy *cis*–*trans* isomerization, and cost. It is also possible that the *cis*- and *trans*-dihydride catalysts may form from either *cis*- or *trans*-dichloride precatalysts during activation and hydrogenation. Not wanting to fully dismiss the usage of **176**, the mixture was investigated against in situ prepared catalysts.
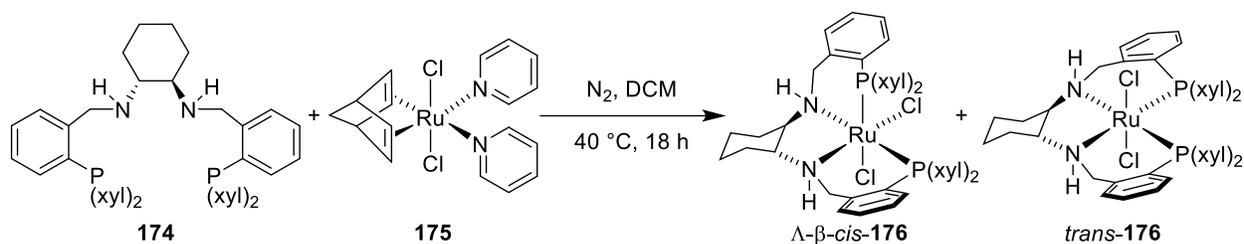
Scheme 2-14. Synthesis of Ru–dichloride precatalysts Λ-β-*cis*-**176** and *trans*-**176**.

The asymmetric hydrogenations of **171** and **173** were investigated with **176** and in situ prepared cationic precatalysts. In the Bergens group's previous investigation on asymmetric hydrogenation of α-chiral amides, NaO^{i}Pr (250 mol%) with ^{i}PrOH (200 mol%) gave optimal results.[140] Hence, NaO^{i}Pr and added ^{i}PrOH were examined with **176** and the cationic precatalyst of **172** and **174**. The results of the precatalyst investigations are summarized in Table 2-2. The asymmetric hydrogenation of **173** with **176**, NaO^{i}Pr, and ^{i}PrOH resulted in high ee (80%) but moderate activity (34% conv, Table 2-2, entry 1). A higher conversion (45%) and ee (83%) were obtained for the same reaction without added ^{i}PrOH (entry 2). Substituting NaO^{i}Pr with KO^{t}Bu resulted in higher activity (43% conv) but lower ee (76%, entry 1 vs 3) for **173** hydrogenation with added ^{i}PrOH. These three results (entries 1–3) support that the usage of NaO^{i}Pr results in higher ee than KO^{t}Bu and that ^{i}PrOH may mildly hinder the enantioselective hydrogenation. The cationic precatalyst of **172** and **174**, with KO^{t}Bu, was significantly more active (>99% conv) but less enantioselective for the hydrogenation of **173** (entry 4 vs entries 1–3). This activity difference supports that the cationic precatalyst forms the active catalyst faster than **176**. The 2% difference in ee between entries 3 and 4 may be the result of the different precatalysts and/or the metathesis reaction between KO^{t}Bu and ^{i}PrOH (eq 2-4).

$$KO^tBu \quad + \quad {^i}PrOH \quad \longrightarrow \quad KO^iPr \quad + \quad {^t}BuOH \quad (\textbf{2-4})$$

Table 2-2. Precatalyst and preliminary base investigations on the asymmetric hydrogenations of **171** and **173**.

Precatalyst (2 mol%)
Base (50 mol%)

^{i}PrOH (0 or 200 mol%)
THF (2.0 mL)
H$_2$ (4 atm), rt

171 (R=CH$_3$, ~70 mg)
173 (R=CH$_2$CH$_3$, ~75 mg)

+ EtOH

entry	ester	precatalyst	base	^{i}PrOH	time (h)	conv (%)[c]	ee (%)[d]
1[a]		**176**	NaO^{i}Pr	Added	3	34	80
2[b]		**176**	NaO^{i}Pr	None	3	45	83
3[a]		**176**	KO^{t}Bu	Added	3	43	76
4[b]		**172+174**	KO^{t}Bu	None	3	>99	74
5[a]		**176**	NaO^{i}Pr	Added	3	16	88
6[a]		**172+174**	NaO^{i}Pr	Added	3	>99	88
7[b]		**172+174**	NaO^{i}Pr	None	0.5	99	90
8[b]		**177+174**	NaO^{i}Pr	None	0.5	>99	90

[a]Precatalyst/base/**171** or **173**/^{i}PrOH = 1:25:50:100, [**171** or **173**] = 0.18 M in THF. [b]Precatalyst/base/**171** or **173** = 1:25:50, [**171** or **173**] = 0.18 M in THF. [c]Determined by ^{1}H NMR spectroscopy. [d]Determined by GC–MS with a β-DEX™ 225 (30 m × 0.25 mm, d$_f$ 0.25 μm) and normalized to the racemic products.

Like NaO^{i}Pr, KO^{i}Pr may result in higher ees than KO^{t}Bu. It is also possible that ^{t}BuOH does not hinder the asymmetric hydrogenation as much as ^{i}PrOH. The asymmetric hydrogenation of **171** with **176**, NaO^{i}Pr, and ^{i}PrOH (entry 5) gave a higher ee (88%) and lower activity (16% conv) than **173** under the same conditions (entry 1). The cationic precatalyst of **172** and **174**, with NaO^{i}Pr and ^{i}PrOH (entry 6) resulted in significantly higher activity (>99% conv) and the same ee (88%) as **176** did for **171** hydrogenation (entry 5). This further supports that the cationic precatalyst forms the active catalyst faster than **176**.

A 30 min reaction time was investigated for the asymmetric hydrogenation of **171** with NaO^{i}Pr and in situ prepared cationic precatalysts. The cationic precatalyst prepared from **172** and **174** resulted in 99% conversion and 90% ee over 30 min under the incredibly mild conditions (entry 7). The cationic precatalyst prepared from [Ru(1-3:5,6-η^5-C$_8$H$_{11}$)(η^6-anthracene)]BF$_4$ (**177**) and **174** resulted in quantitative conversion (>99%) and 90% ee over 30 min (entry 8). These two reactions further support that NaO^{i}Pr results in higher ee.

The apparent differences in activity between the dichloride **176** and the in situ prepared cationic precatalysts are thought to be due to the different rates of formation of the putative dihydride catalyst **178** (Figure 2-11) under the mild conditions. Based on this assumption, **176** takes significantly longer to form **178** than either in situ prepared cationic precatalysts. A similar situation occurred during the Bergens group's study on the asymmetric hydrogenation of *meso*-cyclic imides by desymmetrization.[142] The catalyst *trans*-[Ru((*R*)-BINAP)(H)$_2$((*R*,*R*)-dpen)] (**85**) was not formed from *trans*-[RuCl$_2$((*R*)-BINAP)((*R*,*R*)-dpen)], but was formed in situ through [Ru((*R*)-BINAP)(1-5-η^5-C$_8$H$_{11}$)]BF$_4$ (0 °C, ~2 atm H$_2$).[142] The slightly lower activity of the cationic precatalyst prepared from **172** and **174** is speculated to be caused by coordinating MeCN

(entry 7 vs 8). The cationic precatalyst prepared from **177** and **174** became my precatalyst of choice for further optimizations.
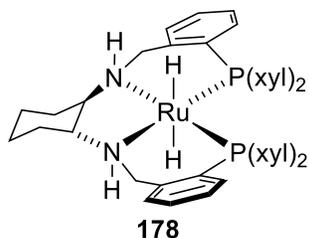
Figure 2-11. Chemical structure of the putative dihydride catalyst **178**.

Complex **177** has been reported by the Bergens group in theses[156, 157] and literature.[144, 145] The complex is an effective cationic precursor for preparing precatalysts for hydrogenations. Former members of the Bergens group have shown that the anthracene of **177** is labile and readily replaced with diphosphines.[156] Hass used **177** to prepare ROMP active (*R*)-BINAP precatalysts for asymmetric ketone hydrogenation,[156] and John used **177** to prepare a cationic precatalyst for lactam hydrogenation.[144, 157]

The asymmetric hydrogenations of **171** and **173** were screened with a considerable amount of base (50 mol%). A large amount of base was used for two reasons. Firstly, as previously mentioned, the base is used for racemization of the esters throughout the DKR. A large amount of base ensures sufficient substrate racemization. Secondly, the base is thought to generate the active catalyst by deprotonation. This belief is supported by the Bergens group's previous low temperature study with *trans*-[Ru((*R*)-BINAP)(H)$_2$((*R*,*R*)-dpen)] (**85**).[158] The dihydride complex **85** was deprotonated at the N–H groups of dpen, by KO^{t}Bu, ^{n}BuLi and LiN[Si(CH$_3$)$_3$]$_2$.[158] These deprotonated complexes, of **85**, were more active towards reducing imides and amides.[158] Therefore, **178** is believed to undergo an analogous deprotonation at an N–H group to **179** (Scheme 2-15).
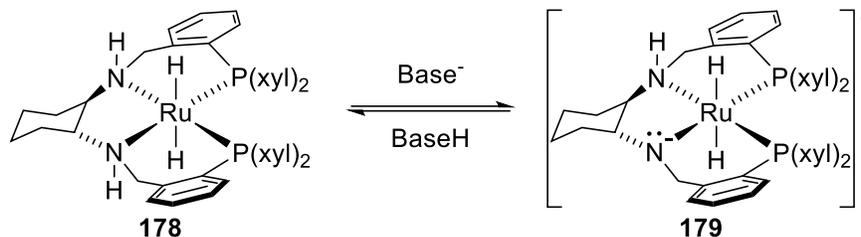
Scheme 2-15. Deprotonation of *trans*-**178** to the active deprotonated catalyst **179**.

As demonstrated in the precatalyst investigation, a change in base significantly impacts the asymmetric hydrogenation. Therefore, a variety of bases and base-alcohol mixtures were examined for the hydrogenation of **171** with the in situ prepared cationic precatalyst of **177** and **174**. The results of this screening are summarized in Table 2-3. The base screening reaction time was extended to 4 h as the efficiency of some bases were unknown. NaOMe, Cs_2CO_3, and K_3PO_4 were delivered as slurries as they did not dissolve well in dry THF. The asymmetric hydrogenations of **171** with these bases did not proceed, likely due to their poor solubilities (Table 2-3, entries 1, 5, and 6). Freshly prepared NaOEt was also poorly soluble in dry THF but did result in trace activity (entry 2). As expected, the NaO^{i}Pr reaction (entry 3) went to completion with high ee (90%). When EtOH was added with NaO^{i}Pr a minor decrease in ee occurred (87%, entry 4). This decrease in ee might be the result of less base being in solution, because of rather insoluble NaOEt forming from the reaction of Na^{i}OPr and EtOH (eq 2-5).

$$Na^iOPr \quad + \quad EtOH \quad \longrightarrow \quad NaOEt \quad + \quad {}^iPrOH \quad \textbf{(2-5)}$$

If this is the case, the EtOH formed, from hydrogenation of **171**, would remove base from the reaction. The asymmetric hydrogenations of **171** with freshly sublimed KO^{t}Bu and KO^{t}Bu alcohol mixtures all went to completion (entries 7–10). Addition of MeOH appeared to have no effect on the ee (84%) when KO^{t}Bu was used as base (entry 7 vs 8). When EtOH was added with KO^{t}Bu a minor increase in ee occurred (85%, entry 9). This is unlike when EtOH was added with NaO^{i}Pr (entry 4) and may be due to KOEt having a higher solubility than NaOEt in THF.

80

This also supports that ethoxide may result in higher ee if in solution. The KO^{t}Bu with ^{i}PrOH

reaction (entry 10) was similar to earlier results with the cationic precatalyst made from **172** and

174 (Table 2-2, entry 6). In summary, the base screening supported that NaO^{i}Pr, without added

alcohol, was the optimal choice. This study also supports that base may be removed during the

hydrogenation due to the EtOH product forming insoluble NaOEt in THF.

Table 2-3. Base and base-alcohol mixture screening for the asymmetric hydrogenation of **171** via DKR.
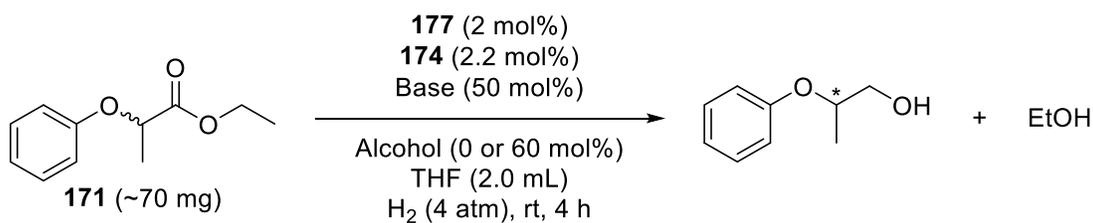
entry	base	alcohol	conv (%)^c	ee (%)^d
1^a	NaOMe	None	None	-
2^a	NaOEt	None	Trace	ND
3^a	NaO^{i}Pr	None	>99	90
4^b	NaO^{i}Pr	EtOH	>99	87
5^a	Cs$_2$CO$_3$	None	None	-
6^a	K$_3$PO$_4$	None	None	-
7^a	KO^{t}Bu	None	>99	84
8^b	KO^{t}Bu	MeOH	>99	84
9^b	KO^{t}Bu	EtOH	>99	85
10^b	KO^{t}Bu	^{i}PrOH	>99	87

^{a}**177**/**174**/base/**171** = 1:1.1:25:50, [**171**] = 0.18 M in THF.
^{b}**177**/**174**/base/alcohol/**171** = 1:1.1:25:30:50, [**171**] = 0.18 M in THF.
^{c}Determined by ^{1}H NMR spectroscopy. ^{d}Determined by GC–MS with a
β-DEX™ 225 (30 m × 0.25 mm, d$_f$ 0.25 μm) and normalized to the racemic
product.

Realizing that THF may not be the optimal solvent for asymmetric ester hydrogenation, a solvent study was performed. Different solvents were examined for the hydrogenation of **171** with NaO^{i}Pr and the in situ prepared cationic precatalyst of **177** and **174**. The results of the solvent screening are summarized in Table 2-4.

Table 2-4. Solvent screening for the asymmetric hydrogenation of (±)-ethyl 2-phenoxypropionate (**171**) via DKR.[a]
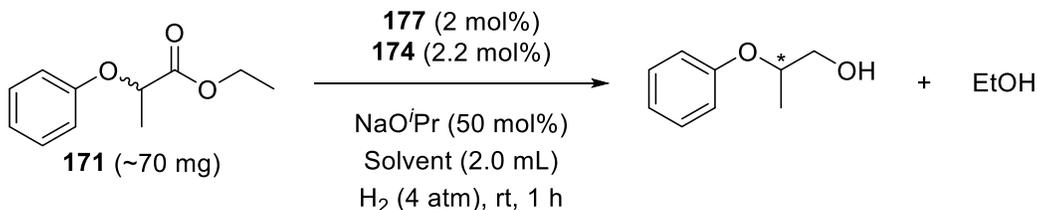
entry	solvent	conv (%)[b]	ee (%)[b]
1	Toluene	0	-
2	MTBE	~50	65
3	1,4-Dioxane	>99	84
4	2-MeTHF	>99	83
5	DME	>99	90

[a]**177**/**174**/base/**171** = 1:1.1:25:50, [**171**] = 0.18 M in solvent. [b]Determined by GC–MS with a β-DEX™ 225 (30 m × 0.25 mm, d$_f$ 0.25 μm) and normalized to the racemic product.

Toluene did not result in catalyst formation due to insolubility at room temperature. Therefore, the hydrogenation of **171** did not proceed in toluene (Table 2-4, entry 1). When methyl *tert*-butyl ether (MTBE) was used as solvent another solubility issue arose. NaO^{i}Pr was found to be sparingly soluble in MTBE and was delivered as a slurry. Due to this insolubility, the asymmetric hydrogenation of **171** was hindered in MTBE (entry 2). The asymmetric hydrogenations of **171** in 1,4-dioxane and 2-MeTHF (entries 3 and 4, respectively) went to completion, but both gave lower ee than the hydrogenation in THF. The usage of

1,2-dimethoxyethane (DME) gave the same results (>99% conv, 90% ee, entry 5) as THF. With

no increase in ee, the solvent investigation did not immediately change the optimized system.

With a significant interest in acquiring the highest ee possible, (1*R*,2*R*)-DACH–PNNP

ligands similar to **174** were purchased, synthesized, and examined for asymmetric hydrogenation

of **171** with **177**, NaO*i*Pr, and THF (Scheme 2-16). The in situ prepared cationic precatalyst of

177 and the bis(diphenylphosphino) ligand **180** resulted in full conversion and 75% ee. The

cationic precatalyst prepared from the Trost ligand **181** and **177** performed significantly worse,

resulting in 30% conversion and only 9% ee. Being that the only difference between **180** and **181**

is the carbonyl groups, it is reasonable to assume that these groups negatively interfere with the

hydrogenation performance. They may negatively interfere by steric hindrance and/or via

withdrawing electron density from the N–H groups. The cationic precatalyst prepared from **177**

and the bis(di(*p*-tolylphosphino)) ligand **182** gave full conversion but only 65% ee. This result

supports that increased steric bulk at the *para*-position diminishes enantioselectivity. The

differences in enantioselectivity between the commercially available phenyl ligand **180**, *p*-tolyl

ligand **182**, and xylyl ligand **174** are substantial. The high ee (90%) that results from usage of the

xylyl ligand **174** is speculated to be caused by the *meta*-positioned methyl groups. Influenced by

this, (1*R*,2*R*)-*N*,*N*′-bis{2-[bis(3,5-di-*tert*-butyl-4-

methoxyphenyl)phosphino]benzyl}cyclohexane-1,2-diamine (**183**) was synthesized. The in situ

prepared cationic precatalyst of **183** and **177** resulted in low ee (8%) and incomplete conversion

(95%) for **171** hydrogenation. Ideally, the 3,5-*tert*-butyl groups of **183** were supposed to result in

an increased ee, but the *para*-positioned methoxy groups may have significantly hindered that

result. In any case, **174** remained the optimal ligand for asymmetric hydrogenation of esters.
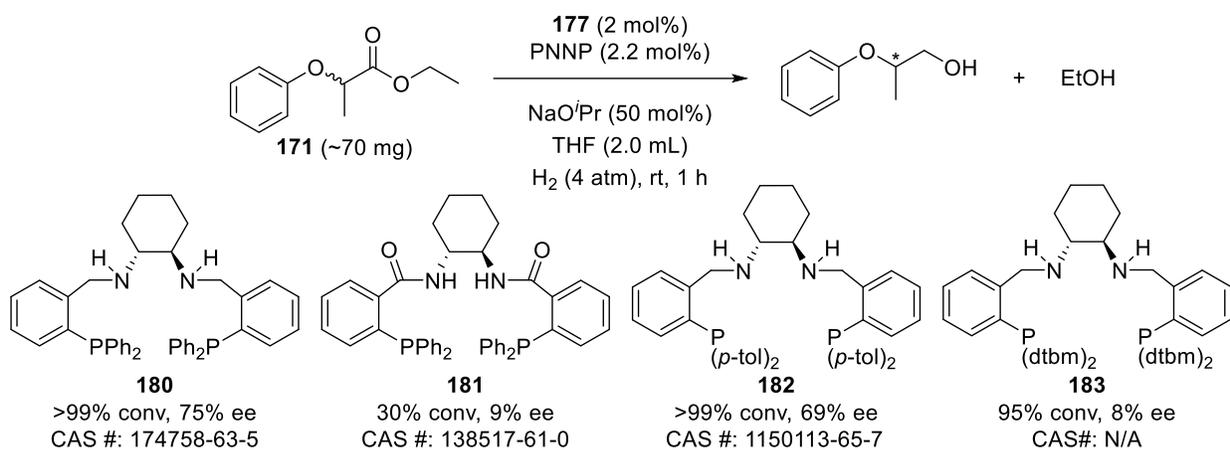
Scheme 2-16. Similar PNNP ligand screening for the asymmetric hydrogenation of **171** via DKR.

Examination of the ethyl esters hydrogenations that did not go to completion with NaO^{i}Pr as base supported that the reactions partially proceed through the transesterification products. The ethyl esters **171** and **173** readily react with NaO^{i}Pr to form their respective ^{i}Pr esters and NaOEt. The transesterification of **171** with NaO^{i}Pr is shown in Scheme 2-17.
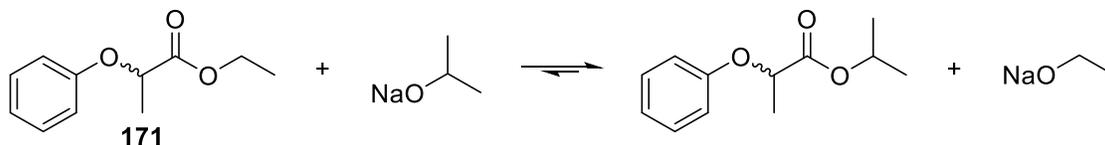
Scheme 2-17. Transesterification reaction between (±)-ethyl 2-phenoxypropionate (**171**) and NaO^{i}Pr.

This reaction is presumably driven by the stronger basicity of isopropoxide than ethoxide and the precipitation of NaOEt in dry THF. Attempting to take advantage of transesterification and use chirality transfer, the chiral base sodium (S)-(+)-1-methoxy-2-propanoxide (**184**) was prepared. Ideally, the usage of **184** would result in the in situ formation of two diastereomers with different reactivities. The transesterification of **171** with **184** is shown in Scheme 2-18.
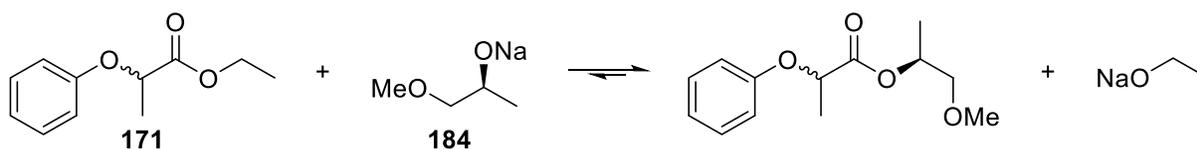
Scheme 2-18. Transesterification reaction between (±)-ethyl 2-phenoxypropionate (**171**) and the chiral base **184**.

The chiral base **184** was used for the asymmetric hydrogenation of **171** with the in situ prepared

cationic precatalyst of **177** and **174** (Scheme 2-19). The resulting ee was 4% lower than when

NaO^{i}Pr was used. Even when the loading of **184** was increased to 100 mol% (1 equiv to **171**) the

ee remained at 86%.

177 (2 mol%)
174 (2.2 mol%)

184 (50 mol%)
DME (2.0 mL)
H$_2$ (4 atm), rt, 1 h

171 (~70 mg)

>99% conv, 86% ee

+ EtOH
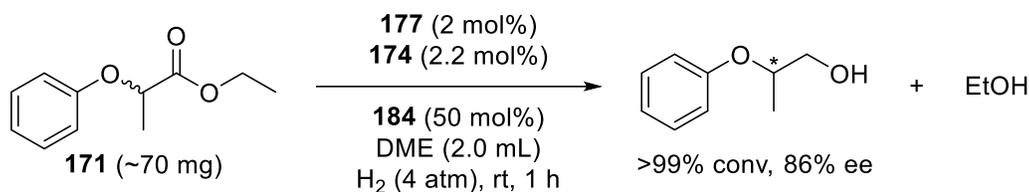
Scheme 2-19. Asymmetric hydrogenation of **171** with the chiral base **184**.

In a last-ditch effort to increase ee, the combination of NaOEt and DME was examined.

NaOEt was found to be sufficiently soluble in dry DME, unlike its solubility in dry THF. Due to

this finding, the asymmetric hydrogenation of **171** was performed with NaOEt in DME (Scheme

2-20). The hydrogenation went to completion and resulted in a 93% ee under the mild reaction

conditions. The 3% higher ee, obtained with NaOEt, may be the result of removing the formation

of the isopropyl ester from the transesterification reaction with NaO^{i}Pr (Scheme 2-17).

Evidently, the usage of NaOEt with ethyl esters, such as **171**, does not result in a composition

change through transesterification. Following this finding and having exhausted several avenues,

a substrate study was performed.

177 (2 mol%)
174 (2.2 mol%)

NaOEt (50 mol%)
DME (2.0 mL)
H$_2$ (4 atm), rt, 1 h

171 (~70 mg)

>99% conv, 93% ee

+ EtOH
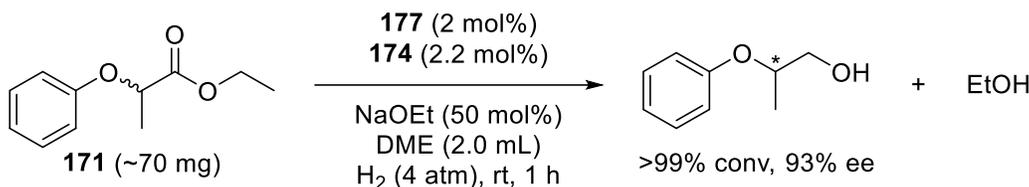
Scheme 2-20. Asymmetric hydrogenation of (±)-ethyl 2-phenoxypropionate (**171**) with 50 mol% NaOEt in DME.

2.2.2 Substrate Screening and Further Hydrogenations

A series of α-phenoxy esters were synthesized and asymmetrically hydrogenated utilizing the in situ prepared cationic precatalyst of **177** and **174**. The results of the α-phenoxy ester screening are summarized in Table 2-5. Several of the esters were examined with both NaOEt in DME and NaO^{i}Pr in THF. For the esters examined with both, the product ees were generally higher with the NaOEt in DME. The ees of the β-phenoxy alcohols, formed from the non-α-Ph substituted esters, ranged from 79 to 93% (Table 2-5, entries 1–24). Esters with halides at the *para*-position, of the phenoxy (PhO) group, resulted in similar product ees (entries 3–8). Oddly, the usage of NaOEt in DME, instead of NaO^{i}Pr in THF, did not result in higher ees for the asymmetric hydrogenations of the *para*-fluoro– and *para*-chloro–PhO esters (entries 3 vs 4 and 5 vs 6). Notably, the hydrogenations of the *para*-bromo– and *para*-iodo–PhO esters (entries 7 and 8, respectively) did not result in halide substitution. Conversely, the LiAlH₄ reduction of these esters resulted in partial halide substitution. The asymmetric hydrogenations of the *meta*-fluoro–PhO ester (entries 13 and 14) resulted in 82 and 85% ee for NaOEt in DME and NaO^{i}Pr in THF, respectively. Both of these ees are substantially lower than the hydrogenations with the *para*-fluoro–PhO ester (entries 3 vs 13 and 4 vs 14). The *ortho*-chloro–PhO ester resulted in a similar ee (86%, entry 15) as the *para*-chloro–PhO ester (87% ee, entry 5) with NaOEt in DME. A 7% lower ee was obtained for the hydrogenation of the *ortho*-chloro–PhO ester when NaO^{i}Pr in THF was used (entry 16). A similar difference in ee occurred with the methoxy substituted esters (entries 9–12). The *para*-methoxy–PhO ester resulted in 90% ee with NaOEt in DME (entry 9) but only 82% ee with NaO^{i}Pr in THF (entry 10). The *meta*-methoxy–PhO ester resulted in 87% ee with NaOEt in DME (entry 11) and 81% ee with NaO^{i}Pr in THF (entry 12). The catalyst appears to be more enantioselective with *para*-substituted PhO esters than the *ortho*- or *meta*-substituted PhO esters. Overall, these results demonstrate that the asymmetric hydrogenation can

Table 2-5. Asymmetric hydrogenation of racemic α-phenoxy esters via DKR.[a]
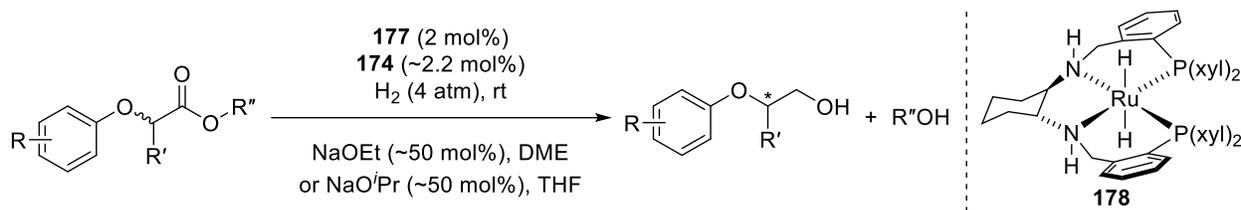
entry	ester	% conv[c] (% yield)[c]	ee (%)[d]	entry	ester	% conv[c] (% yield)[c]	ee (%)[d]
1		>99 (99)	93 (R)[e]	15		>99 (94)	86
2[b]		>99	90 (R)[e]	16[b]		>99	79
3		>99 (93)	88	17		>99 (97)	89 (R)[e]
4[b]		>99	88	18[b]		>99	87 (R)[e]
5		>99 (94)	87 (R)[e]	19		>99 (>99)	83
6[b]		>99	87 (R)[e]	20[b]		>99	79
7		>99 (93)	87	21		55 (44)	89
				22[b]		66[f]	89
8		>99 (95)	85	23		36[f] (32)	90
9		>99 (81)	90	24		>99 (89)	91 (R)[e]
10[b]		>99	82				
11		>99 (89)	87				
12[b]		>99	81	25[g]		>99 (74)	52[h]
13		>99 (91)	82				
14[b]		>99	85				

[a]Reaction conditions (unless otherwise noted): **177**/**174**/NaOEt/ester = 1:25:50, [ester] = 0.18 M in DME, 1 h. [b]**177**/**174**/NaO[i]Pr/ester = 1:1.1:25:50, [ester] = 0.18 M in THF, 4 h. [c]Determined by ^{1}H NMR spectroscopy with 1,3,5-trimethoxybenzene as internal standard. [d]Determined by GC–MS with a β-DEX™ 225 (30 m × 0.25 mm, d_f 0.25 μm) and normalized to the racemic products. [e]Assigned based on the GC–MS chromatograms and the Bergens group's previous publication.[140] [f]Conversion to alcohol product. [g]12 h reaction time. [h]Determined by HPLC with a Daicel CHIRALPAK® IB chiral column (250 × 4.6 mm) and normalized to the racemic product.

tolerate halides and alkoxides on the α-phenoxy group with only minor decreases in ee. Varying the α-alkyl group from Me to Et to ^{i}Pr caused the ee to fluctuate and the α-^{i}Pr (isovalerate) ester was significantly less reactive (entries 1, 2, 19–22). The lower reactivity of the isovalerate esters (entries 21–23) is likely caused by the increased steric bulk. This is further supported by the asymmetric hydrogenation of the α-Ph ester (entry 25) which required a 12 h reaction time for completion. The asymmetric hydrogenation of the α-Ph-PhO ester (entry 25) also resulted in a 52% ee. Varying the alkoxy group of the propionate ester between EtO, ^{i}PrO, and ^{s}BuO did not noticeably influence reactivity but did result in minor differences in enantioselectivity (entries 1, 2, 17, 18, and 24). Varying the alkoxy group of the isovalerate esters between EtO and ^{i}PrO had a noticeable influence on the hydrogenation with NaOEt in DME (entry 21 vs 23). More ethyl isovalerate was converted (55% conv, entry 21) to the alcohol product than isopropyl isovalerate (36% conv, entry 23). This supports that isopropyl esters are less reactive than ethyl esters for asymmetric hydrogenation with NaOEt in DME. The major absolute configurations of a couple enantioenriched products (entries 1, 2, 5, 6, 17, 18, and 24) were determined as *R*. Specifically, the asymmetric hydrogenations of **171** (entries 1 and 2), with **174** as ligand, forms mostly (*R*)-2-phenoxypropan-1-ol (**185**).

A couple of non-α-PhO esters were later examined for asymmetric hydrogenation under the mild conditions. The phenylthio ester **186** was synthesized and hydrogenated with the in situ prepared cationic precatalyst of **177** and **174** (Scheme 2-21).
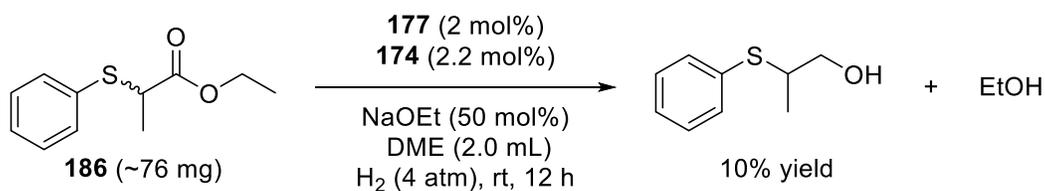
Scheme 2-21. Attempted asymmetric hydrogenation of (±)-ethyl 2-(phenylthio)propionate (**186**).

The hydrogenation of **186** did not proceed to a sufficient extent (10% yield), over 12 h, for ee

determination. This low reactivity is speculated to be caused by the S forming a strong bond to

the Ru and therefore poisoning the catalyst. The racemic ethyl ester of ibuprofen **187** was

purchased and hydrogenated with the in situ prepared cationic precatalyst of **177** and **174**

(Scheme 2-22).
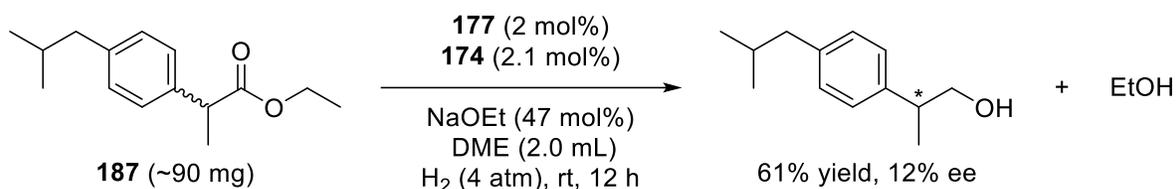
Scheme 2-22. Attempted asymmetric hydrogenation of ethyl 2-(4-isobutylphenyl)propionate (**187**).

The 12 h hydrogenation of **187** proceeded to a sufficient extent (61% yield) for ee determination.

The products ee was low (12% ee). This result demonstrates the importance of the oxygen

between the aryl group and the chiral centre for high activity and enantioselectivity.

Practically all of the aforementioned hydrogenations have used a 50 mol% base loading,

4 atm H₂, and room temperature. Deviations from these conditions were examined with **171** as

substrate. A 10 mol% NaOEt loading was examined for the asymmetric hydrogenation of **171**

(Scheme 2-23).
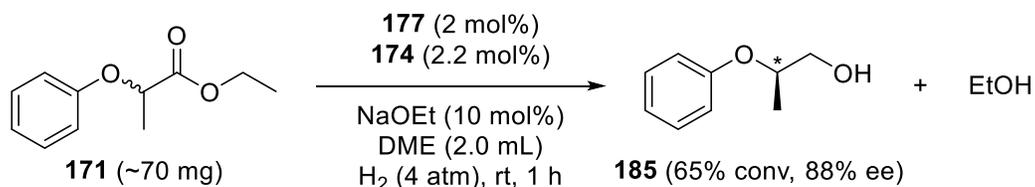
Scheme 2-23. Asymmetric hydrogenation of (±)-ethyl 2-phenoxypropionate (**171**) with 10 mol% NaOEt in DME.

As expected, the substantially reduced base loading decreased both activity (65% conv) and ee

(88%) for the hydrogenation of **171**. The base loading was decreased in higher TON

hydrogenations with **171**. A higher TON hydrogenation of **171** was performed with 20 mol%

NaOEt in DME (Scheme 2-24).
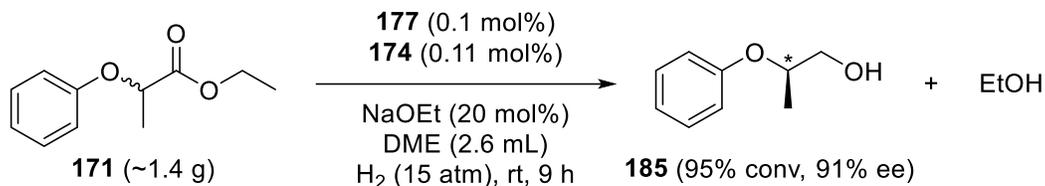
Scheme 2-24. Higher TON asymmetric hydrogenation of (±)-ethyl 2-phenoxypropionate (**171**) with NaOEt in DME.

This higher TON hydrogenation gave a significant result, as ~950 turnovers were performed over

9 h (TOF = ~106 h^{-1}) while maintaining a high ee (91%). This result was achieved with a

decreased base loading (20 mol% NaOEt), moderately higher pressure (15 atm H$_2$), and room

temperature. A similar higher TON hydrogenation was performed with NaO^{i}Pr in THF (Scheme

2-25).
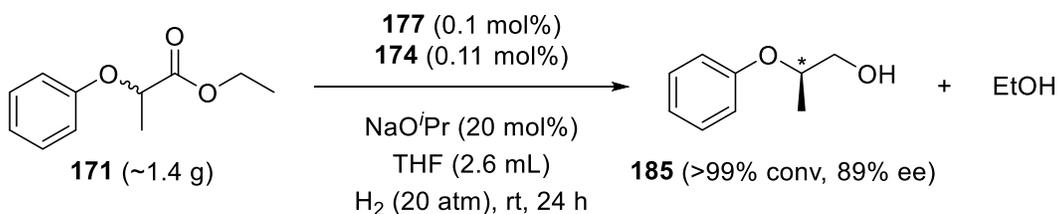
Scheme 2-25. Higher TON asymmetric hydrogenation of (±)-ethyl 2-phenoxypropionate (**171**) with NaO^{i}Pr in THF.

A 1,000 turnovers of **171** was performed with a slightly higher pressure (20 atm H$_2$) and longer

reaction time (24 h) than the higher TON hydrogenation in DME. The hydrogenation used a

decreased base loading (20 mol% NaO^{i}Pr) and room temperature to produce **185** in 89% ee.

Notably, these higher TON hydrogenations only resulted in 2 and 1% lower ees than the

optimized low-pressure counterparts (Table 2-5, entries 1 and 2). A lower pressure (~1 atm H$_2$)

balloon hydrogenation was also performed on **171** (Scheme 2-26) and resulted in a lower

conversion (67%) and ee (86%).

90
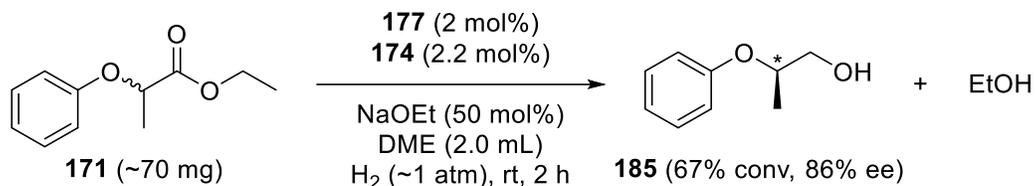
Scheme 2-26. Asymmetric hydrogenation of (±)-ethyl 2-phenoxypropionate (**171**) under ~1 atm H$_2$.

Significantly, hydrogenation of **171** at 0 °C went to completion and resulted in the highest ee (95%) observed (Scheme 2-27).
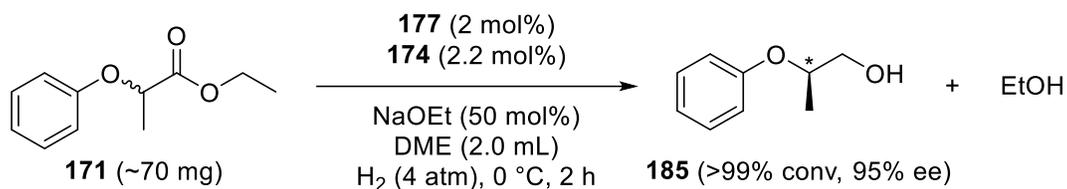
Scheme 2-27. Asymmetric hydrogenation of (±)-ethyl 2-phenoxypropionate (**171**) at 0 °C.

These exploratory reactions illustrate that the activity and enantioselectivity of the developed system could be further optimized for large-scale asymmetric hydrogenation. These further optimizations will likely require undesirable condition changes, such as higher pressure and temperatures below 0 °C.

There are several challenges related to this reaction. As previously mentioned, the esters undergo transesterification with the added base (Schemes 2-17 and 2-18). Presumably, the transesterification reaction can also occur between the racemic ester and the deprotonated β-chiral products. This is demonstrated with **171** and deprotonated **185** in Scheme 2-28. Although not observed throughout the hydrogenation studies, up to four diastereomers can form. These diastereomers were likely not observed due to the low concentration of deprotonated β-chiral product. Likewise, the alcohol produced from the alkoxy portion of the ester can also participate in transesterification. The formation of two alcohols, from every ester hydrogenated, results in the system's polarity and hydrogen-bonding ability increasing throughout the catalytic

reaction. This is significantly more relevant to higher TON ester hydrogenations where a minimal amount of solvent is used, and the concentration of formed alcohols is greater. The formed alcohols are also thought to cause product inhibition through the formation of Ru–alkoxides. This will be further discussed in the mechanism section (Section 2.2.3). The ability of the catalyst to tolerate these challenges and be active and enantioselective is formidable.
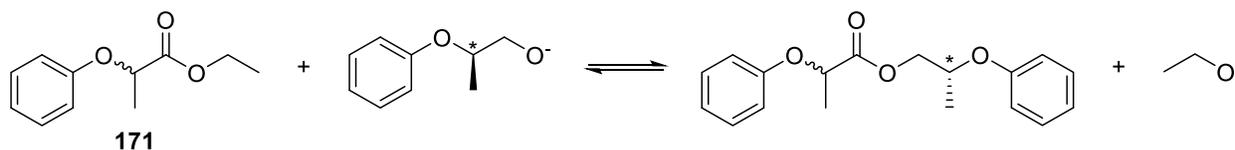
Scheme 2-28. Transesterification reaction between **171** and deprotonated (*R*)-2-phenoxypropan-1-ol (**185**).

2.2.3 Preliminary Investigation of the Mechanism

The developed system, with **178** as the catalyst, is believed to operate through an outer-sphere ligand assisted bifunctional mechanism. My putative mechanism for ester hydrogenation with NaOEt (Scheme 2-29) is based on prior low-temperature mechanistic studies by former group members.[158, 159] In this mechanism, complex **178** is activated via base to form the mono-deprotonated complex **178$_a$**. This complex quickly reacts with an ester to form a six-membered transition state (**178$_b$**) with a partial bond between the Ru and the acyl oxygen. The activated carbonyl group undergoes hydride attack to form a Ru–hemiacetalate species with a partial bond to the N–H group (**178$_c$**). This partial bond is broken to form an 18-electron Ru–hemiacetalate complex **178$_d$**. This complex undergoes elimination to form the Ru–amido complex **178$_e$**, aldehyde, and an alkoxide. The Ru–amido complex then reacts with H$_2$ to reform **178**, and the aldehyde is hydrogenated through a similar process.
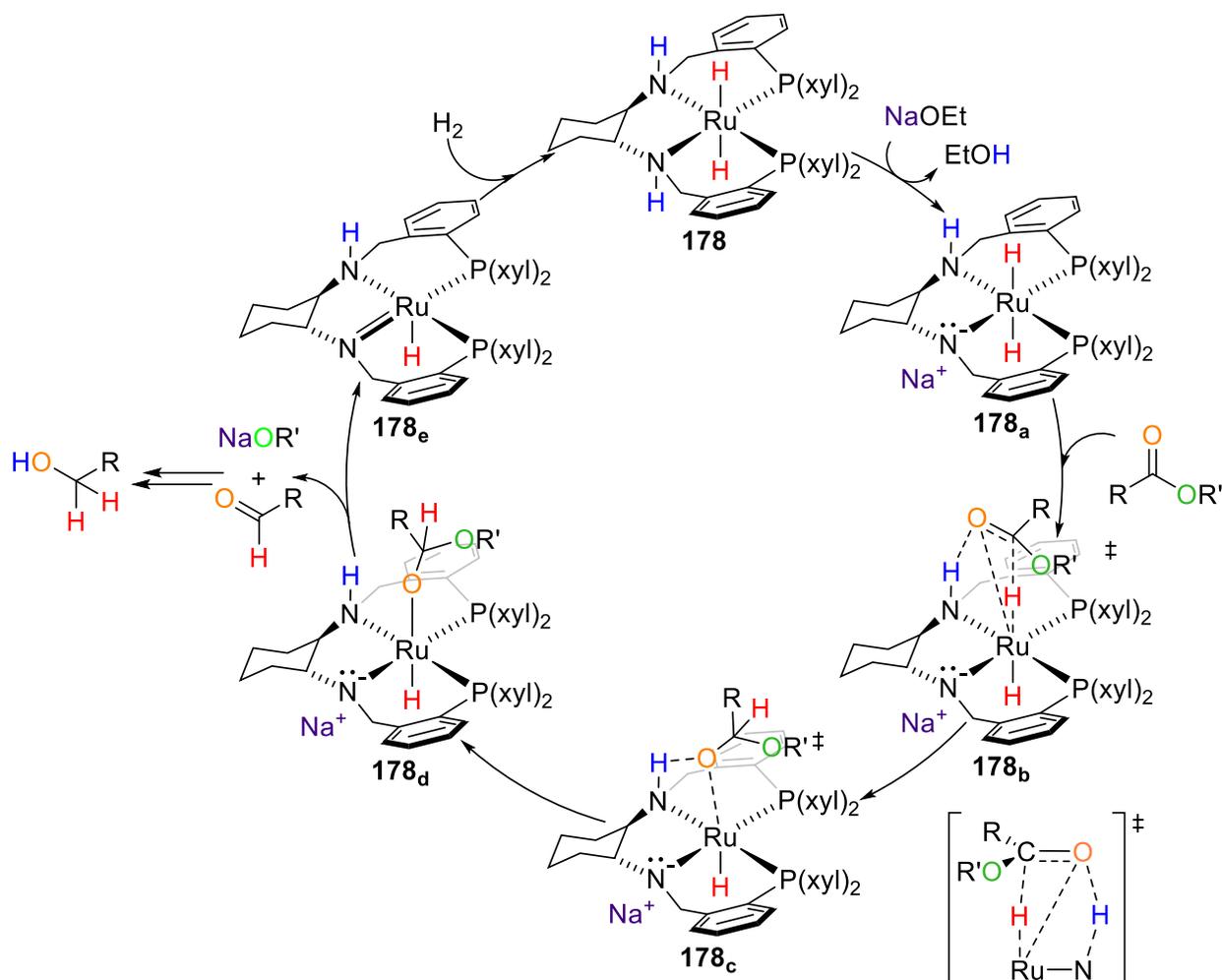
Scheme 2-29. Putative ester hydrogenation mechanism with **178** as catalyst and NaOEt as base.

Another possible mechanism to consider is one similar to Morris' DFT ester hydrogenation mechanism (Chapter 1, Scheme 1-57).[99] The analogous hydrogenation with **178** is shown in Scheme 2-30. In this mechanism, complex **178** is not activated by base prior to forming the six-membered transition state with the ester (**178f**). The carbonyl group undergoes hydride attack to form the dangling hemiacetal species **178g**. The hemiacetal species rearranges to form a partial bond between the Ru and the alkoxy oxygen (**178h**). This six-membered transition state undergoes elimination to form the Ru–amido complex **178i**, aldehyde, and an alcohol. The Ru–

93

amido complex then reacts with H₂ to reform **178**, and the aldehyde is hydrogenated through a

similar process.
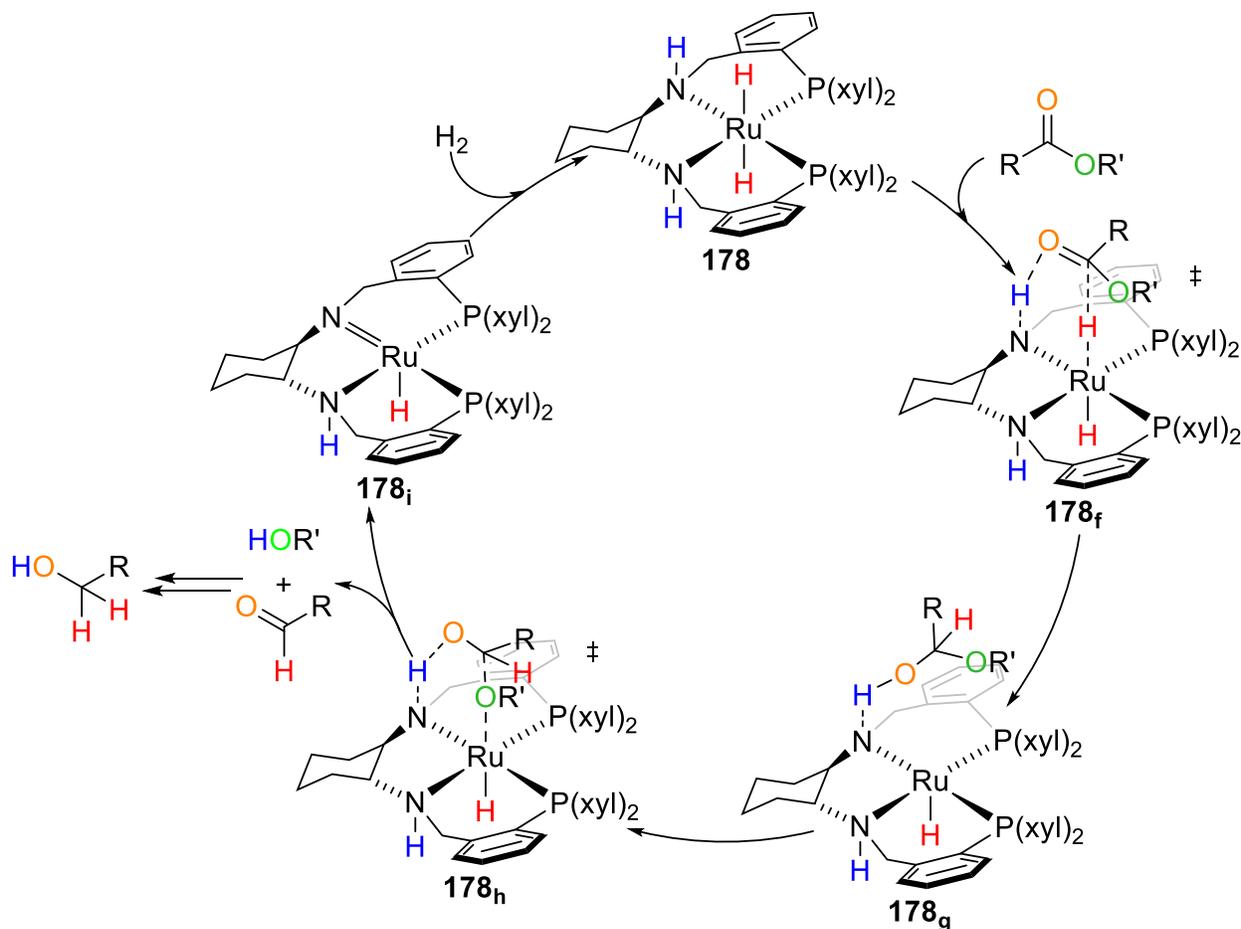
Scheme 2-30. The analogous Morris' ester DFT hydrogenation mechanism with **178** as catalyst.

Although this later mechanism is possible, it suggests that added base does not play a role

in the activity of the catalyst. As previously discussed, the activity of **178** was affected by the

base loading. Therefore, it is supported that the former mechanism, based on prior experimental

work, is more probable.

The mechanism was investigated through reactions. The hydrogenation of the potential

intermediate aldehyde (±)-2-phenoxypropionaldehyde (**188**) was performed (Scheme 2-31).
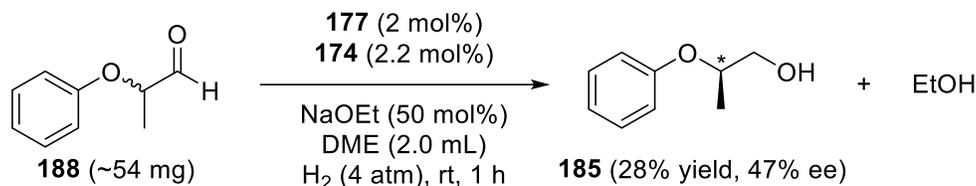
Scheme 2-31. Asymmetric hydrogenation of the possible intermediate (±)-2-phenoxypropionaldehyde (**188**).

The hydrogenation of **188** went to completion but resulted in both low yield (28%) and ee (47%) for the expected β-chiral alcohol. The remaining products were undetermined but were consistent with base catalyzed aldol-type reactions. These side-products did not form during the asymmetric hydrogenation of esters. Thus, the aldehyde is either not an intermediate of asymmetric ester hydrogenation or that the aldehyde is not sufficiently free for side reactions to occur. The lack of free aldehyde could result from either its fast hydrogenation or association with the catalyst. The aldehyde may remain associated to the catalyst through the protic N–H group (Scheme 2-32). The difference in ee between the asymmetric hydrogenations of **188** and **171** further supports that free aldehyde, which could undergo base-assisted racemization, is not present.
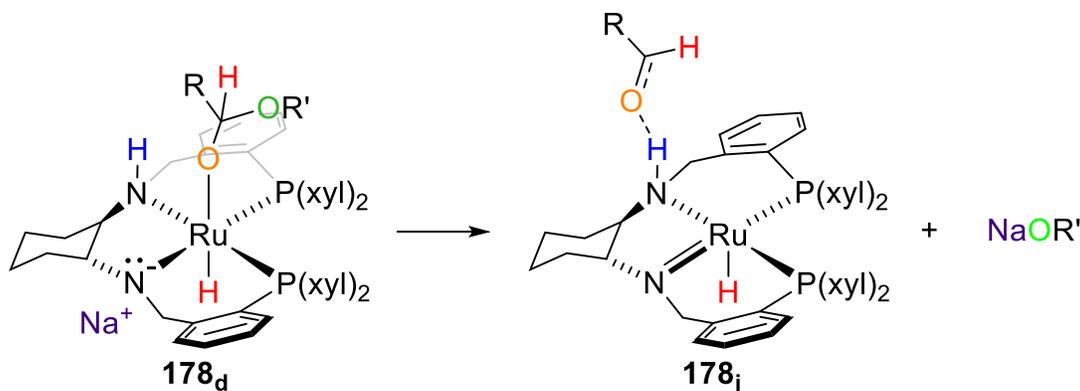
Scheme 2–32. Possible association of intermediate aldehyde through the N–H group of **178**.

The mechanism was further investigated with deuterium gas. The hydrogenation of **171** with deuterium gas (Scheme 2-33) resulted in deuterium at both the α- and β-positions of
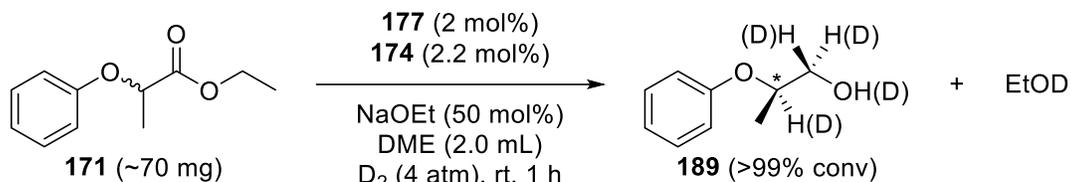
Scheme 2-33. Asymmetric deuteration of (±)-ethyl 2-phenoxypropionate (**171**) with NaOEt in DME.

2-phenoxypropan-1-ol-d_n (**189**). This was supported by the deuterium NMR spectrum (Figure 2-12), in non-deuterated DCM. Both the ^{1}H NMR (Figure 2-13) and ^{2}H NMR spectra supported the absence of deuterium at the alcohol functionality of **189**. This lack of O–D was likely caused by H–D exchanged with water during work-up. The distribution of deuterium in **189** was approximated from its ESI mass spectrum, with consideration for its natural isotope abundance (9.7%). The product's isotope mixture contained 6% with no deuterium (d_0), 17% with one deuterium (d_1), 30% with two deuterium (d_2), and 46% with three deuterium (d_3). Analysis of the isotope mixture, from the ^{1}H NMR spectrum (Figure 2-13), was complicated by overlapping signals and higher-order effects. The relative abundance of the three isotopomers of d_1 and three isotopomers of d_2 could not be reliably determined. However, the presence of these isotopomers provides insight into the reactions taking place.
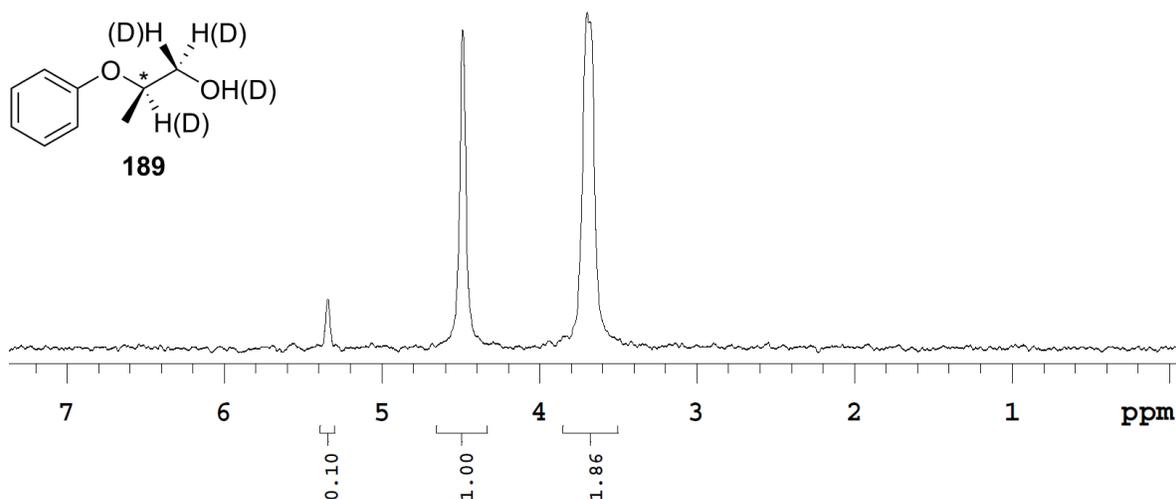
Figure 2-12. ^{2}H NMR spectrum of 2-phenoxypropan-1-ol-d_n (**189**) in CH$_2$Cl$_2$.
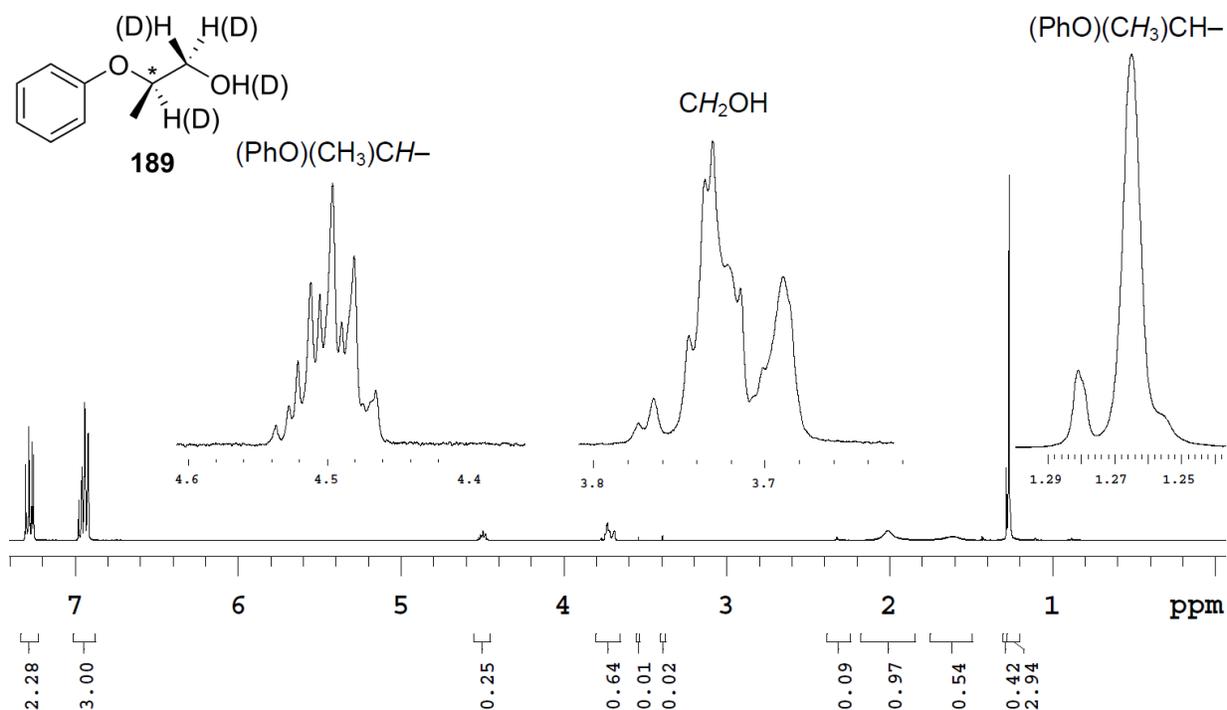
Figure 2-13. ^1H NMR spectrum of 2-phenoxypropan-1-ol-d_n (**189**) in CDCl$_3$.

Deuterium at the $-CH_2OH$ position, of **189**, came from deuteride on the Ru. In the same matter, hydrogen at this position comes from hydride on the Ru. As hydrogen is apparent at this position (Figure 2-13), hydrides must have formed during the deuteration. The hydrides are thought to have formed through a series of H–D exchanges and reactions. Previously, the Bergens group reported that the N–H groups of dpen, in *trans*-[Ru((*R*)-BINAP)(H)(η^2-H$_2$)((*R,R*)-dpen)], undergo H–D exchange with ^{i}PrOH-d_8, even at -80 °C.[91, 160, 161] Therefore, the N–H groups of **178** are believed to undergo analogous H–D exchange with EtOD rapidly at room temperature (Scheme 2-34).
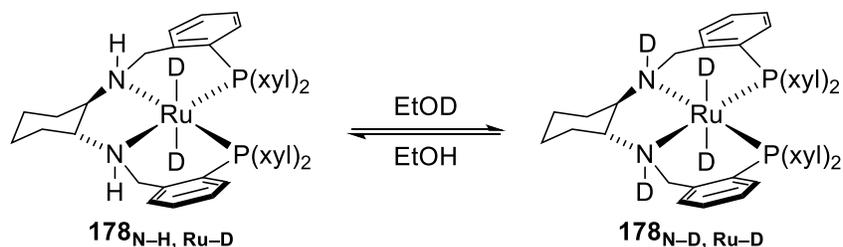
Scheme 2-34. H–D exchange of the N–H groups of **178** with EtOD.

The N–H groups of **178** are also thought to undergo deprotonation via NaOEt, which results in

EtOH formation. EtOH is also produced from the deprotonation of **171**. Therefore, at the start of

the deuteration there is likely more EtOH present than EtOD. This EtOH is believed to also H–D

exchange with the deuteride and η^2-D$_2$ ligands of **178** at room temperature (Scheme 2-35).
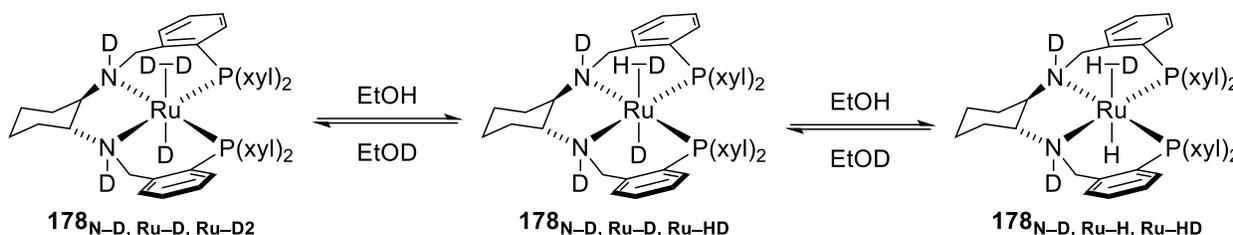
Scheme 2-35. H–D exchanges of Ru–D and Ru–η^2-D$_2$ of **178** with EtOH.

This is supported by the Bergens group's previous work, where the hydride and η^2-H$_2$ ligands

H–D exchanged with ^{i}PrOH-d_8 at ~-60 °C.[91] Therefore, EtOH is responsible for the H–D

exchange throughout **178** and the presence of hydrogen at the –C*H*$_2$OH position of **189**.

The (PhO)(CH$_3$)C*H*– position, of **189**, is also heavily deuterated (Figures 2-12 and 2-13).

This deuterium is caused by the enolate of **171** reacting with EtOD (Scheme 2-36). The amount

of **171** with deuterium at this position is likely to increase over the course of the hydrogenation,

because of the decreasing concentration of EtOH and increasing concentration of EtOD. If **171**

did not undergo deprotonation the ^{1}H NMR spectrum (Figure 2-13) would have one equivalent

of hydrogen at the (PhO)(CH$_3$)C*H*– position of **189**. Therefore, this hydrogen is likely spread

between the (PhO)(CH$_3$)C*H*– and –C*H*$_2$OH positions. The ^{1}H NMR spectrum supports this

theory as the peak area, of the two positions, is 0.89 equivalents of hydrogen. The remaining

0.11 equivalents of hydrogen is believed to have been consumed by ethoxide or ended up in the

O–H groups of the products.
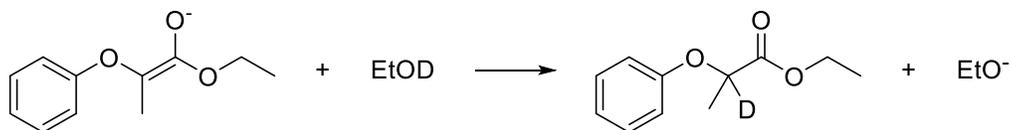
Scheme 2-36. Enolate of (±)-ethyl 2-phenoxypropionate (**171**) reacting with EtOD.

As previously mentioned, the alcohols formed during hydrogenation are believed to cause product inhibition through the formation of Ru–alkoxides. The formation of Ru–alkoxide species, from alcohol addition, has been reported by the Bergens group[90, 91, 159, 161] and an example has been previously discussed (Chapter 1, Scheme 1-47).[90] These Ru–alkoxide complexes require base to reform the Ru–amido species that can participate in the catalytic hydrogenation. Analogous reactions are expected to occur with the developed system. The Ru–amido species **178$_e$** is expected to react with alcohols to form Ru–alkoxide complexes (**178$_{Ru–OR}$**) (Scheme 2-37). These complexes can be converted back to the Ru–amido via reaction with base. This further illustrates the importance of base in the system.
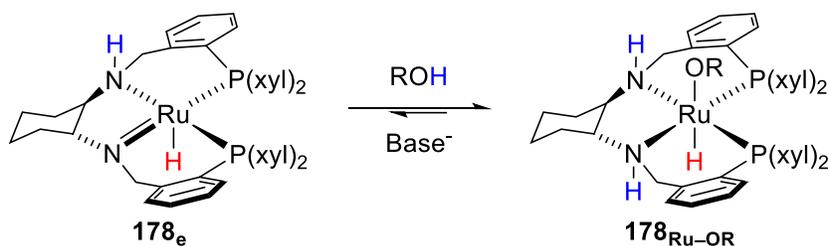
Scheme 2-37. Formation of Ru–alkoxide species from the Ru–amido **178$_e$** reacting with alcohols.

This brief investigation, with deuterium gas, demonstrates the complexity of the developed system. Further studies utilizing deuterated components (substrate, ligand, solvent, and base) and low temperature may aid in the experimental mechanistic investigation. Although further investigations into the mechanism may be beneficial, they are expected to be costly and not significantly change the conclusions made.

99

2.3 Conclusion

The development of the first highly active and enantioselective hydrogenation of acyclic esters has been presented. The Ru-based system was developed through screenings of ligands, bases, and solvents. The optimal system used a cationic precatalyst made from the chiral ligand **174** and labile precursor **177**. The small-scale hydrogenations were performed under 4 atm H_2 and room temperature. A variety of esters were hydrogenated with these conditions over 1 h. Both THF and DME were found to be suitable solvents for high ee. The impacts of lower base loading, temperature, and pressure were examined. Gram-scale asymmetric hydrogenations that maintained high activity and enantioselectivity with low catalyst (0.1 mol%) and base loadings (20 mol%) were discovered. A preliminary mechanism was proposed, and the mechanism was experimentally investigated with a possible intermediate aldehyde and deuterium gas. Further studies are required to gain more mechanistic insight.

2.4 Experimental Details

2.4.1 General Information

2.4.1.1 Purchased Chemicals

Reagents were obtained and used without further purification, unless otherwise stated, from a variety of suppliers. The 2-bromoisovaleric acid (97%), 4-chlorophenol (99%), (1*R*,2*R*)-(+)-dpen (98%), ethyl α-bromophenylacetate (97%), 4-fluorophenol (99%), 4-iodophenol (98+%), 3-methoxyphenol (97%), 4-methoxyphenol (98+%), 2-phenoxypropionyl chloride (98%), and tetrafluoroboric acid diethyl ether complex (50–55% w/w HBF_4) were obtained from Alfa Aesar. Na metal (Technical) was obtained from Anachemia. $MgSO_4$ (Reagent) and molecular sieves (4 Å, 1/16-inch pellets) were obtained from Caledon Laboratory Chemicals. Phenol (≥99.5%) was obtained from EM Science. NH_4Cl (Certified ACS),

benzophenone (Certified/Crystalline Flakes), CaO (Powder/Certified), Florisil® (60–100 mesh),

Mg metal (Turnings for Grignard Reaction), $SOCl_2$ (99.5+%), and triethylamine (Reagent grade,

99%) were obtained from Fisher Scientific. Ar (High Purity, 99.998%, 4.8), D_2 (Research,

Isotopic Enrichment 99.8%, 5.0), H_2 (High Purity, 99.995%, 4.5), and N_2 (High Purity, 99.995%,

4.5) were obtained from Praxair. 2-Chlorophenol (>98%) was obtained from Merck Schuchardt

OHG. Allyl bromide (ReagentPlus®, 99%), Al_2O_3 (Activated, neutral, Brockmann I), anthracene

(Reagent grade, 97%), 4-bromophenol (99%), Cs_2CO_3 (ReagentPlus®, 99%), CaH_2 (Reagent

grade, 95%), DIBAL-H solution (1.0 M in toluene), ethyl 2-bromobutyrate (99%), ethyl

2-bromopropionate (99%), (±)-ethyl 2-(4-isobutylphenyl)propionate (Aldrich[CPR]), $LiAlH_4$

(Reagent grade, 95%), (*S*)-(+)-1-methoxy-2-propanol (≥98.5%), K_3PO_4 (Anhydrous, ≥98%),

KO^tBu (Sublimed), $NaBH_4$ (ReagentPlus®, 99%), NaOMe (Reagent grade, 95%), Na_2SO_4 (ACS

reagent, ≥99%), thiophenol (97%), and 1,3,5-trimethoxybenzene (≥99%) were obtained from

Sigma-Aldrich. The (1*R*,2*R*)-(-)-DACH (99%), $[Ru(COD)Cl_2]_n$ (≥97%),

2-[bis(dtbm)phosphino]benzaldehyde (≥97%), and the 38 ligands listed in Table 2-6 were

obtained from Strem Chemicals. 3-Fluorophenol (≥98.0%) was obtained from TCI Chemicals.

Solvents were obtained and used without further purification, unless otherwise stated,

from a variety of suppliers. MTBE (Extra pure, 99.9%) was obtained from Acros Organics. The

sec-butanol (Distilled in glass, ≥98.0%), 1,4-dioxane (Reagent, ≥99.0%), hexanes (ACS reagent),

and *i*PrOH (HPLC grade, ≥99.7%), were obtained from Caledon Laboratory Chemicals. The

CD_2Cl_2 (99.8% D) was obtained from Cambridge Isotope Laboratories. EtOH (Dehydrated,

100%) was obtained from Commercial Alcohols. DME (Certified, ≥99.9%) was obtained from

Fisher Scientific. The $CDCl_3$ (99.8% D), DCM (ACS reagent, ≥99.5%), Et_2O (ACS reagent,

≥99.0%), hexane (CHROMASOLV® for HPLC, ≥98.5%), *i*PrOH (ACS reagent, ≥99.5%), MeOH

(ACS reagent, ≥99.8%), 2-MeTHF (Anhydrous, ≥99.0%), THF (ACS reagent, ≥99.0%), and

toluene (HPLC, 99.9%) were obtained from Sigma-Aldrich.

Table 2-6. Commercially available ligands examined for the asymmetric hydrogenation of esters.

type	CAS #	MFCD #	purity	type	CAS #	MFCD #	purity
NP	164858-78-0	02684553	98%	PP	149968-36-5	01630850	99%
NP	192057-60-6	17013986	≥97%	PP	244261-66-3	09753005	98%
NP	422509-53-3	04973053	≥95%	PP	255897-36-0	07368358	≥97%
NP	443965-14-8	08459340	≥98%	PP	256390-47-3	09753007	≥97%
NP	452304-59-5	17013996	≥97%	PP	325168-88-5	03840578	≥97%
NP	500103-26-4	08277032		PP	503538-69-0	05861607	97%
NP	607389-84-4	11045439	≥97%	PP	505092-86-4	07781992	≥97%
NP	736158-72-8	17018756	≥98%	PP	610304-81-9	06658119	97%
NP	799297-44-2	17018768	≥97%	PP	729572-46-7		≥95%
NP	960128-64-7	16621442	≥97%	PP	868851-47-2	09908236	96%
NP	1091606-68-6	17013982	≥97%	PP	917377-74-3	08459344	≥97%
NP	1400149-69-0	17013992	≥97%	PP	917377-75-4	08459343	≥97%
NP	1493790-73-0	18827637	≥97%	PP	1020670-88-5	11045085	98%
PP	37002-48-5	00009760	99.5%	PNNP	138517-61-0	01631273	98%
PP	55739-58-7	05863546	98%	PNNP	174758-63-5	16618374	≥97%
PP	71042-55-2	00085365	95%	PNNP	208248-67-3	04974231	
PP	133545-24-1	09753006	97%	PNNP	494227-35-9	04117702	≥97%
PP	136705-64-1	00142335	98+%	PNNP	1150113-65-7	17014023	≥97%
PP	147253-67-6	00142336	≥98%	PNNP	1150113-66-8	17014020	≥97%

2.4.1.2 Air- and Moisture-Sensitivity

Air- and moisture-sensitive materials were manipulated under Ar or N_2 using standard

Schlenk techniques. All glassware, stainless-steel needles, et cetera were dried in an oven before

immediate usage. Solvents were delivered via gas-tight syringes or cannulas (stainless steel).

All solvents for hydrogenations, LiAlH$_4$ reductions, base, ligand, and catalyst syntheses were freshly distilled or inertly collected from a SPS. The solvents were deaerated by bubbling with Ar or N$_2$ for ≥30 min before usage. Specifically, EtOH (CaO), DCM (CaH$_2$), Et$_2$O (Na/benzophenone), DME (Na/benzophenone), 1,4-dioxane (Na/benzophenone), ^{i}PrOH (CaO), MTBE (Na/benzophenone), 2-MeTHF (Na/benzophenone), THF (Na/benzophenone), and toluene (CaH$_2$) were dried by distillation, over the appropriate drying agent, under Ar or N$_2$. MeOH was collected under N$_2$ from a LC Technology Solutions Inc. SPS.

2.4.1.3 Chemical Characterization Methods

NMR spectroscopy was performed on a variety of instruments. The ^{1}H NMR spectra were acquired using one of four spectrometers: 400 MHz Varian Inova, 500 MHz Varian Inova, 500 MHz Varian VNMRS, and 600 MHz Varian Inova. The ^{2}H{^{1}H} NMR spectrum was acquired using a 400 MHz Varian Inova spectrometer. The ^{13}C{^{1}H} NMR spectra were acquired using a 500 MHz Varian VNMRS spectrometer. The ^{31}P{^{1}H} NMR spectra were acquired on a 500 MHz Varian Inova spectrometer and a 400 MHz Varian Inova spectrometer. The ^{19}F NMR spectra were acquired on a 400 MHz Varian DD2 MR spectrometer. Chemical shifts (δ values) are reported in ppm. Coupling constants (J values) are reported in Hz and multiplicities abbreviated as follows: s (singlet), d (doublet), t (triplet), q (quartet), sext (sextet), sept (septet), br (broad), m (multiplet), dd (doublet of doublets), ddd (doublet of doublets of doublets), dt (doublet of triplets), td (triplet of doublets), tt (triplet of triplets), qd (quartet of doublets), and sepd (septet of doublets). The internal standard used for NMR yield determinations was 1,3,5-trimethoxybenzene.

A variety of other chemical characterization techniques were performed. HRMS spectra were acquired using either electron ionization in a Kratos Analytical MS-50G or electrospray

ionization in an Agilent 6220 oaTOF. Elemental analyses were performed with a Carlo Erba

EA1108 Elemental Analyzer. The GC chromatograms and LRMS spectra were acquired using a

Hewlett Packard 5890 GC equipped with a 5970B MSD and a Supelco β-DEX™ 225 capillary

column (30 m × 0.25 mm, d_f 0.25 μm). HPLC was carried out on an Agilent (HP) 1100 series

(G1322A degasser; G1312A binary pump; G1313A autosampler; G1316A TCC; G1314A VWD)

with a Daicel CHIRALPAK® IB chiral column (250 × 4.6 mm). Enantiomeric excess (ee) values

were normalized to the racemic products, which were prepared separately via $LiAlH_4$.

2.4.1.4 Hydrogenation Equipment and General Methods

Screening hydrogenations were performed with a Parr™ 4635 pressure vessel that was

adapted for eight simultaneous hydrogenations. A circular stainless-steel block was machined to

sit in the pressure vessel. Nine wells were drilled into the block to fit Pyrex 9800-16 test tubes.

The test tubes were trimmed to 100 mm, equipped with 6 mm stir bars, and fitted with 14/20

rubber septa. A custom glass test tube, with a 24/40 neck, was fitted with a septum and placed in

the centre well. Each outer reaction test tube was connected to the centre tube with small

double-ended needles. Gasses were supplied to the central tube via long double-tipped needle

that was pierced through a septum on the gauge adapter of the pressure vessel's lid. Vent needles

were pierced through the reaction tubes' septa. With this system, reactions could be set up in the

reaction test tubes under Ar, N_2, or H_2 with the lid suspended over the pressure vessel. Before the

hydrogenations were set to the desired pressure, the lid was lowered, clamped, and the pressure

vessel flushed with H_2. Under positive H_2 pressure, the long central purge needle was removed,

and the septum in the lid was replaced with a pressure gauge. The vessel was then set to the

desired pressure. The vent needles were left in each reaction test tube during the hydrogenations.

The pressure of the screening hydrogenations was limited to 4 atm gauge pressure. Further

details are provided in the preliminary ligand and substrate screening procedures (Sections 2.4.2.1 and 2.4.2.3, respectively). The other screenings hydrogenations (base, solvent, and similar PNNP ligands) were carried out using similar procedures.

Gram-scale and single hydrogenations above 1 atm were performed with a Parr™ 4750 pressure vessel that was fitted with a glass insert. The oven-dried vessel was purged with Ar and cooled before addition of reagents. Reagents were delivered through a long double-tipped needle (i.e., cannula) that was pierced through a septum on the gauge adapter. Further details are provided in the procedures in Section 2.4.3.3.2.

2.4.2 General Procedures

2.4.2.1 Preliminary Ligand Screening

Inside a glovebox, *cis*-[Ru(MeCN)$_2$(η^3-C$_3$H$_5$)(COD)]BF$_4$ (**172**, 3.0 mg, 7.2 μmol), was weighed into each reaction test tube (≤8). Each test tube contained a 6 mm magnetic stir bar. Diphosphine (PP, 1 equiv), bidentate NP (2 equiv), or tetradentate PNNP (1 equiv) ligands were then weighed into different test tubes. The (1*R*,2*R*)-(+)-dpen (18.2 mg, 85.7 μmol, 12 equiv), for reactions with PP ligand, was weighed into a 100 mL Schlenk flask. Freshly sublimed KO^{t}Bu (200.7 mg, 1.789 mmol, 250 equiv) was also weighed into a 100 mL Schlenk flask. The test tubes and Schlenk flasks were sealed with 14/20 rubber septa and brought out of the glovebox. On a Schlenk line, THF was added via syringe to the (1*R*,2*R*)-(+)-dpen (6.0 mL, 0.014 M) and the KO^{t}Bu (5.0 mL, 0.36 M). (±)-Ethyl 2-phenoxypropionate (**171**, 625.0 mg, 3.220 mmol, 450 equiv) or (±)-ethyl 2-phenoxybutyrate (**173**, 670.6 mg, 3.220 mmol, 450 equiv) was weighed into a third 100 mL Schlenk flask, sealed, and purged with an inert gas. THF (4.5 mL) was added to the ester via syringe to make a stock solution (0.72 M). A custom test tube fitted with a 24/40 septum was placed in the central well of the machined block inside the pressure vessel. A long

double-tipped needle was used to connect an empty Schlenk flask, on a Schlenk line, to the custom tube. This needle was also passed through a 14/20 septum in the gauge adapter of the lid. The lid was held over the pressure vessel with a clamp. The central custom tube was evacuated and refilled with Ar several times, and then flushed with ~1 atm H_2. On a Schlenk line, 1.0 mL THF was added to each reaction test tube not containing a PP ligand. Test tubes containing PP ligand received 0.5 mL of THF. The tubes were stirred and heated at 60 °C, under Ar, for 30 min. The (1R,2R)-(+)-dpen solution (0.5 mL, 1 equiv/Ru) was added to the tubes containing a PP ligand. These tubes were heated and stirred for an additional 30 min at 60 °C. The reaction tubes were cooled to rt, placed into the outer wells of the block, and connected to the central tube with small double-ended needles. H_2 was supplied under slightly positive pressure to the central custom tube using the long needle passed through the lid. Each reaction tube's septum was pierced with an 18-gauge vent needle to allow H_2 to flush from the central tube through the reaction tubes. H_2 was flushed in this manner through the reaction tubes for 5 min. Each tube was then charged with 0.50 mL of ester solution (50 equiv) and 0.50 mL of KO^{t}Bu solution (25 equiv) via syringe. The lid of the pressure vessel was lowered, sealed, and the vessel was flushed with H_2 from the pressure vessel feed line for 5 min. Then, while flushing with H_2, the long needle supplying H_2 to the central tube was removed and the septum in the gauge adapter was replaced with the gauge. The vessel was then pressurized to 4 atm H_2. The reaction mixtures were stirred at rt for 3 h. The reaction vessel was depressurized and opened to air. The catalysts were removed by passing aliquots through Florisil® plugs, with DCM, into 15 mL vials. Volatiles were removed using a rotary evaporator. The reaction aliquots were analyzed using NMR and GC–MS.

2.4.2.2 Synthesis of Na Bases

The NaOEt and NaO^{i}Pr were always prepared the day prior to hydrogenation. Although time consuming, this was done because both bases would change colour over time. NaOEt would turn from white to yellow and NaO^{i}Pr would turn from white to pink.

A 100 mL Schlenk flask, with a stir bar and reflux condenser, was attached to a N$_2$ Schlenk line. The reflux condenser was attached to a bubbler via adapter. The flask was evacuated and refilled with N$_2$ in triplicate. Freshly cut Na metal (0.1–0.2 g, 4–9 mmol) was placed into the 100 mL Schlenk flask. Under N$_2$ pressure, the flask was sealed with a septum and the reflux condenser was sealed with a small dry RBF. The flask and condenser were evacuated and refilled with N$_2$. Freshly distilled and deaerated EtOH or ^{i}PrOH (20 mL) was then transferred, via cannula, into the Schlenk flask. With N$_2$ pressure, from the side-arm, the reflux condenser was reconnected to the Schlenk flask. The valve of the side-arm was closed, and the bubbler was used to constantly purge with N$_2$. The solution was stirred and refluxed at the alcohol's boiling point until no Na metal was visible. The solution was refluxed for a further 10 min and then cooled to rt. The side-arm's valve was opened, and the condenser was quickly replaced with a septum. The Schlenk flask was then placed under a medium vacuum (0.4 Torr) and the excess alcohol was removed to produce a white powder. The white powder was dried overnight (12–18 h) under the medium vacuum (0.4 Torr).

The chiral base sodium (*S*)-(+)-1-methoxy-2-propanoxide (**184**) was prepared in a similar manner as above, but on a smaller scale with (*S*)-(+)-1-methoxy-2-propanol and no refluxing.

Inside a glovebox, $[Ru(1\text{-}3{:}5,6\text{-}\eta^5\text{-}C_8H_{11})(\eta^6\text{-anthracene})]BF_4$ (**177**, 3.4 mg, 7.2 μmol) and $(1R,2R)\text{-}N,N'\text{-bis}\{2\text{-}[bis(3,5\text{-dimethylphenyl})phosphino]benzyl\}cyclohexane\text{-}1,2\text{-diamine}$ (**174**, 6.1 mg, 7.9 μmol, 1.1 equiv) were weighed into each reaction test tube (≤8). Each test tube contained a 6 mm magnetic stir bar. Freshly prepared NaO^iPr (147.4 mg, 1.796 mmol, 250 equiv) or NaOEt (122.2 mg, 1.796 mmol, 250 equiv) was weighed into a 100 mL Schlenk flask, inside the glovebox. The test tubes and Schlenk flask were sealed with 14/20 rubber septa and brought out of the glovebox. On a Schlenk line, THF or DME (0.5 mL) was syringed into each test tube under Ar pressure. The test tubes were stirred and heated at 60 °C, under Ar, for 30 min. During this heating, a custom test tube fitted with a 24/40 septum was placed in the central well of the machined block inside the pressure vessel. A long double-tipped needle was used to connect an empty Schlenk flask, on a Schlenk line, to the custom tube. This needle was also passed through a 14/20 septum in the gauge adapter of the lid. The lid was held over the pressure vessel with a clamp. The central custom tube was evacuated and refilled with Ar several times, and then flushed with ~1 atm H_2. On a Schlenk line, THF or DME (5.0 mL) was syringed into the Schlenk flask with base to prepare a stock base solution (0.36 M). The NaOEt and DME mixture was sonicated for 30 min. The reaction tubes were cooled to rt, placed into the outer wells of the machined block, and connected to the central tube with small double-ended needles. H_2 was supplied under slightly positive pressure to the central custom tube using the long needle passed through the lid. Each reaction tube's septum was pierced with an 18-gauge vent needle to allow H_2 to flush from the central tube through the reaction tubes. H_2 was flushed in this manner through the reaction tubes for 5 min. The esters (0.359 mmol, 50 equiv) were weighed in air into NMR tubes. The tubes were sealed with septa and purged with Ar or N_2. Dry, deaerated THF or DME was then transferred though a cannula into the NMR tubes (1.0 mL total). These solutions

were then transferred, through cannulas, to their corresponding reaction tube with H_2 pressure. The stock base solution (0.50 mL, 25 equiv) was added to each reaction tube in the pressure vessel using a syringe. The lid of the pressure vessel was lowered, sealed, and the vessel was flushed with H_2 from the pressure vessel feed line for 5 min. Then, while flushing with H_2, the long needle supplying H_2 to the central tube was removed and the septum in the gauge adapter was replaced with the gauge. The vessel was then pressurized to 4 atm H_2. The THF reaction mixtures were stirred at rt for 4 h. The DME reaction mixtures were stirred at rt for 1 h. The reactions were depressurized and opened to air. 1,3,5-Trimethoxybenzene in THF or DME (0.14 M) was syringed (0.5 mL) into each reaction mixture. Aliquots were passed through Florisil® plugs, with DCM, into 15 mL vials. Volatiles were removed using a rotary evaporator. The aliquots were then analyzed using NMR and GC–MS.

2.4.2.4 Synthesis of (±)-Ethyl 2-phenoxypropionates
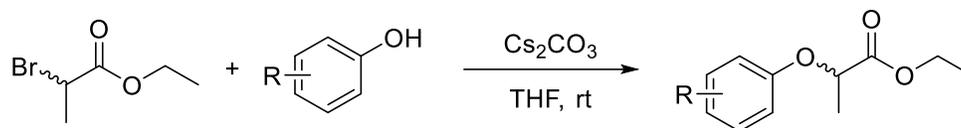
Scheme 2-38. General reaction for synthesis of (±)-ethyl 2-phenoxypropionates.

Two general procedures were used for the synthesis of racemic ethyl 2-phenoxypropionates. The general procedures were modified from a literature procedure[162] and not optimized. The two procedures are based on whether the phenol is a solid or a liquid.

Solid Phenol Procedure:

Ethyl 2-bromopropionate (3.0 g, 17 mmol) was weighed into a 15 mL vial. An oven-dried 100 mL RBF, equipped with a magnetic stir bar, was charged with Cs_2CO_3 (5.5–7.5 g, 17–23 mmol, 1.0–1.4 equiv) and a solid phenol (1.5–3.5 g, 16–18 mmol, 0.94–1.1 equiv). Phenols were weighed inside a fume hood. The phenol was dissolved in 10.0 mL of dry THF.

Dry THF (5.0 mL) was added to the ester and the solution was transferred dropwise, by a disposable pipet, to the RBF. Additional THF (2 × 5.0 mL) was used to quantitatively transfer the solution to the reaction mixture. The reaction mixture was stirred overnight (12–18 h) at rt. The reaction was filtered into a 250 mL RBF with DCM as eluent. Volatiles were removed using a rotary evaporator. A crude oil was then passed through an Al_2O_3 plug, with DCM as eluent, into a 25 mL RBF. The DCM was removed using a rotary evaporator. The crude product was purified by distillation under a medium vacuum (0.4 Torr).

Liquid Phenol Procedure:

Ethyl 2-bromopropionate (3.0 g, 17 mmol) was weighed into a 15 mL vial. An oven-dried 100 mL RBF, equipped with a magnetic stir bar, was charged with Cs_2CO_3 (5.4–7.7 g, 17–24 mmol, 1.0–1.4 equiv). A liquid phenol (1.8–2.3 g, 16–19 mmol, 0.95–1.1 equiv) was weighed, inside a fume hood, into a 15 mL vial. Dry THF (5.0 mL) was added to the phenol. The phenol was then added, by disposable pipet, to the Cs_2CO_3. Additional THF (2 × 2.5 mL) was used to quantitatively transfer the phenol. Dry THF (5.0 mL) was added to the ester and the solution was transferred dropwise, by a disposable pipet, to the RBF. Additional THF (2 × 5.0 mL) was used to quantitatively transfer the solution to the reaction mixture. The reaction mixture was stirred overnight (12–18 h) at rt. The reaction was filtered into a 250 mL RBF with DCM as eluent. Volatiles were removed using a rotary evaporator. A crude oil was then passed through an Al_2O_3 plug, with DCM as eluent, into a 25 mL RBF. The DCM was removed using a rotary evaporator. The crude product was purified by distillation under a medium vacuum (0.4 Torr).

2.4.2.5 Synthesis of Racemic Alcohols
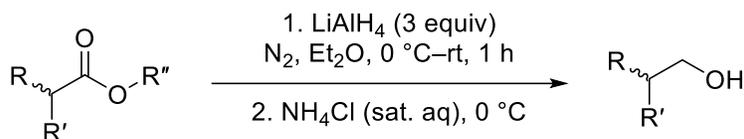
Scheme 2-39. General reaction for racemic alcohol synthesis.

A similar procedure was previously reported for the synthesis of (±)-2-phenoxypropan-1-ol from (±)-ethyl 2-phenoxypropionate.[163]

A racemic ester (149–218 mg, 0.64–1.06 mmol) was weighed into a 15 mL vial. An oven-dried 100 mL RBF, equipped with a stir bar, was brought into a glovebox. LiAlH$_4$ (72–119 mg, 1.9–3.1 mmol, ~3 equiv) was weighed out into the RBF. The RBF was sealed with a septum and brought outside the glovebox. A double-tipped needle from a Schlenk flask, under N$_2$ and attached to a bubbler, was pierced through the septum of the RBF. The RBF was cooled to 0 °C using an ice-water bath. Distilled Et$_2$O (10.0 mL) was syringed into the RBF. Et$_2$O (5.0 mL) was added to the ester via syringe. The ester was then added dropwise into the RBF via syringe. Additional Et$_2$O (2 × 2.5 mL) was used to ensure quantitative transfer. The sides of the RBF were rinsed with additional Et$_2$O (5.0 mL). The ice-water bath was removed, and the reaction was stirred for 1 h under N$_2$. The reaction mixture was then cooled to 0 °C. A saturated NH$_4$Cl solution (0.5 mL) was syringed into the RBF dropwise. The mixture was stirred until bubbles were not produced. The double-tipped needle and septum were removed. The reaction mixture was filtered, in air, into a 250 mL RBF, with DCM as eluent. Volatiles were removed using a rotary evaporator. DCM (20 mL) was added to the product and the solution transferred to a separatory funnel. The organic layer was washed with distilled H$_2$O (4 × 50 mL). The organic layer was dried over Na$_2$SO$_4$ and filtered, with DCM as eluent, into a 250 mL RBF. DCM was removed via rotary evaporator. The product was then passed through an Al$_2$O$_3$ plug, with DCM

as eluent, into a 15 mL vial. Most of the DCM was then removed via rotary evaporator. The

product was placed, with the vial open, in a fume hood overnight (12–18 h) to remove volatiles.

The racemic products were weighed and analyzed by NMR and GC–MS.

2.4.3 Syntheses and Spectroscopic Data

The NMR spectra, mass spectra, and GC chromatograms of the synthesized compounds

are not included due to their volume. The exception being the deuteration experiment's ^{2}H and

^{1}H NMR spectra (Figure 2-12 and 2-13, respectively). The data from the spectra and

chromatograms are reported below. To view most of the acquired spectra and chromatograms,

please refer to the supporting information (S39-S188) of the published version of this chapter.[145]

2.4.3.1 Ru-Based Precursors and Ligand

cis-[Ru(MeCN)$_2$(η^3-C$_3$H$_5$)(COD)]BF$_4$ (**172**) and *trans*-[RuCl$_2$(NBD)(py)$_2$] (**175**) are

readily available precursors in the Bergens group. Bergens and co-workers reported the

syntheses of **172**[164] and **175**[165] in 2004 and 2003, respectively.

[Ru(Cl)$_2$(1*R*,2*R*)-*N*,*N*′-bis{2-[bis(3,5-dimethylphenyl)phosphino]benzyl}cyclohexane-1,2-diamine] (176)
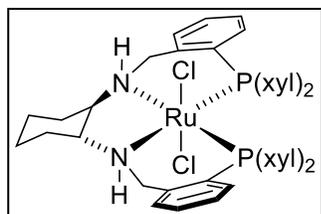
trans-[RuCl$_2$(NBD)(py)$_2$] (**175**, 48.9 mg, 0.116 mmol) was weighed, into a 11 mL vial. The vial was slowly evacuated and refilled with Ar in triplicate. The Ru precursor was dissolved in 3 mL of distilled and

deaerated DCM and then transferred, via cannula, into a triply evacuated and refilled 50 mL

Schlenk bomb. A 2 mL DCM rinse was used for quantitative transfer. (1*R*,2*R*)-*N*,*N*′-Bis{2-

[bis(3,5-dimethylphenyl)phosphino]benzyl}cyclohexane-1,2-diamine (89.8 mg, 0.116 mmol,

1.00 equiv) was weighed, inside a glovebox, into an NMR tube. The NMR tube was sealed with

a septum and brought out of the glovebox. The ligand was quantitatively transferred, via cannula,

into the Schlenk bomb using DCM (3 × 1 mL). The reaction was stirred and heated to 45 °C. The

plug valve was sealed, and the reaction cooled to 40 °C. The reaction was stirred at 40 °C for 18

hours. At rt, the reaction mixture was transferred, through a cannula, into a 100 mL Schlenk flask

with excess DCM. The DCM was removed under a medium vacuum (0.4 Torr) to produce a

reddish-orange solid (109.3 mg, >99% yield). The product contained a mixture of *cis*- and *trans*-

dichloride (57% *cis* and 43% *trans* by $^{31}P\{^1H\}$ NMR spectroscopy). **$^{31}P\{^1H\}$ NMR** (161.839

MHz, CDCl$_3$, 27 °C): δ 42.8 (d, 1P, J_{PP} = 29.6 Hz), 42.8 (s, 2P), 50.6 (d, 1P, J_{PP} = 29.6 Hz).

Purification via recrystallization with DCM and hexanes were unsuccessful. The *trans*-dichloride

was isolated (25.0 mg, 23% yield) by passing the mixture through a 10 mL Al$_2$O$_3$ plug with 20

mL of DCM. **^1H NMR** (499.788 MHz, CD$_2$Cl$_2$, 27 °C): δ 1.13–1.20 (m, 2H), 1.28–1.31 (m, 2H),

1.84–1.91 (m, 2H), 1.96 (s, 12H), 2.05 (s, 12H), 2.80–2.82 (m, 2H), 2.92–3.00 (m, 2H),

3.89–3.93 (m, 2H), 4.11–4.15 (m, 2H), 4.64–4.69 (m, 2H), 6.78–7.33 (m, 20H). **$^{31}P\{^1H\}$ NMR**

(201.641 MHz, CD$_2$Cl$_2$, 27 °C): δ 43.2 (s, 2P). **HRMS (ESI) *m/z***: Calcd for C$_{52}$H$_{60}$Cl$_2$N$_2$P$_2$^{102}Ru

[M]$^+$: 946.2647. Found: 946.2652.

[Ru(1-3:5,6-η^5-C$_8$H$_{11}$)(η^6-anthracene)]BF$_4$ (177)
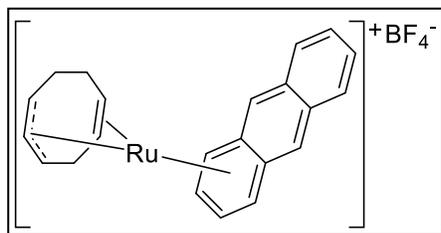
[Ru(COD)Cl$_2$]$_n$ (10.051 g, 35.876 mmol) was weighed into a

500 mL Schlenk flask. The flask was evacuated and refilled

with N$_2$ in triplicate. Distilled Et$_2$O (50 mL) was added to

the Schlenk flask. An ether solution of allylmagnesium

bromide (1.45 M, 150 mL, ~6 equiv) was delivered, through a cannula, into the 500 mL Schlenk

flask and the mixture was stirred overnight (12–18 h). The reaction was cooled to 0 °C using an

ice-water bath. Distilled and deaerated H$_2$O (100 mL) was added to the mixture. The mixture

was stirred for 30 min. The organic layer was transferred to a 500 mL Schlenk flask containing

MgSO$_4$ and a stir bar. The mixture was stirred for 30 min. The dried organic layer was filtered,

via cannula filtration, into a dry 500 mL Schlenk flask. Excess Et$_2$O was used to ensure

quantitative transfer. The Et$_2$O was removed under a medium vacuum (0.4 Torr) to leave a black

solid. The solid was sublimed at 70 °C under vacuum to produce a yellow powder (8.418 g,

81%) of [Ru(η^3-C$_3$H$_5$)$_2$(COD)]. [Ru(η^3-C$_3$H$_5$)$_2$(COD)] (1.738 g, 5.965 mmol) and anthracene

(1.063 g, 5.965 mmol, 1.000 equiv) were weighed into a 250 mL Schlenk flask inside a

glovebox. On a Schlenk line, DCM (70 mL) was added. Tetrafluoroboric acid diethyl ether

complex (0.84 mL, 6.0 mmol, 1.0 equiv) was mixed with 5 mL of DCM in a 100 mL Schlenk

flask under N$_2$. The acid solution was added dropwise to the 250 mL Schlenk tube, via cannula,

to produce a red solution. A black precipitate formed. The solvent was filtered, via cannula

filtration, into a 250 mL Schlenk flask. The black solid was washed with Et$_2$O (15 mL) in

triplicate. The washes were filtered, via cannula filtration, into the filtrate, where more solid

formed. The solids were recrystallized with DCM and Et$_2$O. The product was obtained as a dark

reddish-orange solid (1.581 g) in 56% yield. **^{1}H NMR** (499.788 MHz, CD$_2$Cl$_2$, 27 °C): δ

1.16–1.29 (m, 1H), 1.76–1.88 (m, 2H), 2.06–2.10 (m, 1H), 2.23–2.28 (m, 1H), 2.57–2.62 (m,

1H), 2.65–2.71 (m, 1H), 3.90–3.94 (m, 1H), 4.06 (t, J = 7.2 Hz, 1H), 4.76–4.79 (m, 1H),

5.01–5.06 (m, 1H), 6.39 (t, J = 5.9 Hz, 1H), 6.63–6.67 (m, 2H), 6.87 (d, J = 6.3 Hz, 1H),

7.61–7.64 (m, 2H), 8.03–8.08 (m, 2H), 8.39 (s, 1H), 8.53 (s, 1H). **^{13}C{^{1}H} NMR** (125.688 MHz,

CD$_2$Cl$_2$, 27 °C): δ 19.9, 27.7, 33.8, 35.3, 36.5, 74.0, 80.0, 87.4, 87.8, 88.6, 91.6, 91.8, 102.6,

103.6, 126.9, 128.2, 128.3, 128.3, 128.4, 128.5, 135.2, 135.7. **HRMS (ESI)** *m/z*: Calcd for

C$_{22}$H$_{21}$^{102}Ru [M]$^+$: 387.0681. Found: 387.0682.

(1*R*,2*R*)-*N*,*N*′-bis{2-[bis(3,5-di-*tert*-butyl-4-methoxyphenyl)phosphino]benzyl}cyclohexane-1,2-diamine (183)
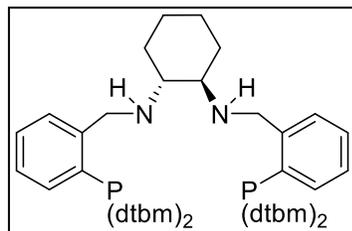
Inside a glovebox, a 100 mL Schlenk flask, equipped with a stir bar, was charged with (1*R*,2*R*)-(-)-DACH (8.6 mg, 0.076 mmol), 2-[bis(dtbm)phosphino]benzaldehyde (86.9 mg, 0.151 mmol, 2 equiv), and activated molecular sieves (4 Å, 23 mg). The Schlenk flask was sealed with a septum and brought out of the glovebox. On a N_2 Schlenk line, ~20 mL of EtOH was added, through a cannula, into the Schlenk flask. Freshly distilled and deaerated triethylamine (25 μL, ~2 equiv) was syringed into the Schlenk flask. The reaction was stirred at rt, under N_2, to completion (7 days). The reaction mixture was filtered, via cannula filtration, into a triply evacuated and N_2 refilled 100 mL Schlenk flask. Volatiles were removed using a medium vacuum (0.4 Torr) to produce a yellow solid. The yellow solid was dissolved in DCM (~5 mL). The dissolved compound was transferred, through a cannula, to a tall, triply evacuated and N_2 refilled, 50 mL Schlenk tube with a stir bar. Quantitative transfer was ensured by using excess DCM (~5 mL). The organic phase was washed with triply distilled and deaerated H_2O (4 × ~10 mL). The organic layer was transferred, through a cannula, into a triply evacuated and N_2 refilled Schlenk flask containing Na_2SO_4. The dried organic phase was filtered, via cannula filtration, into a triply evacuated and N_2 refilled 100 mL Schlenk flask. Quantitative transfer was ensured by using excess DCM (4 × ~10 mL). The DCM was removed using a medium vacuum (0.4 Torr) to produce a yellow solid. The yellow solid was dissolved in EtOH (~10 mL). A 250 mL Schlenk bomb, with a stir bar, was charged with $NaBH_4$ (45.4 mg, 1.20 mmol, ~16 equiv), inside a glovebox. The Schlenk bomb was sealed, brought out of the glovebox, and attached to an Ar bubbler. The plug valve of the Schlenk bomb was replaced with a septum. The Schlenk bomb was slowly evacuated and refilled with Ar in triplicate. The yellow EtOH solution was transferred, through a cannula, into the Schlenk bomb. Quantitative transfer was ensured by

using excess EtOH (2 × ~5 mL). The septum was replaced with the plug valve under Ar pressure. The system was purged with Ar through the bubbler. The reaction was stirred and heated to 85 °C. The plug valve was sealed, and the reaction cooled to 80 °C. The reaction was stirred at 80 °C overnight (12–18 h). The reaction was cooled to rt and plug valve replaced with a septum. The reaction was quenched with triply distilled and deaerated H_2O (~10 mL). DCM (~30 mL) was added to extract the product. The mixture was stirred for 15 min and the layers allowed to separate. The aqueous layer was decanted off. The organic layer was then washed with a saturated solution of NH_4Cl (~20 mL), which was made from the triply distilled H_2O. The mixture was stirred for 10 min and the layers allowed to separate. The aqueous layer was decanted off. The organic layer was washed with more triply distilled H_2O (3 × ~10 mL). After washing, the organic layer was filtered, via cannula filtration, into a triply evacuated and N_2 refilled 100 mL Schlenk flask, which contained Na_2SO_4. Additional DCM (~10 mL) was used to ensure quantitative transfer. After 30 min, the dried organic phase was transferred by filtration, via cannula filtration, into a triply evacuated and N_2 refilled 100 mL Schlenk flask. Additional DCM (3 × ~10 mL) was used to ensure quantitative transfer. The DCM was removed using a medium vacuum (0.4 Torr) to produce a pale-yellow solid. The purified product was dissolved in minimal DCM and transferred, through a cannula, to a weighed Ar purged NMR tube. Visible solvent was evaporated with a stream of Ar and the tube placed under vacuum to remove trace DCM. The NMR tube was refilled with Ar and reweighed. The product was obtained as a pale-yellow solid (92.3 mg) in >99% yield. **^{1}H NMR** (498.119 MHz, CD_2Cl_2, 27 °C): δ 1.07 (br, 4H), 1.32 (s, 36H), 1.33 (s, 36H), 1.34 (br, 2H), 1.62 (br, 2H), 1.96 (br, 2H), 2.39 (br, 2H), 3.69 (s, 6H), 3.70 (s, 6H), 4.02–4.18 (m, 4H), 6.89–6.91 (m, 2H), 7.07–7.11 (m, 8H), 7.20–7.23 (m, 2H), 7.29–7.32 (m, 2H), 7.59–7.62 (m, 2H). **^{31}P{^{1}H} NMR** (201.641 MHz, CD_2Cl_2, 27 °C): δ -16.1 (s,

2P). **HRMS (ESI)** *m/z*: Calcd for $C_{80}H_{117}N_2O_4P_2$ [M+H]$^+$: 1231.8483. Found: 1231.8471. **Anal.**

Calcd for $C_{80}H_{116}N_2O_6P_2$ (Oxidized phosphines): C, 76.03; H, 9.25; N, 2.22. Found: C, 75.66; H,

9.23; N, 2.22.

2.4.3.2 Esters and Aldehyde

(±)-Ethyl 2-phenoxypropionate (171)
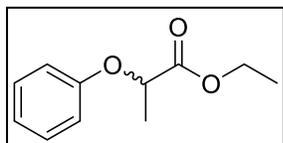
Prepared according to the Solid Phenol Procedure from ethyl

2-bromopropionate (3.04 g, 16.8 mmol), Cs_2CO_3 (5.95 g, 18.3 mmol,

1.09 equiv), and phenol (1.54 g, 16.4 mmol, 0.974 equiv). The crude

product was purified by distillation at 84 °C under a medium vacuum (0.4 Torr). Purified product

was isolated as a colourless oil in 77% yield. **^{1}H NMR** (499.797 MHz, CDCl$_3$, 27.0 °C): δ 1.26

(t, *J* = 7.2 Hz, 3H), 1.63 (d, *J* = 6.8 Hz, 3H), 4.23 (q, *J* = 7.1 Hz, 2H), 4.76 (q, *J* = 6.8 Hz, 1H),

6.89–6.91 (m, 2H), 6.98 (tt, *J* = 7.4, 1.1 Hz, 1H), 7.26–7.31 (m, 2H). **^{13}C{^{1}H} NMR** (125.688

MHz, CDCl$_3$, 27.0 °C): δ 14.1, 18.6, 61.2, 72.6, 115.1, 121.5, 129.5, 157.6, 172.2. **HRMS (EI)**

m/z: Calcd for $C_{11}H_{14}O_3$ [M]$^+$: 194.0943. Found: 194.0942. **Anal.** Calcd for $C_{11}H_{14}O_3$: C, 68.02;

H, 7.27. Found: C, 68.18; H, 7.32.

Large-Scale Synthesis of (±)-Ethyl 2-phenoxypropionate (171)
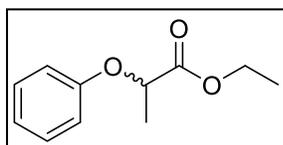
A modified procedure of the Solid Phenol Procedure was performed.

Ethyl 2-bromopropionate (20.0 g, 0.110 mol) was weighed into a 15 mL

vial. An oven-dried 250 mL RBF, equipped with a magnetic stir bar, was

charged with Cs_2CO_3 (39.7 g, 0.122 mol, 1.10 equiv) and phenol (11.5 g, 0.122 mol, 1.10 equiv).

The phenol was weighed inside a fume hood. The phenol was dissolved in 50 mL of dry THF.

The ester was transferred dropwise, by a disposable pipet, to the RBF. Additional THF (15 mL)

was used to quantitatively transfer the solution to the reaction mixture. A further 15 mL of THF

was used to rinse the sides of the RBF. The reaction mixture was stirred for 22 h at rt. The reaction was filtered into a 250 mL RBF with DCM as eluent. Volatiles were removed, using a rotary evaporator, to produce a crude oil. The crude oil was then passed through an Al_2O_3 syringe (5 mL), with DCM as eluent. The DCM was removed using a rotary evaporator. The crude product was purified by distillation at 84 °C under a medium vacuum (0.4 Torr). Purified product was isolated as a colourless oil in 77% yield. Spectroscopic data matched that of the smaller-scale synthesis.

(±)-Ethyl 2-(4-fluorophenoxy)propionate
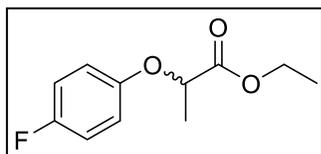
Prepared according to the Solid Phenol Procedure from ethyl 2-bromopropionate (3.00 g, 16.6 mmol), Cs_2CO_3 (5.95 g, 18.3 mmol, 1.10 equiv), and 4-fluorophenol (1.86 g, 16.6 mmol, 1.00 equiv). The crude product was purified by distillation at 120 °C under a medium vacuum (0.4 Torr). Purified product was isolated as a colourless oil in 54% yield. **^{1}H NMR** (499.797 MHz, CDCl$_3$, 27.0 °C): δ 1.24 (t, J = 7.1 Hz, 3H), 1.60 (d, J = 6.9 Hz, 3H), 4.16–4.25 (m, 2H), 4.67 (q, J = 6.8 Hz, 1H), 6.81–6.85 (m, 2H), 6.93–6.98 (m, 2H). **^{13}C{^{1}H} NMR** (125.688 MHz, CDCl$_3$, 27.0 °C): δ 14.1, 18.5, 61.3, 73.4, 115.9 (d, J = 23.1 Hz), 116.5 (d, J = 8.1 Hz), 153.7 (d, J = 2.3 Hz), 157.7 (d, J = 239.5 Hz), 172.0. **^{19}F NMR** (376.318 MHz, CDCl$_3$, 27.0 °C): δ -122.8. **HRMS (EI)** *m/z*: Calcd for $C_{11}H_{13}FO_3$ [M]$^+$: 212.0849. Found: 212.0849. **Anal.** Calcd for $C_{11}H_{13}FO_3$: C, 62.26; H, 6.17. Found: C, 61.91; H, 6.20.

(±)-Ethyl 2-(4-chlorophenoxy)propionate

Prepared according to the Solid Phenol Procedure from ethyl 2-bromopropionate (3.00 g, 16.6 mmol), Cs_2CO_3 (5.94 g, 18.2 mmol, 1.10 equiv), and 4-chlorophenol (2.13 g, 16.6 mmol, 1.00 equiv).

The crude product was purified by distillation at 93 °C under a medium vacuum (0.4 Torr). Purified product was isolated as a colourless oil in 49% yield. **^{1}H NMR** (499.797 MHz, CDCl$_3$, 27.0 °C): δ 1.25 (t, J = 7.2 Hz, 3H), 1.62 (d, J = 6.8 Hz, 3H), 4.22 (q, J = 7.2 Hz, 2H), 4.70 (q, J = 6.8 Hz, 1H), 6.80–6.83 (m, 2H), 7.21–7.24 (m, 2H). **^{13}C{^{1}H} NMR** (125.688 MHz, CDCl$_3$, 27.0 °C): δ 14.1, 18.5, 61.4, 73.0, 116.5, 126.5, 129.4, 156.2, 171.8. **HRMS (EI) *m/z*:** Calcd for $C_{11}H_{13}ClO_3$ [M]$^+$: 228.0553. Found: 228.0557. **Anal.** Calcd for $C_{11}H_{13}ClO_3$: C, 57.78; H, 5.73. Found: C, 57.69; H, 5.62.

(±)-Ethyl 2-(4-bromophenoxy)propionate
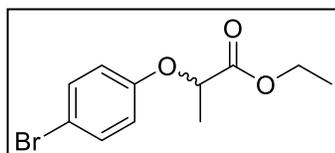
Prepared according to the Solid Phenol Procedure from ethyl 2-bromopropionate (3.00 g, 16.6 mmol), Cs_2CO_3 (5.96 g, 18.3 mmol, 1.10 equiv), and 4-bromophenol (2.87 g, 16.6 mmol, 1.00 equiv).

The crude product was purified by distillation at 129 °C under a medium vacuum (0.4 Torr). Purified product was isolated as a colourless oil in 57% yield. **^{1}H NMR** (499.797 MHz, CDCl$_3$, 27.0 °C): δ 1.25 (t, J = 7.1 Hz, 3H), 1.61 (d, J = 6.8 Hz, 3H), 4.21 (q, J = 7.2 Hz, 2H), 4.70 (q, J = 6.8 Hz, 1H), 6.74–6.78 (m, 2H), 7.35–7.38 (m, 2H). **^{13}C{^{1}H} NMR** (125.688 MHz, CDCl$_3$, 27.0 °C): δ 14.1, 18.5, 61.4, 72.9, 113.8, 116.9, 132.3, 156.7, 171.8. **HRMS (EI) *m/z*:** Calcd for $C_{11}H_{13}BrO_3$ [M]$^+$: 272.0048 and 274.0028. Found: 272.0045 and 274.0028. **Anal.** Calcd for $C_{11}H_{13}BrO_3$: C, 48.37; H, 4.80. Found: C, 48.45; H, 4.84.

(±)-Ethyl 2-(4-iodophenoxy)propionate
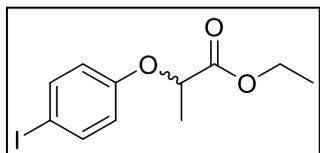
Prepared according to the Solid Phenol Procedure from ethyl 2-bromopropionate (3.04 g, 16.8 mmol), Cs_2CO_3 (5.49 g, 16.8 mmol, 1.00 equiv), and 4-iodophenol (3.47 g, 15.8 mmol, 0.941 equiv). The crude product was purified by distillation at 118 °C under a medium vacuum (0.4 Torr). Purified product was isolated as a colourless oil in 65% yield. **¹H NMR** (499.797 MHz, CDCl₃, 27.0 °C): δ 1.26 (t, $J = 7.2$ Hz, 3H), 1.62 (d, $J = 6.8$ Hz, 3H), 4.22 (q, $J = 7.2$ Hz, 2H), 4.70 (q, $J = 6.8$ Hz, 1H), 6.65–6.68 (m, 2H), 7.54–7.57 (m, 2H). **¹³C{¹H} NMR** (125.688 MHz, CDCl₃, 27.0 °C): δ 14.1, 18.5, 61.4, 72.7, 83.8, 117.5, 138.3, 157.5, 171.8. **HRMS (ESI)** *m/z*: Calcd for $C_{11}H_{13}INaO_3$ [M+Na]⁺: 342.9802. Found: 342.9800. **Anal.** Calcd for $C_{11}H_{13}IO_3$: C, 41.27; H, 4.09. Found: C, 41.25; H, 4.17.

(±)-Ethyl 2-(4-methoxyphenoxy)propionate
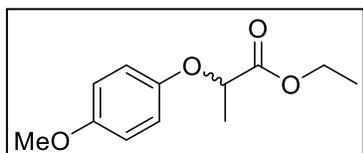
Prepared according to the Solid Phenol Procedure from ethyl 2-bromopropionate (3.04 g, 16.8 mmol), Cs_2CO_3 (7.49 g, 23.0 mmol, 1.37 equiv), and 4-methoxyphenol (2.26 g, 18.2 mmol, 1.09 equiv). The crude product was purified by distillation at 105 °C under a medium vacuum (0.4 Torr). Purified product was isolated as a colourless oil in 76% yield. **¹H NMR** (499.797 MHz, CDCl₃, 27.0 °C): δ 1.26 (t, $J = 7.2$ Hz, 3H), 1.60 (d, $J = 6.8$ Hz, 3H), 3.76 (s, 3H), 4.20–4.24 (m, 2H), 4.66 (q, $J = 6.8$ Hz, 1H), 6.80–6.86 (m, 4H). **¹³C{¹H} NMR** (125.688 MHz, CDCl₃, 27.0 °C): δ 14.1, 18.6, 55.6, 61.2, 73.7, 114.6, 116.5, 151.7, 154.5, 172.4. **HRMS (ESI)** *m/z*: Calcd for $C_{12}H_{16}NaO_4$ [M+Na]⁺: 247.0941. Found: 247.0941. **Anal.** Calcd for $C_{12}H_{16}O_4$: C, 64.27; H, 7.19. Found: C, 64.03; H, 7.24.

(±)-Ethyl 2-(3-methoxyphenoxy)propionate
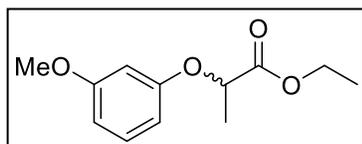
Prepared according to the Liquid Phenol Procedure from ethyl 2-bromopropionate (3.04 g, 16.8 mmol), Cs_2CO_3 (7.67 g, 23.6 mmol, 1.40 equiv), and 3-methoxyphenol (2.29 g, 18.5 mmol, 1.10 equiv). The crude product was purified by distillation at 108 °C under a medium vacuum (0.4 Torr). Purified product was isolated as a colourless oil in 79% yield. **¹H NMR** (499.797 MHz, CDCl₃, 27.0 °C): δ 1.26 (t, J = 7.2 Hz, 3H), 1.62 (d, J = 6.8 Hz, 3H), 3.78 (s, 3H), 4.23 (q, J = 7.1 Hz, 2H), 4.74 (q, J = 6.8 Hz, 1H), 6.46 (ddd, J = 8.2, 2.4, 0.8 Hz, 1H), 6.48 (t, J = 2.3 Hz, 1H), 6.54 (ddd, J = 8.2, 2.4, 0.8 Hz, 1H), 7.16 (t, J = 8.2 Hz, 1H). **¹³C{¹H} NMR** (125.688 MHz, CDCl₃, 27.0 °C): δ 14.1, 18.5, 55.2, 61.2, 72.6, 101.7, 106.8, 107.4, 129.9, 158.8, 160.9, 172.1. **HRMS (ESI)** *m/z*: Calcd for $C_{12}H_{16}NaO_4$ [M+Na]⁺: 247.0941. Found: 247.0941. **Anal.** Calcd for $C_{12}H_{16}O_4$: C, 64.27; H, 7.19. Found: C, 64.39; H, 7.32.

(±)-Ethyl 2-(3-fluorophenoxy)propionate
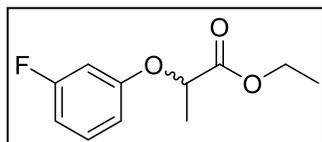
Prepared according to the Liquid Phenol Procedure from ethyl 2-bromopropionate (3.00 g, 16.6 mmol), Cs_2CO_3 (5.39 g, 16.5 mmol, 0.997 equiv), and 3-fluorophenol (1.77 g, 15.8 mmol, 0.950 equiv). The crude product was purified by distillation at 77 °C under a medium vacuum (0.4 Torr). Purified product was isolated as a colourless oil in 76% yield. **¹H NMR** (499.797 MHz, CDCl₃, 27.0 °C): δ 1.26 (t, J = 7.2 Hz, 3H), 1.62 (d, J = 6.9 Hz, 3H), 4.23 (q, J = 7.2 Hz, 2H), 4.73 (q, J = 6.9 Hz, 1H), 6.61 (dt, J = 10.7, 2.4 Hz, 1H), 6.66–6.70 (m, 2H), 7.21 (td, J = 8.3, 6.8 Hz, 1H). **¹³C{¹H} NMR** (125.688 MHz, CDCl₃, 27.0 °C): δ 14.1, 18.4, 61.4, 72.8, 103.0 (d, J = 25.1 Hz), 108.4 (d, J = 21.3 Hz), 110.6 (d, J = 2.9 Hz), 130.3 (d, J = 10.0 Hz), 158.9 (d, J = 11.1 Hz), 163.5 (d, J = 245.5 Hz), 171.7. **¹⁹F NMR** (376.318 MHz, CDCl₃, 27.0 °C): δ -111.4. **HRMS**

(EI) *m/z*: Calcd for $C_{11}H_{13}FO_3$ $[M]^+$: 212.0849. Found: 212.0849. **Anal.** Calcd for $C_{11}H_{13}FO_3$: C, 62.26; H, 6.17. Found: C, 62.34; H, 6.14.
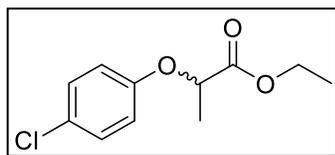
(±)-Ethyl 2-(2-chlorophenoxy)propionate
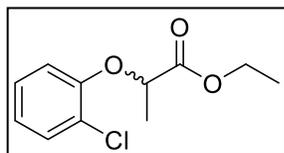
Prepared according to the Liquid Phenol Procedure from ethyl 2-bromopropionate (3.01 g, 16.6 mmol), Cs_2CO_3 (6.06 g, 18.6 mmol, 1.12 equiv), and 2-chlorophenol (2.10 g, 16.3 mmol, 0.981 equiv). The crude product was purified by distillation at 97 °C under a medium vacuum (0.4 Torr). Purified product was isolated as a colourless oil in 80% yield. **¹H NMR** (499.797 MHz, CDCl₃, 27.0 °C): δ 1.24 (t, *J* = 7.1 Hz, 3H), 1.67 (d, *J* = 6.9 Hz, 3H), 4.18–4.24 (m, 2H), 4.75 (q, *J* = 6.9 Hz, 1H), 6.85 (dd, *J* = 8.2, 1.4 Hz, 1H), 6.92 (td, *J* = 7.8, 1.4 Hz, 1H), 7.14–7.17 (m, 1H), 7.36 (dd, *J* = 7.9, 1.6 Hz, 1H). **¹³C{¹H} NMR** (125.688 MHz, CDCl₃, 27.0 °C): δ 14.1, 18.5, 61.3, 74.1, 115.3, 122.6, 123.8, 127.6, 130.5, 153.5, 171.6. **HRMS (ESI)** *m/z*: Calcd for $C_{11}H_{13}ClNaO_3$ $[M+Na]^+$: 251.0445. Found: 251.0444. **Anal.** Calcd for $C_{11}H_{13}ClO_3$: C, 57.78; H, 5.73. Found: C, 57.88; H, 5.83.

(±)-Isopropyl 2-phenoxypropionate
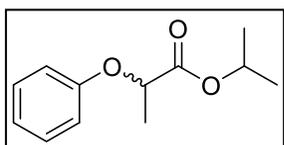
The ester was prepared as previously reported,[140] but the product was filtered through an Al_2O_3 plug, which resulted in a colourless oil. **¹H NMR** (499.797 MHz, CDCl₃, 27.0 °C): δ 1.19 (d, *J* = 6.3 Hz, 3H), 1.28 (d, *J* = 6.3 Hz, 3H), 1.62 (d, *J* = 6.8 Hz, 3H), 4.72 (q, *J* = 6.8 Hz, 1H), 5.09 (sept, *J* = 6.3 Hz, 1H), 6.88–6.90 (m, 2H), 6.97 (tt, *J* = 7.4, 1.0 Hz, 1H), 7.26–7.30 (m, 2H). **¹³C{¹H} NMR** (125.688 MHz, CDCl₃, 27.0 °C): δ 18.5, 21.6, 21.7, 68.8, 72.7, 115.1, 121.5, 129.5, 157.7, 171.8. **HRMS (EI)** *m/z*: Calcd for $C_{12}H_{16}O_3$ $[M]^+$: 208.1099. Found: 208.1099.

(±)-Ethyl 2-phenoxybutyrate (173)
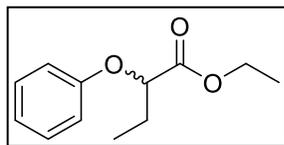
Ethyl 2-bromobutyrate (5.00 g, 25.6 mmol) was weighed into a 15 mL vial. An oven-dried 100 mL RBF, equipped with a magnetic stir bar, was charged with Cs_2CO_3 (8.44 g, 25.9 mmol, 1.01 equiv) and phenol (2.41 g, 25.7 mmol, 1.00 equiv). Phenol was weighed inside a fume hood. The phenol was dissolved in 10 mL of dry THF. Dry THF (5 mL) was added to the ester and the solution was transferred dropwise, by a disposable pipet, to the RBF. Additional THF (2×5 mL) was used to quantitatively transfer the solution to the reaction mixture. The reaction mixture was stirred overnight (12–18 h) at rt. The reaction was filtered into a 250 mL RBF with DCM as eluent. Volatiles were removed using a rotary evaporator. A crude oil was then passed through an Al_2O_3 plug, with DCM as eluent, into a 25 mL RBF. The DCM was removed using a rotary evaporator. The crude product was purified by distillation at 64 °C under a medium vacuum (0.4 Torr). Purified product was isolated as a colourless oil in 84% yield. **^{1}H NMR** (499.797 MHz, CDCl$_3$, 27.0 °C): δ 1.11 (t, J = 7.5 Hz, 3H), 1.26 (t, J = 7.2 Hz, 3H), 2.02 (qd, J = 7.4, 6.3 Hz, 2H), 4.21–4.25 (m, 2H), 4.58 (t, J = 6.2 Hz, 1H), 6.91–6.93 (m, 2H), 6.98 (tt, J = 7.4, 1.0 Hz, 1H), 7.26–7.31 (m, 2H). **^{13}C{^{1}H} NMR** (125.688 MHz, CDCl$_3$, 27.0 °C): δ 9.7, 14.2, 26.2, 61.1, 77.8, 115.1, 121.5, 129.5, 158.0, 171.7. **HRMS (EI)** *m/z*: Calcd for $C_{12}H_{16}O_3$ [M]$^+$: 208.1099. Found: 208.1101. **Anal.** Calcd for $C_{12}H_{16}O_3$: C, 69.21; H, 7.74. Found: C, 69.10; H, 7.60.

(±)-α-Phenoxy-isovaleric acid ethyl ester
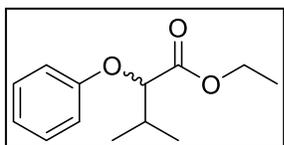
2-Bromoisovaleric acid (10.0 g, 55.3 mmol) was weighed into a 100 mL Schlenk flask equipped with a stir bar. The flask was sealed with a septum and purged with N_2. $SOCl_2$ (24 mL, 0.33 mol, 6.0 equiv) was added dropwise, to the acid, by syringe. The septum was replaced with a condenser that was

123

attached to a bubbler via adapter. The mixture was refluxed at 75 °C for 2 h under N_2. Excess

$SOCl_2$ was removed using a water aspirator. Hexanes (4×5 mL) was added to the mixture and

removed with the water aspirator. DCM (50 mL) was added to the acid chloride and the solution

cooled to 0 °C using an ice-water bath. Anhydrous EtOH (17 mL, 0.29 mol, 5.3 equiv) was

added to the acid chloride solution dropwise. The reaction mixture warmed to rt and stirred

overnight (12–18 h). The reaction was transferred to a 250 mL RBF, with excess DCM to ensure

quantitative transfer. Volatiles were removed, using a rotary evaporator, to leave a yellow oil.

DCM (50 mL) was added to the oil and the solution transferred to a separatory funnel. The

organic layer was washed with distilled H_2O (3×50 mL) and brine (50 mL). The organic layer

was dried over Na_2SO_4 and filtered, with DCM as eluent, into a 100 mL RBF. DCM was

removed using a rotary evaporator. Ethyl 2-bromoisovalerate was obtained as a yellow oil in

91% yield. Ethyl 2-bromoisovalerate (3.00 g, 14.4 mmol) was weighed into a 15 mL vial. An

oven-dried 100 mL RBF, equipped with a magnetic stir bar, was charged with Cs_2CO_3 (5.15 g,

15.8 mmol, 1.10 equiv) and phenol (1.48 g, 15.8 mmol, 1.10 equiv). Phenol was weighed inside

a fume hood. The phenol was dissolved in 10 mL of dry THF. Dry THF (5 mL) was added to the

ester and the solution was transferred dropwise, by a disposable pipet, to the RBF. Additional

THF (2×5 mL) was used to quantitatively transfer the solution to the reaction mixture. THF (5

mL) was used to rinse the sides of the RBF. The reaction mixture was stirred for 42 h at rt.

Additional Cs_2CO_3 (6.54 g, 20.1 mmol, 1.40 equiv) and phenol (2.99 g, 31.8 mmol, 2.21 equiv)

was added. The reaction mixture was stirred for a further 4 days at rt. The reaction was filtered

into a 250 mL RBF with DCM as eluent. Volatiles were removed using a rotary evaporator. A

yellow oil was then passed through two Al_2O_3 plugs, with DCM as eluent, into a 25 mL RBF.

The DCM was removed using a rotary evaporator. The crude product was purified by distillation

at 74 °C under a medium vacuum (0.4 Torr). Purified product was isolated as a colourless oil in

22% yield. **^{1}H NMR** (499.797 MHz, CDCl$_3$, 27.0 °C): δ 1.09 (d, J = 6.9 Hz, 3H), 1.12 (d, J = 6.8

Hz, 3H), 1.26 (t, J = 7.1 Hz, 3H), 2.30 (sepd, J = 6.8, 5.7 Hz, 1H), 4.23 (q, J = 7.1 Hz, 2H), 4.37

(d, J = 5.7 Hz, 1H), 6.89–6.92 (m, 2H), 6.98 (tt, J = 7.4, 1.0 Hz, 1H), 7.26–7.30 (m, 2H).

^{13}C{^{1}H} NMR (125.688 MHz, CDCl$_3$, 27.0 °C): δ 14.2, 17.9, 18.6, 31.7, 61.0, 81.7, 115.2,

121.4, 129.5, 158.3, 171.4. **HRMS (EI) *m/z*:** Calcd for C$_{13}$H$_{18}$O$_3$ [M]$^+$: 222.1256. Found:

222.1258. **Anal.** Calcd for C$_{13}$H$_{18}$O$_3$: C, 70.24; H, 8.16. Found: C, 70.50; H, 8.34.
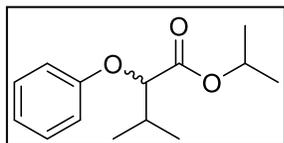
(±)-α-Phenoxy-isovaleric acid isopropyl ester

2-Bromoisovaleric acid (10.0 g, 55.3 mmol) was weighed into a 100 mL

Schlenk flask equipped with a stir bar. The flask was sealed with a

septum and purged with N$_2$. SOCl$_2$ (24 mL, 0.33 mol, 6.0 equiv) was

added dropwise, to the acid, by syringe. The septum was replaced with a condenser that was

attached to a bubbler via adapter. The mixture was refluxed at 75 °C for 2 h under N$_2$. Excess

SOCl$_2$ was removed using a water aspirator. Hexanes (2 × 10 mL) was added to the mixture and

removed with the water aspirator. DCM (50 mL) was added to the acid chloride and the solution

cooled to 0 °C using an ice-water bath. Isopropyl alcohol (22 mL, 0.29 mol, 5.2 equiv) was

added to the acid chloride solution dropwise. The reaction mixture was warmed to rt and stirred

overnight (12–18 h). The reaction was transferred to a 250 mL RBF, with excess DCM to ensure

quantitative transfer. DCM and excess isopropyl alcohol were removed, using a rotary

evaporator, to leave a yellow oil. DCM (50 mL) was added to the oil and the solution transferred

to a separatory funnel. The organic layer was washed with distilled H$_2$O (3 × 50 mL) and brine

(50 mL). The organic layer was dried over Na$_2$SO$_4$ and filtered, with DCM as eluent, into a 100

mL RBF. DCM was removed under reduced pressure using a rotary evaporator. Isopropyl

2-bromoisovalerate was obtained as a yellow oil in 80% yield. Isopropyl 2-bromoisovalerate (3.00 g, 13.5 mmol) was weighed into a 15 mL vial. An oven-dried 100 mL RBF, equipped with a magnetic stir bar, was charged with Cs_2CO_3 (4.88 g, 15.0 mmol, 1.11 equiv) and phenol (1.41 g, 14.9 mmol, 1.10 equiv). Phenol was weighed inside a fume hood. The phenol was dissolved in 10 mL of dry THF. Dry THF (5 mL) was added to the ester and the solution was transferred dropwise, by a disposable pipet, to the RBF. Additional THF (2×5 mL) was used to quantitatively transfer the solution to the reaction mixture. THF (5 mL) was used to rinse the sides of the RBF. The reaction mixture was stirred for 42 h at rt. Additional Cs_2CO_3 (5.52 g, 16.9 mmol, 1.25 equiv) and phenol (2.84 g, 30.1 mmol, 2.23 equiv) was added. The reaction mixture was stirred for a further 4 days at rt. The reaction was filtered into a 250 mL RBF with DCM as eluent. Volatiles were removed, using a rotary evaporator, to produce a crude oil. The yellow oil was then passed through two Al_2O_3 plugs, with DCM as eluent, into a 25 mL RBF. The DCM was removed using a rotary evaporator. The crude product was purified by distillation at 89 °C under a medium vacuum (0.4 Torr). Purified product was isolated as a colourless oil in 18% yield. **¹H NMR** (499.797 MHz, CDCl₃, 27.0 °C): δ 1.08 (d, J = 6.9 Hz, 3H), 1.11 (d, J = 6.9 Hz, 3H), 1.18 (d, J = 6.3 Hz, 3H), 1.28 (d, J = 6.3 Hz, 3H), 2.29 (sepd, J = 6.9, 5.9 Hz, 1H), 4.33 (d, J = 5.9 Hz, 1H), 5.11 (sept, J = 6.3 Hz, 1H), 6.89–6.91 (m, 2H), 6.95–6.98 (m, 1H), 7.25–7.29 (m, 2H). **¹³C{¹H} NMR** (125.688 MHz, CDCl₃, 27.0 °C): δ 17.9, 18.6, 21.7, 21.8, 31.6, 68.6, 81.7, 115.2, 121.3, 129.4, 158.3, 170.8. **HRMS (EI) *m/z*:** Calcd for $C_{14}H_{20}O_3$ [M]⁺: 236.1413. Found: 236.1414. **Anal.** Calcd for $C_{14}H_{20}O_3$: C, 71.16; H, 8.53. Found: C, 71.26; H, 8.69.

(±)-Butan-2-yl 2-phenoxypropionate
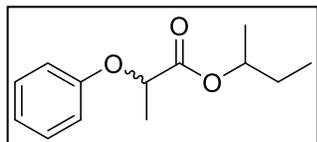
The ester was prepared from 2-phenoxypropionyl chloride (5 mL, 0.03 mol). DCM (50 mL) was added to the acid chloride and the solution cooled to 0 °C using an ice-water bath. Triethylamine (5 mL, 0.04 mol, 1 equiv) was added and then 2-butanol (15 mL, 0.16 mol, 5.1 equiv) was added dropwise. The mixture was warmed to rt and stirred overnight (12–18 h). The reaction mixture was transferred to a separatory funnel and washed with distilled H_2O (4 × 25 mL) and brine (30 mL). The organic layer was dried over Na_2SO_4 and filtered, with DCM as eluent. Volatiles were removed, using a rotary evaporator, to produce a crude oil. The crude product was purified by distillation at 81 °C under a medium vacuum (0.4 Torr). Purified product was isolated as a colourless oil in 18% yield. The product is a mixture of diastereomers (de = 14%). Major: **^{1}H NMR** (499.797 MHz, CDCl$_3$, 27.0 °C): δ 0.92 (t, J = 7.5 Hz, 3H), 1.14 (d, J = 6.3 Hz, 3H), 1.47–1.69 (m, 5H), 4.75 (q, J = 6.8 Hz, 1H), 4.88–4.96 (m, 1H), 6.88–6.91 (m, 2H), 6.95–6.98 (m, 1H), 7.25–7.29 (m, 2H). **^{13}C{^{1}H} NMR** (125.688 MHz, CDCl$_3$, 27.0 °C): δ 9.7, 18.5, 19.2, 28.7, 72.7, 73.3, 115.1, 121.4, 129.4, 157.7, 171.9. Minor: **^{1}H NMR** (499.797 MHz, CDCl$_3$, 27.0 °C): δ 0.77 (t, J = 7.5 Hz, 3H), 1.25 (d, J = 6.3 Hz, 3H), 1.47–1.69 (m, 5H), 4.75 (q, J = 6.8 Hz, 1H), 4.88–4.96 (m, 1H), 6.88–6.91 (m, 2H), 6.95–6.98 (m, 1H), 7.25–7.29 (m, 2H). **^{13}C{^{1}H} NMR** (125.688 MHz, CDCl$_3$, 27.0 °C): δ 9.4, 18.6, 19.5, 28.6, 72.6, 73.4, 115.0, 121.4, 129.5, 157.7, 172.0. Mixture: **HRMS (EI) *m/z*:** Calcd for C$_{13}$H$_{18}$O$_3$ [M]$^+$: 222.1256. Found: 222.1257. **Anal.** Calcd for C$_{13}$H$_{18}$O$_3$: C, 70.24; H, 8.16. Found: C, 70.07; H, 7.91.

(±)-Ethyl 2-phenoxy-2-phenylethanoate
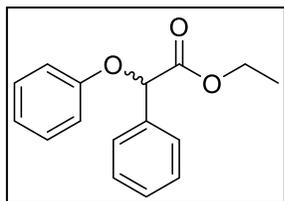
Ethyl α-bromophenylacetate (1.03 g, 4.25 mmol) was weighed into a 15 mL vial. A dried 100 mL RBF, equipped with a magnetic stir bar, was charged with Cs_2CO_3 (1.62 g, 4.97 mmol, 1.17 equiv) and phenol (0.470 g, 4.99 mmol, 1.17 equiv). Phenol was weighed inside a fume hood. The phenol was dissolved in 10 mL of dry THF. Dry THF (5 mL) was added to the ester and the solution was transferred dropwise, by a disposable pipet, to the RBF. Additional THF (2 × 5 mL) was used to quantitatively transfer the solution to the reaction mixture. The reaction mixture was stirred overnight (12–18 h) at rt. The reaction was filtered into a 250 mL RBF with DCM as eluent. Volatiles were removed using a rotary evaporator. A crude oil was then passed through an Al_2O_3 plug, with DCM as eluent, into a 25 mL RBF. The DCM was removed using a rotary evaporator. The crude product was purified by distillation at 127 °C under a medium vacuum (0.4 Torr). Purified product was isolated as a colourless oil in 54% yield. **^{1}H NMR** (499.797 MHz, CDCl$_3$, 27 °C): δ 1.23 (t, J = 7.1 Hz, 3H), 4.17–4.29 (m, 2H), 5.67 (s, 1H), 6.99–7.02 (m, 3H), 7.29–7.32 (m, 2H), 7.37–7.45 (m, 3H), 7.62–7.64 (m, 2H). **^{13}C{^{1}H} NMR** (125.688 MHz, CDCl$_3$, 27 °C): δ 14.1, 61.6, 78.7, 115.5, 121.8, 127.1, 128.8, 128.9, 129.6, 135.6, 157.4, 169.9. **HRMS (EI)** *m/z*: Calcd for $C_{16}H_{16}O_3$ [M]$^+$: 256.1100. Found: 256.1100. **Anal.** Calcd for $C_{16}H_{16}O_3$: C, 74.98; H, 6.29. Found: C, 74.72; H, 6.33.

(±)-Ethyl 2-(phenylthio)propionate (186)
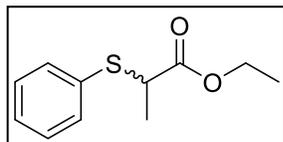
Ethyl 2-bromopropionate (3.00 g, 16.6 mmol) was weighed into a 15 mL vial. Dry THF (5 mL) was added to the 15 mL vial. A dried 100 mL RBF, equipped with a magnetic stir bar, was charged with Cs_2CO_3 (6.00 g, 18.4 mmol, 1.1 equiv) and purged with Ar for 20 min. Dry THF (10 mL) was added to the RBF by syringe. Thiophenol (1.80 mL, 17.5 mmol, 1.1 equiv), from a sure seal bottle, was syringe injected into the RBF. THF (2.5 mL) was used to ensure quantitative transfer from the syringe. A second syringe was used to inject the ester solution into the RBF. Additional THF (2 × 5 mL) was used to quantitatively transfer the solution to the reaction mixture. The reaction mixture was stirred overnight (12–18 h) at rt. The reaction was filtered into a 250 mL RBF with DCM as eluent. Volatiles were removed using a rotary evaporator. A crude oil was then passed through an Al_2O_3 plug, with DCM as eluent, into a 25 mL RBF. The DCM was removed using a rotary evaporator. The crude product was purified by distillation at 83 °C under a medium vacuum (0.4 Torr). Purified product was isolated as a colourless oil in 85% yield. **¹H NMR** (499.797 MHz, CDCl₃, 27 °C): δ 1.16 (t, J = 7.3 Hz, 3H), 1.48 (d, J = 7.1 Hz, 3H), 3.78 (q, J = 7.2 Hz, 1H), 4.07–4.13 (m, 2H), 7.25–7.31 (m, 3H), 7.45–7.47 (m, 2H). **¹³C{¹H} NMR** (125.688 MHz, CDCl₃, 27 °C): δ 14.0, 17.4, 45.2, 61.1, 127.9, 128.9, 133.0, 133.3, 172.6. **HRMS (EI)** *m/z*: Calcd for $C_{11}H_{14}O_2S$ [M]⁺: 210.0715. Found: 210.0709. **Anal.** Calcd for $C_{11}H_{14}O_2S$: C, 62.83; H, 6.71; S, 15.25. Found: C, 63.06; H, 6.80; S, 15.06.

(±)-2-Phenoxypropionaldehyde (188)
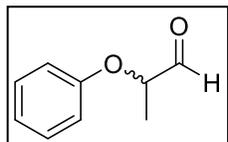
The aldehyde was prepared with modification to a previously reported procedure.[140] Ethyl 2-phenoxypropionate (1.51 g, 7.77 mmol) was weighed into a 15 mL vial. Distilled anhydrous DCM (5.0 mL) was added to the ester. The ester was syringed injected into a 100 mL Schlenk flask, which was previously evacuated and refilled with N_2 in triplicate. Additional DCM (3×5.0 mL) was used to ensure quantitative transfer. The ester solution was cooled to ~-78 °C using an acetone dry ice bath. DIBAL-H (7.0 mL, 7.0 mmol, 0.9 equiv) was added to the ester solution dropwise. The reaction was quenched with 0.5 mL of SPS dried MeOH. The reaction was stirred for 30 min and then warmed to rt. The reaction mixture was transferred into a separatory funnel with 50 mL of DCM. The mixture was washed with 10 mL of 1 M HCl and then 10 mL of brine. The solvent was removed, using a rotary evaporator, to produce a crude oil. The crude product was purified by distillation at 41 °C under a medium vacuum (0.4 Torr). Purified product was isolated as a colourless oil in 45% yield. **¹H NMR** (499.797 MHz, CDCl₃, 27.0 °C): δ 1.50 (d, $J = 6.9$ Hz, 3H), 4.65 (qd, $J = 6.9$, 1.9 Hz, 1H), 6.90–6.93 (m, 2H), 7.02 (tt, $J = 7.4$, 1.0 Hz, 1H), 7.30–7.34 (m, 2H), 9.74 (d, $J = 1.9$ Hz, 1H). **¹³C{¹H} NMR** (125.688 MHz, CDCl₃, 27.0 °C): δ 15.6, 77.8, 115.3, 121.9, 129.8, 157.3, 202.4. **HRMS (EI) *m/z*:** Calcd for $C_9H_{10}O_2$ [M]⁺: 150.0681. Found: 150.0680.

2.4.3.3 Alcohols

Three general methods were used to determine the ees for the product alcohols.

Method A: Products were made up as THF solutions (0.5 mg sample/mL THF) and injected (0.25 µL) into a Hewlett Packard 5890 GC equipped with a 5970B MSD and a Supelco β-DEX™ 225 capillary column (30 m × 0.25 mm, d_f 0.25 µm) at a 1.0 mL/min He flow rate. The standard temperature programming used was from 100 to 220 °C at 5 °C/min.

Method B: Is Method A but with a 2 °C/min gradient from 100 to 220 °C.

Method C: Products were made up as THF solutions (1.0 mg sample/mL THF) and injected (5.00 µL) into an Agilent 1100 series HPLC with a Daicel CHIRALPAK® IB chiral column (250 × 4.6 mm) set at 30 °C. The solvent system used was hexane:^{i}PrOH (97:3) at a flow rate of 1.0 mL/min.

The ees were determined from the resulting chromatograms. Enantioenriched products' ees were normalized to their respective racemic mixtures.

2.4.3.3.1 Small-Scale Asymmetric Ester Hydrogenations

The syntheses and spectroscopic data from the smaller-scale (<1 g of ester) low-pressure screening hydrogenations (4 atm H$_2$) has been limited to the optimized rt conditions with DME and NaOEt (50 mol%). This was done to help remove redundant data from being presented.

(R)-2-Phenoxypropan-1-ol (Table 2-5, entry 1, 185)
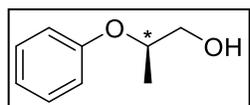
Prepared according to Substrate Screening from **177** (3.4 mg, 7.2 µmol), **174** (6.1 mg, 7.9 µmol, 1.1 equiv), NaOEt (12 mg, 0.18 mmol, 25 equiv), DME (2.0 mL), H$_2$ (4 atm), and **171** (70.2 mg, 0.361 mmol, 50 equiv) at rt for 1 h. Colourless oil, 99% yield, 93% ee. **^{1}H NMR** (498.118 MHz, CDCl$_3$, 27.0 °C): δ 1.30 (d, J = 6.2 Hz, 3H), 2.00 (dd, J = 7.5, 5.2 Hz, 1H), 3.71–3.80 (m, 2H), 4.50–4.56 (m, 1H), 6.95–7.00 (m, 3H), 7.29–7.33 (m, 2H). **^{13}C{^{1}H} NMR** (125.688 MHz, CDCl$_3$, 27.0 °C): δ 15.8, 66.4, 74.7, 116.2, 121.2, 129.6, 157.7. **LRMS (EI) *m/z*:** Calcd for C$_9$H$_{12}$O$_2$ [M]$^+$: 152. Found: 152. **Retention times (Method A):** t_R(minor) = 10.89 min, t_R(major) = 11.10 min.

2-(4-Fluorophenoxy)propan-1-ol (Table 2-5, entry 3)
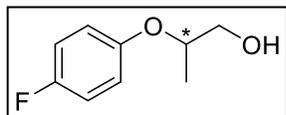
Prepared according to Substrate Screening from **177** (3.4 mg, 7.2 μmol), **174** (6.1 mg, 7.9 μmol, 1.1 equiv), NaOEt (12 mg, 0.18 mmol, 25 equiv), DME (2.0 mL), H_2 (4 atm), and (±)-ethyl 2-(4-fluorophenoxy)propionate (77.0 mg, 0.363 mmol, 51 equiv) at rt for 1 h. Colourless oil, 93% yield, 88% ee. **^{1}H NMR** (498.118 MHz, CDCl$_3$, 27.0 °C): δ 1.27 (d, J = 6.2 Hz, 3H), 2.01 (br, 1H), 3.74 (br, 2H), 4.39–4.45 (m, 1H), 6.88–6.92 (m, 2H), 6.97–7.02 (m, 2H). **^{13}C{^{1}H} NMR** (125.688 MHz, CDCl$_3$, 27.0 °C): δ 15.7, 66.3, 75.9, 116.0 (d, J = 23.1 Hz), 117.6 (d, J = 8.0 Hz), 153.7 (d, J = 1.9 Hz), 157.6 (d, J = 239.0 Hz). **LRMS (EI) *m/z*:** Calcd for C$_9$H$_{11}$FO$_2$ [M]$^+$: 170. Found: 170. **Retention times (Method A)**: t_R(minor) = 11.62 min, t_R(major) = 11.80 min.

(*R*)-2-(4-Chlorophenoxy)propan-1-ol (Table 2-5, entry 5)

Prepared according to Substrate Screening from **177** (3.4 mg, 7.2 μmol), **174** (6.1 mg, 7.9 μmol, 1.1 equiv), NaOEt (12 mg, 0.18 mmol, 25 equiv), DME (2.0 mL), H_2 (4 atm), and (±)-ethyl 2-(4-chlorophenoxy)propionate (82.0 mg, 0.359 mmol, 50 equiv) at rt for 1 h. Colourless oil, 94% yield, 87% ee. **^{1}H NMR** (498.118 MHz, CDCl$_3$, 27.0 °C): δ 1.28 (d, J = 6.2 Hz, 3H), 1.98 (dd, J = 7.2, 5.3 Hz, 1H), 3.70–3.79 (m, 2H), 4.44–4.50 (m, 1H), 6.87–6.90 (m, 2H), 7.24–7.28 (m, 2H). **^{13}C{^{1}H} NMR** (125.688 MHz, CDCl$_3$, 27.0 °C): δ 15.7, 66.2, 75.3, 117.5, 126.1, 129.5, 156.3. **LRMS (EI) *m/z*:** Calcd for C$_9$H$_{11}$ClO$_2$ [M]$^+$: 186. Found: 186. **Retention times (Method A)**: t_R(minor) = 16.62 min, t_R(major) = 16.77 min.

2-(4-Bromophenoxy)propan-1-ol (Table 2-5, entry 7)

Prepared according to Substrate Screening from **177** (3.4 mg, 7.2 μmol), **174** (6.3 mg, 8.1 μmol, 1.1 equiv), NaOEt (12 mg, 0.18 mmol, 25 equiv), DME (2.0 mL), H_2 (4 atm), and (±)-ethyl 2-(4-bromophenoxy)propionate (98.6 mg, 0.361 mmol, 50 equiv) at rt for 1 h. Colourless oil, 93% yield, 87% ee. **^{1}H NMR** (498.118 MHz, CDCl$_3$, 27.0 °C): δ 1.28 (d, J = 6.2 Hz, 3H), 1.96 (br, 1H), 3.75 (br, 2H), 4.44–4.50 (m, 1H), 6.82–6.85 (m, 2H), 7.38–7.41 (m, 2H). **^{13}C{^{1}H} NMR** (125.688 MHz, CDCl$_3$, 27.0 °C): δ 15.7, 66.2, 75.2, 113.4, 117.9, 132.4, 156.8. **LRMS (EI) *m/z*****: Calcd for C$_9$H$_{11}$BrO$_2$ [M]$^+$: 230 and 232. Found: 230 and 232. **Retention times (Method A)**: t_R(minor) = 18.92 min, t_R(major) = 19.05 min.

2-(4-Iodophenoxy)propan-1-ol (Table 2-5, entry 8)

Prepared according to Substrate Screening from **177** (3.4 mg, 7.2 μmol), **174** (6.3 mg, 8.1 μmol, 1.1 equiv), NaOEt (12 mg, 0.18 mmol, 25 equiv), DME (2.0 mL), H_2 (4 atm), and (±)-ethyl 2-(4-iodophenoxy)propionate (115.1 mg, 0.3595 mmol, 50 equiv) at rt for 1 h. Colourless oil, 95% yield, 85% ee. **^{1}H NMR** (498.118 MHz, CDCl$_3$, 27.0 °C): δ 1.28 (d, J = 6.2 Hz, 3H), 1.94 (br, 1H), 3.75 (br, 2H), 4.45–4.50 (m, 1H), 6.72–6.75 (m, 2H), 7.56–7.59 (m, 2H). **^{13}C{^{1}H} NMR** (125.688 MHz, CDCl$_3$, 27.0 °C): δ 15.6, 66.2, 75.0, 83.3, 118.4, 138.4, 157.6. **LRMS (EI) *m/z*****: Calcd for C$_9$H$_{11}$IO$_2$ [M]$^+$: 278. Found: 278. **Retention times (Method A)**: t_R(minor) = 21.63 min, t_R(major) = 21.75 min.

2-(4-Methoxyphenoxy)propan-1-ol (Table 2-5, entry 9)

Prepared according to Substrate Screening from **177** (3.4 mg, 7.2 µmol), **174** (6.1 mg, 7.9 µmol, 1.1 equiv), NaOEt (12 mg, 0.18 mmol, 25 equiv), DME (2.0 mL), H_2 (4 atm), and (±)-ethyl 2-(4-methoxyphenoxy)propionate (80.6 mg, 0.359 mmol, 50 equiv) at rt for 1 h. Colourless oil, 81% yield, 90% ee. **^{1}H NMR** (498.118 MHz, CDCl₃, 27.0 °C): δ 1.26 (d, J = 6.2 Hz, 3H), 2.05 (dd, J = 7.3, 4.9 Hz, 1H), 3.68–3.78 (m, 2H), 3.79 (s, 3H), 4.35–4.41 (m, 1H), 6.84–6.87 (m, 2H), 6.89–6.92 (m, 2H). **^{13}C{^{1}H} NMR** (125.688 MHz, CDCl₃, 27.0 °C): δ 15.9, 55.7, 66.4, 76.0, 114.7, 117.8, 151.6, 154.4. **LRMS (EI) *m/z*:** Calcd for $C_{10}H_{14}O_3$ [M]$^+$: 182. Found: 182. **Retention times (Method A):** t_R(minor) = 16.98 min, t_R(major) = 17.10 min.

2-(3-Methoxyphenoxy)propan-1-ol (Table 2-5, entry 11)

Prepared according to Substrate Screening from **177** (3.4 mg, 7.2 µmol), **174** (6.2 mg, 8.0 µmol, 1.1 equiv), NaOEt (12 mg, 0.18 mmol, 25 equiv), DME (2.0 mL), H_2 (4 atm), and (±)-ethyl 2-(3-methoxyphenoxy)propionate (80.9 mg, 0.361 mmol, 50 equiv) at rt for 1 h. Colourless oil, 89% yield, 87% ee. **^{1}H NMR** (498.118 MHz, CDCl₃, 27.0 °C): δ 1.30 (d, J = 6.3 Hz, 3H), 1.98 (dd, J = 7.9, 5.1 Hz, 1H), 3.70–3.78 (m, 2H), 3.81 (s, 3H), 4.48–4.54 (m, 1H), 6.52 (t, J = 2.3 Hz, 1H), 6.54–6.57 (m, 2H), 7.19–7.22 (m, 1H). **^{13}C{^{1}H} NMR** (125.688 MHz, CDCl₃, 27.0 °C): δ 15.8, 55.3, 66.3, 74.7, 102.6, 106.7, 108.1, 130.0, 158.9, 160.9. **LRMS (EI) *m/z*:** Calcd for $C_{10}H_{14}O_3$ [M]$^+$: 182. Found: 182. **Retention times (Method A):** t_R(minor) = 16.95 min, t_R(major) = 17.09 min.

2-(3-Fluorophenoxy)propan-1-ol (Table 2-5, entry 13)

Prepared according to Substrate Screening from **177** (3.4 mg, 7.2 μmol), **174** (6.2 mg, 8.0 μmol, 1.1 equiv), NaOEt (12 mg, 0.18 mmol, 25 equiv), DME (2.0 mL), H$_2$ (4 atm), and (±)-ethyl 2-(3-fluorophenoxy)propionate (76.3 mg, 0.360 mmol, 50 equiv) at rt for 1 h. Colourless oil, 91% yield, 82% ee. **^{1}H NMR** (498.118 MHz, CDCl$_3$, 27.0 °C): δ 1.30 (d, J = 6.3 Hz, 3H), 1.97 (br, 1H), 3.76 (br, 2H), 4.47–4.53 (m, 1H), 6.65–6.71 (m, 2H), 6.73 (dd, J = 8.3, 2.3 Hz, 1H), 7.22–7.26 (m, 1H). **^{13}C{^{1}H} NMR** (125.688 MHz, CDCl$_3$, 27.0 °C): δ 15.7, 66.2, 75.1, 103.7 (d, J = 24.7 Hz), 108.0 (d, J = 21.5 Hz), 111.6 (d, J = 2.9 Hz), 130.3 (d, J = 10.2 Hz), 159.1 (d, J = 10.9 Hz), 163.7 (d, J = 245.5 Hz). **LRMS (EI) m/z**: Calcd for C$_9$H$_{11}$FO$_2$ [M]$^+$: 170. Found: 170. **Retention times (Method A)**: t_R(minor) = 11.68 min, t_R(major) = 11.91 min.

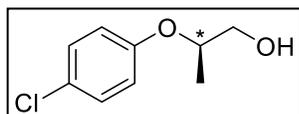**2-(2-Chlorophenoxy)propan-1-ol (Table 2-5, entry 15)**

Prepared according to Substrate Screening from **177** (3.4 mg, 7.2 μmol), **174** (6.3 mg, 8.1 μmol, 1.1 equiv), NaOEt (12 mg, 0.18 mmol, 25 equiv), DME (2.0 mL), H$_2$ (4 atm), and (±)-ethyl 2-(2-chlorophenoxy)propionate (82.4 mg, 0.360 mmol, 50 equiv) at rt for 1 h. Colourless oil, 94% yield, 86% ee. **^{1}H NMR** (498.118 MHz, CDCl$_3$, 27.0 °C): δ 1.35 (d, J = 6.3 Hz, 3H), 2.22 (br, 1H), 3.78 (br, 2H), 4.48–4.54 (m, 1H), 6.93–6.97 (m, 1H), 7.03 (dd, J = 8.2, 1.4 Hz, 1H), 7.21–7.25 (m, 1H), 7.39 (dd, J = 7.9, 1.6 Hz, 1H). **^{13}C{^{1}H} NMR** (125.688 MHz, CDCl$_3$, 27.0 °C): δ 16.1, 66.2, 77.4, 116.6, 122.3, 124.5, 127.8, 130.5, 153.5. **LRMS (EI) m/z**: Calcd for C$_9$H$_{11}$ClO$_2$ [M]$^+$: 186. Found: 186. **Retention times (Method A)**: t_R(minor) = 14.40 min, t_R(major) = 14.50 min.
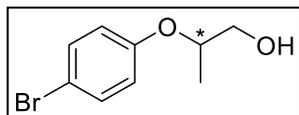
(*R*)-2-Phenoxypropan-1-ol (Table 2-5, entry 17, 185)
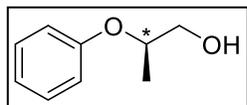
 Prepared according to Substrate Screening from **177** (3.4 mg, 7.2 μmol),
174 (6.1 mg, 7.9 μmol, 1.1 equiv), NaOEt (12 mg, 0.18 mmol, 25 equiv),
DME (2.0 mL), H_2 (4 atm), and (±)-isopropyl 2-phenoxypropionate (76.4 mg, 0.367 mmol, 51
equiv) at rt for 1 h. Colourless oil, 97% yield, 89% ee. **^{1}H NMR** (498.118 MHz, CDCl$_3$, 27.0
°C): δ 1.30 (d, *J* = 6.2 Hz, 3H), 2.00 (br, 1H), 3.76 (br, 2H), 4.50–4.56 (m, 1H), 6.94–7.00 (m,
3H), 7.29–7.33 (m, 2H). **^{13}C{^{1}H} NMR** (125.688 MHz, CDCl$_3$, 27.0 °C): δ 15.8, 66.4, 74.7,
116.1, 121.2, 129.6, 157.7. **LRMS (EI) *m/z*:** Calcd for $C_9H_{12}O_2$ [M]$^+$: 152. Found: 152.

Retention times (Method A): t_R(minor) = 10.95 min, t_R(major) = 11.16 min.

2-Phenoxybutan-1-ol (Table 2-5, entry 19)
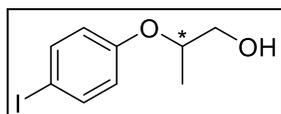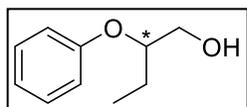
 Prepared according to Substrate Screening from **177** (3.4 mg, 7.2 μmol),
174 (6.4 mg, 8.3 μmol, 1.1 equiv), NaOEt (12 mg, 0.18 mmol, 25 equiv),
DME (2.0 mL), H_2 (4 atm), and **173** (74.7 mg, 0.359 mmol, 50 equiv) at rt for 1 h. Colourless
oil, >99% yield, 83% ee. **^{1}H NMR** (498.118 MHz, CDCl$_3$, 27.0 °C): δ 1.00 (t, *J* = 7.5 Hz, 3H),
1.66–1.82 (m, 2H), 1.90 (br, 1H), 3.80 (br, 2H), 4.30–4.34 (m, 1H), 6.96–7.00 (m, 3H),
7.28–7.32 (m, 1H). **^{13}C{^{1}H} NMR** (125.688 MHz, CDCl$_3$, 27.0 °C): δ 9.6, 23.4, 64.1, 80.1,
116.2, 121.2, 129.6, 158.2. **LRMS (EI) *m/z*:** Calcd for $C_{10}H_{14}O_2$ [M]$^+$: 166. Found: 166.

Retention times (Method A): t_R(minor) = 12.30 min, t_R(major) = 12.48 min.

3-Methyl-2-phenoxybutan-1-ol (Table 2-5, entry 21)
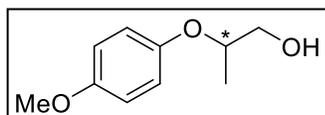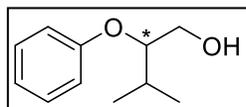
Prepared according to Substrate Screening from **177** (3.4 mg, 7.2 μmol), **174** (6.1 mg, 7.9 μmol, 1.1 equiv), NaOEt (12 mg, 0.18 mmol, 25 equiv), DME (2.0 mL), H_2 (4 atm), and (±)-α-phenoxy-isovaleric acid ethyl ester (79.6 mg, 0.358 mmol, 50 equiv) at rt for 1 h. Colourless oil, 44% yield, 89% ee. **^{1}H NMR** (498.118 MHz, CDCl$_3$, 27.0 °C): δ 0.99 (d, J = 6.9 Hz, 3H), 1.03 (d, J = 6.9 Hz, 3H), 1.78 (br, 1H), 2.09–2.15 (m, 1H), 3.79–3.88 (m, 2H), 4.17 (td, J = 6.1, 3.6 Hz, 1H), 6.95–7.00 (m, 3H), 7.26–7.32 (m, 2H). **^{13}C{^{1}H} NMR** (125.688 MHz, CDCl$_3$, 27.0 °C): δ 18.1, 18.6, 29.3, 62.3, 84.0, 116.4, 121.2, 129.6, 158.9. **LRMS (EI) *m/z*:** Calcd for C$_{11}$H$_{16}$O$_2$ [M]$^+$: 180. Found: 180. **Retention times (Method B):** t_R(minor) = 21.94 min, t_R(major) = 22.13 min.

3-Methyl-2-phenoxybutan-1-ol (Table 2-5, entry 23)
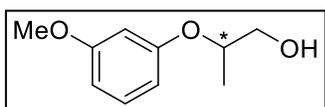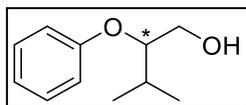
Prepared according to Substrate Screening from **177** (3.4 mg, 7.2 μmol), **174** (6.2 mg, 8.0 μmol, 1.1 equiv), NaOEt (12 mg, 0.18 mmol, 25 equiv), DME (2.0 mL), H_2 (4 atm), and (±)-α-phenoxy-isovaleric acid isopropyl ester (84.7 mg, 0.358 mmol, 50 equiv) at rt for 1 h. Colourless oil, 32% yield, 90% ee. **^{1}H NMR** (498.118 MHz, CDCl$_3$, 27.0 °C): δ 0.99 (d, J = 6.9 Hz, 3H), 1.04 (d, J = 6.9 Hz, 3H), 1.78 (br, 1H), 2.09–2.15 (m, 1H), 3.79–3.85 (m, 2H), 4.17 (td, J = 6.1, 3.6 Hz, 1H), 6.96–7.01 (m, 3H), 7.26–7.32 (m, 2H). **^{13}C{^{1}H} NMR** (125.688 MHz, CDCl$_3$, 27.0 °C): δ 18.1, 18.6, 29.3, 62.3, 84.0, 116.4, 121.2, 129.6, 158.9. **LRMS (EI) *m/z*:** Calcd for C$_{11}$H$_{16}$O$_2$ [M]$^+$: 180. Found: 180. **Retention times (Method B):** t_R(minor) = 21.96 min, t_R(major) = 22.15 min.

(*R*)-2-Phenoxypropan-1-ol (Table 2-5, entry 24, 185)
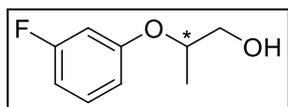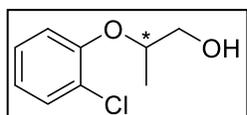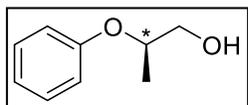
Prepared according to Substrate Screening from **177** (3.4 mg, 7.2 μmol), **174** (6.1 mg, 7.9 μmol, 1.1 equiv), NaOEt (12 mg, 0.18 mmol, 25 equiv), DME (2.0 mL), H$_2$ (4 atm), and (±)-butan-2-yl 2-phenoxypropionate (79.7 mg, 0.367 mmol, 50 equiv) at rt for 1 h. Colourless oil, 89% yield, 91% ee. **^{1}H NMR** (498.118 MHz, CDCl$_3$, 27.0 °C): δ 1.30 (d, *J* = 6.2 Hz, 3H), 2.02 (br, 1H), 3.76 (br, 2H), 4.50–4.56 (m, 1H), 6.94–7.00 (m, 3H), 7.29–7.33 (m, 2H). **^{13}C{^{1}H} NMR** (125.688 MHz, CDCl$_3$, 27.0 °C): δ 15.8, 66.4, 74.7, 116.1, 121.2, 129.6, 157.7. **LRMS (EI) *m/z*:** Calcd for C$_9$H$_{12}$O$_2$ [M]$^+$: 152. Found: 152.

Retention times (Method A): t_R(minor) = 10.93 min, t_R(major) = 11.13 min.

2-Phenoxy-2-phenylethan-1-ol (Table 2-5, entry 25)
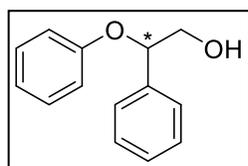
Prepared with modification to the reaction time of Substrate Screening from **177** (3.4 mg, 7.2 μmol), **174** (6.1 mg, 7.9 μmol, 1.1 equiv), NaOEt (12 mg, 0.18 mmol, 25 equiv), DME (2.0 mL), H$_2$ (4 atm), and (±)-ethyl 2-phenoxy-2-phenylethanoate (92.9 mg, 0.362 mmol, 50 equiv) at rt for 12 h. White solid, 74% yield, 52% ee. **^{1}H NMR** (498.118 MHz, CDCl$_3$, 27.0 °C): δ 2.23 (br, 1H), 3.82–3.87 (m, 1H), 3.93–3.97 (m, 1H), 5.29 (dd, *J* = 8.2, 3.6 Hz, 1H), 6.89–6.94 (m, 3H), 7.20–7.24 (m, 2H), 7.29–7.33 (m, 1H), 7.35–7.41 (m, 4H). **^{13}C{^{1}H} NMR** (125.688 MHz, CDCl$_3$, 27.0 °C): δ 67.6, 81.1, 116.0, 121.3, 126.3, 128.2, 128.8, 129.4, 137.8, 157.8. **Retention times (Method C):** t_R(major) = 11.51 min, t_R(minor) = 17.14 min.

2-(Phenylthio)propan-1-ol
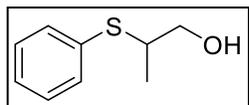
Prepared with modification to the reaction time of Substrate Screening from **177** (3.4 mg, 7.2 μmol), **174** (6.4 mg, 8.3 μmol, 1.1 equiv), NaOEt (12 mg, 0.18 mmol, 25 equiv), DME (2.0 mL), H$_2$ (4 atm), and **186** (76.0 mg, 0.361 mmol, 50 equiv) at rt for 12 h. Colourless oil, 10% yield. **^{1}H NMR** (599.926 MHz, CDCl$_3$, 27.0 °C): δ 1.33 (d, J = 7.0 Hz, 3H), 2.09 (br, 1H), 3.30–3.36 (m, 1H), 3.53 (br, 1H), 3.62 (br, 1H), 7.29–7.34 (m, 3H), 7.46–7.49 (m, 2H).

2-(4-Isobutylphenyl)propan-1-ol
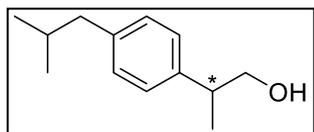
Prepared with modification to the reaction time of Substrate Screening from **177** (3.4 mg, 7.2 μmol), **174** (6.1 mg, 7.9 μmol, 1.1 equiv), NaOEt (12 mg, 0.18 mmol, 25 equiv), DME (2.0 mL), H$_2$ (4 atm), and **187** (89.5 mg, 0.382 mmol, 53 equiv) at rt for 12 h. Colourless oil, 61% yield, 12% ee. **^{1}H NMR** (599.926 MHz, CDCl$_3$, 27.0 °C): δ 0.93 (d, J = 6.6 Hz, 6H), 1.28 (d, J = 7.0 Hz, 3H), 1.58 (br, 1H), 1.83–1.92 (m, 1H), 2.47 (d, J = 7.2 Hz, 2H), 2.95 (sext, J = 6.9 Hz, 1H), 3.71 (d, J = 7.0 Hz, 2H), 7.12–7.17 (m, 4H). **LRMS (EI)** *m/z*: Calcd for C$_{13}$H$_{20}$O [M]$^+$: 192. Found: 192. **Retention times (Method B)**: t_R = 27.22 min, t_R = 27.41 min.

Asymmetric Hydrogenation of (±)-Ethyl 2-phenoxypropionate (171) Under ~1 atm
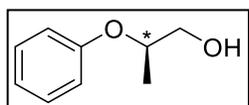
An oven-dried 10 mL Schlenk flask, with a stir bar, was evacuated and refilled with H$_2$ on a bubbler. A double-layered balloon attached to a glass barrel of a syringe was evacuated and refilled with H$_2$ via 50 mL Schlenk flask. The ester **171** (70.0 mg, 0.360 mmol, 50 equiv/Ru) was weighed, in air, into an NMR tube. The NMR tube was sealed with a septum and purged with Ar for 2 min. Freshly distilled, deaerated DME was added to the NMR tube, via cannula, to a 0.25 mL mark. The deaerated solution was then transferred,

through a cannula, into the 10 mL Schlenk flask with H_2 pressure. More freshly distilled, deaerated DME (0.25 mL) was used for quantitative transfer. In a glovebox, the precursor **177** (3.4 mg, 7.2 μmol) and ligand **174** (6.1 mg, 7.9 μmol, 1.1 equiv/Ru) were weighed into an NMR tube that was then fitted with a septum. On a Schlenk line, DME (0.5 mL) was transferred, through a cannula, into the NMR tube with Ar pressure. The tube was heated for 30 min at 60 °C with shaking every 10 min. The tube's solution was cooled to rt and then transferred, through a cannula, into the 10 mL Schlenk flask with H_2 pressure. Inside a glovebox, NaOEt (12.2 mg, 0.179 mmol, 25 equiv/Ru) was weighed into an NMR tube, which was then fitted with a septum. On a Schlenk line, DME (1.0 mL) was transferred, through a cannula, into the NMR tube with Ar pressure. The NMR tube was sonicated for 30 min and the resulting solution was transferred, through a cannula, into the 10 mL Schlenk flask with H_2 pressure. The H_2 filled balloon syringe was quickly transferred to the 10 mL Schlenk flask. The bubbler was opened to ensure the pressure of the Schlenk flask was equalized with that of the balloon. The reaction mixture was stirred for 2 h at rt. An aliquot was passed through a Florisil® plug, with DCM as eluent, into a 15 mL vial. Volatiles were removed using a rotary evaporator to produce a colourless oil, which was analyzed using NMR and GC–MS. Some spectroscopic data matched that of **185** (67% yield, 86% ee).

Asymmetric Hydrogenation of (±)-Ethyl 2-phenoxypropionate (171) at 0 °C
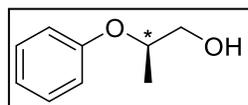
An oven-dried autoclave with a stir bar was assembled hot. While cooling to rt, the autoclave was purged with Ar through a long double-tipped needle that was pierced through a septum on the gauge adapter. The autoclave was cooled to 0 °C with an ice-water bath. Once cooled, the autoclave was flushed with H_2 (~1 atm). The ester **171** (70.0 mg, 0.360 mmol, 50 equiv/Ru) was weighed, in air, into an NMR tube. The NMR tube was

140

sealed with a septum and purged with Ar for 2 min. Freshly distilled, deaerated DME was added to the NMR tube, via cannula, to a 0.25 mL mark. The deaerated solution was cooled to 0 °C and then transferred, through the long double-tipped needle (i.e., cannula), into the autoclave with H_2 pressure. Freshly distilled, deaerated DME (0.25 mL) was used to ensure quantitative transfer from the NMR tube. In a glovebox, the precursor **177** (3.4 mg, 7.2 μmol) and ligand **174** (6.3 mg, 8.1 μmol, 1.1 equiv/Ru) were weighed into an NMR tube that was then fitted with a septum. On a Schlenk line, DME (0.5 mL) was transferred, through a cannula, into the NMR tube with Ar pressure. The tube was heated for 30 min at 60 °C with shaking every 10 min. The tube's solution was cooled to 0 °C and then transferred, through the long double-tipped needle (i.e., cannula), into the autoclave with H_2 pressure. Inside a glovebox, NaOEt (12.2 mg, 0.179 mmol, 25 equiv/Ru) was weighed into an NMR tube, which was then fitted with a septum. On a Schlenk line, DME (0.5 mL) was transferred, through a cannula, into the NMR tube with Ar pressure. The resulting mixture was sonicated for 30 min, cooled to 0 °C, and then transferred, through the long double-tipped needle (i.e., cannula), into the autoclave with H_2 pressure. Additional DME (0.5 mL) was used to ensure quantitative transfer of the base. The autoclave was sealed and pressurized to 4 atm H_2. The reaction mixture was stirred at 0 °C for 2 h. The reaction was depressurized and opened to air. 1,3,5-Trimethoxybenzene (25.0 mg, 0.149 mmol) was dissolved in DME (1.0 mL) and 0.5 mL was syringed into the reaction mixture. An aliquot was passed through a Florisil® plug, with DCM as eluent, into a 15 mL vial. Volatiles were removed using a rotary evaporator to produce a colourless oil, which was analyzed using NMR and GC–MS. Spectroscopic data matched that of **185** (>99% conv, 95% ee).

2.4.3.3.2 Miscellaneous Asymmetric Hydrogenations and Deuteration

Higher TON Asymmetric Hydrogenation of (±)-Ethyl 2-phenoxypropionate (171) with NaOEt in DME

 An oven-dried autoclave with a stir bar was assembled hot. While cooling to rt, the autoclave was purged with Ar through a long double-tipped needle that was pierced through a septum on the gauge adapter. Once cooled the autoclave was flushed with H_2 (~1 atm). The ester **171** (1.398 g, 7.198 mmol, 1002 equiv/Ru) was weighed, in air, into an NMR tube. The NMR tube was sealed with a septum and purged with Ar for 5 min. The deaerated ester was transferred, through the long double-tipped needle (i.e., cannula), into the autoclave with H_2 pressure. Freshly distilled, deaerated DME (~0.60 mL) was used to ensure quantitative transfer from the NMR tube. In a glovebox, the precursor **177** (3.4 mg, 7.2 μmol) and ligand **174** (6.1 mg, 7.9 μmol, 1.1 equiv/Ru) were weighed into an NMR tube that was then fitted with a septum. On a Schlenk line, DME (0.5 mL) was transferred, through a cannula, into the NMR tube with Ar pressure. The tube was heated for 30 min at 60 °C with shaking every 10 min. The tube's solution was cooled to rt and then transferred, through the long double-tipped needle (i.e., cannula), into the autoclave with H_2 pressure. Inside a glovebox, NaOEt (98.0 mg, 1.44 mmol, 200 equiv/Ru) was weighed into an NMR tube, which was then fitted with a septum. On a Schlenk line, DME (1.0 mL) was transferred, through a cannula, into the NMR tube with Ar pressure. The resulting mixture was sonicated for 30 min and then transferred, through the long double-tipped needle (i.e., cannula), into the autoclave with H_2 pressure. Additional DME (0.5 mL) was used to ensure quantitative transfer of the base. The autoclave was sealed and pressurized to 15 atm H_2. The reaction mixture was stirred at rt for 9 h. The reaction was depressurized and opened to air. 1,3,5-Trimethoxybenzene (243.0 mg, 1.445 mmol) was added to the reaction mixture. An aliquot was passed through a Florisil® plug, with DCM as eluent, into a 15 mL vial. Volatiles were removed using a rotary evaporator to produce a colourless oil, which

was analyzed using NMR and GC–MS. Some spectroscopic data matched that of **185** (95% conv, 91% ee).

Higher TON Asymmetric Hydrogenation of (±)-Ethyl 2-phenoxypropionate (171) with NaO^{i}Pr in THF

An oven-dried autoclave with a stir bar was assembled hot. While cooling to rt, the autoclave was purged with Ar through a long double-tipped needle that was pierced through a septum on the gauge adapter. Once cooled the autoclave was flushed with H$_2$ (~1 atm). The ester **171** (1.398 g, 7.198 mmol, 1002 equiv/Ru) was weighed, in air, into an NMR tube. The NMR tube was sealed with a septum and purged with Ar for 5 min. The deaerated ester was transferred, through the long double-tipped needle (i.e., cannula), into the autoclave with H$_2$ pressure. Freshly distilled, deaerated THF (~0.60 mL) was used to ensure quantitative transfer from the NMR tube. In a glovebox, the precursor **177** (3.4 mg, 7.2 μmol) and ligand **174** (6.1 mg, 7.9 μmol, 1.1 equiv/Ru) were weighed into an NMR tube that was then fitted with a septum. On a Schlenk line, THF (1.0 mL) was transferred, through a cannula, into the NMR tube with Ar pressure. The tube was heated for 30 min at 60 °C with shaking every 10 min. The tube's solution was cooled to rt and then transferred, through the long double-tipped needle (i.e., cannula), into the autoclave with H$_2$. Inside a glovebox, NaO^{i}Pr (119.0 mg, 1.45 mmol, 202 equiv/Ru) was weighed into an NMR tube, which was then fitted with a septum. On a Schlenk line, THF (1.0 mL) was transferred, through a cannula, into the NMR tube with Ar pressure. The resulting solution was transferred, through the long double-tipped needle (i.e., cannula), into the autoclave with H$_2$ pressure. The autoclave was sealed and pressurized to 20 atm H$_2$. The reaction mixture was stirred at rt for 24 h. The reaction was depressurized and opened to air. 1,3,5-Trimethoxybenzene (246.8 mg, 1.467 mmol) was added to the reaction mixture. An aliquot was passed through a Florisil® plug, with DCM as eluent, into a 15 mL vial.

Volatiles were removed using a rotary evaporator to produce a colourless oil, which was analyzed using NMR and GC–MS. Spectroscopic data matched that of **185** (>99% conv, 89% ee).

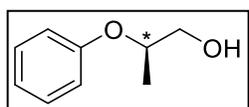**Asymmetric Hydrogenation of (±)-2-Phenoxypropionaldehyde (188)**
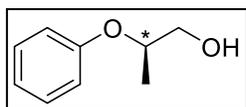
An oven-dried autoclave with stir bar was assembled hot. While cooling to rt, the autoclave was purged with Ar through a long double-tipped needle that was pierced through a septum on the gauge adapter. Once cooled the autoclave was flushed with H_2 (~1 atm). The aldehyde **188** (54.4 mg, 0.362 mmol, 50 equiv/Ru) was weighed, in air, into an NMR tube. The NMR tube was sealed with a septum and purged with Ar for 2 min. Freshly distilled, deaerated DME was added to the NMR tube, via cannula, to a 0.25 mL mark. The deaerated solution was then transferred, through the long double-tipped needle (i.e., cannula), into the autoclave with H_2 pressure. More freshly distilled, deaerated DME (0.25 mL) was used to ensure quantitative transfer from the NMR tube. In a glovebox, the precursor **177** (3.4 mg, 7.2 μmol) and ligand **174** (6.2 mg, 8.0 μmol, 1.1 equiv/Ru) were weighed into an NMR tube that was then fitted with a septum. On a Schlenk line, DME (0.5 mL) was transferred, through a cannula, into the NMR tube with Ar pressure. The tube was heated for 30 min at 60 °C with shaking every 10 min. The tube's solution was cooled to rt and then transferred, through the long double-tipped needle (i.e., cannula), into the autoclave with H_2 pressure. Inside a glovebox, NaOEt (12.3 mg, 0.181 mmol, 25 equiv/Ru) was weighed into an NMR tube, which was then fitted with a septum. On a Schlenk line, DME (0.5 mL) was transferred, through a cannula, into the NMR tube with Ar pressure. The resulting mixture was sonicated for 30 min and then transferred, through the long double-tipped needle (i.e., cannula), into the autoclave with H_2 pressure. Additional DME (0.5 mL) was used to ensure quantitative transfer of the base. The

autoclave was sealed and pressurized to 4 atm H_2. The reaction mixture was stirred at rt for 1 h. The reaction was depressurized and opened to air. An aliquot was passed through a Florisil® plug, with DCM as eluent, into a 15 mL vial. Volatiles were removed using a rotary evaporator to produce a colourless oil, which was analyzed using NMR and GC–MS. Some spectroscopic data matched that of **185** (28% yield, 47% ee).
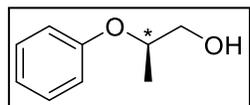
Asymmetric Deuteration of (±)-Ethyl 2-phenoxypropionate (171) with NaOEt in DME (189)
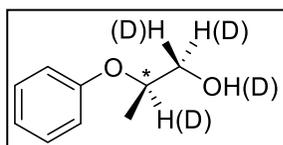
An oven-dried autoclave with stir bar was assembled hot. While cooling to rt, the autoclave was purged with Ar through a long double-tipped needle that was pierced through a septum on the gauge adapter. Once cooled the autoclave was flushed with D_2 (~1 atm). The ester **171** (70.3 mg, 0.362 mmol, 50 equiv/Ru) was weighed, in air, into an NMR tube. The NMR tube was sealed with a septum and purged with Ar for 2 min. Freshly distilled, deaerated DME was added to the NMR tube, via cannula, to a 0.25 mL mark. The deaerated solution was then transferred, through the long double-tipped needle (i.e., cannula), into the autoclave with D_2 pressure. More freshly distilled, deaerated DME (0.25 mL) was used to ensure quantitative transfer from the NMR tube. In a glovebox, the precursor **177** (3.4 mg, 7.2 μmol) and ligand **174** (6.1 mg, 7.9 μmol, 1.1 equiv/Ru) were weighed into an NMR tube that was then fitted with a septum. On a Schlenk line, DME (0.5 mL) was transferred, through a cannula, into the NMR tube with Ar pressure. The tube was heated for 30 min at 60 °C with shaking every 10 min. The tube's solution was cooled to rt and then transferred, through the long double-tipped needle (i.e., cannula), into the autoclave with D_2 pressure. Inside a glovebox, NaOEt (12.2 mg, 0.179 mmol, 25 equiv/Ru) was weighed into an NMR tube, which was then fitted with a septum. On a Schlenk line, DME (0.5 mL) was transferred, through a cannula, into the NMR tube with Ar pressure. The resulting mixture was

sonicated for 30 min and then transferred, through the long double-tipped needle (i.e., cannula), into the autoclave with D_2 pressure. Additional DME (0.5 mL) was used to ensure quantitative transfer of the base. The autoclave was sealed and pressurized to 4 atm D_2. The reaction mixture was stirred at rt for 1 h. The reaction was depressurized and opened to air. An aliquot was passed through a Florisil® plug, with DCM as eluent, into a 15 mL vial. Volatiles were removed using a rotary evaporator to produce a colourless oil, which was analyzed using NMR and GC–MS. **^{1}H NMR** (399.947 MHz, CDCl$_3$, 27.0 °C): δ 1.27 (br, 3H), 2.01 (br, 1H), 3.71 (br, 0.6H), 4.50 (br, 0.3H), 6.94 (br, 3H), 7.28 (br, 2H). **^{2}H{^{1}H} NMR** (61.394 MHz, CH$_2$Cl$_2$, 27.0 °C): δ 3.70 (br, 1.9D), 4.49 (br, 1D)

2.4.3.3.3 LiAlH$_4$ Reductions

(±)-2-Phenoxypropan-1-ol
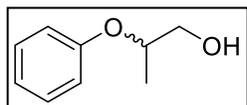
Prepared according to Synthesis of Racemic Alcohols from **171** (206 mg, 1.06 mmol) and LiAlH$_4$ (119 mg, 3.14 mmol, 2.96 equiv). Colourless oil, 68% yield. **^{1}H NMR** (499.797 MHz, CDCl$_3$, 27.0 °C): δ 1.29 (d, J = 6.2 Hz, 3H), 2.30 (br, 1H), 3.71–3.77 (m, 2H), 4.48–4.54 (m, 1H), 6.94–7.00 (m, 3H), 7.29–7.32 (m, 2H). **^{13}C{^{1}H} NMR** (125.688 MHz, CDCl$_3$, 27.0 °C): δ 15.8, 66.3, 74.7, 116.2, 121.2, 129.6, 157.7. **HRMS (EI) *m/z*:** Calcd for C$_9$H$_{12}$O$_2$ [M]$^+$: 152.0837. Found: 152.0840. **LRMS (EI) *m/z*:** Calcd for C$_9$H$_{12}$O$_2$ [M]$^+$: 152. Found: 152. **Retention times (Method A):** t_R = 10.89 min, t_R = 11.11 min.

(±)-2-(4-Fluorophenoxy)propan-1-ol
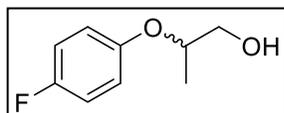
Prepared according to Synthesis of Racemic Alcohols from (±)-ethyl 2-(4-fluorophenoxy)propionate (210 mg, 0.990 mmol) and LiAlH$_4$ (110 mg, 2.89 mmol, 2.92 equiv). Colourless oil, 83% yield. **^{1}H NMR** (499.797 MHz, CDCl$_3$, 27.0 °C): δ 1.26 (d, J = 6.2 Hz, 3H), 2.09 (dd, J = 6.9, 5.4 Hz, 1H), 3.68–3.77 (m, 2H), 4.38–4.44 (m,

1H), 6.87–6.91 (m, 2H), 6.96–7.01 (m, 2H). ^{13}C{^{1}H} NMR (125.688 MHz, CDCl$_3$, 27.0 °C): δ

15.7, 66.3, 75.9, 115.9 (d, J = 22.9 Hz), 117.6 (d, J = 8.0 Hz), 153.7 (d, J = 2.3 Hz), 157.6 (d, J =

239.0 Hz). ^{19}F NMR (376.318 MHz, CDCl$_3$, 27.0 °C): δ -123.0. HRMS (EI) *m/z*: Calcd for

C$_9$H$_{11}$FO$_2$ [M]$^+$: 170.0743. Found: 170.0744. LRMS (EI) *m/z*: Calcd for C$_9$H$_{11}$FO$_2$ [M]$^+$: 170.

Found: 170. Retention times (Method A): t_R = 11.64 min, t_R = 11.85 min.

(±)-2-(4-Chlorophenoxy)propan-1-ol

 Prepared according to Synthesis of Racemic Alcohols from (±)-ethyl

2-(4-chlorophenoxy)propionate (152 mg, 0.664 mmol) and LiAlH$_4$ (76

mg, 2.0 mmol, 3.0 equiv). Colourless oil, 98% yield. ^{1}H NMR (499.797 MHz, CDCl$_3$, 27.0 °C):

δ 1.27 (d, J = 6.2 Hz, 3H), 2.05 (dd, J = 7.2, 5.3 Hz, 1H), 3.69–3.78 (m, 2H), 4.42–4.48 (m, 1H),

6.85–6.89 (m, 2H), 7.23–7.26 (m, 2H). ^{13}C{^{1}H} NMR (125.688 MHz, CDCl$_3$, 27.0 °C): δ 15.7,

66.2, 75.3, 117.4, 126.1, 129.5, 156.3. HRMS (EI) *m/z*: Calcd for C$_9$H$_{11}$ClO$_2$ [M]$^+$: 186.0448.

Found: 186.0449. LRMS (EI) *m/z*: Calcd for C$_9$H$_{11}$ClO$_2$ [M]$^+$: 186. Found: 186. Retention

times (Method A): t_R = 16.65 min, t_R = 16.82 min.

(±)-2-(4-Bromophenoxy)propan-1-ol
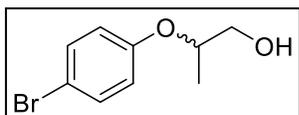
 Prepared according to Synthesis of Racemic Alcohols from (±)-ethyl

2-(4-bromophenoxy)propionate (214 mg, 0.784 mmol) and LiAlH$_4$ (88

mg, 2.3 mmol, 3.0 equiv). Colourless oil, 89% yield. ^{1}H NMR (499.797 MHz, CDCl$_3$, 27.0 °C):

δ 1.27 (d, J = 6.2 Hz, 3H), 2.02 (dd, J = 7.3, 5.4 Hz, 1H), 3.70–3.78 (m, 2H), 4.43–4.49 (m, 1H),

6.81–6.84 (m, 2H), 7.37–7.40 (m, 2H). ^{13}C{^{1}H} NMR (125.688 MHz, CDCl$_3$, 27.0 °C): δ 15.7,

66.2, 75.2, 113.4, 117.9, 132.4, 156.8. HRMS (EI) *m/z*: Calcd for C$_9$H$_{11}$BrO$_2$ [M]$^+$: 229.9943

and 231.9922. Found: 229.9945 and 231.9923. LRMS (EI) *m/z*: Calcd for C$_9$H$_{11}$BrO$_2$ [M]$^+$: 230

and 232. Found: 230 and 232. Retention times (Method A): t_R = 18.95 min, t_R = 19.10 min.

(±)-2-(4-Iodophenoxy)propan-1-ol
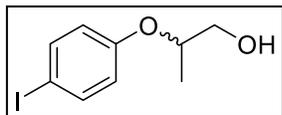
 Prepared according to Synthesis of Racemic Alcohols from (±)-ethyl 2-(4-iodophenoxy)propionate (218 mg, 0.680 mmol) and LiAlH$_4$ (72 mg, 1.9 mmol, 2.8 equiv). Colourless oil, 28% yield. **^{1}H NMR** (499.797 MHz, CDCl$_3$, 27.0 °C): δ 1.27 (d, J = 6.2 Hz, 3H), 1.99 (dd, J = 7.6, 5.3 Hz, 1H), 3.70–3.77 (m, 2H), 4.44–4.49 (m, 1H), 6.71–6.74 (m, 2H), 7.55–7.58 (m, 2H). **^{13}C{^{1}H} NMR** (125.688 MHz, CDCl$_3$, 27.0 °C): δ 15.7, 66.2, 75.0, 83.3, 118.4, 138.4, 157.6. **HRMS (EI)** *m/z*: Calcd for C$_9$H$_{11}$IO$_2$ [M]$^+$: 277.9804. Found: 277.9803. **LRMS (EI)** *m/z*: Calcd for C$_9$H$_{11}$IO$_2$ [M]$^+$: 278. Found: 278. **Retention times (Method A)**: t_R = 21.67 min, t_R = 21.79 min.

(±)-2-(4-Methoxyphenoxy)propan-1-ol
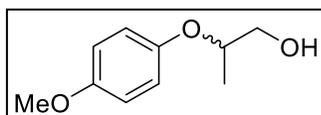
 Prepared according to Synthesis of Racemic Alcohols from (±)-ethyl 2-(4-methoxyphenoxy)propionate (162 mg, 0.721 mmol) and LiAlH$_4$ (82 mg, 2.2 mmol, 3.0 equiv). Colourless oil, 80% yield. **^{1}H NMR** (499.797 MHz, CDCl$_3$, 27.0 °C): δ 1.24 (d, J = 6.2 Hz, 3H), 2.15 (dd, J = 7.2, 5.0 Hz, 1H), 3.67–3.77 (m, 2H), 3.78 (s, 3H), 4.34–4.40 (m, 1H), 6.82–6.85 (m, 2H), 6.88–6.91 (m, 2H). **^{13}C{^{1}H} NMR** (125.688 MHz, CDCl$_3$, 27.0 °C): δ 15.9, 55.7, 66.4, 76.1, 114.7, 117.8, 151.6, 154.4. **HRMS (EI)** *m/z*: Calcd for C$_{10}$H$_{14}$O$_3$ [M]$^+$: 182.0943. Found: 182.0947. **LRMS (EI)** *m/z*: Calcd for C$_{10}$H$_{14}$O$_3$ [M]$^+$: 182. Found: 182. **Retention times (Method A)**: t_R = 17.00 min, t_R = 17.14 min.

(±)-2-(3-Methoxyphenoxy)propan-1-ol
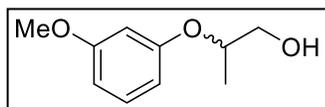
Prepared according to Synthesis of Racemic Alcohols from (±)-ethyl 2-(3-methoxyphenoxy)propionate (211 mg, 0.940 mmol) and LiAlH$_4$ (106 mg, 2.80 mmol, 2.98 equiv). Colourless oil, 87% yield. **^{1}H NMR** (499.797 MHz, CDCl$_3$, 27.0 °C): δ 1.29 (d, J = 6.2 Hz, 3H), 2.08 (br, 1H), 3.69–3.78 (m, 2H), 3.80 (s, 3H), 4.47–4.53 (m, 1H), 6.51 (t, J = 2.3 Hz, 1H), 6.53–6.56 (m, 2H), 7.19 (t, J = 8.2 Hz, 1H). **^{13}C{^{1}H} NMR** (125.688 MHz, CDCl$_3$, 27.0 °C): δ 15.8, 55.3, 66.3, 74.8, 102.6, 106.7, 108.1, 130.0, 158.9, 160.9. **HRMS (EI) *m/z*:** Calcd for C$_{10}$H$_{14}$O$_3$ [M]$^+$: 182.0943. Found: 182.0945. **LRMS (EI) *m/z*:** Calcd for C$_{10}$H$_{14}$O$_3$ [M]$^+$: 182. Found: 182. **Retention times (Method A):** t_R = 16.97 min, t_R = 17.11 min.

(±)-2-(3-Fluorophenoxy)propan-1-ol
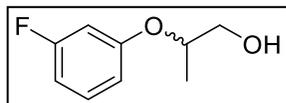
Prepared according to Synthesis of Racemic Alcohols from (±)-ethyl 2-(3-fluorophenoxy)propionate (153 mg, 0.720 mmol) and LiAlH$_4$ (83 mg, 2.2 mmol, 3.0 equiv). Colourless oil, 90% yield. **^{1}H NMR** (499.797 MHz, CDCl$_3$, 27.0 °C): δ 1.29 (d, J = 6.2 Hz, 3H), 2.09 (br, 1H), 3.70–3.78 (m, 2H), 4.46–4.51 (m, 1H), 6.64–6.70 (m, 2H), 6.72 (dd, J = 8.3, 2.2 Hz, 1H), 7.20–7.25 (m, 1H). **^{13}C{^{1}H} NMR** (125.688 MHz, CDCl$_3$, 27.0 °C): δ 15.7, 66.2, 75.1, 103.7 (d, J = 24.5 Hz), 108.0 (d, J = 21.3 Hz), 111.6 (d, J = 3.0 Hz), 130.3 (d, J = 10.1 Hz), 159.1 (d, J = 10.9 Hz), 163.7 (d, J = 245.7 Hz). **^{19}F NMR** (376.318 MHz, CDCl$_3$, 27.0 °C): δ -111.5. **HRMS (EI) *m/z*:** Calcd for C$_9$H$_{11}$FO$_2$ [M]$^+$: 170.0743. Found: 170.0744. **LRMS (EI) *m/z*:** Calcd for C$_9$H$_{11}$FO$_2$ [M]$^+$: 170. Found: 170. **Retention times (Method A):** t_R = 11.67 min, t_R = 11.92 min.
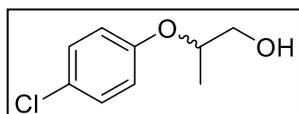
(±)-2-(2-Chlorophenoxy)propan-1-ol
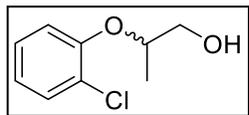
Prepared according to Synthesis of Racemic Alcohols from (±)-ethyl 2-(2-chlorophenoxy)propionate (207 mg, 0.906 mmol) and LiAlH$_4$ (104 mg, 2.75 mmol, 3.04 equiv). Colourless oil, 60% yield. **^{1}H NMR** (499.797 MHz, CDCl$_3$, 27.0 °C): δ 1.34 (d, J = 6.3 Hz, 3H), 2.30 (t, J = 6.7 Hz, 1H), 3.75–3.80 (m, 2H), 4.47–4.53 (m, 1H), 6.93–6.96 (m, 1H), 7.02 (dd, J = 8.3, 1.3 Hz, 1H), 7.20–7.24 (m, 1H), 7.38 (dd, J = 7.9, 1.6 Hz, 1H). **^{13}C{^{1}H} NMR** (125.688 MHz, CDCl$_3$, 27.0 °C): δ 16.1, 66.2, 77.4, 116.6, 122.3, 124.5, 127.8, 130.5, 153.5. **HRMS (EI)** *m/z*: Calcd for C$_9$H$_{11}$ClO$_2$ [M]$^+$: 186.0448. Found: 186.0449. **LRMS (EI)** *m/z*: Calcd for C$_9$H$_{11}$ClO$_2$ [M]$^+$: 186. Found: 186. **Retention times (Method A)**: t_R = 14.32 min, t_R = 14.43 min.

(±)-2-Phenoxybutan-1-ol
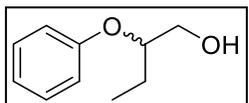
Prepared according to Synthesis of Racemic Alcohols from **173** (209 mg, 1.00 mmol) and LiAlH$_4$ (111 mg, 2.91 mmol, 2.91 equiv). Colourless oil, 80% yield. **^{1}H NMR** (499.797 MHz, CDCl$_3$, 27.0 °C): δ 0.99 (t, J = 7.5 Hz, 3H), 1.65–1.81 (m, 2H), 2.04 (t, J = 6.1 Hz, 1H), 3.74–3.85 (m, 2H), 4.29–4.31 (m, 1H), 6.96–6.99 (m, 3H), 7.28–7.31 (m, 1H). **^{13}C{^{1}H} NMR** (125.688 MHz, CDCl$_3$, 27.0 °C): δ 9.6, 23.4, 64.1, 80.1, 116.2, 121.2, 129.6, 158.2. **HRMS (EI)** *m/z*: Calcd for C$_{10}$H$_{14}$O$_2$ [M]$^+$: 166.0994. Found: 166.0996. **LRMS (EI)** *m/z*: Calcd for C$_{10}$H$_{14}$O$_2$ [M]$^+$: 166. Found: 166. **Retention times (Method A)**: t_R = 12.29 min, t_R = 12.46 min.

(±)-3-Methyl-2-phenoxybutan-1-ol
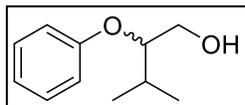
 Prepared with modification of the reaction time, of Synthesis of Racemic Alcohols, to 3 h from (±)-α-phenoxy-isovaleric acid isopropyl ester (201 mg, 0.849 mmol) and LiAlH$_4$ (101 mg, 2.65 mmol, 3.13 equiv). Colourless oil, 80% yield. **^{1}H NMR** (499.797 MHz, CDCl$_3$, 27.0 °C): δ 0.99 (d, J = 6.9 Hz, 3H), 1.03 (d, J = 6.9 Hz, 3H), 1.91 (br, 1H), 2.06–2.16 (m, 1H), 3.78–3.85 (m, 2H), 4.16 (td, J = 6.1, 3.6 Hz, 1H), 6.95–7.00 (m, 3H), 7.27–7.31 (m, 2H). **^{13}C{^{1}H} NMR** (125.688 MHz, CDCl$_3$, 27.0 °C): δ 18.1, 18.6, 29.3, 62.3, 84.0, 116.4, 121.2, 129.6, 158.9. **HRMS (EI) *m/z*:** Calcd for C$_{11}$H$_{16}$O$_2$ [M]$^+$: 180.1150. Found: 180.1154. **LRMS (EI) *m/z*:** Calcd for C$_{11}$H$_{16}$O$_2$ [M]$^+$: 180. Found: 180. **Retention times (Method B)**: t_R = 21.80 min, t_R = 22.00 min.

(±)-2-Phenoxy-2-phenylethan-1-ol
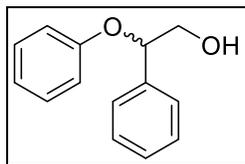
 Prepared with modification of the reaction time, of Synthesis of Racemic Alcohols, to 3 h from (±)-ethyl 2-phenoxy-2-phenylethanoate (200 mg, 0.781 mmol) and LiAlH$_4$ (89 mg, 2.34 mmol, 3.00 equiv). White solid, 84% yield. **^{1}H NMR** (499.787 MHz, CDCl$_3$, 27.0 °C): δ 2.35 (br, 1H), 3.84–3.88 (m, 1H), 3.94–3.98 (m, 1H), 5.31 (dd, J = 8.2, 3.6 Hz, 1H), 6.91–6.96 (m, 3H), 7.21–7.26 (m, 2H), 7.31–7.34 (m, 1H), 7.36–7.42 (m, 4H). **^{13}C{^{1}H} NMR** (125.688 MHz, CDCl$_3$, 27.0 °C): δ 67.6, 81.2, 116.0, 121.3, 126.3, 128.2, 128.8, 129.5, 137.9, 157.8. **HRMS (EI) *m/z*:** Calcd for C$_{14}$H$_{14}$O$_2$ [M]$^+$: 214.0994. Found: 214.0992. **Retention times (Method C)**: t_R = 11.51 min, t_R = 17.11 min.

(±)-2-(Phenylthio)propan-1-ol
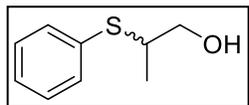
Prepared according to Synthesis of Racemic Alcohols from **186** (201 mg, 0.956 mmol) and LiAlH$_4$ (108 mg, 2.86 mmol, 2.99 equiv). Colourless oil, 70% yield. **^{1}H NMR** (499.787 MHz, CDCl$_3$, 27.0 °C): δ 1.33 (d, J = 7.0 Hz, 3H), 2.18 (br, 1H), 3.30–3.37 (m, 1H), 3.51–3.56 (m, 1H), 3.60–3.65 (m, 1H), 7.28–7.35 (m, 3H), 7.46–7.48 (m, 2H). **^{13}C{^{1}H} NMR** (125.685 MHz, CDCl$_3$, 27.0 °C): δ 17.6, 46.6, 65.4, 127.6, 129.0, 133.0. **HRMS (EI)** *m/z*: Calcd for C$_9$H$_{12}$OS [M]$^+$: 168.0609. Found: 168.0610.

(±)-2-(4-Isobutylphenyl)propan-1-ol
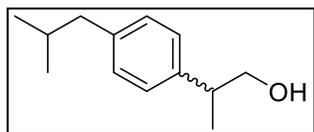
Prepared according to Synthesis of Racemic Alcohols from **187** (149 mg, 0.635 mmol) and LiAlH$_4$ (72 mg, 1.90 mmol, 2.99 equiv). Colourless oil, 90% yield. **^{1}H NMR** (499.787 MHz, CDCl$_3$, 27.0 °C): δ 0.94 (d, J = 6.6 Hz, 6H), 1.30 (d, J = 7.1 Hz, 3H), 1.44 (br, 1H), 1.83–1.94 (m, 1H), 2.49 (d, J = 7.2 Hz, 2H), 2.95 (sext, J = 6.9 Hz, 1H), 3.71 (d, J = 6.8 Hz, 2H), 7.13–7.18 (m, 4H). **^{13}C{^{1}H} NMR** (125.685 MHz, CDCl$_3$, 27.0 °C): δ 17.6, 22.4, 30.2, 42.1, 45.1, 68.8, 127.2, 129.4, 140.0, 140.1. **HRMS (EI)** *m/z*: Calcd for C$_{13}$H$_{20}$O [M]$^+$: 192.1514. Found: 192.1513.

Chapter 3:

Syntheses of Ru(II)–Polypyridyl Complexes for Photoredox Catalysis

3.1 Introduction

3.1.1 General Intro

Ru–polypyridyl complexes are of significant interest for organic photochemical transformations since the seminal reports by MacMillan and Yoon in 2008.[166, 167] MacMillan and Nicewicz used [Ru(bipy)$_3$]Cl$_2$ and the organocatalyst **190** for the dual-catalytic photoredox asymmetric alkylation of aldehydes (Scheme 3-1).[166]
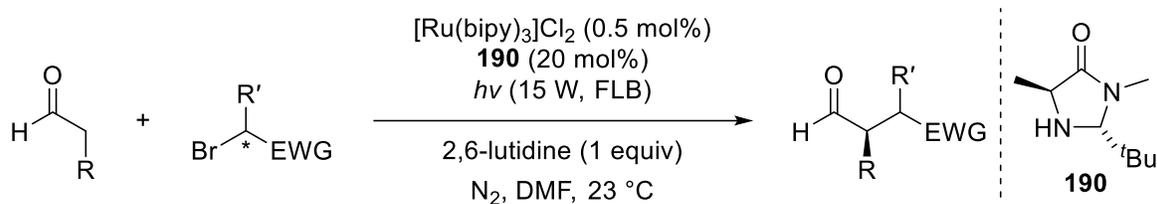
Scheme 3-1. MacMillan's dual-catalytic photoredox asymmetric alkylation of aldehydes with [Ru(bipy)$_3$]Cl$_2$.[166]

Yoon and co-workers reported the use of [Ru(bipy)$_3$]Cl$_2$ for photocatalytic [2+2] enone cycloadditions.[167] For example, (2*E*,7*E*)-1,9-bis(4-methoxyphenyl)nona-2,7-diene-1,9-dione (**191**) was mostly transformed into (1*R*,5*S*,6*R*,7*S*)-6,7-bis-(4-methoxybenzoyl)bicyclo[3.2.0]heptane (**192**) in sunlight (Scheme 3-2).
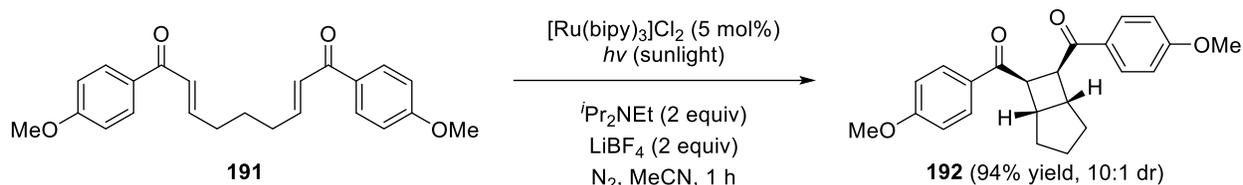
Scheme 3-2. Yoon's photocatalytic [2+2] enone cycloaddition of **191** to **192** with [Ru(bipy)$_3$]Cl$_2$.[167]

Since these seminal reports, several researchers have reported new organometallic polypyridyl complexes as photoredox catalysts for organic transformations.[168]

Polypyridyl complexes, such as [Ru(bipy)$_3$]Cl$_2$, exhibit unique photophysical properties, which make them suitable photoredox catalysts.[169] Specifically, these complexes have long-lived triplet excited state lifetimes that allow them to undergo single-electron transfer (SET) events with other molecules. A SET event can result in the catalyst undergoing either reduction or oxidation and a molecule becoming either a radical anion or cation, respectively. These radical species then undergo chemical transformations to form more stable compounds.

The combination of a photoredox catalyst and a hydrogenation catalyst, in the homogeneous phase, has been underexplored. To the best of my knowledge, the only successful application of a Ru(II)–polypyridyl photoredox catalyst and hydrogenation catalyst, in the homogeneous phase, was that reported by Rau and co-workers.[170]

In 2006, Rau and co-workers reported the synthesis of the Ru(II)–polypyridyl photoredox catalyst **193**.[170] This chelating photocatalyst was combined with Pd(MeCN)$_2$Cl$_2$ to form a Ru–Pd complex **194** (Scheme 3-3).[170]
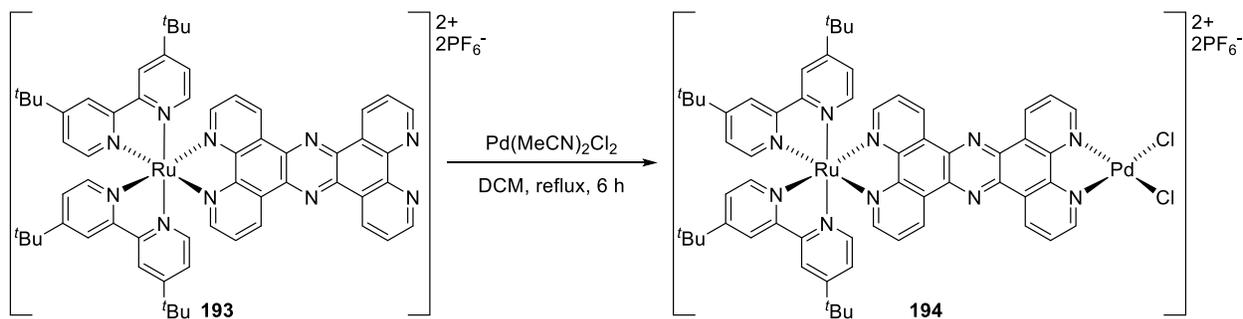
Scheme 3-3. Rau's synthesis of their Ru–Pd photohydrogenation precatalyst **194**.[170]

Complex **194** photocatalyzed the hydrogenation of diphenylacetylene (**195**) to *cis*-stilbene (**196**) using triethylamine as the H$_2$ equivalent (Scheme 3-4).[170]

154

194 (0.2 mol%)
hv (470 nm)

NEt$_3$ (~138 equiv)
Ar, MeCN, 116 h

195 (0.24 g)   **196** (13% conv)

^{t}Bu

2+
2PF$_6^-$

Cl
Cl

194
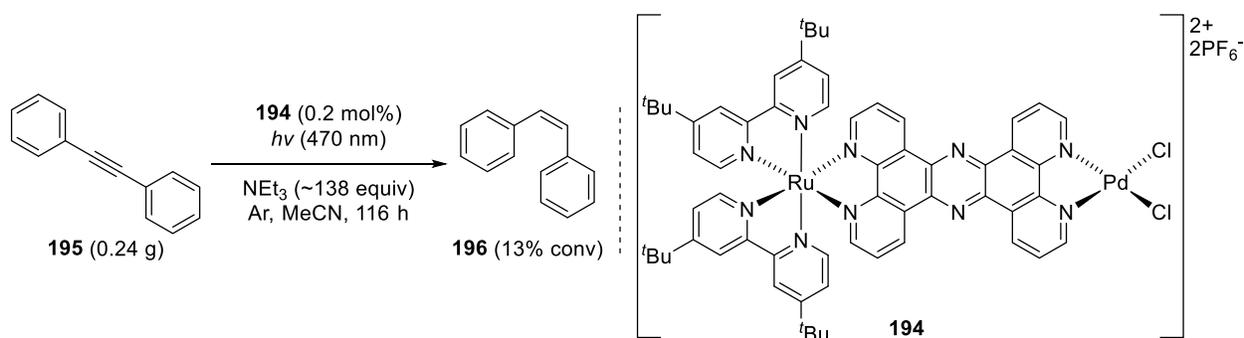
Scheme 3-4. Rau's homogeneous photocatalytic hydrogenation of diphenylacetylene (**195**).[170]

The production of the H$_2$ equivalent is believed to occur through several steps. The triplet excited

state of the Ru chromophore, formed via metal-to-ligand charge transfer (MLCT), likely

transfers an electron to Pd(II), reducing it to Pd(I). The Ru(III) is reduced back to Ru(II) by a

one-electron oxidation of triethylamine. The resulting cationic triethylamine radical loses a

proton and then undergoes a second one-electron oxidation to form a cationic iminium species. It

is also possible that the cationic triethylamine reduces Pd(I) to Pd(0) with loss of a proton, to

form the cationic iminium. The cationic iminium exists in equilibrium with its respective

enamine.[171] The oxidation of triethylamine and its resulting products are illustrated in Scheme

3-5. It is proposed that the Pd(I) species is eventually reduced to Pd(0).[170] The Pd(0) reacts

further with photogenerated protons and electrons to generate H$_2$ or its equivalent to net

hydrogenate **195**.[170] Therefore, this dual-catalytic system is believed to operate via MLCT and

ligand-to-metal charge transfer (LMCT). The hydrogenation of **195** proceeded with only 63

turnovers over 5 days (TOF = 0.54 h^{-1}).[170] The hydrogenation of **195** did not proceed without

irradiation. Substitution of the Ar atmosphere with H$_2$ significantly increased activity (97% conv,

TON = 485, TOF = 4.85 h^{-1}).[170] This example shows that MLCT and LMCT events can occur

between a photoexcited Ru dye and a connected site for hydrogenation.
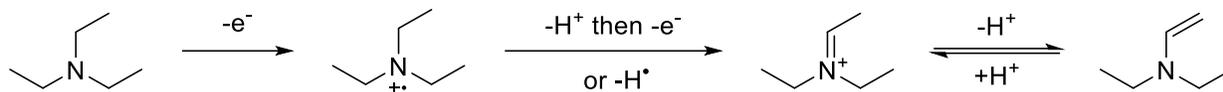
Scheme 3-5. The oxidation of triethylamine and its product cationic triethylamine radical.

In the interest of developing my own Ru(II)–polypyridyl photoredox catalysts, for photohydrogenation, three target compounds were devised for screening (Figure 3-1).
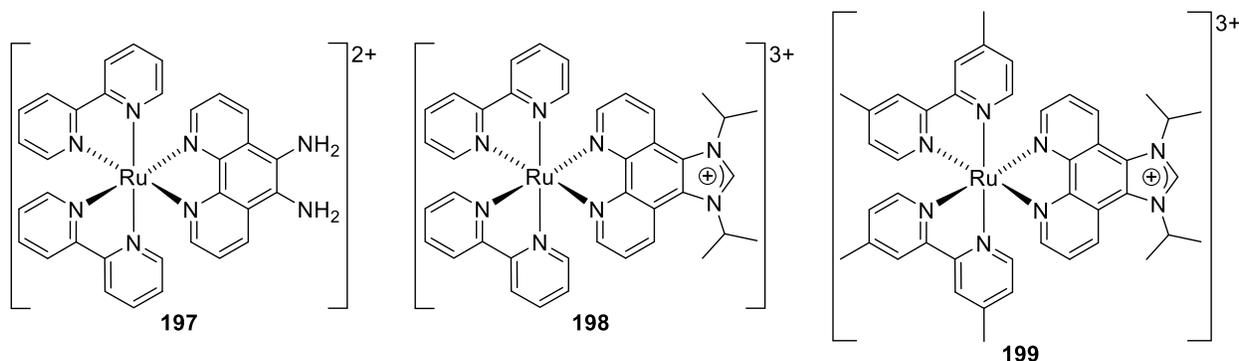
Figure 3-1. Selected target Ru(II)–polypyridyl complexes for photohydrogenation screenings.

[Ru(bipy)$_2$(1,10-phenanthroline-5,6-diamine)]$^{2+}$ (**197**) was of interest due to its diamine functionality. Specifically, the diamine could be used as a ligand to form a Noyori-type photohydrogenation catalyst with an N–H functionality. The premise to be explored with **197** is based upon whether its excited state increases the activity of a Noyori-type active site. More specifically, the excitation of the Ru–polypyridyl complex involves MLCT and intersystem crossing to form a relatively long-lived triplet state with an electron in the π* molecular orbitals of the polypyridyl ligands. The Bergens group reported that deprotonation of the N–H groups of Noyori-type bifunctional catalysts dramatically increases their activity towards amides and imides.[158] Chianese and co-workers reported that the Ru(0) analogs of related catalysts are more active than Ru(II).[114] These results indicate that increasing the electron density at the Ru hydrogenation site increases its reactivity towards carbonyl reduction. Further, the acidity of the O–H functionality of 1-naphthol increases dramatically upon photoexcitation.[172] Perhaps a

similar photoenhanced acidity can occur in the diamino fragment of a Noyori-type species incorporating **197**. Finally, Ru–amido species (Ru=N) are common intermediates in Noyori-type bifunctional hydrogenations. A dinuclear Ru species incorporating **197** as ligand would allow direct π-conjugation between the excited triplet state of the chromophore and the bifunctional active site. The effects of such π-conjugation during hydrogenation under photoexcitation are unknown.

The Ru–imidazolium complexes **198** and **199** were of synthetic interest for deprotonation to their respective NHC chromophores. Ideally, the NHC chromophores can be bonded to active sites for photoactivated hydrogenation. Ru–imidazolium complexes similar to **198** and **199** have been reported,[173-177] but the free NHCs could not be prepared. The published analogs did not contain isopropyl groups to sterically stabilize the target NHCs. I reasoned that the isopropyl groups in **198** and **199** would provide sufficient steric crowding to allow the free NHC to form and bond to active sites.

3.1.2 Prior Syntheses

Complex **197** is previously reported[178-188] and has been used to synthesize dinuclear Ru–polypyridyl complexes[178-180] and luminescent sensors.[181-185] It has also been used as a luminescent sensor without prior derivatization.[183, 186, 187]

The first synthesis of **197**, as a chloride salt (**197–Cl**), was reported in 1998. Gourdon and co-workers reduced the amino-nitro derivative **200** with hydrazine hydrate over Pd/C to synthesize **197** (Scheme 3-6).[178] The reaction proceeded in high yield (89%), but the authors did not provide several reaction conditions, such as time, temperature, and solvent.[178]

157
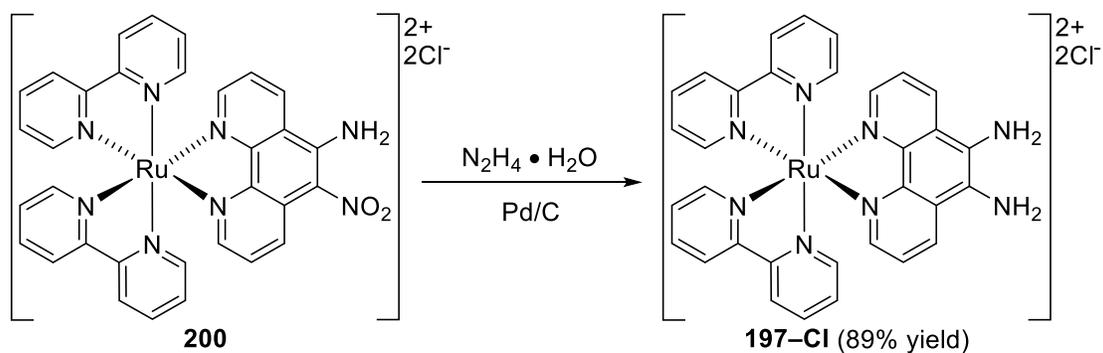
Scheme 3-6. Gourdon's original synthesis of [Ru(bipy)$_2$(1,10-phenanthroline-5,6-diamine)]$^{2+}$ (**197**) as a Cl salt.[178]

A year later, Gourdon and co-workers reported the synthesis of dihydrated **197** with PF$_6^-$ anions (**197–PF$_6$**).[179] This synthesis followed the method of the previous report but included the missing reactions conditions (Scheme 3-7).[179] The nitro group of **200** was reduced using 10 equivalents of hydrazine hydrate (55%), 10% Pd/C, in a refluxing solution of EtOH/MeOH (1:1).[179] This reaction resulted in exactly the same yield (89%) of **197** as the prior report.[179] Gourdon and co-workers stated that the attempted preparation of **197** via [Ru(Cl)$_2$(bipy)$_2$] (**201**), 1,10-phenanthroline-5,6-diamine (**202**), and AgOTf resulted in a mixture containing the dinuclear species [(bipy)$_2$Ru(tpphz)Ru(bipy)$_2$]$^{4+}$.
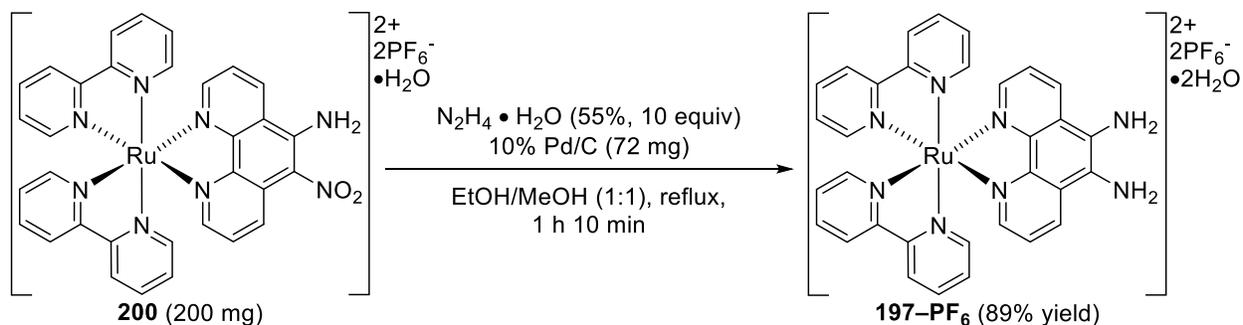
Scheme 3-7. Gourdon's detailed synthesis of [Ru(bipy)$_2$(1,10-phenanthroline-5,6-diamine)]$^{2+}$ (**197**) as a PF$_6$ salt.[179]

In the same year, Ward and co-workers reported their reaction of **201** with **202** and subsequent anion exchange with NH$_4$PF$_6$ (Scheme 3-8).[180]

158
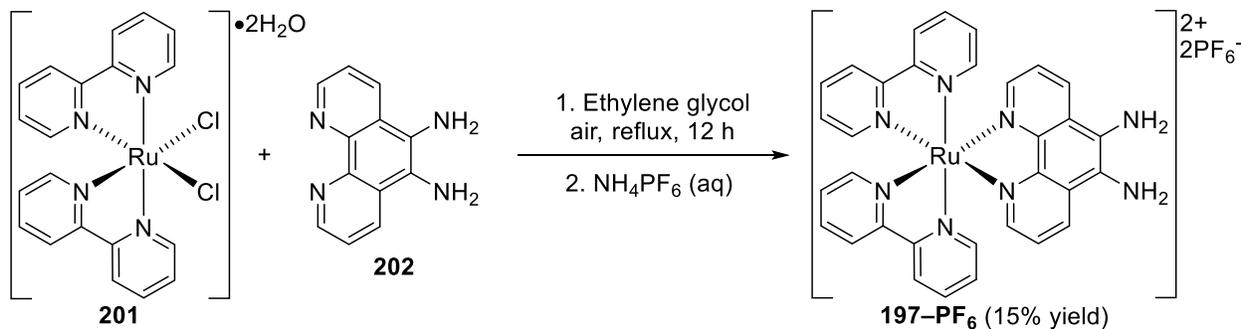
Scheme 3-8. Ward's synthesis of **197** from $[Ru(Cl)_2(bipy)_2]$ (**201**) and 1,10-phenanthroline-5,6-diamine (**202**).[180]

The reaction formed **197–PF$_6$** in poor yield (15%).[180] The poor yield was partially due to the formation of the dinuclear Ru complex **203** (Figure 3-2) as the major product (40% yield). Complex **203** is speculated to have formed via two-electron oxidation of the diamine in air.[180]
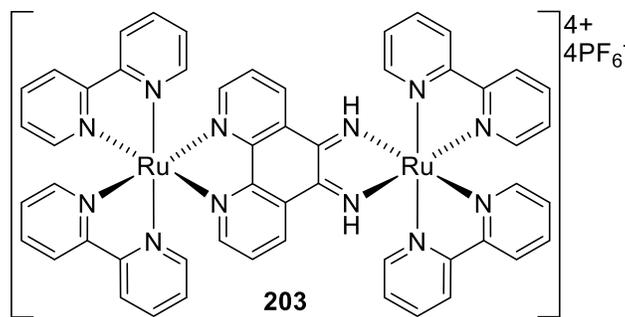
Figure 3-2. Chemical structure of Ward's dinuclear Ru complex **203**.[180]

In 2010, Paul and co-workers were able to synthesize **197–PF$_6$**, from **201** and **202**, by refluxing in EtOH/H$_2$O, anion exchange, and then column chromatography to obtain a 60% yield of **197–PF$_6$** (Scheme 3-9).[183] This yield is significantly greater than that obtained by Ward and co-workers. Perhaps the solvent participates in the formation of **197** and/or lower temperature prevents formation of dinuclear Ru species like **203**.
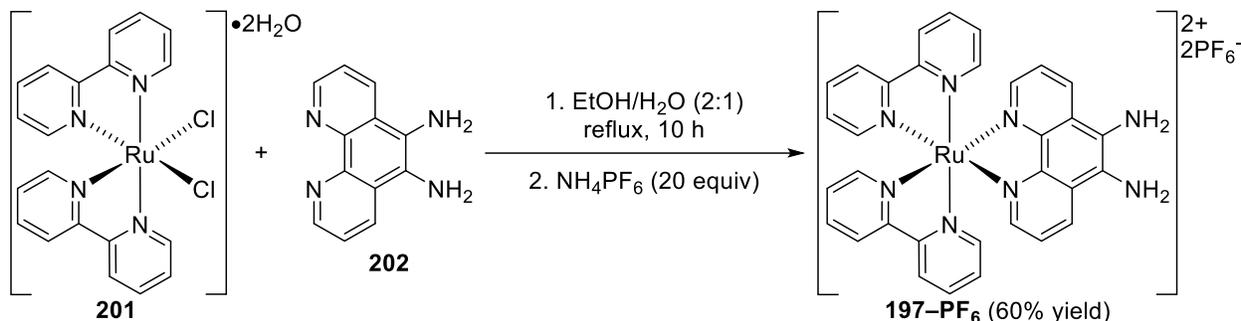
Scheme 3-9. Paul's synthesis of **197** from [Ru(Cl)$_2$(bipy)$_2$] (**201**) and 1,10-phenanthroline-5,6-diamine (**202**).[183]

3.2 Results and Discussion

3.2.1 Synthesis of [Ru(bipy)$_2$(1,10-phenanthroline-5,6-diamine)]$^{2+}$

The precursor *cis*-[Ru(MeCN)$_2$(bipy)$_2$](OTf)$_2$ (**204**) was prepared from **201**, AgOTf, and MeCN (Scheme 3-10). The exchange of the chlorides was complete within 2 h at room temperature to give **204**.
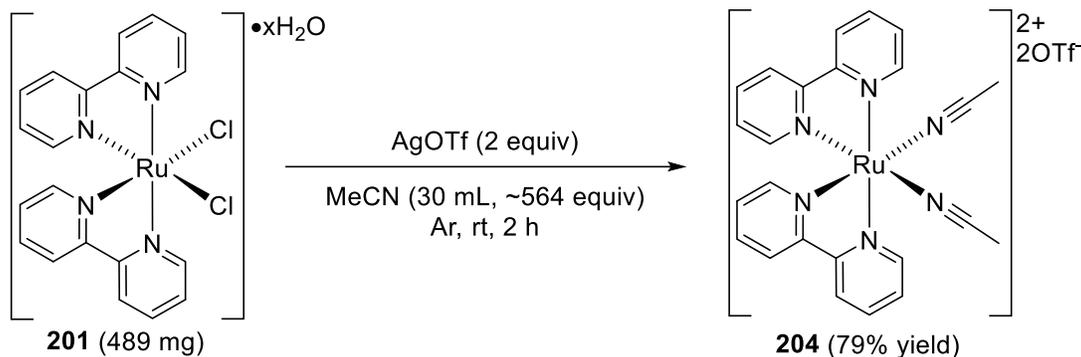
Scheme 3-10. Synthesis of *cis*-[Ru(MeCN)$_2$(bipy)$_2$](OTf)$_2$ (**204**) from **201** and AgOTf in MeCN.

Complex **204** refluxed with **202**, in MeOH, formed **197** with triflate anions (**197–OTf**) (Scheme 3-11). The long reaction time (3 days) may be attributed to the displacement of MeCN occurring by a dissociative mechanism and the increasing concentration of MeCN as the reaction proceeds. NMR spectroscopy supported the formation of complex **197–OTf** as the major product. The preference for **197–OTf**, over the NH$_2$ groups bonding, is believed to be controlled

by stronger bonding between the Ru and sp^2 nitrogen. Specifically, the Ru and sp^2 nitrogen will

have π-interactions and perhaps a more optimal ring size than the sp^3 nitrogen.
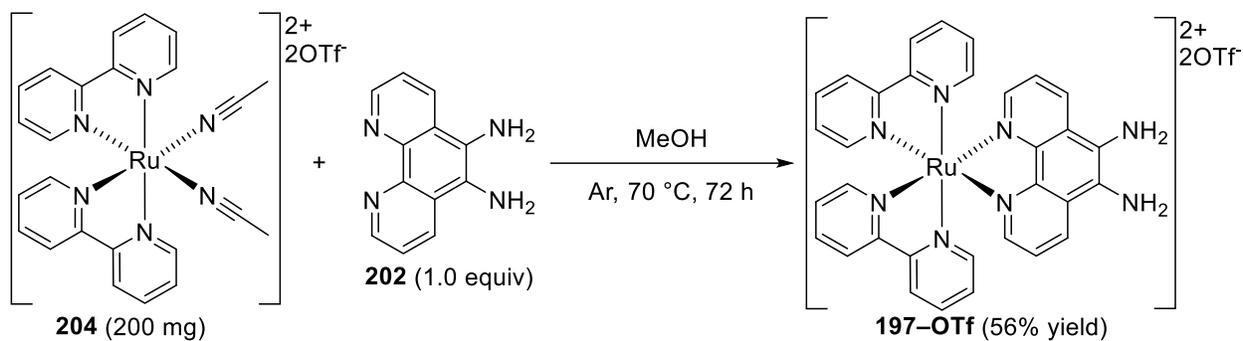
Scheme 3-11. Synthesis of [Ru(bipy)$_2$(1,10-phenanthroline-5,6-diamine)](OTf)$_2$ (**197–OTf**) in MeOH.

3.2.2 Syntheses of Ru–Polypyridyl–Imidazolium Salts

The retrosynthetic strategy to obtain **205** from **202** is shown in Scheme 3-12.
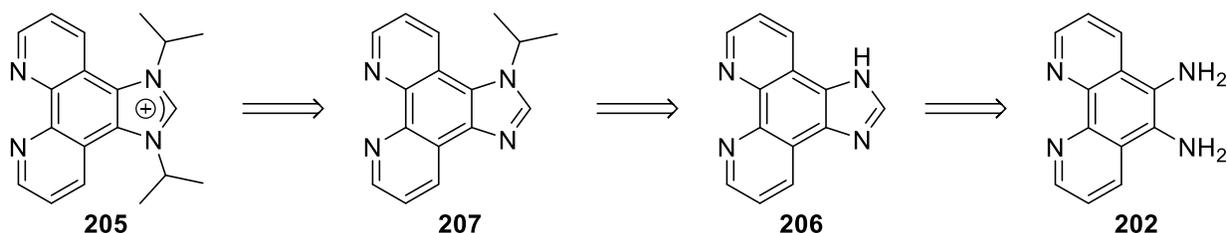
Scheme 3-12. Planned retrosynthesis for 1,3-di(propan-2-yl)-1*H*-imidazol[4,5-*f*][1,10]phenanthrolin-3-ium (**205**).

The synthesis of the known compound imidazo[4,5-*f*][1,10]-phenanthroline (**206**) was

performed using **202**, triethyl orthoformate, and sulfamic acid (Scheme 3-13). A similar

procedure was reported for 1,2-diamino-benzene to benzoimidazole.[189] To the best of my

knowledge, this method has not been reported for the synthesis of **206**. Notably, **206** was

acquired in 95% yield.
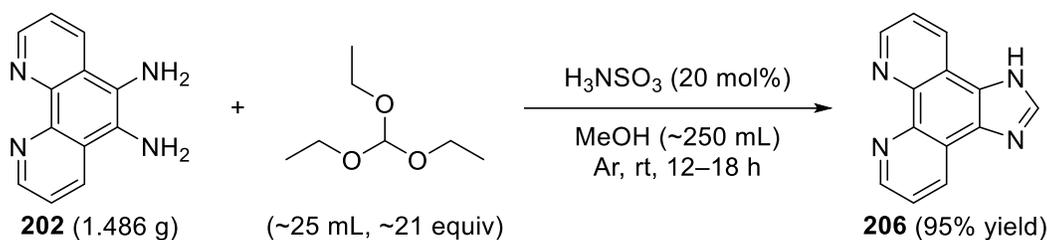
Scheme 3-13. Synthesis of imidazo[4,5-*f*][1,10]-phenanthroline (**206**) from **202** and triethyl orthoformate.

The compound 1-(propan-2-yl)-1*H*-imidazo[4,5-*f*][1,10]-phenanthroline (**207**) was

prepared from **206**, 2-iodopropane, and Cs₂CO₃ in MeCN (Scheme 3-14). Similar methods have

been reported for the alkylation of **206** with primary alkyl halides.[173-175, 190] Most of these

previously reported alkylations of **206** required less than 7 h.[173-175] The full conversion of **206**

required a longer reaction time (39 h), even under reflux and using an alkyl iodide. The

sluggishness of this alkylation is likely caused by the steric hindrance of the secondary amine

approaching the secondary alkyl halide. Although the reaction is slow, a good yield (86%) of **207**

was obtained under optimized conditions.
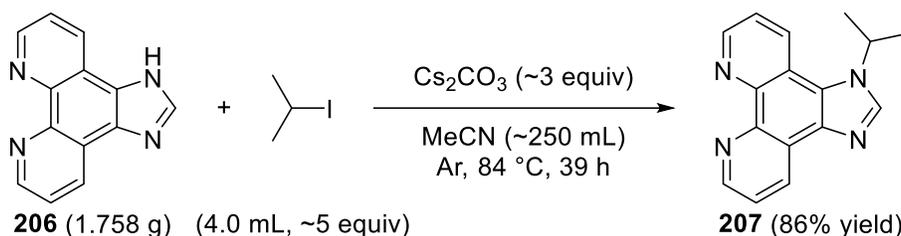
Scheme 3-14. Alkylation of **206** to form 1-(propan-2-yl)-1*H*-imidazo[4,5-*f*][1,10]-phenanthroline (**207**).

The synthesis and isolation of **205** was not successful. Several attempts to alkylate **207** to

form **205** with 2-iodopropane were performed. A low-temperature alkylation with isopropyl

triflate was also attempted but did not provide **205** in reasonable yield. Similar challenges were

reported by Rau and co-workers in alkylating their derivatives.[175] Microwave irradiation may be

required to obtain **205** from **207**. Efforts to selectively alkylate the diamine **202** with

2-iodopropane and then form **205** were also unsuccessful. Due to these difficulties, an alternative derivative was synthesized.

Instead of continuing attempts at preparing **205**, the asymmetrical ligand 1-benzyl-3-(propan-2-yl)-1*H*-imidazol[4,5-*f*][1,10]phenanthroline-3-ium bromide (bpip–Br, **208**) was prepared. The imidazolium salt **208** was prepared by simply reacting **207** with benzyl bromide for 5 h at 120 °C (Scheme 3-15). A similar procedure was reported to prepare a dibenzyl derivative.[174] To the best of my knowledge, **208** has not been reported in the literature. Importantly, **208** was obtained in 67% yield and could be used for complexation reactions.
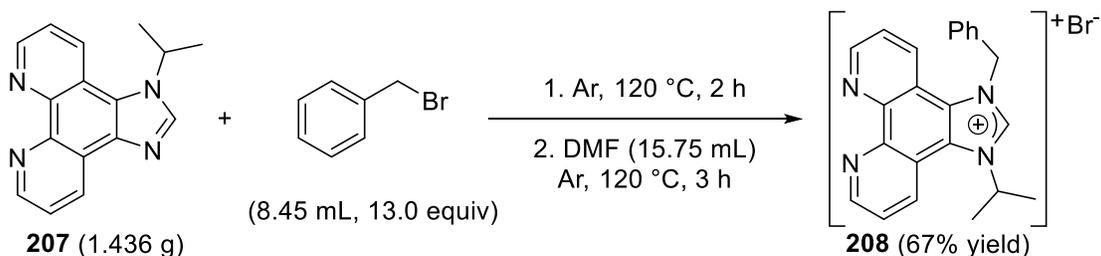
Scheme 3-15. Alkylation of **207** with benzyl bromide to form the imidazolium salt bpip–Br (**208**).

The complexation of **208** (bpip–Br) to the dichloride precursor **201** proceeded smoothly to the tricationic complex **209–BrCl₂** (Scheme 3-16) in excellent yield (98%). Although the reaction proceeded smoothly, a long reaction time (36 h) was required. The long reaction time is likely a result of several factors, including the rigidity of **208**'s backbone, the electronic effects of **208**'s imidazolium group on coordinating ability, and the difficulty of two positively charged species reacting with each other.
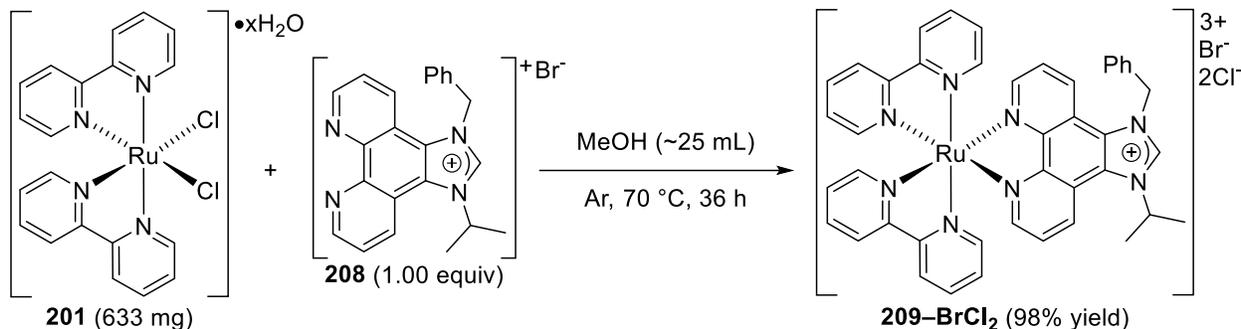
Scheme 3-16. Formation of [Ru(bpip)(bipy)$_2$]BrCl$_2$ (**209–BrCl$_2$**) from complexation of bpip–Br (**208**) to **201**.

Anion exchange of the halides in concentrated aqueous solutions of ammonium salts (i.e., NH$_4$BF$_4$, NH$_4$PF$_6$, and NH$_4$OTf) proceeded smoothly. For example, the bromide and chlorides of **209–BrCl$_2$** were easily replaced with triflate anions via concentrated aqueous solution of NH$_4$OTf (Scheme 3-17). The products were recrystallized in hot MeOH.
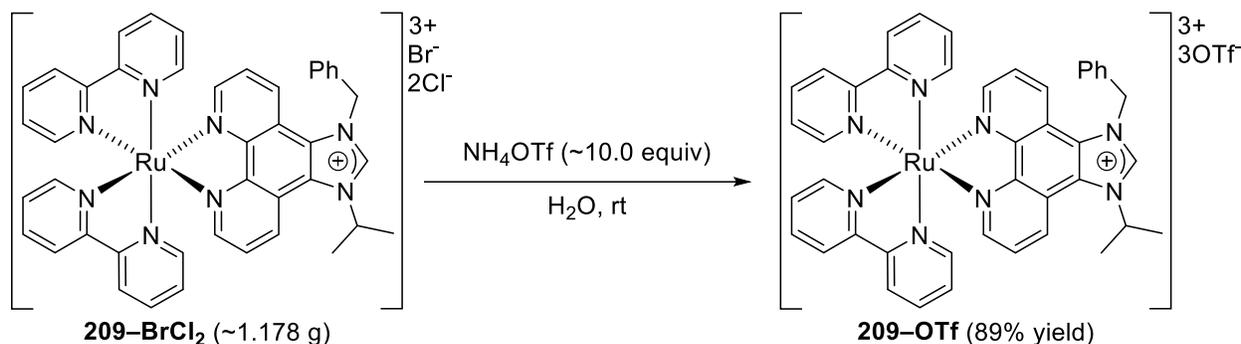
Scheme 3-17. Anion exchange reaction of **209–BrCl$_2$** to [Ru(bpip)(bipy)$_2$](OTf)$_3$ (**209–OTf**) with NH$_4$OTf.

Satisfyingly, crystals suitable for X-ray crystallography were obtained for **209** with tetrafluoroborate anions (**209–BF$_4$**). The crystal structure (Figure 3-3) and accompanying data confirmed the structure and several aspects about **209–BF$_4$**. The crystallographic data (Table 3-1 and 3-2) and selected interatomic angles (Table 3-3) are included in the experimental details section of this chapter. The crystal system of **209–BF$_4$** is highly asymmetrical as all of its vectors and angles between the vectors are unequal (Table 3-1). Thus, the crystal system of **209–BF$_4$** is triclinic. Belonging specifically to the $P\bar{1}$ space group, the crystal system contains an inversion

centre as its only symmetry element. Unsurprisingly, the bite angles of the bidentate polypyridyl

ligands were found to be less than <90° (Table 3-3). As a result, the octahedral geometry of

209–**BF₄** is slightly distorted. This is further supported by the closest right and straight angles,

between the Ru and coordinating N atoms, to be 87.84(11) and 174.52(10)°, respectively.

Notably, the interatomic bond distances between the N atoms and the C of the imidazolium

moiety (N7 to C33 and N8 to C33) are both 1.322(5) Å. This supports an equal distribution of

the double-bond character and that the N-alkyl substituents have equal or no impact on the

charge distribution. This is contrary to previous literature on similar

Ru(II)–polypyridyl–imidazolium complexes, which noted slightly differing bond lengths on the

imidazolium moiety when different alkyl substituents were present.[175]
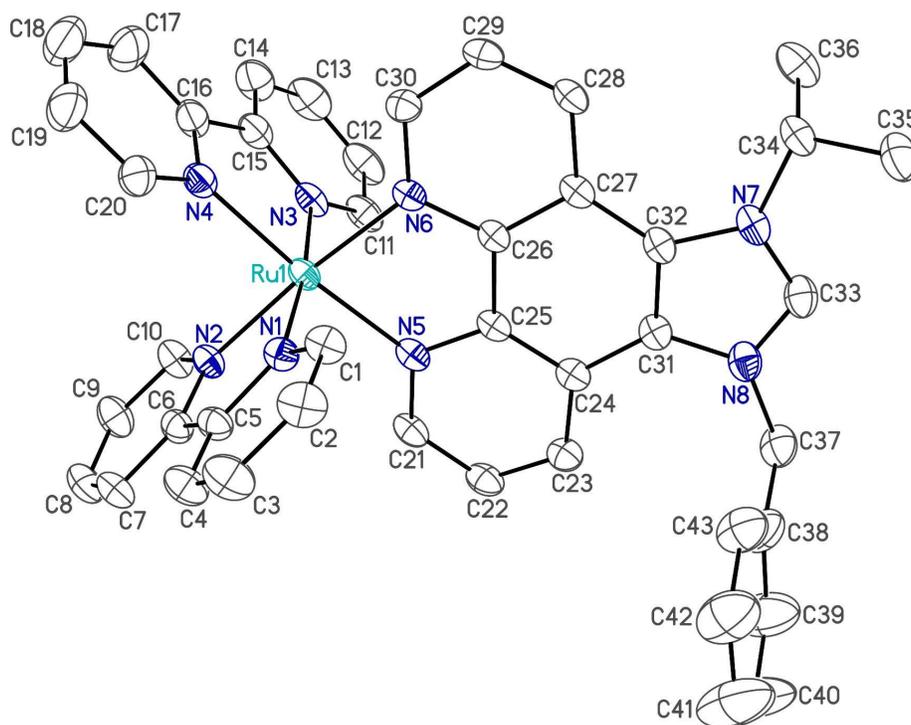
Figure 3-3. Perspective view of [Ru(bpip)(bipy)₂](BF₄)₃ (**209**–**BF₄**). Non-hydrogen atoms are represented by Gaussian ellipsoids at the 30% probability level. The hydrogen atoms and three BF₄⁻ are omitted for clarity.

The complexation of **208** (bpip–Br) to the dichloride precursor *cis*-[Ru(Cl)₂(dmbipy)₂] (**210**) and the subsequent triflate anion exchange proceeded smoothly to **211** (Scheme 3-18). A long reaction time (24 h) was required and is likely the result of the several factors previously mentioned for the formation of **209–BrCl₂**. The bromide and chlorides were also easily replaced with triflate anions via concentrated aqueous solution of NH₄OTf. The hot recrystallization of **211** resulted in 73% yield of **211**.
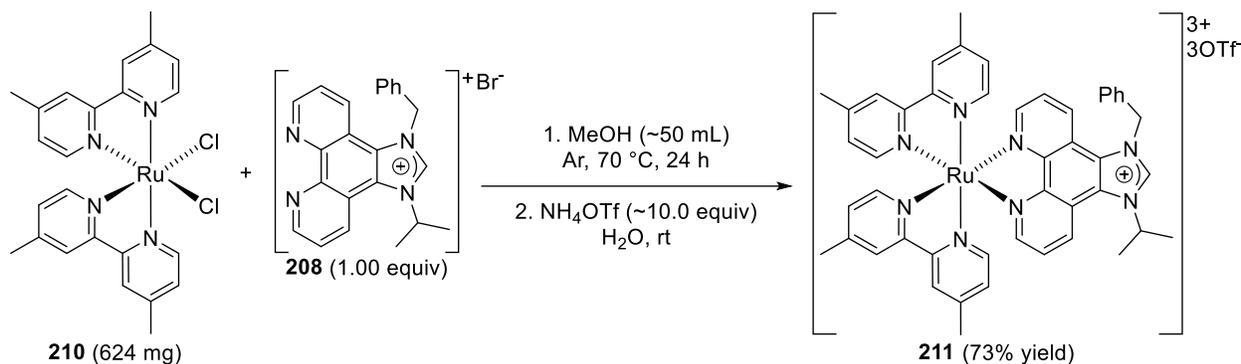
Scheme 3-18. Two-step synthesis of [Ru(bpip)(dmbipy)₂](OTf)₃ (**211**) from *cis*-[Ru(Cl)₂(dmbipy)₂] (**210**).

3.3 Conclusion

The target Ru(II)–polypyridyl diamine complex **197** was successfully prepared. The target Ru–polypyridyl–imidazolium complexes **198** and **199** were not prepared due to complications with obtaining the symmetrical ligand **205**. The alternative Ru(II)–polypyridyl–imidazolium complexes **209** and **211** were prepared from reactions with the asymmetrical ligand **208**. Anion exchange reactions with **209** and **211** were straightforward. The preliminary studies on whether the synthesized Ru(II)–polypyridyl complexes are able to facilitate an electron transfer to catalyze a hydrogenation is presented in Chapter 4. The usage of these complexes for other purposes is also being explored by fellow group members.

3.4 Experimental Details

3.4.1 General Information

3.4.1.1 Purchased Chemicals

Reagents were obtained and used without further purification, unless otherwise stated, from a variety of suppliers. Na metal (Technical) was obtained from Anachemia. Benzophenone (Certified/Crystalline Flakes) and sulfamic acid (LabChem™, ACS Grade, $\geq$99.3%) were obtained from Fisher Scientific. Ar (High Purity, 99.998%, 4.8) and N_2 (High Purity, 99.995%, 4.5) were obtained from Praxair. The 1,10-phenanthroline-5,6-diamine ($\geq$98%) was purchased from Shanghai UCHEM Inc. The NH_4BF_4 ($\geq$97%), NH_4OTf (99%), benzyl bromide (Reagent grade, 98%), CaH_2 (Reagent grade, 95%), Cs_2CO_3 (ReagentPlus®, 99%), Celite® 545 (Filter aid, treated with Na_2CO_3), *cis*-[Ru(Cl)$_2$(bipy)$_2$]•xH_2O (97%), 2-iodopropane (99%), 4,4′-dimethyl-2,2′-bipyridine (99%), AgOTf ($\geq$99%), and triethyl orthoformate (98%) were purchased from Sigma-Aldrich. SiO_2 (SiliaFlash® P60) was obtained from Silicycle. [Ru(COD)Cl$_2$]$_n$ ($\geq$97%) was obtained from Strem Chemicals.

Solvents were obtained from a variety of suppliers. The 1,2-dichlorobenzene (99%) was obtained from Anachemia. CD_3OD (99.8% D) was obtained from Cambridge Isotope Laboratories. Hexanes (ACS reagent) was obtained from Caledon Laboratory Chemicals. DMF (Certified ACS, 99.9%) was obtained from Fisher Scientific. Acetone (ACS reagent, $\geq$99.5%), MeCN (HPLC, gradient grade, $\geq$99.9%), CD_3CN ($\geq$99.8% D), DCM (ACS reagent, $\geq$99.5%), DMSO-d_6 (99.9% D), Et_2O (ACS reagent, $\geq$99.0%), MeOH (ACS reagent, $\geq$99.8%), were obtained from Sigma-Aldrich.

3.4.1.2 Air- and Moisture-Sensitivity

Most reactions were performed under air- and moisture-free conditions. Standard Schlenk techniques were used where applicable. All glassware and stainless-steel needles for air- and moisture-sensitive reactions were oven-dried prior to immediate usage.

Most solvents and liquid reagents were freshly distilled or inertly collected from a SPS. Solvents and liquid reagents were deaerated by bubbling with Ar or N_2 for $\geq$30 min before usage. Specifically, MeCN (CaH_2), DCM (CaH_2), DMF (CaH_2), and Et_2O (Na/benzophenone) were dried by distillation, over the appropriate drying agent, under Ar or N_2. MeOH was collected under N_2 from a LC Technology Solutions Inc. SPS. Dried and deaerated solvents and reagents were delivered via gas-tight syringes or cannulas (stainless steel).

3.4.1.3 Chemical Characterization Methods

A variety of chemical characterization techniques were performed. NMR spectroscopy was performed on a variety of instruments. The ^{1}H NMR spectra were acquired using one of four spectrometers: 400 MHz Varian Inova, a 500 MHz Varian Inova, a 500 MHz Varian VNMRS, and a 600 MHz Varian Inova. The ^{13}C$\{^1$H$\}$ NMR spectra were acquired using either a 500 MHz Varian VNMRS or a 600 MHz Varian Inova. Chemical shifts (δ values) are reported in ppm. Coupling constants (*J* values) are reported in Hz and multiplicities abbreviated as follows: s (singlet), d (doublet), sept (septet), br (broad), m (multiplet), dd (doublet of doublets), and ddd (doublet of doublets of doublets). HRMS spectra were acquired using electrospray ionization in an Agilent 6220 oaTOF. Elemental analyses were performed with a Carlo Erba EA1108 Elemental Analyzer. X-ray crystallography was performed on a Bruker D8 Duo diffractometer with a SMART APEX II CCD area detector.

3.4.2 X-ray Crystallography

Crystals suitable for X-ray diffraction were obtained for [Ru(bpip)(bipy)$_2$](BF$_4$)$_3$

(**209–BF$_4$**) via slow evaporation of MeOH in air. A suitable crystal was mounted on a glass fiber

and placed in a -80 °C stream of N$_2$ on a Bruker D8 Duo diffractometer's sample holder. The

diffractometer used graphite-monochromated Mo K$_\alpha$ radiation and the reflections were collected

on a SMART APEX II CCD area detector. The collected crystal data for **209–BF$_4$** is presented in

Table 3-1.

Table 3-1. Crystal data for [Ru(bpip)(bipy)$_2$](BF$_4$)$_3$ (**209–BF$_4$**).

[Ru(bpip)(bipy)$_2$](BF$_4$)$_3$	
formula	C$_{43}$H$_{37}$B$_3$F$_{12}$N$_8$Ru
formula weight	1027.30
crystal dimensions (mm)	0.23 x 0.17 x 0.12
crystal system	triclinic
space group	$P\bar{1}$ (No. 2)
unit cell parameters^a	
a (Å)	9.0867(5)
b (Å)	14.5057(7)
c (Å)	18.9938(10)
α (°)	71.0106(7)
β (°)	89.5568(7)
γ (°)	75.2895(7)
V (Å^3)	2282.0(2)
Z	2
ρ_{calcd} (g cm^{-3})	1.495
μ (mm^{-1})	0.434
^{a}Obtained from least-squares refinement of 9918 reflections with 4.40° < 2θ < 47.80°.	

The data collection and refinement conditions are presented in Table 3-2. The crystal

structure was solved using intrinsic phasing (*SHELXT-2014*)[191] and refined using full-matrix

least-squares on F^2 (SHELXL-2017)[192]. The refinement required the usage of the SQUEEZE

procedure, as implemented in *PLATON*.[193] This procedure was implemented due to unsuccessful

Table 3-2. Data collection and refinement data for [Ru(bpip)(bipy)$_2$](BF$_4$)$_3$ (**209–BF$_4$**).

[Ru(bpip)(bipy)$_2$](BF$_4$)$_3$	
diffractometer	Bruker D8 / Apex II CCD[a]
radiation (λ [Å])	graphite-monochromated Mo Kα (0.71073)
temperature (°C)	-80
scan type	ω scan (0.3°) (20 s exposures)
data collection 2θ limit (°)	52.86
total data collected	18726
index ranges	$-11 \leq h \leq 11$
	$-18 \leq k \leq 18$
	$-23 \leq l \leq 23$
independent reflections (R_{int})	9396 (0.0234)
observed reflections	7834 [$F_o^2 \geq 2\sigma(F_o^2)$]
structure solution method	intrinsic phasing (*SHELXT-2014*[b])
refinement method	full-matrix least-squares on F^2 (*SHELXL-2017*[c,d])
absorption correction method	gaussian integration (face-indexed)
range of transmission factors	0.9960–0.9258
data/restraints/parameters	9396 / 174[e] / 644
goodness-of-fit (S)[f] [all data]	1.035
final R indices	
R_1 [$F_o^2 \geq 2\sigma(F_o^2)$][g]	0.0472
wR_2 [all data][h]	0.1358
largest difference peak and hole	0.886 and -0.595 e$^-$ Å^{-3}

[a]Programs for diffractometer operation, data collection, data reduction and absorption correction were those supplied by Bruker. [b]Sheldrick, G. M. *Acta Crystallogr., Sect. A: Found. Crystallogr.* **2015**, *71* (1), 3–8. (Ref. 191). [c]Sheldrick, G. M. *Acta Crystallogr., Sect. C: Struct. Chem.* **2015**, *71* (1), 3–8. (Ref. 192). [d]Attempts to refine peaks of residual electron density as disordered or partial-occupancy solvent (MeOH) O or C atoms were unsuccessful. The data were corrected for disordered electron density through use of the SQUEEZE procedure as implemented in *PLATON* (Spek, A. *Acta Crystallogr., Sect. C: Struct. Chem.* **2015**, *71* (1), 9–18. Ref. 193) A total solvent-accessible void volume of 150 Å^3 with a total electron count of 12 (consistent with two-thirds of a molecule of solvent (MeOH), or 0.33 molecules per formula unit of the Ru complex) was found in the unit. [e]The geometry (bond lengths and angles) of the disordered BF$_4^-$ was restrained to be approximately the same as that for the ordered BF$_4^-$, with the central atom B1, by use of the *SHELXL* SAME instruction. Additionally, the anisotropic displacement parameters of the atoms of the disordered anion were restrained to be similar by use of the *SHELXL* SIMU instruction. The central boron atoms (B3 and B3A) were constrained to have identical anisotropic displacement parameters. [f]$S = [\sum w(F_o^2 - F_c^2)^2/(n - p)]^{1/2}$ ($n =$ number of data; $p =$ number of parameters varied; $w = [\sigma^2(F_o^2) + (0.0772P)^2 + 1.8084P]^{-1}$ where $P = [\text{Max}(F_o^2, 0) + 2F_c^2]/3$). [g]$R_1 = \sum||F_o|-|F_c||/\sum|F_o|$. [h]$wR_2 = [\sum w(F_o^2-F_c^2)^2/\sum w(F_o^4)]^{1/2}$.

attempts at refining the residual electron density as disordered or partial occupancy solvent (MeOH) O or C atoms. A total solvent-accessible void volume of 150 $Å^3$ with a total electron count of 12 (consistent with two-thirds of a molecule of solvent (MeOH), or 0.33 molecules per formula unit of the Ru complex) was found in the unit cell. The refinement also required that a disordered BF_4^- be restrained to approximately the same as that for an ordered BF_4^- by the use of the *SHELXL* SAME instruction. The anisotropic displacement parameters of the disordered anion were restrained to be similar by the use of the *SHELXL* SIMU instruction. The central boron atoms (B3 and B3A) were constrained to have identical anisotropic displacement parameters.

The crystal structure of **209–BF₄** with its three BF_4^- is illustrated in Figure 3-4.
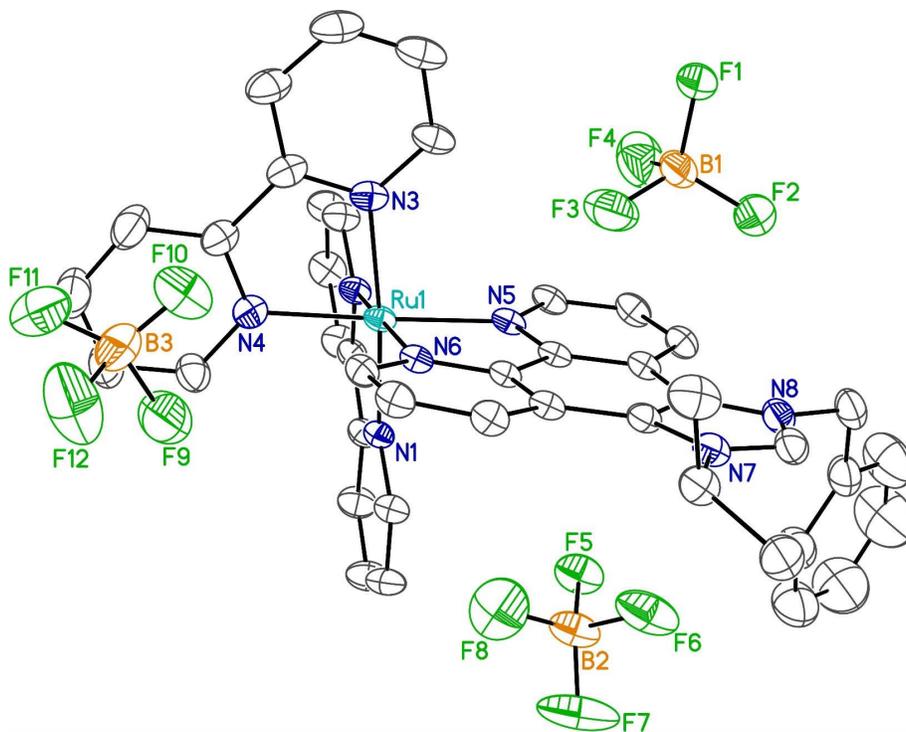
Figure 3-4. Perspective view of [Ru(bpip)(bipy)₂](BF₄)₃ (**209–BF₄**) with its three BF_4^-. Non-hydrogen atoms are represented by Gaussian ellipsoids at the 30% probability level. The hydrogen atoms are omitted for clarity.

Selected interatomic angles of **209–BF₄** are presented in Table 3-3. The interatomic bond distances between the N atoms (N7 and N8) and the C of the imidazolium moiety are 1.322 Å.

Table 3-3. Selected interatomic angles for [Ru(bpip)(bipy)₂](BF₄)₃ (**209–BF₄**).

Atom 1	Atom 2	Atom 3	Angle (°)	Atom 1	Atom 2	Atom 3	Angle (°)
N1	Ru1	N2	78.87(11)	N2	Ru1	N6	174.07(11)
N1	Ru1	N3	174.18(11)	N3	Ru1	N4	78.76(12)
N1	Ru1	N4	96.51(11)	N3	Ru1	N5	97.71(11)
N1	Ru1	N5	87.25(10)	N3	Ru1	N6	87.34(10)
N1	Ru1	N6	96.62(10)	N4	Ru1	N5	174.52(10)
N2	Ru1	N3	97.45(10)	N4	Ru1	N6	96.55(11)
N2	Ru1	N4	87.84(11)	N5	Ru1	N6	79.01(10)
N2	Ru1	N5	96.82(11)				

3.4.3 Syntheses and Spectroscopic Data

The NMR and mass spectra of reported compounds are not included. Selected ^{1}H NMR spectra of unreported compounds are provided in Section 3.4.4. The ^{13}C{^{1}H} NMR spectra of the unreported compounds are not included. The syntheses and spectroscopic data are reported for all synthesized compounds.

cis-[Ru(MeCN)₂(bipy)₂](OTf)₂ (204)
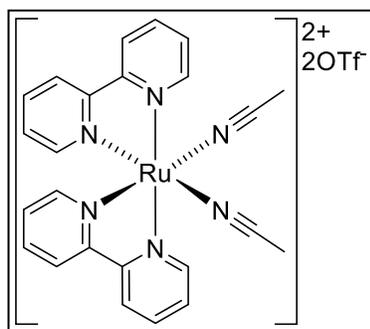
Inside a glovebox, *cis*-[Ru(Cl)₂(bipy)₂]•xH₂O (**201**, 489 mg, 1.01 mmol) and AgOTf (519 mg, 2.02 mmol, 2 equiv) were weighed and transferred into a 500 mL Schlenk flask, which contained a stir bar. The flask was sealed with a 24/40 septum, brought out of the glovebox, and attached to an Ar Schlenk line. Freshly distilled and deaerated MeCN (~30 mL, 0.57 mol, ~560 equiv) was added through a cannula, with Ar pressure. The resulting solution was stirred for 2 h at rt. The blood-red solution was filtered, via cannula filtration, into a triply evacuated and Ar refilled 100 mL Schlenk flask. The excess MeCN was removed under a medium vacuum (0.4 Torr) to produce a reddish-orange solid. The

solid was dissolved in a minimal amount of distilled and deaerated DCM. The resulting solution was filtered with excess DCM, via cannula filtration into a Celite® plug, into a triply evacuated and Ar refilled 100 mL Schlenk flask. The filtration was repeated. The DCM was removed under the medium vacuum (0.4 Torr) to produce a reddish-orange solid. The solid was dissolved in a minimal amount of DCM. Freshly distilled and deaerated Et$_2$O was added to precipitate out an orange solid. A red liquid was filtered off, via cannula filtration, into a triply evacuated and Ar refilled 100 mL Schlenk flask. The orange compound was washed with excess Et$_2$O and the washes collected into the filtrate. More orange solid formed in the filtrate. This solid was isolated in the same manner. The orange solids were dried under the medium vacuum (0.4 Torr) for 2 h. The dried product was obtained as an orange solid (0.636 g) in 79% yield. **^{1}H NMR** (499.789 MHz, CD$_3$OD, 27.0 °C): δ 2.43 (s, 6H), 7.33 (ddd, J = 7.5, 5.8, 1.2 Hz, 2H), 7.65 (d, J = 5.6 Hz, 2H), 7.93 (ddd, J = 7.6, 5.6, 1.2 Hz, 2H), 7.99 (ddd, J = 7.9, 7.8, 1.3 Hz, 2H), 8.32 (ddd, J = 7.9, 7.8, 1.4 Hz, 2H), 8.55 (d, J = 8.2 Hz, 2H), 8.69 (d, J = 8.2 Hz, 2H), 9.43 (d, J = 5.5 Hz, 2H). **^{13}C{^{1}H} NMR** (125.686 MHz, CD$_3$OD, 27.0 °C): δ 2.0, 123.6, 123.8, 126.1, 126.7, 127.6, 137.9, 138.3, 151.6, 153.3, 157.1, 158.0. **HRMS (ESI) *m/z*:** Calcd for C$_{25}$H$_{22}$F$_3$N$_6$O$_3$^{102}RuS [M]$^+$: 645.0464. Found: 645.0468.

[Ru(bipy)$_2$(1,10-phenanthroline-5,6-diamine)](OTf)$_2$ (197–OTf)
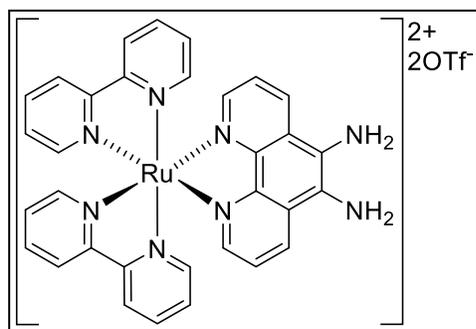
Inside a glovebox, *cis*-[Ru(MeCN)$_2$(bipy)$_2$](OTf)$_2$ (**204**, 200 mg, 0.251 mmol) and 1,10-phenanthroline-5,6-diamine (**202**, 53 mg, 0.25 mmol) were weighed and transferred into a 500 mL Schlenk flask. The flask was sealed with a 24/40 septum, brought out of the glovebox, and attached to an Ar Schlenk line. A minimum volume of anhydrous deaerated MeOH was

added, through a cannula, to dissolve the compounds. The solution was transferred, through a

cannula, into a triply evacuated and Ar refilled 250 mL Schlenk bomb, which contained a stir

bar. The reaction was stirred and heated to 75 °C. The plug valve was sealed, and the reaction

cooled to 70 °C. The reaction was stirred at 70 °C for 3 days. At rt, the reaction was transferred,

through a cannula, into a triply evacuated and refilled 500 mL Schlenk flask. Volatiles were

removed under a medium vacuum (0.4 Torr) to produce a black crude solid. Freshly distilled and

deaerated DCM was added to the flask and the flask sonicated. The black solution was removed,

via cannula filtration, to leave a reddish-orange solid. Enough DCM was added to remove the

black material. The product was obtained as a reddish-orange solid (130 mg) in 56% yield. **¹H

NMR** (399.796 MHz, CD₃OD, 27.0 °C): δ 7.30 (ddd, J = 7.6, 5.7, 1.1 Hz, 2H), 7.51 (ddd, J =

7.7, 5.6, 1.2 Hz, 2H), 7.56 (d, J = 5.7 Hz, 2H), 7.63 (dd, J = 8.6, 5.0 Hz, 2H), 7.84 (dd, J = 5.0,

0.8 Hz, 2H), 7.91 (d, J = 5.7 Hz, 2H), 8.03 (ddd, J = 8.0, 7.9, 1.4 Hz, 2H), 8.13 (ddd, J = 8.0, 7.9,

1.4 Hz, 2H), 8.66 (d, J = 8.2 Hz, 2H), 8.66 (dd, J = 8.7, 1.0 Hz, 2H), 8.70 (d, J = 8.1 Hz, 2H).

¹³C{¹H} NMR (125.688 MHz, CD₃OD, 27.0 °C): δ 125.4, 125.5, 125.6, 126.3, 128.7, 128.8,

131.0, 138.9, 139.0, 143.2, 148.5, 152.5, 152.8, 158.6, 158.8. **HRMS (ESI)** *m/z*: Calcd for

$C_{33}H_{26}F_3N_8O_3^{102}RuS$ [M]⁺: 773.0839. Found: 773.0835.

Imidazo[4,5-*f*][1,10]-phenanthroline (206)
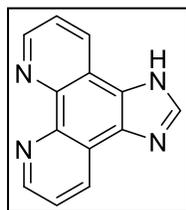
Inside a glovebox, 1,10-phenanthroline-5,6-diamine (**202**, 1.486 g, 7.069 mmol)

was weighed and transferred into a 500 mL RBF, which contained a stir bar. The

flask was sealed with a 24/40 septum, brought out of the glovebox, and attached

to an Ar Schlenk line. SPS dried MeOH (250 mL) was added to the RBF, through a cannula,

with Ar pressure. Freshly distilled and deaerated triethyl orthoformate (~25 mL, ~150 mmol, ~21

equiv) was added to the RBF, through a cannula, with Ar pressure. Sulfamic acid (138 mg, 1.42

mmol, ~0.2 equiv) was quickly added via removing the septum and pouring the solid in. The

RBF was then purged with Ar for 30 min. The black solution was stirred overnight (12–18 h) at

rt. A banana-yellow precipitate formed. The RBF was opened to air and volatiles were removed

using a rotary evaporator. The solid was transferred as a slurry to a Büchner funnel, under

vacuum, using SPS dried MeOH (~50 mL). The solid was washed with additional MeOH (~50

mL). The solid was then washed with triply distilled H_2O (~5 mL) and then MeOH (~5 mL). A

watch glass was placed on the Büchner funnel and the solid dried under vacuum overnight

(12–18 h). The dried product was obtained as a yellow solid (1.481 g) in 95% yield. The low

solubility of the compound made acquiring a ^{13}C NMR difficult. **^{1}H NMR** (499.799 MHz,

DMSO-d_6, 27.0 °C): δ 7.81 (br, 2H), 8.45 (br, 1H), 8.82 (br, 2H), 9.02 (br, 2H). **HRMS (ESI)**

m/z: Calcd for $C_{13}H_8N_4Na$ [M+Na]$^+$: 243.0641. Found: 243.0641.

1-(propan-2-yl)-1*H*-imidazo[4,5-*f*][1,10]phenanthroline (207)
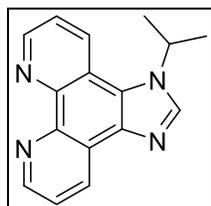
An oven-dried 500 mL Schlenk flask, with a stir bar, was charged with

imidazo[4,5-*f*][1,10]-phenanthroline (**206**, 1.758 g, 7.982 mmol) and Cs_2CO_3

(7.819 g, 24.00 mmol, ~3 equiv). The flask was sealed with a 24/40 septum

and evacuated and refilled with Ar in triplicate. Dry and deaerated MeCN (~250 mL) was added

to the Schlenk flask, through a cannula, with Ar pressure. The mixture was stirred for 30 min.

Deaerated 2-iodopropane (4.0 mL, 40 mmol, ~5 equiv) was added via syringe. The septum was

replaced with a triply evacuated and Ar refilled condenser, which was attached to a bubbler. The

reaction was stirred and heated to 84 °C. The reaction was stirred at 84 °C for 39 h and then

cooled to rt. The reaction mixture was opened to air and gravity filtered into a 500 mL RBF, with

MeCN as eluent. Volatiles were removed using a rotary evaporator to produce a crude oil. The

crude oil was purified via SiO_2 column chromatography (9:1 DCM:MeOH) to produce a dark

brown liquid. The liquid solidified into a dark brown solid. The product was obtained as a dark

brown solid (1.792 g) in 86% yield. *R$_f$*. 0.64. **^{1}H NMR** (599.928 MHz, CD$_3$OD, 27.0 °C): δ 1.71

(d, *J* = 6.6 Hz, 6H), 5.17 (sept, *J* = 6.6 Hz, 1H), 7.67 (dd, *J* = 8.4, 4.3 Hz, 1H), 7.70 (dd, *J* = 8.1,

4.3 Hz, 1H), 8.35 (s, 1H), 8.62 (dd, *J* = 8.5, 1.3 Hz, 1H), 8.76 (dd, *J* = 8.1, 1.7 Hz, 1H), 8.90 (dd,

J = 4.3, 1.4 Hz, 1H), 8.92 (dd, *J* = 4.3, 1.7 Hz, 1H). **^{13}C{^{1}H} NMR** (150.869 MHz, CD$_3$OD, 27.0

°C): δ 21.9, 49.8, 119.7, 122.9, 123.4, 123.4, 123.5, 129.1, 129.8, 135.7, 139.5, 143.0, 143.4,

146.9, 147.8. **HRMS (ESI) *m/z*:** Calcd for C$_{16}$H$_{15}$N$_4$ [M+H]$^+$: 263.1291. Found: 263.1288.

1-benzyl-3-(propan-2-yl)-1*H*-imidazol[4,5-*f*][1,10]phenanthrolin-3-ium bromide (208, bpip–Br)
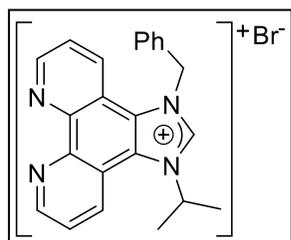
The imidazolium salt was prepared with modification to a previously

reported procedure.[175] A 100 mL Schlenk flask was charged with

1-isopropyl-1*H*-imidazo[4,5-*f*][1,10]phenanthroline (**207**, 1.436 g, 5.474

mmol), sealed with a 14/20 septum. The Schlenk flask was then

evacuated and refilled with Ar in triplicate. Freshly distilled and deaerated benzyl bromide (8.45

mL, 71.0 mmol, 13.0 equiv) was syringed into the Schlenk flask. The septum was replaced with

a triply evacuated and Ar refilled condenser, which was attached to a bubbler. The reaction was

stirred and heated to 120 °C. Over 2 h, a yellow solid appeared. The reaction was cooled to rt and

the condenser replaced with a septum. Freshly distilled and deaerated DMF (15.75 mL) was

added via syringe to partially dissolve the solid. The condenser was reattached, and the reaction

mixture reheated to 120 °C. The reaction was stirred at 120 °C for 3 h. During this time, the solid

fully dissolved and then reappeared. The reaction mixture was cooled to rt and condenser

replaced with a septum. The excess benzyl bromide and DMF were filtered off, via cannula

filtration, into a 500 mL evacuated and refilled Schlenk flask. The solid was washed with freshly

distilled and deaerated Et$_2$O (3 × ~50 mL). The Et$_2$O washes were collected into the 500 mL

Schlenk flask. The addition of Et$_2$O to the 500 mL Schlenk flask precipitated out solid. The liquids were filtered off the solid. The solid was washed with more Et$_2$O. The solids were dried for 1 h under a medium vacuum (0.4 Torr). An off-white solid (1.583 g) was isolated in 67% yield. **^{1}H NMR** (499.789 MHz, CD$_3$OD, 27.0 °C): δ 1.96 (d, J = 6.5 Hz, 6H), 5.81 (sept, J = 6.5 Hz, 1H), 6.35 (s, 2H), 7.33–7.42 (m, 5H), 7.75 (dd, J = 8.5, 4.4 Hz, 1H), 8.03 (dd, J = 8.6, 4.4 Hz, 1H), 8.74 (dd, J = 8.5, 1.2 Hz, 1H), 9.09 (dd, J = 4.3, 1.1 Hz, 1H), 9.16 (d, J = 8.6 Hz, 1H), 9.19 (dd, J = 4.3, 1.0 Hz, 1H), 10.09 (s, 1H). **^{13}C{^{1}H} NMR** (125.686 MHz, CD$_3$OD, 27.0 °C): δ 23.0, 54.8, 55.4, 119.1, 119.9, 125.4, 126.0, 127.1, 127.2, 127.5, 130.0, 130.7, 132.6, 132.8, 134.5, 142.1, 145.7, 145.9, 151.3, 151.5. **HRMS (ESI)** ***m/z***: Calcd for C$_{23}$H$_{21}$N$_4$ [M]$^+$: 353.1761. Found: 353.1760.

[Ru(bpip)(bipy)$_2$]BrCl$_2$ (209–BrCl$_2$)
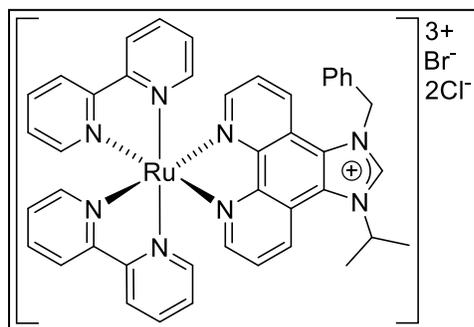
Inside a glovebox, **201** (633 mg, 1.31 mmol) and bpip–Br (**208**, 566 mg, 1.31 mmol, 1.00 equiv) were weighed and transferred into a 200 mL Schlenk flask, which contained a stir bar. The flask was sealed with a 14/20 septum, brought out of the glovebox, and attached to an Ar Schlenk line. The Schlenk flask was then evacuated and refilled with Ar. SPS dried MeOH (~25 mL) was added to the flask, through a cannula, with Ar pressure. The septum was replaced with a triply evacuated and Ar refilled condenser, which was attached to a bubbler. The reaction was stirred and heated to 70 °C. The reaction was stirred at 70 °C for 36 h and then cooled to rt. Volatiles were removed under a medium vacuum (0.4 Torr) to produce a dark orange-red product. The solid was dried for 2 h. The product was obtained as a dark orange-red solid (1.178 g) in 98% yield. **^{1}H NMR** (499.789 MHz, DMSO-d$_6$, 27.0 °C): δ 1.85 (d, J = 6.4 Hz, 3H), 1.88

(d, J = 6.4 Hz, 3H), 5.78 (sept, J = 6.6 Hz, 1H), 6.36–6.44 (m, 2H), 7.32–7.43 (m, 7H),

7.51–7.54 (m, 2H), 7.56–7.61 (m, 2H), 7.75–7.77 (m, 2H), 7.89 (dd, J = 8.6, 5.4 Hz, 1H), 8.06

(dd, J = 8.7, 5.4 Hz, 1H), 8.09–8.13 (m, 2H), 8.19–8.24 (m, 3H), 8.28 (d, J = 5.3 Hz, 1H),

8.83–8.92 (m, 5H), 9.33 (d, J = 8.8 Hz, 1H), 10.65 (s, 1H). **HRMS (ESI)** *m/z*: Calcd for

$C_{43}H_{37}N_8{}^{102}Ru$ $[M]^{3+}$: 255.7389. Found: 255.7385.; Calcd for $C_{43}H_{37}BrN_8{}^{102}Ru$ $[M]^{2+}$: 423.0679.

Found: 423.0673.; Calcd for $C_{43}H_{37}ClN_8{}^{102}Ru$ $[M]^{2+}$: 401.0931. Found: 401.0933.

[Ru(bpip)(bipy)₂](OTf)₃ (209–OTf)
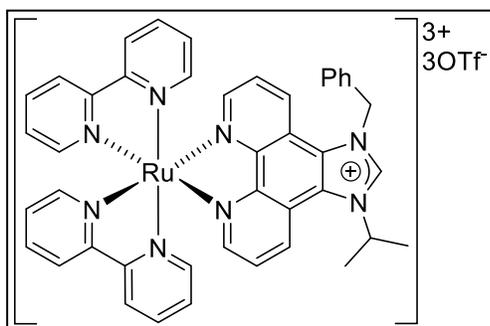
The Schlenk flask containing [Ru(bpip)(bipy)₂]BrCl₂ (**209–BrCl₂,** ~1.178 g, ~1.284 mmol) and stir bar was opened to air. A 11 mL vial was charged with NH₄OTf (2.149 g, 12.86 mmol, ~10.0 equiv). Both solids were dissolved in a minimal amount of triply distilled H₂O.

The NH₄OTf solution was added dropwise, via disposable pipet, to the Schlenk flask. Orange

solid formed on addition. The solid was agitated with the stir bar and a spatula. The solution was

filtered off, via cannula filtration, with Ar pressure. The solid was washed with triply distilled

H₂O (2 × 20 mL). The solid was dried and then dissolved in SPS dried MeOH. Black particles

were removed via filtration through cotton plugs. The product was purified via recrystallization

in hot MeOH. The product was obtained as an orange solid (1.394 g) in 89% yield. The residual

MeOH, in the recrystallized solid, can be removed via crushing the crystals and placing the

powder under a medium vacuum (0.4 Torr) overnight (12–18 h). **¹H NMR** (499.789 MHz,

CD₃CN, 27.0 °C): δ 1.88 (d, J = 6.5 Hz, 3H), 1.93 (d, J = 6.5 Hz, 3H), 5.70 (sept, J = 6.4 Hz,

1H), 6.25 (s, 2H), 7.24–7.28 (m, 2H), 7.38–7.50 (m, 7H), 7.54 (d, J = 5.6 Hz, 1H), 7.57 (d, J =

5.7 Hz, 1H), 7.72 (dd, J = 8.6, 5.3 Hz, 1H), 7.80–7.83 (m, 2H), 7.95 (dd, J = 8.7, 5.3 Hz, 1H),

8.01–8.06 (m, 2H), 8.10–8.15 (m, 2H), 8.21 (d, J = 5.3 Hz, 1H), 8.30 (d, J = 5.4 Hz, 1H),

8.52–8.60 (m, 4H), 8.74 (d, J = 8.7 Hz, 1H), 9.14 (d, J = 8.8 Hz, 1H), 9.57 (s, 1H). **^{13}C{^{1}H}**

NMR (125.685 MHz, CD$_3$CN, 27.0 °C): δ 21.5, 21.5, 53.7, 54.5, 120.7, 121.0 (d, J = 320.9 Hz),

121.5, 124.4, 124.4, 124.4, 124.4, 126.6, 126.8, 126.8, 127.0, 127.0, 127.5, 127.5, 127.7, 127.7,

129.0, 129.4, 131.0, 131.4, 132.2, 138.0, 138.0, 138.1, 138.1, 141.6, 147.5, 147.7, 151.8, 151.8,

152.1, 152.1, 153.0, 153.1, 156.9, 156.9, 157.0, 157.0. **HRMS (ESI)** *m/z*: Calcd for

C$_{43}$H$_{37}$N$_8$^{102}Ru [M]$^{3+}$: 255.7389. Found: 255.7388.; Calcd for C$_{44}$H$_{37}$F$_3$N$_8$O$_3$^{102}RuS [M]$^{2+}$:

458.0847. Found: 458.0847. **Anal.** Calcd for C$_{46}$H$_{37}$F$_9$N$_8$O$_9$RuS$_3$: C, 45.51; H, 3.07; N, 9.23; S,

7.92. Found: C, 45.51; H, 3.09; N, 8.92; S, 8.24.

[Ru(bpip)(bipy)$_2$](BF$_4$)$_3$ (209–BF$_4$)
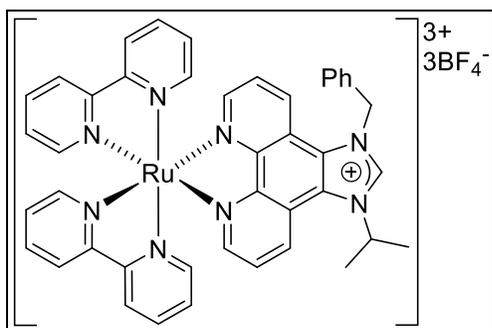
A 15 mL vial was charged with [Ru(bpip)(bipy)$_2$]BrCl$_2$ (**209–BrCl$_2$,** 52 mg, 56 µmol) and dissolved in triply distilled H$_2$O. A second 15 mL vial was charged with NH$_4$BF$_4$ (252 mg, 2.40 mmol) and dissolved in triply distilled H$_2$O. The NH$_4$BF$_4$ solution was added

dropwise, via disposable pipet, to the solution containing the Ru. Red solid formed on addition.

Drops were added until the solution became colourless. The solid was collected and dried via

Büchner filtration. The solid was dissolved and passed through a cotton plug, into a 25 mL RBF,

with minimal MeCN. The MeCN was removed using a rotary evaporator. The solid was

dissolved and passed through a cotton plug, into a 25 mL RBF, with minimal acetone. The

acetone was removed using a rotary evaporator. The product was obtained as a red solid (57.8

mg) in >99% yield. Crystals suitable for X-ray crystallography were obtained by slow

evaporation of MeOH. **^{1}H NMR** (499.789 MHz, CD$_3$CN, 27.0 °C): δ 1.88 (d, J = 6.5 Hz, 3H),

1.91 (d, J = 6.5 Hz, 3H), 5.67 (sept, J = 6.5 Hz, 1H), 6.22 (s, 2H), 7.23–7.26 (m, 2H), 7.35–7.37 (m, 2H), 7.42–7.49 (m, 5H), 7.51–7.54 (m, 2H), 7.71 (dd, J = 8.6, 5.3 Hz, 1H), 7.79–7.82 (m, 2H), 7.94 (dd, J = 8.7, 5.3 Hz, 1H), 8.00–8.06 (m, 2H), 8.10–8.16 (m, 2H), 8.20 (d, J = 5.4 Hz, 1H), 8.29 (d, J = 5.3 Hz, 1H), 8.50–8.58 (m, 4H), 8.73 (d, J = 8.7 Hz, 1H), 9.12 (d, J = 8.8 Hz, 1H), 9.50 (s, 1H). **$^{13}C\{^1H\}$ NMR** (125.685 MHz, CD$_3$CN, 27.0 °C): δ 21.4, 21.5, 53.7, 54.5, 120.5, 121.3, 124.4, 124.4, 124.4, 124.4, 126.7, 126.7, 126.8, 126.9, 127.1, 127.4, 127.4, 127.7, 127.7, 129.1, 129.4, 130.9, 131.3, 132.1, 138.1, 138.1, 138.1, 138.2, 141.6, 147.5, 147.6, 151.8, 151.8, 152.0, 152.0, 153.1, 153.2, 156.9, 156.9, 157.0, 157.0. **HRMS (ESI)** *m/z*: Calcd for C$_{43}$H$_{37}$BF$_4$N$_8$^{102}Ru [M]$^{2+}$: 427.1101. Found: 427.1091.

cis-[Ru(Cl)$_2$(dmbipy)$_2$] (210)
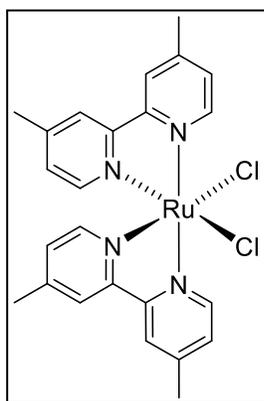
cis-[Ru(Cl)$_2$(dmbipy)$_2$] was prepared with modification to a previously reported procedure.[194] [Ru(COD)Cl$_2$]$_n$ (1.005 g, 3.587 mmol of monomer) and 4,4′-dimethyl-2,2′-bipyridine (1.322 g, 7.174 mmol, 2.00 equiv) were weighed and transferred into a 200 mL Schlenk flask, which contained a stir bar. The flask was sealed with a 14/20 septum. On a Schlenk line, the flask was evacuated and refilled with Ar in duplicate. Freshly distilled and deaerated 1,2-dichlorobenzene (80 mL) was added to the Schlenk flask, through a cannula, with Ar pressure. The septum was replaced with an Ar purged condenser attached to a bubbler. The reaction was stirred and heated to 150 °C. The reaction was stirred overnight (12–18 h) at 150 °C. The reaction was cooled to rt and opened to air. A large quantity of hexanes was added to precipitate out a dark purple product. The solid was collected and dried overnight (12–18 h) via Büchner filtration. The product still contained 1,2-dichlorobenzene (~30 mol%). With the weight of the solvent subtracted, the product was obtained as a purple solid (1.789 g) in 92% yield. **^{1}H**

NMR (498.120 MHz, CD$_3$CN, 27.0 °C): δ 2.38 (s, 6H), 2.63 (s, 6H), 6.82 (dd, J = 6.0, 1.2 Hz, 2H), 7.43 (d, J = 5.9 Hz, 2H), 7.49 (dd, J = 5.9, 1.1 Hz, 2H), 8.06 (s, 2H), 8.21 (s, 2H), 9.87 (d, J = 5.8 Hz, 2H).

[Ru(bpip)(dmbipy)$_2$](OTf)$_3$ (211)
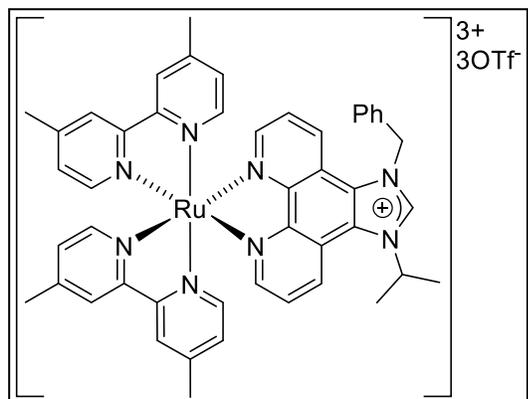
A 200 mL Schlenk flask, with a stir bar, was charged with *cis*-[Ru(Cl)$_2$(dmbipy)$_2$] (624 mg, 1.16 mmol) and bpip–Br (**208**, 501 mg, 1.16 mmol, 1.00 equiv). The flask was sealed with a 14/20 septum. On a Schlenk line, the flask was evacuated and refilled with Ar in triplicate. SPS dried MeOH (~50 mL) was added to the flask, through a cannula, with Ar pressure. The septum was replaced with a triply evacuated and Ar refilled condenser, which was attached to a bubbler. The reaction mixture was stirred and heated to 70 °C. The reaction was stirred at 70 °C for 24 h and then cooled to rt. The reaction mixture was opened to air and filtered through a cotton plug into a 250 mL RBF. Volatiles were removed using a rotary evaporator. A second cotton plug filtration was performed with a minimal amount of SPS dried MeOH. The MeOH was removed using a rotary evaporator. The solid was dissolved in a minimal amount of triply distilled H$_2$O. A 15 mL vial was charged with NH$_4$OTf (1.935 g, 11.58 mmol, ~10.0 equiv) and dissolved in a minimal amount of triply distilled H$_2$O. The NH$_4$OTf solution was added dropwise, via disposable pipet, to the solution containing the Ru. Solid formed on addition and was agitated with a spatula. The solution was filtered off, via cannula filtration, with Ar pressure. The solid was washed with triply distilled H$_2$O (3 × 20 mL). The crude solid was dried (1.313 g, 90% yield) and then dissolved in SPS dried MeOH. The product was purified via recrystallization in hot MeOH. The product was

obtained as a red solid (1.069 g) in 73% yield. The residual MeOH, in the recrystallized solid, can be removed via crushing the crystals and placing the powder under a medium vacuum (0.4 Torr) overnight (12–18 h). **^{1}H NMR** (499.789 MHz, CD$_3$CN, 27.0 °C): δ 1.88 (d, J = 6.5 Hz, 3H), 1.92 (d, J = 6.5 Hz, 3H), 2.48 (s, 3H), 2.49 (s, 3H), 2.57 (s, 3H), 2.59 (s, 3H), 5.69 (sept, J = 6.5 Hz, 1H), 6.24 (s, 2H), 7.06–7.08 (m, 2H), 7.29–7.35 (m, 4H), 7.37–7.45 (m, 5H), 7.59–7.62 (m, 2H), 7.70 (dd, J = 8.6, 5.4 Hz, 1H), 7.94 (dd, J = 8.6, 5.3 Hz, 1H), 8.21 (d, J = 5.3 Hz, 1H), 8.30 (d, J = 5.3 Hz, 1H), 8.37 (s, 1H), 8.40 (s, 1H), 8.41 (s, 1H), 8.44 (s, 1H), 8.71 (d, J = 8.6 Hz, 1H), 9.11 (d, J = 8.7 Hz, 1H), 9.55 (s, 1H). **^{13}C{^{1}H} NMR** (125.685 MHz, CD$_3$CN, 27.0 °C): δ 20.2, 20.3, 20.3, 21.5, 21.5, 53.7, 54.4, 120.5, 121.1 (d, J = 320.8 Hz), 121.3, 125.0, 125.0, 126.5, 126.8, 126.9, 127.0, 128.1, 128.1, 128.3, 128.3, 129.0, 129.4, 130.5, 131.0, 132.2, 141.5, 147.7, 147.9, 150.5, 150.5, 150.6, 150.6, 150.7, 150.7, 151.2, 152.8, 152.9, 156.4, 156.4, 156.5, 156.5. **HRMS (ESI)** *m/z*: Calcd for C$_{47}$H$_{45}$N$_8$^{102}Ru [M]$^{3+}$: 274.4265. Found: 274.4264.; Calcd for C$_{48}$H$_{45}$F$_3$N$_8$O$_3$^{102}RuS [M]$^{2+}$: 486.1160. Found: 486.1158. **Anal.** Calcd for C$_{50}$H$_{45}$F$_9$N$_8$O$_9$RuS$_3$: C, 47.28; H, 3.57; N, 8.82; S, 7.57. Found: C, 47.25; H, 3.52; N, 8.51; S, 7.81.

3.4.4 Selected ^{1}H NMR Spectra

Most of the ^{1}H NMR spectra of the unreported synthesized compounds are included to support the syntheses and demonstrate relative purities. The ^{1}H NMR spectrum of the imidazolium precursor, 1-(propan-2-yl)-1*H*-imidazo[4,5-*f*][1,10]phenanthroline (**207**), is shown in Figure 3-5. The ^{1}H NMR spectrum of the imidazolium bromide, 1-benzyl-3-(propan-2-yl)-1*H*-imidazol[4,5-*f*][1,10]phenanthrolin-3-ium bromide (**208**, bpip–Br), is shown in Figure 3-6. The ^{1}H NMR spectrum of [Ru(bpip)(bipy)$_2$](OTf)$_3$ (**209–OTf**) is shown in Figure 3-7. The ^{1}H NMR spectrum of [Ru(bpip)(dmbipy)$_2$](OTf)$_3$ (**211**) is shown in Figure 3-8.
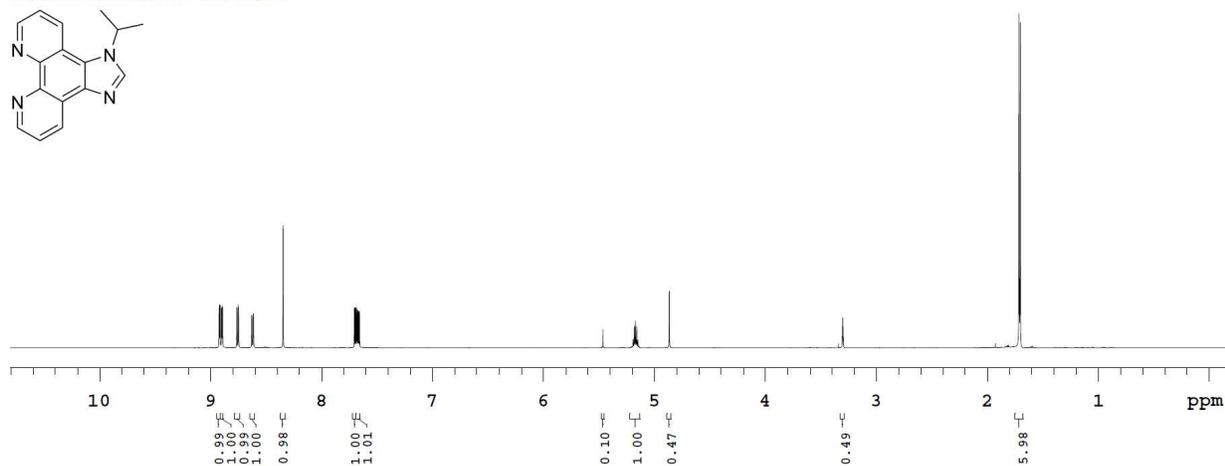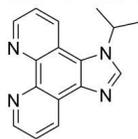
Figure 3-5. ¹H NMR spectrum of 1-(propan-2-yl)-1*H*-imidazo[4,5-*f*][1,10]phenanthroline (**207**) in CD₃OD.
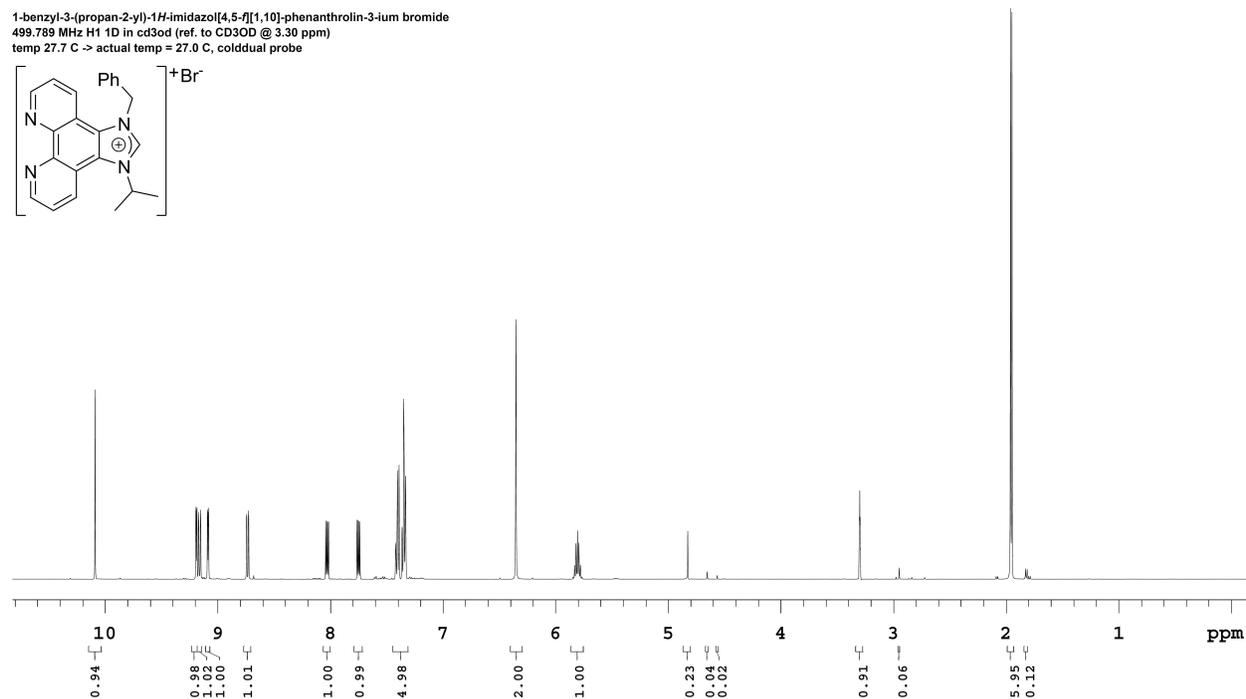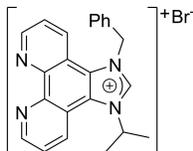
Figure 3-6. ¹H NMR spectrum of 1-benzyl-3-(propan-2-yl)-1*H*-imidazol[4,5-*f*][1,10]phenanthroline-3-ium bromide (bpip–Br, **208**) in CD₃OD.
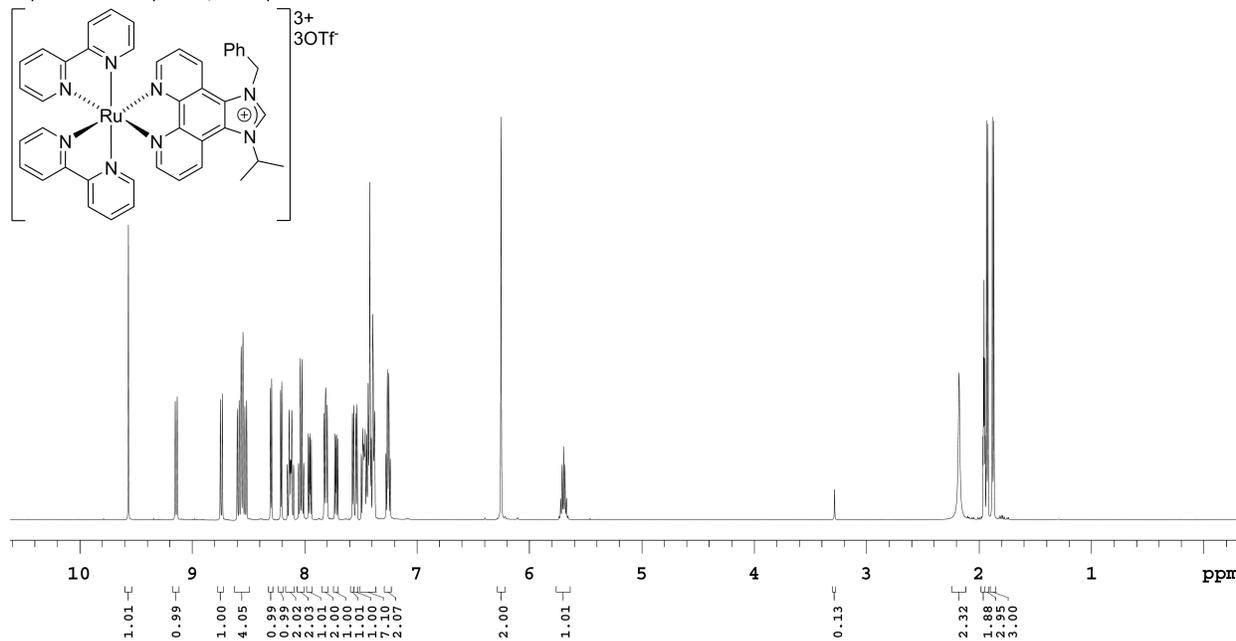
Figure 3-7. ¹H NMR spectrum of [Ru(bpip)(bipy)₂](OTf)₃ (**209–OTf**) in CD₃CN.
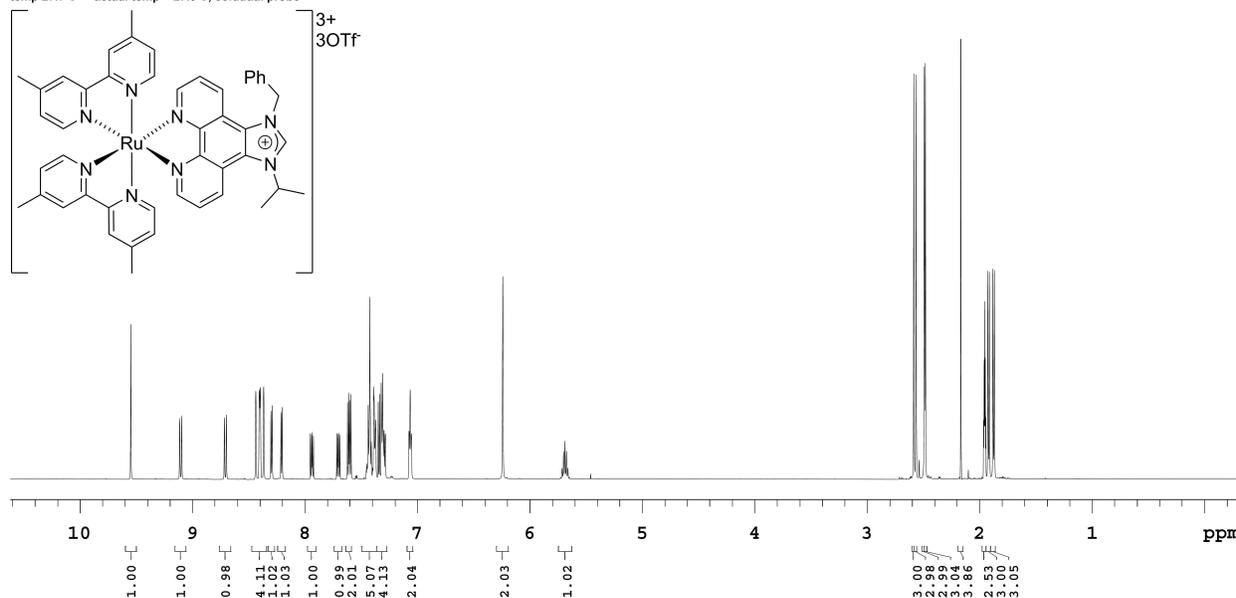
Figure 3-8. ¹H NMR spectrum of [Ru(bpip)(dmbipy)₂](OTf)₃ (**211**) in CD₃CN.

Chapter 4:

Preliminary Photohydrogenation Trials with Ru(II) Complexes

4.1 Introduction

The usage of Ru–polypyridyl complexes as photoredox catalysts was introduced in Chapter 3 (Section 3.1.1). As previously discussed, the bimetallic Ru–Pd complex **194** hydrogenated diphenylacetylene (**195**) through MLCT and LMCT processes (Chapter 3, Scheme 3-4).[170] This chapter describes exploratory attempts to utilize the Ru(II)–polypyridyl synthesized in Chapter 3 in known hydrogenation systems.

4.1.1 Incorporation into a Noyori-Type System

A large focus of the Bergens group's previous work and my work has involved hydrogenation utilizing Noyori-type catalysts. Of particular relevance to this chapter, is the system developed by Wiles et al.[164, 195] The system uses cationic Ru–diphosphine (PP) precursors with 1-5-η^5-coordinated cyclooctadienyl to form Ru–solvento–hydride complexes (eq 4-1).

$$[Ru(PP)(1\text{-}5\text{-}\eta^5\text{-}C_8H_{11})]BF_4 \quad + \quad 3\,H_2 \quad + \quad 3\,solv \quad \longrightarrow \quad [Ru(PP)(H)(solv)_3]BF_4 \quad + \quad C_8H_{16} \quad \textbf{(4-1)}$$

$$solv = THF,\ ^iPrOH,\ or\ Acetone$$
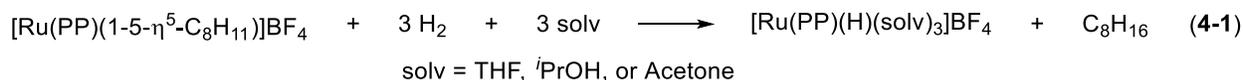
These solvento–hydride complexes are prepared in high yields and are stable at low temperatures.[164, 195] The solvento ligands are labile and readily replaced with diamine ligands, under H_2 and low temperatures, to form Noyori-type hydrogenation catalysts. This has been demonstrated, by the Bergens group, with *fac*-[Ru((*R*)-BINAP)(H)(solv)$_3$]BF$_4$ (**212**) and (1*R*,2*R*)-(+)-dpen for the hydrogenation of ketones,[91, 160] esters,[90] imides, and amides.[158] Ideally, the Ru–polypyridyl–diamine complex **197–OTf** can be combined with **212** to form the dinuclear Ru species **213** for photohydrogenation (Scheme 4-1). Furthermore, this dinuclear species may

be able to operate without the addition of base, as the MLCT from the Ru–polypyridyl moiety may activate the N–H functionality. As described in Chapter 3, this activation was envisaged to occur by increasing the negative charge at the Noyori-type active site, by rendering the N–H more acidic or by conjugation through the Ru=N linkage. This admittedly exploratory approach, if successful, might eliminate the need for high concentrations of base in the hydrogenation of carboxylic acid derivatives.
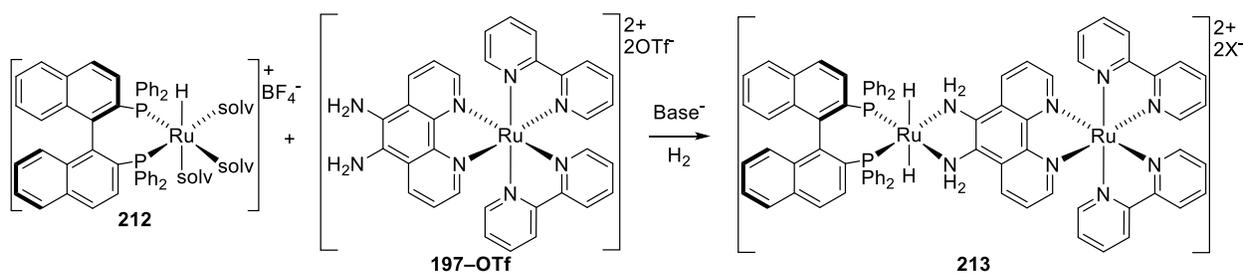
Scheme 4-1. Possible in situ formation of the Noyori-type dinuclear Ru species **213**.

4.1.2 Incorporation into a Co–NHC Hydrogenation System

Ideally, complexes **209** and **211** can be converted into Ru–polypyridyl–NHC derivatives and then coordinated to an earth-abundant hydrogenation catalyst. Once coordinated, the effect of light on hydrogenation activity can be examined. The earth-abundant hydrogenation system chosen to incorporate the Ru–polypyridyl–NHC derivatives into was that developed by Walter and co-workers.

In 2018, Walter and co-workers reported their syntheses of Co(II)–NHC–dialkyl complexes by displacing TMEDA with the free NHC ligand (eq 4-2).[196] The Co–NHC–dialkyl

$$[Co(TMEDA)(R)_2] \;+\; NHC \;\longrightarrow\; [Co(NHC)(R)_2] \;+\; TMEDA \qquad (\textbf{4-2})$$

complexes are precatalysts for alkene hydrogenation.[196] Notably, the Co–NHC complex [Co(1,3-di-*tert*-butylimidazolin-2-ylidene)(CH$_2$SiMe$_3$)] (**214**) catalyzed the hydrogenation of alkenes and an alkyne under low pressure (4 atm H$_2$) at room temperature.[196] The authors

proposed that the active hydrogenation catalyst was the dihydride species

[Co(1,3-di-*tert*-butylimidazolin-2-ylidene)H$_2$] (**215**). They also proposed the mechanism shown

in Scheme 4-2.[196] Complex **215** undergoes olefin insertion and reductive elimination to form the

alkane product and [Co(1,3-di-*tert*-butylimidazolin-2-ylidene)] (**216**).[196] The active catalyst **215**

is then reformed by oxidative addition of H$_2$. Notably, the authors observed that the olefins can

coordinate to the Co and hinder the formation of the active catalyst.[196]
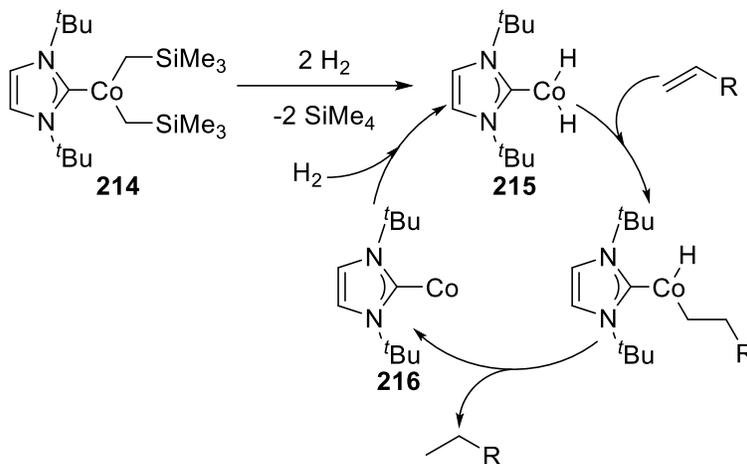
Scheme 4-2. Walter's proposed mechanism for olefin hydrogenation with the Co–NHC complex **214**.

My target bimetallic Ru–Co–dialkyl species, complexes **217** and **218**, are shown in

Figure 4-1. These dialkyl species should react with H$_2$ to form their respective dihydride species,

analogous of **214** to **215**. I wanted to investigate whether the Ru(II) photoredox moieties would

activate the Co towards alkene hydrogenation by either a one-electron reduction, analogous to

Rau and co-workers Ru–Pd system,[170] or by simply increasing the negative charge of the

putative Co(H)$_2$ centre. The activation of Co(II) species to Co(I) and Co(0) with Zn has recently

received significant recognition for the asymmetric reduction of the C=C bond in enamides.[197]
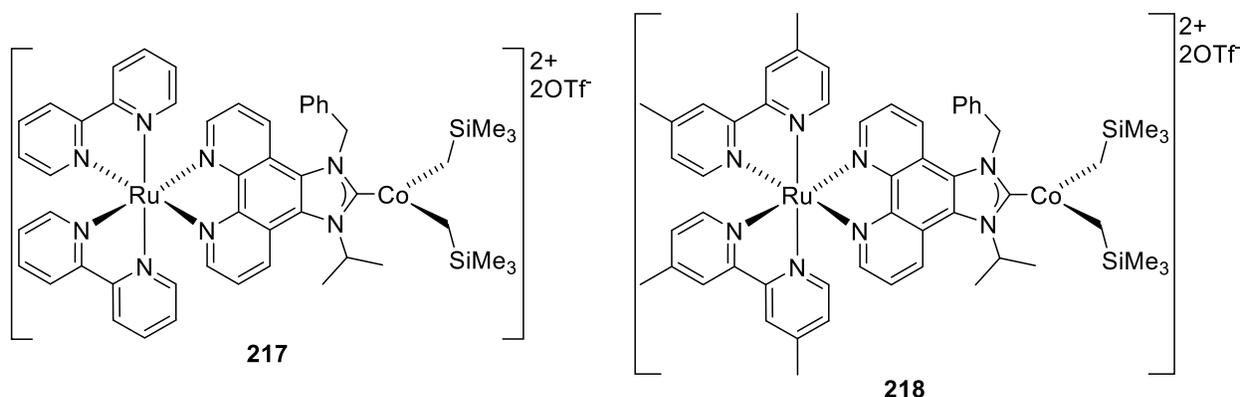
Figure 4-1. Chemical structures of target bimetallic Ru–Co species **217** and **218**.

The preliminary photohydrogenation attempts, with the Ru(II) complexes reported in Chapter 3, are now presented.

4.2 Results and Discussion

4.2.1 Attempted Photohydrogenations of Acetophenone with the Noyori-Type System

The trisolvento hydride complex *fac*-[Ru((*R*)-BINAP)(H)(*i*PrOH)$_3$]BF$_4$ (**212–*i*PrOH**) was chosen for the formation of **212** because **197–OTf** was soluble in *i*PrOH, and it avoided possible reactions between **197** and acetone. Complex **212–*i*PrOH** was prepared in situ from [Ru((*R*)-BINAP)(1-5-η^5-C$_8$H$_{11}$)]BF$_4$ (**219**, Scheme 4-3) by a method previously reported by the Bergens group.[164] Complex **212–*i*PrOH** decomposes upon warming to -40 °C,[164] so the temperature was kept below -60 °C.
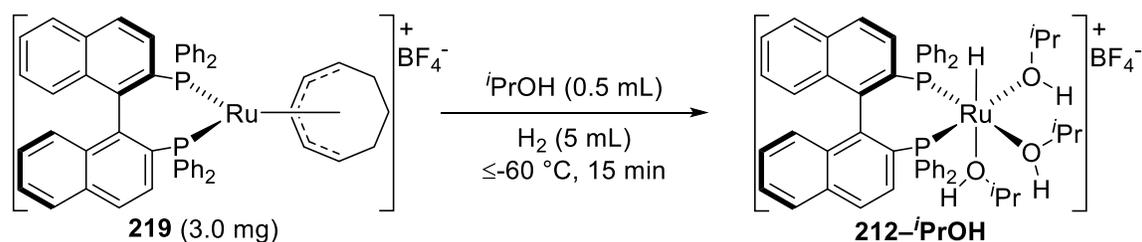
Scheme 4-3. Preparation of the labile trisolvento complex **212–*i*PrOH**.

Complex **212–*i*PrOH** was mixed with an *i*PrOH solution of **197–OTf**, and the resulting

putative dinuclear Ru complex **213** was investigated for the photohydrogenation of acetophenone

(**220**) to 1-phenylethanol (**221**) at 0 °C (Scheme 4-4). The reaction only resulted in trace product

(~1% conv, ~5 turnovers) over 2 h (1 h of 400–700 nm *hv*) with the initial conditions (0.2 mol%

213, 0.6 mol% KO*t*Bu, 4.0 mL *i*PrOH, ~1 atm H$_2$, 0 °C). The in situ preparation of **212–*i*PrOH**

was extended to 30 min and different reactions conditions were explored. The highest conversion

of **220** was ~2% (~10 turnovers) over 45 min (15 min of 400–700 nm *hv*) with a 10% base

loading, decreased *i*PrOH volume, and room temperature (0.2 mol% **213**, 10 mol% KO*t*Bu, 3.0

mL *i*PrOH, ~1 atm H$_2$, rt). To check that the method was appropriate for hydrogenation, a control

reaction was performed with (1*R*,2*R*)-(+)-dpen instead of **197–OTf**. The control reaction went to

96% conversion (480 turnovers) over 45 min (0.2 mol% **212–*i*PrOH**, 0.2 mol% (1*R*,2*R*)-(+)-

dpen, 10 mol% KO*t*Bu, 3.0 mL *i*PrOH, ~1 atm H$_2$, rt). The low activity of the hydrogenations

with **212–*i*PrOH** and **197–OTf** support that **213** is not a catalyst for ketone hydrogenation. It is

also possible that **213** becomes inactivated, or **213** does not form under the conditions examined.

This system was not pursued further.
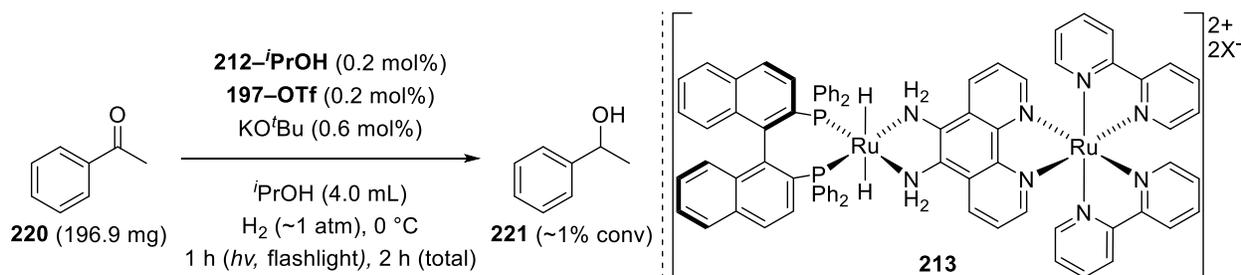
Scheme 4-4. Attempted photohydrogenation of acetophenone (**220**) with speculated in situ formed **213**.

4.2.2 Attempted Photohydrogenation of Styrene with a Ru–Co–NHC System

To examine the bimetallic Ru–Co–dialkyl species **217** and **218** (shown in Figure 4-1) as possible photohydrogenation catalysts the Co precursor [Co(TMEDA)(CH$_2$SiMe$_3$)] (**222**) was prepared from [Co(acac)$_2$(TMEDA)] (**223**) and [Mg(CH$_2$SiMe$_3$)$_2$] (**224**) (Scheme 4-5). Complex **222** was obtained, with modification to a previously reported procedure,[196] as a purplish-blue solid in 83% yield and was found to be extremely air-sensitive.
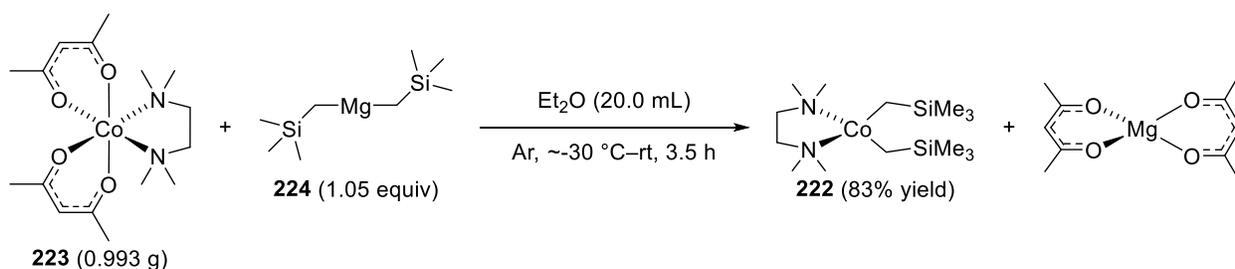
Scheme 4-5. Synthetic preparation of [Co(TMEDA)(CH$_2$SiMe$_3$)$_2$] (**222**).

The synthesis of the bimetallic Ru–Co species **218** from **211** and **222** was attempted but did not result in product (Scheme 4-6). The complexation of the Ru–NHC derivatives of **209** and **211** to other metal species has proven difficult and methods are still being investigated by fellow group members. The Ru–polypyridyl–imidazolium complexes **209** and **211** decompose in the presence of strong bases, such as KO^{t}Bu, at temperatures above 0 °C. They are also poorly soluble in several solvents.
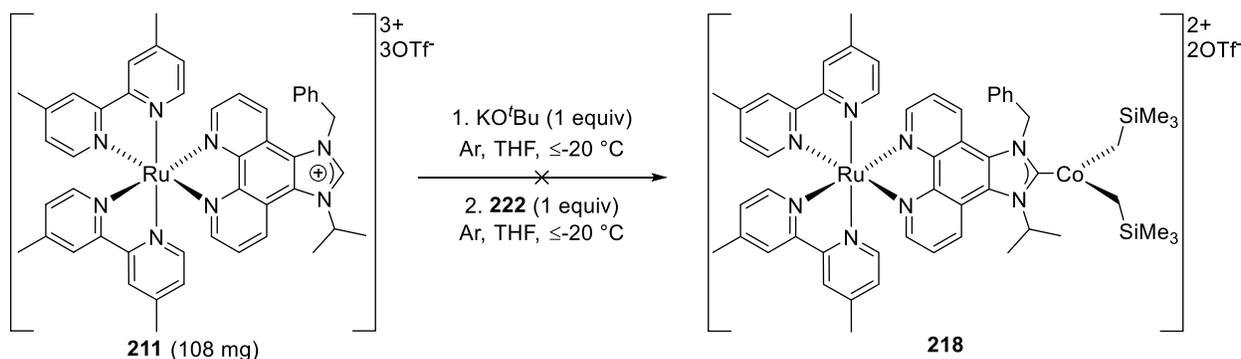
Scheme 4-6. Attempted synthesis of the bimetallic Ru–Co species **218**.

Although the bimetallic Ru–Co species **218** was not obtained, the photohydrogenation of styrene (**225**) to ethylbenzene (**17**) was attempted with the potential in situ formation of **218** (Scheme 4-7). The reaction did not proceed under the conditions examined. There are several possible reasons that the reaction did not proceed. Particularly, the solubility of **222** in MeOH was low and may undergo decomposition prior to reaction with **211**. Overall, the reaction may require more forcing conditions and a proper preparation of **218**.
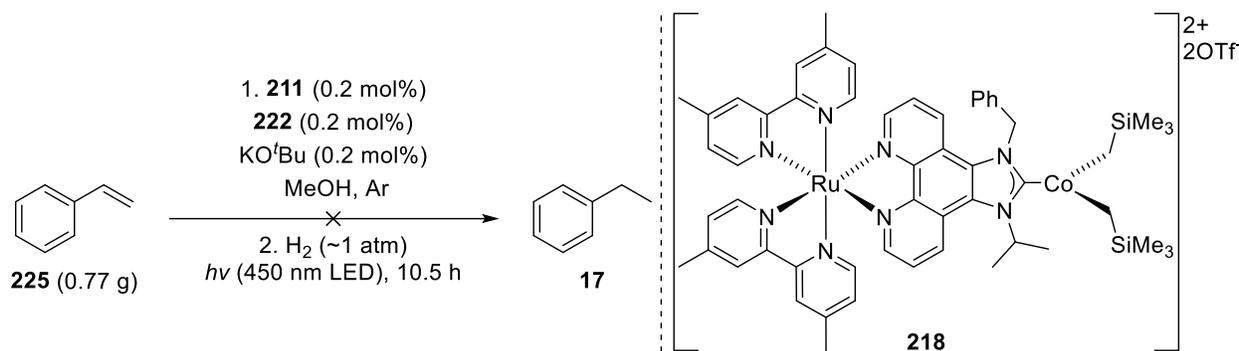
Scheme 4-7. Attempted photohydrogenation of styrene (**225**) with in situ catalyst formation from **218**.

4.3 Conclusion

The synthesized Ru(II)–polypyridyl complexes **197–OTf** and **211** were used for preliminary and in situ examinations of possible photohydrogenation catalysts. The diamine complex **197–OTf** was mixed with **212–^{i}PrOH** to provide low activity (2% conv) for the hydrogenation of **220** to **221**. The NHC precursor **211** did not coordinate to **222** with KO^{t}Bu as base. The photohydrogenation of **225** to **17** with **211** and **222** did not proceed under the conditions used. Further investigations into these photohydrogenation systems and other catalytic systems involving **197**, **209**, and **211** is feasible as a large synthetic workload has been performed.

4.4 Experimental Details

4.4.1 General Information

4.4.1.1 Purchased Chemicals and Equipment

Reagents and solvents were obtained and used without further purification, unless otherwise stated, from a variety of suppliers. The (1*R*,2*R*)-(+)-dpen (98%) was obtained from Alfa Aesar. Na metal (Technical) was obtained from Anachemia. The acetophenone (Certified ACS), CaO (Powder/Certified), and *n*-pentane (Certified) were obtained from Fisher Scientific. Ar (High Purity, 99.998%, 4.8), H_2 (High Purity, 99.995%, 4.5), and N_2 (High Purity, 99.995%, 4.5) were obtained from Praxair. The C_6D_6 (99.6% D), cobalt(II) acetylacetonate (≥99.0%), $CDCl_3$ (99.8% D), Et_2O (ACS reagent, ≥99.0%), *^{i}PrOH* (ACS reagent, ≥99.5%), KO^tBu (Sublimed), styrene (ReagentPlus®, ≥99%), *N,N,N′,N′*-tetramethylethylenediamine (99%), (trimethylsilyl)methylmagnesium chloride solution (1.0 M in Et_2O), and toluene (HPLC, 99.9%) were obtained from Sigma-Aldrich. The 1,4-dioxane (Reagent, ≥99.0%) was obtained from Caledon Laboratory Chemicals.

A Coast HP8R LED flashlight was purchased and used as a light source. An ALITOVE blue LED flexible strip ribbon light was purchased and used as a blue light source.

4.4.1.2 Air- and Moisture-Sensitivity

Most reactions were performed under air- and moisture-free conditions. Standard Schlenk techniques were used where applicable. All glassware and stainless-steel needles for air- and moisture-sensitive reactions were oven-dried prior to immediate usage.

Most solvents and liquid reagents were freshly distilled or inertly collected from a SPS. Solvents and liquid reagents were deaerated by bubbling with Ar or N_2 for ≥30 min before usage. Specifically, Et_2O (Na/benzophenone), *^{i}PrOH* (CaO), *n*-pentane (CaH_2), and 1,4-dioxane

(Na/benzophenone) were dried by distillation, over the appropriate drying agent, under Ar or N_2.

MeOH was collected under N_2 from a LC Technology Solutions Inc. SPS. Dried and deaerated

solvents and reagents were delivered via gas-tight syringes or cannulas (stainless steel).

4.4.1.3 Chemical Characterization Methods

A variety of chemical characterization techniques were performed. ^{1}H NMR spectra were

acquired using a 500 MHz Varian VNMRS. Chemical shifts (δ values) are reported in ppm. The

paramagnetic compounds provided broad peaks. The HRMS spectrum was acquired using

electrospray ionization in an Agilent 6220 oaTOF. The elemental analysis data was performed

with a Carlo Erba EA1108 Elemental Analyzer. The NMR and mass spectra of the reported

compounds are not included, but the spectroscopic data acquired are reported in Section 4.4.3.

4.4.2 General Procedures

4.4.2.1 Attempted Noyori-Type Photohydrogenations of Acetophenone

A two-neck 10 mL RBF, containing a stir bar, was sealed with two 14/20 septa. The RBF

evacuated and refilled with Ar in triplicate. The RBF was then flushed with H_2 for ≥30 min and

set to the desired reaction temperature. Inside a glovebox, $[Ru((R)\text{-BINAP})(1\text{-}5\text{-}\eta^5\text{-}C_8H_{11})]BF_4$

(**219**, 3.0 mg, 3.3 μmol), $[Ru(bipy)_2(1,10\text{-phenanthroline-5,6-diamine})](OTf)_2$ (**197–OTf**, 3.0

mg, 3.3 μmol, 1 equiv), and KO^{t}Bu were weighed into separate NMR tubes. The NMR tubes

were sealed with septa and brought out of the glovebox. Freshly distilled and deaerated ^{i}PrOH

(0.5 mL) was added to each NMR tube containing a Ru compound. The tubes were cooled below

-60 °C with an acetone dry ice bath. A 5 mL gas-tight syringe was evacuated and refilled with H_2

in triplicate. H_2 (5 mL) was syringed into the NMR tube containing $[Ru((R)\text{-BINAP})(1\text{-}5\text{-}\eta^5\text{-}$

$C_8H_{11})]BF_4$. The tube was shaken periodically over 15–30 min while maintaining the

temperature below -60 °C. The resulting $[Ru((R)\text{-BINAP})(H)(^iPrOH)_3]BF_4$ (**212–^{i}PrOH**) was

transferred, through a double-ended needle, into the two-neck RBF with H_2 pressure.

Quantitative transfer was ensured with 0.25 mL of ^{i}PrOH. At this point the room's lights were

turned off. The NMR tube containing **197–OTf** was then transferred, through a double-ended

needle, into the two-neck RBF with H_2 pressure. Quantitative transfer was ensured with 0.5 mL

of ^{i}PrOH. The solution was stirred for 15 min. Acetophenone (**220**, 196.9 mg, 1.639 mmol, ~500

equiv) was weighed into an NMR tube in air. The NMR tube was sealed with a septum and

purged with Ar for 5 min. ^{i}PrOH was then added to the NMR tube to make a 0.5 mL solution.

The solution was transferred, through a double-ended needle, into the two-neck RBF with H_2

pressure. Quantitative transfer was ensured with 0.25 mL of ^{i}PrOH. The KO^{t}Bu was dissolved in

1.0 mL of ^{i}PrOH and transferred, through a double-ended needle, into the reaction mixture with

H_2 pressure. Quantitative transfer of the base was ensured with 0.5 mL of ^{i}PrOH. A Coast HP8R

LED flashlight was placed directly on the surface of the two-neck RBF. The flashlight's beam

was directed towards the reaction mixture. The flashlight was turned on or off at desired timings.

The reaction mixture was stirred at the desired reaction temperature under H_2 pressure (~1 atm).

A double-ended needle and H_2 pressure were used to take aliquots at desired timings. The

aliquots were delivered into 15 mL vials and volatiles were removed using a rotary evaporator.

The remainder was examined by ^{1}H NMR in CDCl$_3$.

4.4.2.2 Attempted Ru–Co–NHC Photohydrogenation of Styrene

In air, a Pyrex 9800-16 test tube, with a 6 mm stir bar, was charged with

[Ru(bpip)(dmbipy)$_2$](OTF)$_3$ (**211**, 19.1 mg, 15.0 μmol) and sealed with a 14/20 septa. The test

tube was evacuated and refilled with Ar in triplicate. SPS dried MeOH (0.5 mL) was then

syringed into the test tube with Ar pressure. The test tube was cooled to ~-35 °C with an

acetonitrile dry ice bath. Inside a glovebox, [Co(TMEDA)(CH$_2$SiMe$_3$)$_2$] (**223**, 5.3 mg, 15 μmol,

194

1 equiv) and KO^{t}Bu (~4.0 mg, ~36 μmol, ~2.4 equiv) were weighed into separate NMR tubes. The tubes were sealed with septa and brought out of the glovebox. At this point the room's lights were turned off. SPS dried MeOH (0.5 mL) was added to the KO^{t}Bu, through a double-ended needle, with Ar pressure. The NMR tube was shaken, cooled to ~-35 °C, and half of the 0.07M base solution (~1.2 equiv) was transferred, through a double-ended needle, into the test tube with Ar pressure. The mixture was stirred for 5 min at ~-35 °C. The [Co(TMEDA)(CH$_2$SiMe$_3$)$_2$] (**223**) was partially dissolved in SPS dried MeOH (0.5 mL). The slurry was transferred, through a double-ended needle, into the test tube with Ar pressure. A 0.25 mL rinse with SPS dried MeOH was used to ensure near quantitative transfer. The mixture was stirred and slowly warmed to rt. At approximately rt, deaerated styrene (0.85 mL, 7.4 mmol, ~500 equiv) was syringed into the test tube. The solution was then flushed with H$_2$ for 3 min. A double-layered balloon attached to a plastic syringe barrel was flushed with H$_2$. The H$_2$ filled balloon syringe was quickly transferred to the test tube. The test tube, under ~1 atm H$_2$, was placed in a glass vial that was wrapped in an ALITOVE blue LED flexible strip ribbon light. The test tube was ~1 cm from the LED strip. The reaction was stirred, and the blue light turned on. A double-ended needle and H$_2$ pressure were used to take aliquots at desired timings. The aliquots were delivered into 15 mL vials and volatiles were removed using a rotary evaporator. The remainder was examined by ^{1}H NMR in CDCl$_3$.

4.4.3 Syntheses and Spectroscopic Data

[Ru((*R*)-BINAP)(1-5-η^5-C$_8$H$_{11}$)]BF$_4$ (**219**) is a readily available precursor in the Bergens group and did not require synthesis. The synthesis of this precursor was reported by Bergens and co-workers in 2001[195] and an alternative synthesis in 2004.[164] The conversion of **219** to Ru–trisolvento–hydride complexes has been examined by the Bergens group.[160, 164, 195] The

syntheses and spectroscopic data of complexes **197–OTf** and **211** were described in Chapter 3.

Although previously reported, the syntheses and acquired spectroscopic data for

[Co(acac)₂(TMEDA)] (**223**), [Mg(CH₂SiMe₃)₂] (**224**), and [Co(TMEDA)(CH₂SiMe₃)₂] (**222**) are

provided.

[Co(acac)₂(TMEDA)] (223)
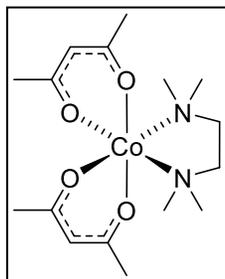
[Co(acac)₂(TMEDA)] was prepared with modification to previously reported procedures.[198, 199] A doubly evacuated and Ar refilled 200 mL Schlenk flask was charged with a stir bar and [Co(acac)₂] (5.00 g, 19.4 mmol). Toluene (150 mL, deaerated) was added, through a double-ended needle, into the

Schlenk flask with Ar pressure. With stirring, freshly distilled and deaerated

N,N,N′,N′-tetramethylethylenediamine (TMEDA, 3.20 mL, 21.3 mmol, 1.10 equiv) was syringed

into the Schlenk flask. The reaction was stirred overnight (12–18 h). Excess TMEDA and

toluene were removed under a medium vacuum (0.4 Torr). A red crude solid (7.153 g, 99%

yield) was purified via sublimation under the medium vacuum (0.4 Torr) at 80 °C. The purified

product was obtained as a red solid (6.624 g) in 91% yield. **¹H NMR** (499.803 MHz, CDCl₃, 27

°C): δ -13.10 (br, 8H), 10.59 (br, 6H), 37.45 (br, 2H), 45.90 (br, 6H), 66.75 (br, 2H), 76.45 (br,

6H). **HRMS (ESI)** *m/z*: Calcd for $C_{11}H_{23}CoN_2O_2$ [M]⁺: 274.1086 Found: 274.1084. **Anal.** Calcd

for $C_{16}H_{30}CoN_2O_4$: C, 51.47; H, 8.10; N, 7.50. Found: C, 51.55; H, 8.09; N, 7.41.

[Mg(CH₂SiMe₃)₂] (224)
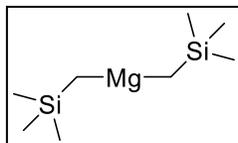
[Mg(CH₂SiMe₃)₂] was prepared with substantial modification to a previously reported procedure.[200] An oven-dried 200 mL Schlenk flask, containing a stir bar, was evacuated and refilled with Ar in triplicate. While

under Ar pressure, a 25 mL solution of (trimethylsilyl)methylmagnesium chloride (1.0 M in

Et$_2$O, 25 mmol ClMgCH$_2$SiMe$_3$) was removed via syringe from its Sure/Seal™ bottle and quickly transferred into the Schlenk flask. With stirring, freshly distilled and deaerated 1,4-dioxane (2.3 mL, 27 mmol, ~1.1 equiv) was added dropwise via syringe over 1 h. The reaction mixture was stirred overnight (12–18 h). The stirring was stopped and the white precipitate, MgCl$_2$•2(1,4-dioxane), was allowed to settle. The solution was inertly filtered, through a double-ended needle and celite plug, into a 500 mL Schlenk flask. Excess freshly distilled and deaerated Et$_2$O was used to aid the filtration. The filtration was repeated until a solution without white particles was obtained. The Et$_2$O was then removed under a medium vacuum (0.4 Torr) to produce a white solid. The white solid was dried under the medium vacuum (0.4 Torr) overnight (12–18 h). The product was obtained as a white powder (1.562 g) in 31% yield.

[Co(TMEDA)(CH$_2$SiMe$_3$)$_2$] (222)
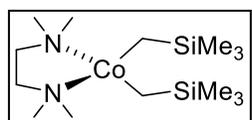
[Co(TMEDA)(CH$_2$SiMe$_3$)$_2$] was prepared with substantial modification to a previously reported procedure.[196] A dried 100 mL Schlenk flask, containing a stir bar, was charged with [Co(acac)$_2$(TMEDA)] (**223**, 0.993 g, 2.66 mmol). The flask was then evacuated and refilled with Ar in duplicate. Inside a glovebox, a 50 mL Schlenk flask was charged with [Mg(CH$_2$SiMe$_3$)$_2$] (**224**, 0.555 g, 2.79 mmol, 1.05 equiv) and sealed with a 24/40 septum. The flask was brought out of the glovebox and attached to an Ar Schlenk line. The flask was evacuated and refilled with Ar. Freshly distilled and deaerated Et$_2$O (10.0 mL) was added to each Schlenk flask via syringe. Both flasks were cooled to ~-30 °C with an acetone dry ice bath. With stirring, the Et$_2$O solution of **224** was added dropwise, through a double-ended needle, into the Schlenk flask containing the dissolved **223**. After addition, the reaction mixture was stirred for 3 h at ~-30 °C. The reaction mixture was then warmed to approximately rt and stirred for an

additional 30 min. The stirring was stopped, and the precipitate allowed to settle. The dark purple

solution was carefully filtered, through a double-ended needle, into a triply evacuated and Ar

refilled 100 mL Schlenk flask. Excess Et_2O was used to ensure quantitative transfer of the purple

product and that the filter paper did not come in contact with the white solid. The Et_2O was then

removed under a medium vacuum (0.4 Torr) to produce a dark bluish-purple solid. The solid was

dissolved in a minimal amount of freshly distilled and deaerated *n*-pentane. The dark purple

mixture was filtered, through a double-ended needle, into a triply evacuated and Ar refilled 50

mL Schlenk flask. Excess *n*-pentane was used to ensure quantitative transfer. The *n*-pentane was

then removed under a medium vacuum (0.4 Torr). The dark purple solid was dissolved in a

minimal amount of *n*-pentane (7.5 mL). The solution was stored in a -20 °C freezer overnight

(12–18 h). A purplish-blue solid was isolated by filtering off the *n*-pentane solution, through a

double-ended needle, while maintaining the temperature at ~-20 °C. The solid was dried under a

medium vacuum (0.4 Torr) for 4 h. The product was obtained as a purplish-blue solid (0.768 g)

in 83% yield. **^{1}H NMR** (499.809 MHz, C_6D_6, 27 °C): δ 9.47 (br, 18H), 78.15 (br, 16).

Chapter 5:

Summary and Possible Future Directions

5.1 Chapter 1

Chapter 1 presented a thorough overview into esters and their reductions. A large focus was placed on the literature involving homogeneous hydrogenation of esters. Ideally, that portion can be converted into a review article with some further work and discussion.

5.2 Chapter 2

Chapter 2 presented the first successful development of a highly active and enantioselective system for the asymmetric hydrogenation of α-chiral acyclic esters via DKR. The Ru-based system was discovered and optimized through a developed in-house screening method. The optimal system used a cationic precatalyst made from the chiral ligand (1R,2R)-N,N'-bis{2-[bis(3,5-dimethylphenyl)phosphino]benzcyclohexane-1,2-diamine (**174**) and cationic precursor [Ru(1-3:5,6-η^5-C$_8$H$_{11}$)(η^6-anthracene)]BF$_4$ (**177**). A 50 mol% base loading was used to ensure sufficient racemization and activity in small-scale hydrogenations. High activity and enantioselectivity were obtained for the hydrogenation of α-phenoxy esters with either THF and Na^{i}OPr or DME and NaOEt. The in situ formed catalyst operates under extremely mild pressure (4 atm H$_2$) and room temperature to give β-chiral phenoxy alcohols in up to >99% conversion, 93% ee, and 50 turnovers over 1 h (TOF = 50 h^{-1}). The ee can be increased by decreasing the temperature. Furthermore, the TON and TOF can be increased with moderately increased pressures (15–20 atm H$_2$). The higher TON systems used a decreased base loading (20%) without significantly diminishing the enantioselectivity. The developed system did not perform well with α-chiral phenyl and thiophenyl esters. The latter result supports that the

α-oxygen may be important to obtaining a high enantioselectivity and activity with the discovered catalyst. Preliminary experimental studies with a possible intermediate aldehyde and deuterium gas support that the system is complex. Further experimental and theoretical investigations are required to gain further mechanistic insight. Importantly, this work was published in a respectable journal.[145]

A variety of avenues are available to be explored with the developed catalyst system. For instance, a possibly advantageous and industrially relevant extension to this work would be to examine if α-chiral alcohol esters, such as (±)-methyl lactate, can be asymmetrically hydrogenated with a variant of the developed system. Specifically, both (*R*)-methyl lactate (**98**) and (±)-methyl lactate (**226**) could be investigated on a large-scale. This would provide a direct comparison to the industrial catalyst Ru-MACHO, which provided 2,000 turnovers of **98** to (*R*)-(-)-1,2-propanediol (Chapter 1, Scheme 1-53).[93] Possible starting conditions for these two reactions are shown in Scheme 5-1. The results of these two reactions would provide significant insight into whether **178** is industrially viable.
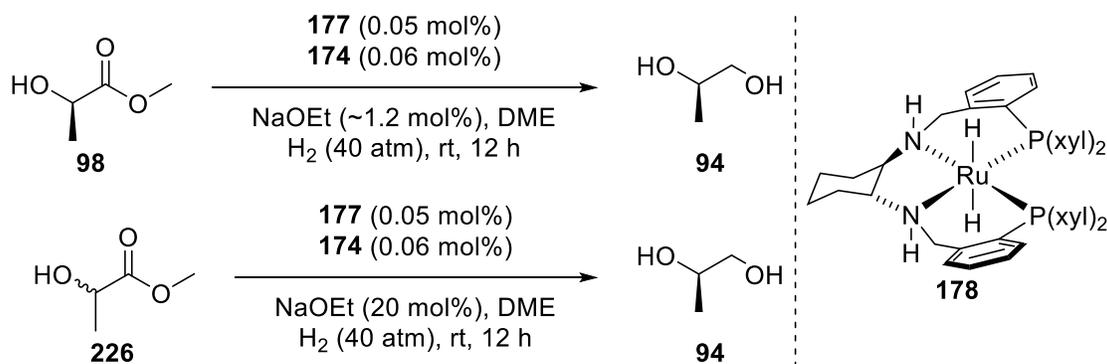
Scheme 5-1. Possible starting reaction conditions for hydrogenations of methyl lactates with **178**.

To possibly increase ee further, I suggest synthesizing the *tert*-butyl DACH ligand **227** (Figure 5-1) and examining it under the optimized conditions. This ligand was not synthesized

due to the lack of availability of its respective aldehyde precursor. Otherwise, the derivative

would have been prepared by the same method as the *para*-methoxy *tert*-butyl DACH ligand

derivative (**183**).
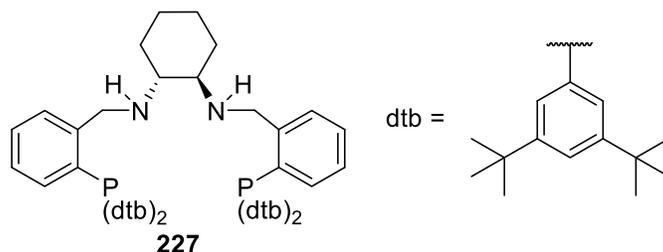
Figure 5-1. (1*R*,2*R*)-*N,N'*-bis{2-[bis(3,5-di-*tert*-butylphenyl)phosphino]benzyl}cyclohexane-1,2-diamine.

The asymmetric hydrogenation of α-chiral phenyl and thiophenyl esters will likely

require the development of an entirely new catalyst system. As a starting point for this matter, I

suggest examining the diphosphine ligands that provided high activity and moderate ee, with

(*R,R*)-(+)-dpen, for hydrogenation of **173** (Chapter 2, Figure 2-10).

Further mechanistic insight, into the developed system, will require stoichiometric

low-temperature experimental studies and theoretical calculations. These studies may provide aid

in developing future systems.

5.3 Chapter 3

Chapter 3 presented the synthesis of three Ru(II)–polypyridyl complexes for photoredox

catalysis. The three Ru(II) complexes are precursors to dinuclear metal complexes as they

contain, or can be converted to contain, a bridging ligand.

The target Ru(II)–diamine complex [Ru(bipy)$_2$(1,10-phenanthroline-5,6-diamine)]$^{2+}$

(**197**) was conveniently synthesized, as a triflate salt, from the bis-bidentate ligand

1,10-phenanthroline-5,6-diamine (**202**) and [Ru(MeCN)$_2$(bipy)$_2$](OTf)$_2$ (**204**). The synthesis was

convenient as it avoided the complexation of 5-amino-6-nitro-1,10-phenanthroline (**200**) and the subsequent reduction with hydrazine hydrate over Pd/C.

Conveniently, **204** was also used, by a fellow group member, for constructing photoanodes on indium tin oxide and titanium dioxide nanoparticles. The results from these photoanodes were published in 2018.[141]

The symmetrical ligand 1,3-di(propan-2-yl)-1*H*-imidazo[4,5-*f*][1,10]-phenanthroline (**205**) was not obtained from 1-(propan-2-yl)-1*H*-imidazo[4,5-*f*][1,10]-phenanthroline (**207**) due to difficulties with the alkylation. Therefore, the target Ru(II) complexes **198** and **199** were not obtained. Similar synthetic challenges have been reported.[175] Although, the symmetrical ligand was not obtained, the asymmetrical ligand 1-benzyl-3-(propan-2-yl)-1*H*-imidazol[4,5-*f*][1,10]phenanthroline-3-ium bromide (bpip, **208**) was obtained. The asymmetrical ligand was used to prepare $[Ru(bpip)(bipy)_2]^{3+}$ (**209**) and $[Ru(bpip)(dmbipy)_2]^{3+}$ (**211**) as halide salts. The halides can be exchanged for more hydrophobic anions with concentrated aqueous solutions of ammonium salts. Furthermore, complexes **209** and **211** are chiral and related compounds have been resolved.[201]

For future work, I suggest attempting the alkylation of **207** with 2-iodopropane when it has been complexed to the desired Ru precursor. Specifically, alkylating complexes **228** and **229** under forcing conditions may produce **198** and **199**, respectively. (Scheme 5-2). Similar conditions have been reported for alkylating the second amine, of the imidazo moiety, with primary halides.[175] This method would protect the phenanthroline moiety from being alkylated.
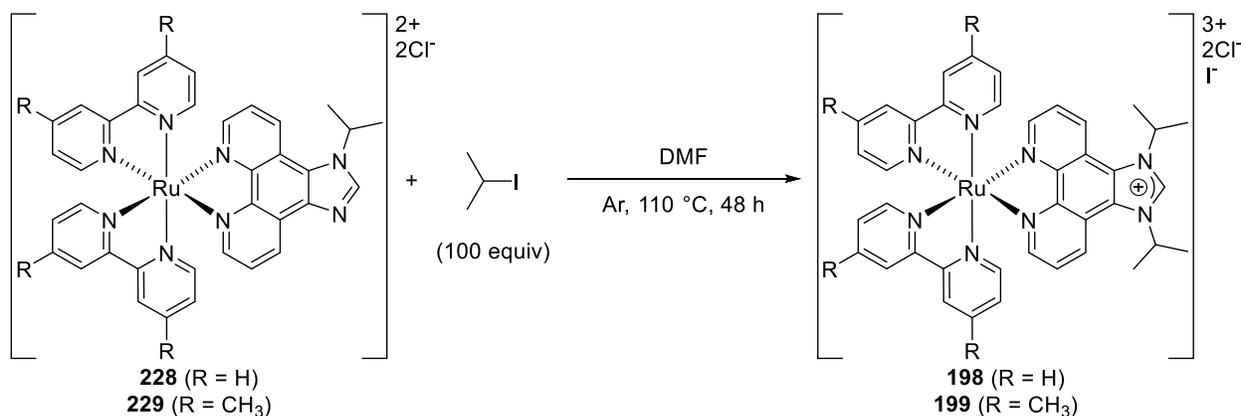
Scheme 5-2. Possible method for synthesizing tricationic Ru–imidazolium complexes **198** and **199**.

5.4 Chapter 4

Chapter 4 presented the preliminary photohydrogenations with complexes **197** and **211**. Complex **197** was mixed with the trisolvento complex *fac*-[Ru((*R*)-BINAP)(H)(*i*PrOH)₃]BF₄ (**212–*i*PrOH**) for in situ catalyst formation and examined for photohydrogenation of acetophenone. The mixture only resulted in poor activity (~2% conv). Although the attempted reactions were not significantly successful, it is interesting that some activity was observed. Further investigations with this system were considered unproductive. I recommend preparing the dichloride derivative **230** from **197** and *trans*-[RuCl₂((*R*)-BINAP)(py)₂] (**231**, Scheme 5-3) and examining it for photohydrogenation under harsher conditions.
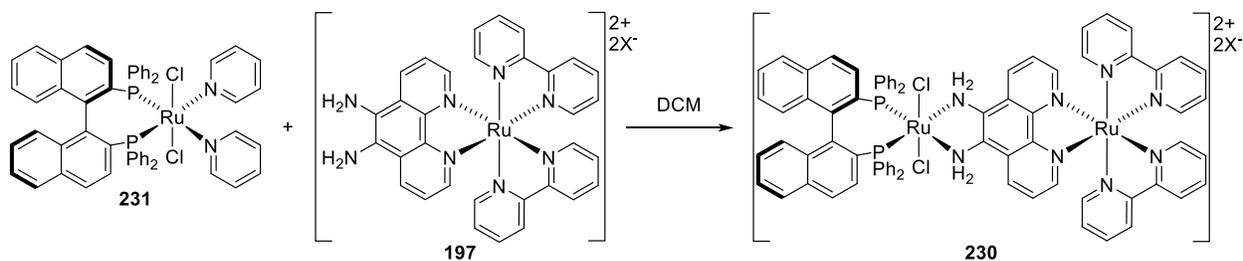

Scheme 5-3. Possible method for preparing the Noyori-type dinuclear Ru–dichloride precatalyst **230**.

Although my usage of complex **197** was not successful, a fellow group member used it for solid-phase synthesis of photoactive dinuclear Ru species.[202]

The Ru(II)–imidazolium complexes **209** and **211** have yet to be coordinated as NHCs to an active site and used for an organic transformation. The attempted photohydrogenation of styrene (**225**) with **211** and **222** was not successful. Prior to further photohydrogenation attempts, the Ru(II)–imidazolium salts should be complexed as NHCs to a metal capable of hydrogenation.

A possible pathway to various bimetallic NHCs of **209** and **211** is through their respective Ru–NHC–AgCl species **232** and **233** (Figure 5-2). These species can likely be prepared from the trichloride salts of **209** and **211** with Ag$_2$O. Similar Ru–NHC–AgCl species have been reported.[203] The AgCl moiety can then undergo substitution to form new bimetallic Ru–NHC species. This method would avoid the decomposition that occured with strong bases but could result in trace Ag impurities that affect catalytic activity. Catalytic hydrogen evolution has been affected by Ag impurities.[203] This is primarily the reason the Ag species were not prepared for the formation of the Ru–Co–dialkyl species.
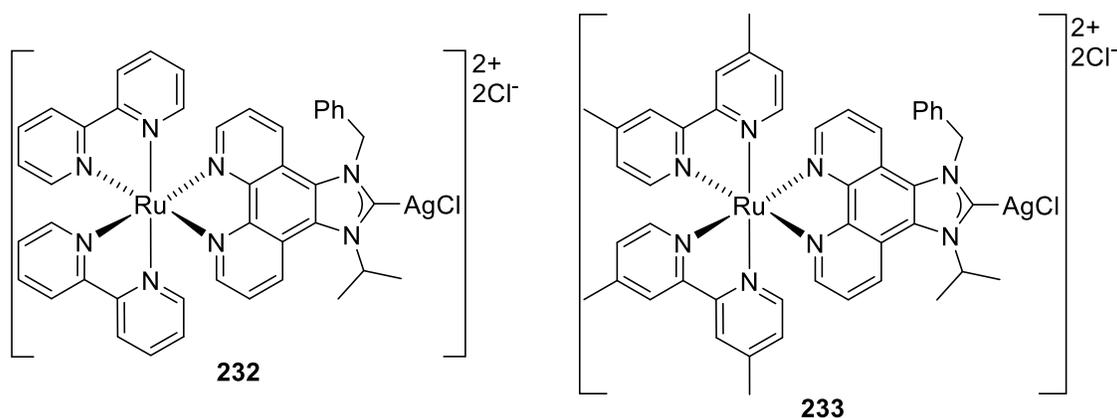
Figure 5-2. Chemical structures of the Ru–NHC–AgCl species **232** and **233**.

References

1. Otera, J.; Nishikido, J. Industrial Uses. In *Esterification: Methods, Reactions, and Applications*, 2nd ed.; Wiley-VCH Verlag GmbH & Co. KGaA: Weinheim, 2009; pp 293–322.

2. Demole, E.; Lederer, E.; Mercier, D. Isolement et Détermination de la Structure du Jasmonate de Méthyle, Constituant Odorant Caractéristique de l'Essence de Jasmin. *Helv. Chim. Acta* **1962**, *45* (2), 675–685.

3. Demole, E.; Lederer, E.; Mercier, D. Synthèse du Dihydrojasmonate de Méthyle (pentyl-2-oxo-3-cyclopentylacétate de Méthyle). *Helv. Chim. Acta* **1962**, *45* (2), 685–692.

4. Chapuis, C. The Jubilee of Methyl Jasmonate and *Hedione*®. *Helv. Chim. Acta* **2012**, *95* (9), 1479–1511.

5. Fischer, E.; Speier, A. Darstellung der Ester. *Ber. Dtsch. Chem. Ges.* **1895**, *28* (3), 3252–3258.

6. Senent, M. L.; Domínguez-Gómez, R.; Carvajal, M.; Kleiner, I. Highly Correlated ab initio Study of the Far Infrared Spectra of Methyl acetate. *J. Chem. Phys.* **2013**, *138* (4), 044319.

7. Venkateswarlu, P.; Gordy, W. Methyl Alcohol. II. Molecular Structure. *J. Chem. Phys.* **1955**, *23* (7), 1200–1202.

8. Juaristi, E.; Cuevas, G. *The Anomeric Effect*. 1st ed.; CRC Press: Boca Raton, 1994.

9. Pawar, D. M.; Khalil, A. A.; Hooks, D. R.; Collins, K.; Elliott, T.; Stafford, J.; Smith, L.; Noe, E. A. *E* and *Z* Conformations of Esters, Thiol Esters, and Amides. *J. Am. Chem. Soc.* **1998**, *120* (9), 2108–2112.

10. Alabugin, I. V. Stereoelectronic Effects with Donor and Acceptor Separated by a Single Bond Bridge. In *Stereoelectronic Effects*, John Wiley & Sons, Ltd.: 2016; pp 97–182.

11. Zhao, Y.; Mouhib, H.; Li, G.; Kleiner, I.; Stahl, W. Conformational Analysis of *tert*-Butyl acetate Using a Combination of Microwave Spectroscopy and Quantum Chemical Calculations. *J. Mol. Spectrosc.* **2016**, *322*, 38–42.

12. Grindley, T. B. Conformational Populations and Rotational Barriers in Esters. *Tetrahedron Lett.* **1982**, *23* (17), 1757–1760.

13. Dugave, C.; Demange, L. Cis−Trans Isomerization of Organic Molecules and Biomolecules: Implications and Applications. *Chem. Rev.* **2003**, *103* (7), 2475–2532.

14. Hiroshi, N.; Hitoshi, F.; Osamu, Y. Nuclear Magnetic Resonance Study of Exchanging Systems. X. Rotational Barriers to *trans-cis* Isomerization in Esters. *Bull. Chem. Soc. Jpn.* **1978**, *51* (1), 214–218.

15. Bach, R. D.; Dmitrenko, O. The Effect of Carbonyl Substitution on the Strain Energy of Small Ring Compounds and Their Six-Member Ring Reference Compounds. *J. Am. Chem. Soc.* **2006**, *128* (14), 4598–4611.

16. Wietelmann, U.; Felderhoff, M.; Rittmeyer, P. Hydrides. In *Ullmann's Encyclopedia of Industrial Chemistry*, Wiley-VCH Verlag GmbH & Co. KGaA: Weinheim, 2016; pp 1–39.

17. Brown, H. C.; Ramachandran, P. V. Sixty Years of Hydride Reductions. In *Reductions in Organic Synthesis*, American Chemical Society: 1996; Vol. 641, pp 1–30.

18. Schlesinger, H. I.; Brown, H. C.; Finholt, A. E. The Preparation of Sodium Borohydride by the High Temperature Reaction of Sodium Hydride with Borate Esters[1]. *J. Am. Chem. Soc.* **1953**, *75* (1), 205–209.

19. Kollonitsch, J.; Fuchs, O.; Gábor, V. New and Known Complex Borohydrides and Some of Their Applications in Organic Syntheses. *Nature* **1954**, *173* (4394), 125–126.

20. Brown, H. C.; Mead, E. J.; Subba Rao, B. C. A Study of Solvents for Sodium Borohydride and the Effect of Solvent and the Metal Ion on Borohydride Reductions[1]. *J. Am. Chem. Soc.* **1955**, *77* (23), 6209–6213.

21. Kollonitsch, J.; Fuchs, O.; Gábor, V. Alkaline-Earth Borohydrides and Their Applications in Organic Syntheses. *Nature* **1955**, *175* (4451), 346–346.

22. Brown, H. C.; Rao, B. C. S. A New Powerful Reducing Agent—Sodium Borohydride in the Presence of Aluminum Chloride and Other Polyvalent Metal Halides[1,2]. *J. Am. Chem. Soc.* **1956**, *78* (11), 2582–2588.

23. Walker, E. R. H. The Functional Group Selectivity of Complex Hydride Reducing Agents. *Chem. Soc. Rev.* **1976**, *5*, 23–50.

24. Brown, H. C.; Narasimhan, S.; Choi, Y. M. Selective Reductions. 30. Effect of Cation and Solvent on the Reactivity of Saline Borohydrides for Reduction of Carboxylic Esters. Improved Procedures for the Conversion of Esters to Alcohols by Metal Borohydrides. *J. Org. Chem.* **1982**, *47* (24), 4702–4708.

25.   Brown, H. C.; Krishnamurthy, S. Forty Years of Hydride Reductions. *Tetrahedron* **1979**, *35* (5), 567–607.

26.   Laïb, T.; Zhu, J. Synthesis of Model of Phomopsin-Ustiloxin-Type Antimitotic Agents. *Synlett* **2000**, (9), 1363–1365.

27.   Hu, B.; Prashad, M.; Har, D.; Prasad, K.; Repič, O.; Blacklock, T. J. An Efficient Synthesis of (*R*)-2-Butyl-3-hydroxypropionic acid. *Org. Process Res. Dev.* **2007**, *11* (1), 90–93.

28.   Finholt, A. E.; Bond, A. C.; Schlesinger, H. I. Lithium Aluminum Hydride, Aluminum Hydride and Lithium Gallium Hydride, and Some of Their Applications in Organic and Inorganic Chemistry[1]. *J. Am. Chem. Soc.* **1947**, *69* (5), 1199–1203.

29.   Allen, L. C. Electronegativity Is the Average One-Electron Energy of the Valence-Shell Electrons in Ground-State Free Atoms. *J. Am. Chem. Soc.* **1989**, *111* (25), 9003–9014.

30.   Abdel-Magid, A. F. 8.01 Reduction of C=O to CHOH by Metal Hydrides. In *Comprehensive Organic Synthesis*, 2nd ed.; Knochel, P.; Molander, G. A., Eds. Elsevier: Amsterdam, 2014; pp 1–84.

31.   Magano, J.; Dunetz, J. R. Large-Scale Carbonyl Reductions in the Pharmaceutical Industry. *Org. Process Res. Dev.* **2012**, *16* (6), 1156–1184.

32.   Saudan, L. A. Hydrogenation of Esters. In *Sustainable Catalysis*, Dunn, P. J.; (Mimi) Hii, K. K.; Krische, M. J.; Williams, M. T., Eds. John Wiley & Sons, Inc.: Hoboken, NJ, 2013; pp 37–61.

33.   Burgey, C. S.; Paone, D. V.; Shaw, A. W.; Deng, J. Z.; Nguyen, D. N.; Potteiger, C. M.; Graham, S. L.; Vacca, J. P.; Williams, T. M. Synthesis of the (3*R*,6*S*)-3-Amino-6-(2,3-difluorophenyl)azepan-2-one of Telcagepant (MK-0974), a Calcitonin Gene-Related Peptide Receptor Antagonist for the Treatment of Migraine Headache. *Org. Lett.* **2008**, *10* (15), 3235–3238.

34.   Patnaik, P. Gases, Common Toxic, and Flammable. In *A Comprehensive Guide to the Hazardous Properties of Chemical Substances*, 3rd ed.; John Wiley & Sons, Inc.: 2006; pp 402–409.

35.   Sheldon, R. A.; Arends, I. W. C. E.; Hanefeld, U. Introduction: Green Chemistry and Catalysis. In *Green Chemistry and Catalysis*, Wiley-VCH Verlag GmbH & Co. KGaA: 2007; pp 1–47.

36.   Adkins, H.; Folkers, K. The Catalytic Hydrogenation of Esters to Alcohols. *J. Am. Chem. Soc.* **1931**, *53* (3), 1095–1097.

37. Adkins, H.; Burgoyne, E. E.; Schneider, H. J. The Copper—Chromium Oxide Catalyst for Hydrogenation[1]. *J. Am. Chem. Soc.* **1950**, *72* (6), 2626–2629.

38. Folkers, K.; Adkins, H. The Catalytic Hydrogenation of Esters to Alcohols. II. *J. Am. Chem. Soc.* **1932**, *54* (3), 1145–1154.

39. Sauer, J.; Adkins, H. The Selective Hydrogenation of Unsaturated Esters to Unsaturated Alcohols. *J. Am. Chem. Soc.* **1937**, *59* (1), 1–3.

40. Ovakimian, G.; Christman, C. C.; Kuna, M.; Levene, P. A. The Reaction of the Esters of *dl*-Leucine and of *l*-Leucine on the Raney Catalyst. *J. Biol. Chem.* **1940**, *134* (1), 151–161.

41. Ovakimian, G.; Kuna, M.; Levene, P. A. The Reaction of the Esters of Phenylaminoacetic acid and of Phenylalanine on the Raney Catalyst. *J. Biol. Chem.* **1940**, *135* (1), 91–98.

42. Pavlic, A. A.; Adkins, H. Preparation of a Raney Nickel Catalyst. *J. Am. Chem. Soc.* **1946**, *68* (8), 1471–1471.

43. Adkins, H.; Billica, H. R. The Preparation of Raney Nickel Catalysts and Their Use Under Conditions Comparable with Those for Platinum and Palladium Catalysts. *J. Am. Chem. Soc.* **1948**, *70* (2), 695–698.

44. Adkins, H.; Pavlic, A. A. Hydrogenation of Esters to Alcohols over Raney Nickel. I. *J. Am. Chem. Soc.* **1947**, *69* (12), 3039–3041.

45. Adkins, H.; Billica, H. R. The Hydrogenation of Esters to Alcohols at 25–150°. *J. Am. Chem. Soc.* **1948**, *70* (9), 3121–3125.

46. Mozingo, R.; Folkers, K. Hydrogenolysis of β-Oxygenated Esters to Glycols. *J. Am. Chem. Soc.* **1948**, *70* (1), 227–229.

47. Mozingo, R.; Folkers, K. Hydrogenolysis of Aromatic Esters to Alcohols. *J. Am. Chem. Soc.* **1948**, *70* (1), 229–231.

48. Adkins, H. Catalytic Hydrogenation of Esters to Alcohols. In *Organic Reactions*, 2011; pp 1–27.

49. Evans, J. W.; Wainwright, M. S.; Cant, N. W.; Trimm, D. L. Structural and Reactivity Effects in the Copper-Catalyzed Hydrogenolysis of Aliphatic Esters. *J. Catal.* **1984**, *88* (1), 203–213.

50. Agarwal, A. K.; Cant, N. W.; Wainwright, M. S.; Trimm, D. L. Catalytic Hydrogenolysis of Esters: A Comparative Study of the Reactions of Simple Formates and Acetates over Copper on Silica. *J. Mol. Catal.* **1987**, *43* (1), 79–92.

51. Turek, T.; Trimm, D. L.; Black, D. S.; Cant, N. W. Hydrogenolysis of Dimethyl succinate on Copper-based Catalysts. *Appl. Catal., A* **1994**, *116* (1), 137–150.

52. van de Scheur, F. T.; Staal, L. H. Effects of Zinc Addition to Silica Supported Copper Catalysts for the Hydrogenolysis of Esters. *Appl. Catal., A* **1994**, *108* (1), 63–83.

53. Brands, D. S.; Poels, E. K.; Krieger, T. A.; Makarova, O. V.; Weber, C.; Veer, S.; Bliek, A. The Relation Between Reduction Temperature and Activity in Copper Catalysed Ester Hydrogenolysis and Methanol Synthesis. *Catal. Lett.* **1996**, *36* (3), 175–181.

54. Brands, D. S.; Poels, E. K.; Bliek, A. Ester Hydrogenolysis over Promoted Cu/SiO_2 Catalysts. *Appl. Catal., A* **1999**, *184* (2), 279–289.

55. Poels, E. K.; Brands, D. S. Modification of $Cu/ZnO/SiO_2$ Catalysts by High Temperature Reduction. *Appl. Catal., A* **2000**, *191* (1), 83–96.

56. Ohlinger, C.; Kraushaar-Czarnetzki, B. Improved Processing Stability in the Hydrogenation of Dimethyl maleate to γ-Butyrolactone, 1,4-Butanediol and Tetrahydrofuran. *Chem. Eng. Sci.* **2003**, *58* (8), 1453–1461.

57. Müller, S. P.; Kucher, M.; Ohlinger, C.; Kraushaar-Czarnetzki, B. Extrusion of Cu/ZnO Catalysts for the Single-Stage Gas-Phase Processing of Dimethyl maleate to Tetrahydrofuran. *J. Catal.* **2003**, *218* (2), 419–426.

58. He, Z.; Lin, H.; He, P.; Yuan, Y. Effect of Boric oxide Doping on the Stability and Activity of a $Cu–SiO_2$ Catalyst for Vapor-Phase Hydrogenation of Dimethyl oxalate to Ethylene glycol. *J. Catal.* **2011**, *277* (1), 54–63.

59. Turek, T.; Trimm, D. L.; Cant, N. W. The Catalytic Hydrogenolysis of Esters to Alcohols. *Catal. Rev.* **1994**, *36* (4), 645–683.

60. Ying, J.; Han, X.; Ma, L.; Lu, C.; Feng, F.; Zhang, Q.; Li, X. Effects of Basic Promoters on the Catalytic Performance of Cu/SiO_2 in the Hydrogenation of Dimethyl maleate. *Catalysts* **2019**, *9* (9), 704.

61. Shu, G.; Ma, K.; Tang, S.; Liu, C.; Yue, H.; Liang, B. Highly Selective Hydrogenation of Diesters to Ethylene glycol and Ethanol on Aluminum-Promoted $CuAl/SiO_2$ Catalysts. *Catal. Today* **2019**.

62. Huang, H.; Wang, S.; Wang, S.; Cao, G. Deactivation Mechanism of Cu/Zn Catalyst Poisoned by Organic Chlorides in Hydrogenation of Fatty Methyl Ester to Fatty Alcohol. *Catal. Lett.* **2010**, *134* (3), 351–357.

63. Hu, Q.; Fan, G.; Yang, L.; Li, F. Aluminum-Doped Zirconia-Supported Copper Nanocatalysts: Surface Synergistic Catalytic Effects in the Gas-Phase Hydrogenation of Esters. *ChemCatChem* **2014**, *6* (12), 3501–3510.

64. Ding, J.; Liu, Y.; Zhang, J.; Liu, K.; Xiao, H.; Kong, F.; Sun, Y.; Chen, J. Excellent Performance in Hydrogenation of Esters over Cu/ZrO$_2$ Catalyst Prepared by Bio-Derived Salicylic acid. *Catal. Sci. Technol.* **2016**, *6* (19), 7220–7230.

65. Li, X.; Wang, H.; Sun, P.; Zhang, S.; Yao, Z. Boron-Promoted Cu/ZrO$_2$ Catalysts for Hydrogenation of *sec*-Butyl acetate: Structural Evolution and Catalytic Performance. *Mol. Catal.* **2020**, *482*, 110698.

66. Guo, P. J.; Chen, L. F.; Yan, S. R.; Dai, W. L.; Qiao, M. H.; Xu, H. L.; Fan, K. N. One-Step Hydrogenolysis of Dimethyl maleate to Tetrahydrofuran over Chromium-Modified Cu–B/γ-Al$_2$O$_3$ Catalysts. *J. Mol. Catal. A: Chem.* **2006**, *256* (1), 164–170.

67. Yuan, P.; Liu, Z.; Zhang, W.; Sun, H.; Liu, S. Cu-Zn/Al$_2$O$_3$ Catalyst for the Hydrogenation of Esters to Alcohols. *Chin. J. Catal.* **2010**, *31* (7), 769–775.

68. Huang, Z.; Barnett, K. J.; Chada, J. P.; Brentzel, Z. J.; Xu, Z.; Dumesic, J. A.; Huber, G. W. Hydrogenation of γ-Butyrolactone to 1,4-Butanediol over CuCo/TiO$_2$ Bimetallic Catalysts. *ACS Catal.* **2017**, *7* (12), 8429–8440.

69. Liu, K.; Pritchard, J.; Lu, L.; van Putten, R.; Verhoeven, M. W. G. M.; Schmitkamp, M.; Huang, X.; Lefort, L.; Kiely, C. J.; Hensen, E. J. M.; Pidko, E. A. Supported Nickel–Rhenium Catalysts for Selective Hydrogenation of Methyl Esters to Alcohols. *Chem. Commun.* **2017**, *53* (70), 9761–9764.

70. Heutz, F. J. L.; Erken, C.; Aguila, M. J. B.; Lefort, L.; Kamer, P. C. J. Heterogeneous Hydrogenation of Esters under Mild Conditions using Solid-Supported Phosphorus–Ruthenium Catalysts. *ChemCatChem* **2016**, *8* (11), 1896–1900.

71. Heutz, F. J. L.; Samuels, M. C.; Kamer, P. C. J. Solid-Phase Synthesis of Recyclable Diphosphine Ligands. *Catal. Sci. Technol.* **2015**, *5* (6), 3296–3301.

72.   Saudan, L. A.; Saudan, C. M.; Debieux, C.; Wyss, P. Dihydrogen Reduction of Carboxylic Esters to Alcohols Under the Catalysis of Homogeneous Ruthenium Complexes: High Efficiency and Unprecedented Chemoselectivity. *Angew. Chem. Int. Ed.* **2007**, *46* (39), 7473–7476.

73.   Spasyuk, D.; Smith, S.; Gusev, D. G. From Esters to Alcohols and Back with Ruthenium and Osmium Catalysts. *Angew. Chem. Int. Ed.* **2012**, *51* (11), 2772–2775.

74.   Spasyuk, D.; Gusev, D. G. Acceptorless Dehydrogenative Coupling of Ethanol and Hydrogenation of Esters and Imines. *Organometallics* **2012**, *31* (15), 5239–5242.

75.   Konrath, R.; Spannenberg, A.; Kamer, P. C. J. Preparation of a Series of Supported Nonsymmetrical PNP-Pincer Ligands and the Application in Ester Hydrogenation. *Chem. Eur. J.* **2019**, *25* (67), 15341–15350.

76.   Samuels, M. C.; Heutz, F. J. L.; Grabulosa, A.; Kamer, P. C. J. Solid-Phase Synthesis and Catalytic Screening of Polystyrene Supported Diphosphines. *Top. Catal.* **2016**, *59* (19), 1793–1799.

77.   Xu, S.; Kalapugama, S.; Rasu, L.; Bergens, S. H. Preparation and Study of Reusable Polymerized Catalysts for Ester Hydrogenation. *ACS Omega* **2019**, *4* (7), 12212–12221.

78.   Grey, R. A.; Pez, G. P. Novel Anionic Phosphine Transition Metal Hydride Complexes and Their Application to the Catalytic Hydrogenation of Polar Organic Compounds. In *Symposium on Homogeneous Catalysis*, American Chemical Society, Division of Petroleum Chemistry, Inc.: Houston, TX, 1980; pp 399–403.

79.   Grey, R. A.; Pez, G. P.; Wallo, A.; Corsi, J. Homogeneous Catalytic Hydrogenation of Carboxylic Acid Esters to Alcohols. *J. Chem. Soc., Chem. Commun.* **1980**, (16), 783–784.

80.   Matteoli, U.; Blanchi, M.; Menchi, G.; Prediani, P.; Piacenti, F. Homogeneous Catalytic Hydrogenation of Dicarboxylic Acid Esters. *J. Mol. Catal.* **1984**, *22* (3), 353–362.

81.   Matteoli, U.; Bianchi, M.; Menchi, G.; Frediani, P.; Piacenti, F. Hydrogenation of Dimethyl oxalate in the Presence of Ruthenium Carbonyl Carboxylates: Ethylene glycol Formation. *J. Mol. Catal.* **1985**, *29* (2), 269–270.

82.   Matteoli, U.; Menchi, G.; Bianchi, M.; Piacenti, F. Homogeneous Catalytic Hydrogenation Dicarboxylic Acid Esters. II. *J. Organomet. Chem.* **1986**, *299* (2), 233–238.

83.   Matteoli, U.; Menchi, G.; Bianchi, M.; Piacenti, F. Homogeneous Catalytic Hydrogenation of the Esters of Bicarboxylic Acids: Part III. Ethylene glycol from Dimethyl oxalate. *J. Mol. Catal.* **1988**, *44* (3), 347–355.

84.   Hara, Y.; Inagaki, H.; Nishimura, S.; Wada, K. Selective Hydrogenation of Cyclic Ester to α,ω-Diol Catalyzed by Cationic Ruthenium Complexes with Trialkylphosphine Ligands. *Chem. Lett.* **1992**, *21* (10), 1983–1986.

85.   Teunissen, H. T.; Elsevier, C. J. Ruthenium Catalysed Hydrogenation of Dimethyl oxalate to Ethylene glycol. *Chem. Commun.* **1997**, (7), 667–668.

86.   Teunissen, H. T.; Elsevier, C. J. Homogeneous Ruthenium Catalyzed Hydrogenation of Esters to Alcohols‡. *Chem. Commun.* **1998**, (13), 1367–1368.

87.   Nomura, K.; Ogura, H.; Imanishi, Y. Direct Synthesis of 2-Phenylethanol by Hydrogenation of Methyl phenylacetate Using Homogeneous Ruthenium-Phosphine Catalysis Under Low Hydrogen Pressure. *J. Mol. Catal. A: Chem.* **2001**, *166* (2), 345–349.

88.   Nomura, K.; Ogura, H.; Imanishi, Y. Ruthenium Catalyzed Hydrogenation of Methyl phenylacetate Under Low Hydrogen Pressure. *J. Mol. Catal. A: Chem.* **2002**, *178* (1), 105–114.

89.   Zhang, J.; Leitus, G.; Ben-David, Y.; Milstein, D. Efficient Homogeneous Catalytic Hydrogenation of Esters to Alcohols. *Angew. Chem. Int. Ed.* **2006**, *45* (7), 1113–1115.

90.   Takebayashi, S.; Bergens, S. H. Facile Bifunctional Addition of Lactones and Esters at Low Temperatures. The First Intermediates in Lactone/Ester Hydrogenations. *Organometallics* **2009**, *28* (8), 2349–2351.

91.   Hamilton, R. J.; Bergens, S. H. An Unexpected Possible Role of Base in Asymmetric Catalytic Hydrogenations of Ketones. Synthesis and Characterization of Several Key Catalytic Intermediates. *J. Am. Chem. Soc.* **2006**, *128* (42), 13700–13701.

92.   Kuriyama, W.; Ino, Y.; Ogata, O.; Sayo, N.; Saito, T. A Homogeneous Catalyst for Reduction of Optically Active Esters to the Corresponding Chiral Alcohols without Loss of Optical Purities. *Adv. Synth. Catal.* **2010**, *352* (1), 92–96.

93.   Kuriyama, W.; Matsumoto, T.; Ogata, O.; Ino, Y.; Aoki, K.; Tanaka, S.; Ishida, K.; Kobayashi, T.; Sayo, N.; Saito, T. Catalytic Hydrogenation of Esters. Development of an Efficient Catalyst and Processes for Synthesising (*R*)-1,2-Propanediol and 2-(L-Menthoxy)ethanol. *Org. Process Res. Dev.* **2012**, *16* (1), 166–171.

94.   Clarke, M. L.; Díaz-Valenzuela, M. B.; Slawin, A. M. Z. Hydrogenation of Aldehydes, Esters, Imines, and Ketones Catalyzed by a Ruthenium Complex of a Chiral Tridentate Ligand. *Organometallics* **2007**, *26* (1), 16–19.

95.   Carpenter, I.; Eckelmann, S. C.; Kuntz, M. T.; Fuentes, J. A.; France, M. B.; Clarke, M. L. Convenient and Improved Protocols for the Hydrogenation of Esters Using Ru Catalysts Derived from (P,P), (P,N,N) and (P,N,O) Ligands. *Dalton Trans.* **2012**, *41* (34), 10136–10140.

96.   Ito, M.; Ikariya, T. Design of Bifunctional Molecular Catalysts for Hydrogenation of Polar Functionalities. *J. Synth. Org. Chem Jpn.* **2008**, *66* (11), 1042–1048.

97.   Ito, M.; Ootsuka, T.; Watari, R.; Shiibashi, A.; Himizu, A.; Ikariya, T. Catalytic Hydrogenation of Carboxamides and Esters by Well-Defined Cp*Ru Complexes Bearing a Protic Amine Ligand. *J. Am. Chem. Soc.* **2011**, *133* (12), 4240–4242.

98.   O, W. W. N.; Lough, A. J.; Morris, R. H. The Hydrogenation of Molecules with Polar Bonds Catalyzed by a Ruthenium(II) Complex Bearing a Chelating N-Heterocyclic Carbene with a Primary Amine Donor. *Chem. Commun.* **2010**, *46* (43), 8240–8242.

99.   O, W. W. N.; Morris, R. H. Ester Hydrogenation Catalyzed by a Ruthenium(II) Complex Bearing an N-Heterocyclic Carbene Tethered with an "NH$_2$" Group and a DFT Study of the Proposed Bifunctional Mechanism. *ACS Catal.* **2013**, *3* (1), 32–40.

100. Sun, Y.; Koehler, C.; Tan, R.; Annibale, V. T.; Song, D. Ester Hydrogenation Catalyzed by Ru-CNN Pincer Complexes. *Chem. Commun.* **2011**, *47* (29), 8349–8351.

101. Fogler, E.; Balaraman, E.; Ben-David, Y.; Leitus, G.; Shimon, L. J. W.; Milstein, D. New CNN-Type Ruthenium Pincer NHC Complexes. Mild, Efficient Catalytic Hydrogenation of Esters. *Organometallics* **2011**, *30* (14), 3826–3833.

102. Zhang, J.; Balaraman, E.; Leitus, G.; Milstein, D. Electron-Rich PNP- and PNN-Type Ruthenium(II) Hydrido Borohydride Pincer Complexes. Synthesis, Structure, and Catalytic Dehydrogenation of Alcohols and Hydrogenation of Esters. *Organometallics* **2011**, *30* (21), 5716–5724.

103. Fogler, E.; Garg, J. A.; Hu, P.; Leitus, G.; Shimon, L. J. W.; Milstein, D. System with Potential Dual Modes of Metal–Ligand Cooperation: Highly Catalytically Active Pyridine-Based PNNH–Ru Pincer Complexes. *Chem. Eur. J.* **2014**, *20* (48), 15727–15731.

104. Spasyuk, D.; Smith, S.; Gusev, D. G. Replacing Phosphorus with Sulfur for the Efficient Hydrogenation of Esters. *Angew. Chem. Int. Ed.* **2013**, *52* (9), 2538–2542.

105. Gusev, D. G. Dehydrogenative Coupling of Ethanol and Ester Hydrogenation Catalyzed by Pincer-Type YNP Complexes. *ACS Catal.* **2016**, *6* (10), 6967–6981.

106. Li, W.; Xie, J.-H.; Yuan, M.-L.; Zhou, Q.-L. Ruthenium Complexes of Tetradentate Bipyridine Ligands: Highly Efficient Catalysts for the Hydrogenation of Carboxylic Esters and Lactones. *Green Chem.* **2014**, *16* (9), 4081–4085.

107. Filonenko, G. A.; Cosimi, E.; Lefort, L.; Conley, M. P.; Copéret, C.; Lutz, M.; Hensen, E. J. M.; Pidko, E. A. Lutidine-Derived Ru-CNC Hydrogenation Pincer Catalysts with Versatile Coordination Properties. *ACS Catal.* **2014**, *4* (8), 2667–2671.

108. Filonenko, G. A.; Aguila, M. J. B.; Schulpen, E. N.; van Putten, R.; Wiecko, J.; Müller, C.; Lefort, L.; Hensen, E. J. M.; Pidko, E. A. Bis-N-Heterocyclic Carbene Aminopincer Ligands Enable High Activity in Ru-Catalyzed Ester Hydrogenation. *J. Am. Chem. Soc.* **2015**, *137* (24), 7620–7623.

109. Tan, X.; Wang, Y.; Liu, Y.; Wang, F.; Shi, L.; Lee, K.-H.; Lin, Z.; Lv, H.; Zhang, X. Highly Efficient Tetradentate Ruthenium Catalyst for Ester Reduction: Especially for Hydrogenation of Fatty Acid Esters. *Org. Lett.* **2015**, *17* (3), 454–457.

110. Wang, Z.; Chen, X.; Liu, B.; Liu, Q.-b.; Solan, G. A.; Yang, X.; Sun, W.-H. Cooperative Interplay Between a Flexible PNN-Ru(II) Complex and a NaBH$_4$ Additive in the Efficient Catalytic Hydrogenation of Esters. *Catal. Sci. Technol.* **2017**, *7* (6), 1297–1304.

111. Kim, D.; Le, L.; Drance, M. J.; Jensen, K. H.; Bogdanovski, K.; Cervarich, T. N.; Barnard, M. G.; Pudalov, N. J.; Knapp, S. M. M.; Chianese, A. R. Ester Hydrogenation Catalyzed by CNN-Pincer Complexes of Ruthenium. *Organometallics* **2016**, *35* (7), 982–989.

112. Le, L.; Liu, J.; He, T.; Kim, D.; Lindley, E. J.; Cervarich, T. N.; Malek, J. C.; Pham, J.; Buck, M. R.; Chianese, A. R. Structure–Function Relationship in Ester Hydrogenation Catalyzed by Ruthenium CNN-Pincer Complexes. *Organometallics* **2018**, *37* (19), 3286–3297.

113. Le, L.; Liu, J.; He, T.; Malek, J. C.; Cervarich, T. N.; Buttner, J. C.; Pham, J.; Keith, J. M.; Chianese, A. R. Unexpected CNN-to-CC Ligand Rearrangement in Pincer–Ruthenium Precatalysts Leads to a Base-Free Catalyst for Ester Hydrogenation. *Organometallics* **2019**, *38* (17), 3311–3321.

114. He, T.; Buttner, J. C.; Reynolds, E. F.; Pham, J.; Malek, J. C.; Keith, J. M.; Chianese, A. R. Dehydroalkylative Activation of CNN- and PNN-Pincer Ruthenium Catalysts for Ester Hydrogenation. *J. Am. Chem. Soc.* **2019**, *141* (43), 17404–17413.

115. Acosta-Ramirez, A.; Bertoli, M.; Gusev, D. G.; Schlaf, M. Homogeneous Catalytic Hydrogenation of Long-Chain Esters by an Osmium Pincer Complex and Its Potential Application in the Direct Conversion of Triglycerides into Fatty Alcohols. *Green Chem.* **2012**, *14* (4), 1178–1188.

116. Spasyuk, D.; Vicent, C.; Gusev, D. G. Chemoselective Hydrogenation of Carbonyl Compounds and Acceptorless Dehydrogenative Coupling of Alcohols. *J. Am. Chem. Soc.* **2015**, *137* (11), 3743–3746.

117. Junge, K.; Wendt, B.; Jiao, H.; Beller, M. Iridium-Catalyzed Hydrogenation of Carboxylic Acid Esters. *ChemCatChem* **2014**, *6* (10), 2810–2814.

118. Brewster, T. P.; Rezayee, N. M.; Culakova, Z.; Sanford, M. S.; Goldberg, K. I. Base-Free Iridium-Catalyzed Hydrogenation of Esters and Lactones. *ACS Catal.* **2016**, *6* (5), 3113–3117.

119. Yang, X.-H.; Yue, H.-T.; Yu, N.; Li, Y.-P.; Xie, J.-H.; Zhou, Q.-L. Iridium-Catalyzed Asymmetric Hydrogenation of Racemic α-Substituted Lactones to Chiral Diols. *Chem. Sci.* **2017**, *8* (3), 1811–1814.

120. Chen, G.-Q.; Lin, B.-J.; Huang, J.-M.; Zhao, L.-Y.; Chen, Q.-S.; Jia, S.-P.; Yin, Q.; Zhang, X. Design and Synthesis of Chiral *oxa*-Spirocyclic Ligands for Ir-Catalyzed Direct Asymmetric Reduction of Bringmann's Lactones with Molecular H_2. *J. Am. Chem. Soc.* **2018**, *140* (26), 8064–8068.

121. Gu, X.-S.; Yu, N.; Yang, X.-H.; Zhu, A.-T.; Xie, J.-H.; Zhou, Q.-L. Enantioselective Hydrogenation of Racemic α-Arylamino Lactones to Chiral Amino Diols with Site-Specifically Modified Chiral Spiro Iridium Catalysts. *Org. Lett.* **2019**, *21* (11), 4111–4115.

122. Elangovan, S.; Garbe, M.; Jiao, H.; Spannenberg, A.; Junge, K.; Beller, M. Hydrogenation of Esters to Alcohols Catalyzed by Defined Manganese Pincer Complexes. *Angew. Chem. Int. Ed.* **2016**, *55* (49), 15364–15368.

123. Espinosa-Jalapa, N. A.; Nerush, A.; Shimon, L. J. W.; Leitus, G.; Avram, L.; Ben-David, Y.; Milstein, D. Manganese-Catalyzed Hydrogenation of Esters to Alcohols. *Chem. Eur. J.* **2017**, *23* (25), 5934–5938.

124. Widegren, M. B.; Harkness, G. J.; Slawin, A. M. Z.; Cordes, D. B.; Clarke, M. L. A Highly Active Manganese Catalyst for Enantioselective Ketone and Ester Hydrogenation. *Angew. Chem. Int. Ed.* **2017**, *56* (21), 5825–5828.

125. van Putten, R.; Uslamin, E. A.; Garbe, M.; Liu, C.; Gonzalez-de-Castro, A.; Lutz, M.; Junge, K.; Hensen, E. J. M.; Beller, M.; Lefort, L.; Pidko, E. A. Non-Pincer-Type Manganese Complexes as Efficient Catalysts for the Hydrogenation of Esters. *Angew. Chem. Int. Ed.* **2017**, *56* (26), 7531–7534.

126. Widegren, M. B.; Clarke, M. L. Manganese Catalyzed Hydrogenation of Enantiomerically Pure Esters. *Org. Lett.* **2018**, *20* (9), 2654–2658.

127. Widegren, M. B.; Clarke, M. L. Towards Practical Earth-Abundant Reduction Catalysis: Design of Improved Catalysts for Manganese Catalysed Hydrogenation. *Catal. Sci. Technol.* **2019**, *9* (21), 6047–6058.

128. Zell, T.; Ben-David, Y.; Milstein, D. Unprecedented Iron-Catalyzed Ester Hydrogenation. Mild, Selective, and Efficient Hydrogenation of Trifluoroacetic Esters to Alcohols Catalyzed by an Iron Pincer Complex. *Angew. Chem. Int. Ed.* **2014**, *53* (18), 4685–4689.

129. Chakraborty, S.; Dai, H.; Bhattacharya, P.; Fairweather, N. T.; Gibson, M. S.; Krause, J. A.; Guan, H. Iron-Based Catalysts for the Hydrogenation of Esters to Alcohols. *J. Am. Chem. Soc.* **2014**, *136* (22), 7869–7872.

130. Werkmeister, S.; Junge, K.; Wendt, B.; Alberico, E.; Jiao, H.; Baumann, W.; Junge, H.; Gallou, F.; Beller, M. Hydrogenation of Esters to Alcohols with a Well-Defined Iron Complex. *Angew. Chem. Int. Ed.* **2014**, *53* (33), 8722–8726.

131. Elangovan, S.; Wendt, B.; Topf, C.; Bachmann, S.; Scalone, M.; Spannenberg, A.; Jiao, H.; Baumann, W.; Junge, K.; Beller, M. Improved Second Generation Iron Pincer Complexes for Effective Ester Hydrogenation. *Adv. Synth. Catal.* **2016**, *358* (5), 820–825.

132. Gajewski, P.; Gonzalez-de-Castro, A.; Renom-Carrasco, M.; Piarulli, U.; Gennari, C.; de Vries, J. G.; Lefort, L.; Pignataro, L. Expanding the Catalytic Scope of (Cyclopentadienone)iron Complexes to the Hydrogenation of Activated Esters to Alcohols. *ChemCatChem* **2016**, *8* (22), 3431–3435.

133. Srimani, D.; Mukherjee, A.; Goldberg, A. F. G.; Leitus, G.; Diskin-Posner, Y.; Shimon, L. J. W.; Ben David, Y.; Milstein, D. Cobalt-Catalyzed Hydrogenation of Esters to Alcohols: Unexpected

Reactivity Trend Indicates Ester Enolate Intermediacy. *Angew. Chem. Int. Ed.* **2015**, *54* (42), 12357–12360.

134. Korstanje, T. J.; Ivar van der Vlugt, J.; Elsevier, C. J.; de Bruin, B. Hydrogenation of Carboxylic Acids with a Homogeneous Cobalt Catalyst. *Science* **2015**, *350* (6258), 298–302.

135. Yuwen, J.; Chakraborty, S.; Brennessel, W. W.; Jones, W. D. Additive-Free Cobalt-Catalyzed Hydrogenation of Esters to Alcohols. *ACS Catal.* **2017**, *7* (5), 3735–3740.

136. Junge, K.; Wendt, B.; Cingolani, A.; Spannenberg, A.; Wei, Z.; Jiao, H.; Beller, M. Cobalt Pincer Complexes for Catalytic Reduction of Carboxylic Acid Esters. *Chem. Eur. J.* **2018**, *24* (5), 1046–1052.

137. Shao, Z.; Zhong, R.; Ferraccioli, R.; Li, Y.; Liu, Q. General and Phosphine-Free Cobalt-Catalyzed Hydrogenation of Esters to Alcohols. *Chin. J. Chem .* **2019**, *37* (11), 1125–1130.

138. Werkmeister, S.; Junge, K.; Beller, M. Catalytic Hydrogenation of Carboxylic Acid Esters, Amides, and Nitriles with Homogeneous Catalysts. *Org. Process Res. Dev.* **2014**, *18* (2), 289–302.

139. Pritchard, J.; Filonenko, G. A.; van Putten, R.; Hensen, E. J. M.; Pidko, E. A. Heterogeneous and Homogeneous Catalysis for the Hydrogenation of Carboxylic Acid Derivatives: History, Advances and Future Directions. *Chem. Soc. Rev.* **2015**, *44* (11), 3808–3833.

140. Rasu, L.; John, J. M.; Stephenson, E.; Endean, R.; Kalapugama, S.; Clément, R.; Bergens, S. H. Highly Enantioselective Hydrogenation of Amides via Dynamic Kinetic Resolution Under Low Pressure and Room Temperature. *J. Am. Chem. Soc.* **2017**, *139* (8), 3065–3071.

141. Wang, C.; Amiri, M.; Endean, R. T.; Martinez Perez, O.; Varley, S.; Rennie, B.; Rasu, L.; Bergens, S. H. Modular Construction of Photoanodes with Covalently Bonded Ru- and Ir-Polypyridyl Visible Light Chromophores. *ACS Appl. Mater. Interfaces* **2018**, *10* (29), 24533–24542.

142. Takebayashi, S.; John, J. M.; Bergens, S. H. Desymmetrization of *meso*-Cyclic Imides via Enantioselective Monohydrogenation. *J. Am. Chem. Soc.* **2010**, *132* (37), 12832–12834.

143. John, J. M.; Bergens, S. H. A Highly Active Catalyst for the Hydrogenation of Amides to Alcohols and Amines. *Angew. Chem. Int. Ed.* **2011**, *50* (44), 10377–10380.

144. John, J. M.; Loorthuraja, R.; Antoniuk, E.; Bergens, S. H. Catalytic Hydrogenation of Functionalized Amides Under Basic and Neutral Conditions. *Catal. Sci. Technol.* **2015**, *5* (2), 1181–1186.

145. Endean, R. T.; Rasu, L.; Bergens, S. H. Enantioselective Hydrogenations of Esters with Dynamic Kinetic Resolution. *ACS Catal.* **2019**, *9* (7), 6111–6117.

146. Seeman, J. I. The Curtin-Hammett principle and the Winstein-Holness Equation: New Definition and Recent Extensions to Classical Concepts. *J. Chem. Educ.* **1986**, *63* (1), 42.

147. Noyori, R.; Ikeda, T.; Ohkuma, T.; Widhalm, M.; Kitamura, M.; Takaya, H.; Akutagawa, S.; Sayo, N.; Saito, T.; Taketomi, T.; Kumobayashi, H. Stereoselective Hydrogenation via Dynamic Kinetic Resolution. *J. Am. Chem. Soc.* **1989**, *111* (25), 9134–9135.

148. Echeverria, P.-G.; Ayad, T.; Phansavath, P.; Ratovelomanana-Vidal, V. Recent Developments in Asymmetric Hydrogenation and Transfer Hydrogenation of Ketones and Imines through Dynamic Kinetic Resolution. *Synthesis* **2016**, *48* (16), 2523–2539.

149. Xie, J.-H.; Zhou, Z.-T.; Kong, W.-L.; Zhou, Q.-L. Ru-Catalyzed Asymmetric Hydrogenation of Racemic Aldehydes via Dynamic Kinetic Resolution: Efficient Synthesis of Optically Active Primary Alcohols. *J. Am. Chem. Soc.* **2007**, *129* (7), 1868–1869.

150. Li, X.; List, B. Catalytic Asymmetric Hydrogenation of Aldehydes. *Chem. Commun.* **2007**, (17), 1739–1741.

151. Wu, G.; Zhu, J.; Ding, Z.; Shen, Z.; Zhang, Y. Dynamic Kinetic Resolution of Racemic α-Sulfonylaldehydes via Asymmetric Transfer Hydrogenation. *Tetrahedron Lett.* **2009**, *50* (4), 427–429.

152. Bai, W.-J.; Xie, J.-H.; Li, Y.-L.; Liu, S.; Zhou, Q.-L. Enantioselective Synthesis of Chiral β-Aryloxy Alcohols by Ruthenium-Catalyzed Ketone Hydrogenation via Dynamic Kinetic Resolution (DKR). *Adv. Synth. Catal.* **2010**, *352* (1), 81–84.

153. Bringmann, G.; Menche, D. Stereoselective Total Synthesis of Axially Chiral Natural Products via Biaryl Lactones. *Acc. Chem. Res.* **2001**, *34* (8), 615–624.

154. Kador, P. F.; Wyman, M.; Betts, D. M. Topical Treatment of Cataracts in Dogs. US 20090082415 A1, August 21, 2007.

155. Stoop, R. M.; Bachmann, S.; Valentini, M.; Mezzetti, A. Ruthenium(II) Complexes with Chiral Tetradentate P_2N_2 Ligands Catalyze the Asymmetric Epoxidation of Olefins with H_2O_2. *Organometallics* **2000**, *19* (20), 4117–4126.

156. Hass, M. J. Reusable Ru and Rh Catalysts for Ester Hydrogenations and Enyne Cycloisomerization. M.Sc. Thesis, University of Alberta, Edmonton, AB, 2011.

157. John, J. M. Design, Development and Mechanistic Study of Ruthenium-Based Catalysts for the Hydrogenation of Imides and Amides. Ph.D. Thesis, University of Alberta, Edmonton, AB, 2014.

158. John, J. M.; Takebayashi, S.; Dabral, N.; Miskolzie, M.; Bergens, S. H. Base-Catalyzed Bifunctional Addition to Amides and Imides at Low Temperature. A New Pathway for Carbonyl Hydrogenation. *J. Am. Chem. Soc.* **2013**, *135* (23), 8578–8584.

159. Takebayashi, S.; Dabral, N.; Miskolzie, M.; Bergens, S. H. Experimental Investigations of a Partial Ru–O Bond During the Metal–Ligand Bifunctional Addition in Noyori-Type Enantioselective Ketone Hydrogenation. *J. Am. Chem. Soc.* **2011**, *133* (25), 9666–9669.

160. Hamilton, R. J.; Leong, C. G.; Bigam, G.; Miskolzie, M.; Bergens, S. H. A Ruthenium−Dihydrogen Putative Intermediate in Ketone Hydrogenation. *J. Am. Chem. Soc.* **2005**, *127* (12), 4152–4153.

161. Hamilton, R. J.; Bergens, S. H. Direct Observations of the Metal−Ligand Bifunctional Addition Step in an Enantioselective Ketone Hydrogenation. *J. Am. Chem. Soc.* **2008**, *130* (36), 11979–11987.

162. Russell, A. G.; Sadler, M. J.; Laidlaw, H. J.; Gutiérrez-Loriente, A.; Wharton, C. W.; Carteau, D.; Bassani, D. M.; Snaith, J. S. Photorelease of Tyrosine from α-Carboxy-6-nitroveratryl (αCNV) Derivatives. *Photochem. Photobiol. Sci.* **2012**, *11* (3), 556–563.

163. Wimmer, Z.; Šaman, D.; Francke, W. Novel Juvenoids of the 2-(4-Hydroxybenzyl)cyclohexan-1-one Series. *Helv. Chim. Acta* **1994**, *77* (2), 502–508.

164. Wiles, J. A.; Daley, C. J. A.; Hamilton, R. J.; Leong, C. G.; Bergens, S. H. An Alternate Route to the Active Chiral Hydrogenation Catalysts [Ru(bisphosphine)(H)(solvent)$_3$]$^+$: Synthesis, Characterization, and Catalytic Evaluation. *Organometallics* **2004**, *23* (20), 4564–4568.

165. Leong, C. G.; Akotsi, O. M.; Ferguson, M. J.; Bergens, S. H. A Ruthenium Catalyst That Does Not Require an N–H Ligand to Achieve High Enantioselectivity for Hydrogenation of an Alkyl-Aryl Ketone. *Chem. Commun.* **2003**, (6), 750–751.

166. Nicewicz, D. A.; MacMillan, D. W. C. Merging Photoredox Catalysis with Organocatalysis: The Direct Asymmetric Alkylation of Aldehydes. *Science* **2008**, *322* (5898), 77–80.

167. Ischay, M. A.; Anzovino, M. E.; Du, J.; Yoon, T. P. Efficient Visible Light Photocatalysis of [2+2] Enone Cycloadditions. *J. Am. Chem. Soc.* **2008**, *130* (39), 12886–12887.

168. Shaw, M. H.; Twilton, J.; MacMillan, D. W. C. Photoredox Catalysis in Organic Chemistry. *J. Org. Chem.* **2016**, *81* (16), 6898–6926.

169. Stephenson, C.; Yoon, T.; MacMillan, D. W. C. *Visible Light Photocatalysis in Organic Chemistry*. 1st ed.; Wiley-VCH Verlag GmbH & Co. KGaA: Weinheim, 2018.

170. Rau, S.; Schäfer, B.; Gleich, D.; Anders, E.; Rudolph, M.; Friedrich, M.; Görls, H.; Henry, W.; Vos, J. G. A Supramolecular Photocatalyst for the Production of Hydrogen and the Selective Hydrogenation of Tolane. *Angew. Chem. Int. Ed.* **2006**, *45* (37), 6215–6218.

171. Beatty, J. W.; Stephenson, C. R. J. Amine Functionalization via Oxidative Photoredox Catalysis: Methodology Development and Complex Molecule Synthesis. *Acc. Chem. Res.* **2015**, *48* (5), 1474–1484.

172. Webb, S. P.; Philips, L. A.; Yeh, S. W.; Tolbert, L. M.; Clark, J. H. Picosecond Kinetics of the Excited-State, Proton-Transfer Reaction of 1-Naphthol in Water. *J. Phys. Chem.* **1986**, *90* (21), 5154–5164.

173. Park, H.-J.; Kim, W.; Choi, W.; Chung, Y. K. Ruthenium(II) Complexes Incorporating the Bidentate Ligand Containing an Imidazolium Moiety: Synthesis, Characterization, and Electrochemical Properties and Their Application in a Visible-Light Induced Hydrogen-Evolving System. *New J. Chem.* **2013**, *37* (10), 3174–3182.

174. Peuntinger, K.; Pilz, T. D.; Staehle, R.; Schaub, M.; Kaufhold, S.; Petermann, L.; Wunderlin, M.; Görls, H.; Heinemann, F. W.; Li, J.; Drewello, T.; Vos, J. G.; Guldi, D. M.; Rau, S. Carbene Based Photochemical Molecular Assemblies for Solar Driven Hydrogen Generation. *Dalton Trans.* **2014**, *43* (36), 13683–13695.

175. Petermann, L.; Staehle, R.; Pilz, T. D.; Sorsche, D.; Görls, H.; Rau, S. Synthetic Strategies for Variably Substituted Ruthenium–Imidazophenanthrolinium Complexes. *Eur. J. Inorg. Chem.* **2015**, 750–762.

176. Webster, A. A.; Prasad, S. K. K.; Hodgkiss, J. M.; Hoberg, J. O. An N-Heterocyclic Carbene Phenanthroline Ligand: Synthesis, Multi-Metal Coordination and Spectroscopic Studies. *Dalton Trans.* **2015**, *44* (8), 3728–3736.

177. Ju, Y.; Park, H.-J.; Shin, I.-S.; Chung, Y. K.; Kim, J. Highly Efficient Low-Oxidation-Potential Electrochemiluminescence of Ruthenium(II) Complex Containing Selone Moiety. *Inorg. Chem. Commun.* **2019**, *106*, 86–90.

178. Ishow, E.; Gourdon, A.; Launay, J.-P. Observation of Supramolecular π–π Dimerization of a Dinuclear Ruthenium Complex by ^{1}H NMR and ESMS. *Chem. Commun.* **1998**, 1909–1910.

179. Ishow, E.; Gourdon, A.; Launay, J.-P.; Chiorboli, C.; Scandola, F. Synthesis, Mass Spectrometry, and Spectroscopic Properties of a Dinuclear Ruthenium Complex Comprising a 20 Å Long Fully Aromatic Bridging Ligand. *Inorg. Chem.* **1999**, *38* (7), 1504–1510.

180. C. Fletcher, N.; C. Robinson, T.; Behrendt, A.; C. Jeffery, J.; R. Reeves, Z.; D. Ward, M. Structural, Electrochemical and UV/VIS/NIR Spectroelectrochemical Properties of Diastereomerically Pure Dinuclear Ruthenium Complexes Based on the Bridging Ligand Phenanthroline-5,6-diimine, and a Mononuclear By-product with a Peripheral Isoimidazole Group. *J. Chem. Soc., Dalton Trans.* **1999**, 2999–3006.

181. Shi, S.; Xie, T.; Yao, T.-M.; Wang, C.-R.; Geng, X.-T.; Yang, D.-J.; Han, L.-J.; Ji, L.-N. Synthesis, Characterization, DNA-Binding and DNA-Photocleavage Studies of $[Ru(bpy)_2(pmip)]^{2+}$ and $[Ru(phen)_2(pmip)]^{2+}$ (pmip=2-(2′-Pyrimidyl)imidazo[4,5-*f*][1,10]phenanthroline. *Polyhedron* **2009**, *28* (7), 1355–1361.

182. Liu, X.-W.; Xu, L.-C.; Li, H.; Chao, H.; Zheng, K.-C.; Ji, L.-N. Synthesis, DNA-Binding and Spectral Properties of Novel Complexes $[RuL_2(idpq)]^{2+}$ (L = bpy, phen) with Embedded CO. *J. Mol. Struct.* **2009**, *920* (1), 163–171.

183. Chakraborty, A.; Gunupuru, R.; Maity, D.; Patra, S.; Suresh, E.; Paul, P. Synthesis and Anion-Sensing Property of a Family of Ru(II)-Based Receptors Containing Functionalized Polypyridine as Binding Site. *Inorg. Chem. Commun.* **2010**, *13* (12), 1522–1526.

184. Liu, X.-W.; Lu, J.-L.; Chen, Y.-D.; Li, L.; Zhang, D.-S. A Novel DNA Light Switch $[Ru(bpy)_2pzip]^{2+}$ Activated by Cobalt(II) Ion. *Inorg. Chem. Commun.* **2010**, *13* (3), 449–451.

185. Liu, X.-W.; Shen, Y.-M.; Lu, J.-L.; Chen, Y.-D.; Li, L.; Zhang, D.-S. Synthesis, DNA-Binding and Photocleavage of "Light Switch" Complexes $[Ru(bpy)_2(pyip)]^{2+}$ and $[Ru(phen)_2(pyip)]^{2+}$. *Spectrochim. Acta, Part A* **2010**, *77* (2), 522–527.

186. Ghosh, A.; Das, P.; Saha, S.; Banerjee, T.; Bhatt, H. B.; Das, A. Diamine Derivative of a Ruthenium(II)-Polypyridyl Complex for Chemodosimetric Detection of Nitrite Ion in Aqueous Solution. *Inorg. Chim. Acta* **2011**, *372* (1), 115–119.

187. Zhang, W.; Zhang, F.; Wang, Y.-L.; Song, B.; Zhang, R.; Yuan, J. Red-Emitting Ruthenium(II) and Iridium(III) Complexes as Phosphorescent Probes for Methylglyoxal in vitro and in vivo. *Inorg. Chem.* **2017**, *56* (3), 1309–1318.

188. Onozawa-Komatsuzaki, N.; Katoh, R.; Himeda, Y.; Sugihara, H.; Arakawa, H.; Kasuga, K. Synthesis and Photochemical Properties of Novel Ruthenium(II)-Nickel(II) and Ruthenium(II)-Copper(II) Dinuclear Complexes. *Bull. Chem. Soc. Jpn.* **2003**, *76* (5), 977–984.

189. Zhang, Z.-H.; Li, T.-S.; Li, J.-J. A Highly Effective Sulfamic Acid/Methanol Catalytic System for the Synthesis of Benzimidazole Derivatives at Room Temperature. *Monatsh. Chem.* **2007**, *138* (1), 89–94.

190. Gök, L.; Türkmen, H. Half-Sandwich η^6-Arene–Ruthenium(II) Complexes Bearing 1-Alkyl(benzyl)-imidazo[4,5-*f*][1,10]-phenanthroline (IP) Derivatives: The Effect of Alkyl Chain Length of Ligands to Catalytic Activity. *Tetrahedron* **2013**, *69* (49), 10669–10674.

191. Sheldrick, G. M. SHELXT - Integrated Space-Group and Crystal-Structure Determination. *Acta Crystallogr., Sect. A: Found. Crystallogr.* **2015**, *71* (1), 3–8.

192. Sheldrick, G. M. Crystal Structure Refinement with SHELXL. *Acta Crystallogr., Sect. C: Struct. Chem.* **2015**, *71* (1), 3–8.

193. Spek, A. PLATON SQUEEZE: A Tool for the Calculation of the Disordered Solvent Contribution to the Calculated Structure Factors. *Acta Crystallogr., Sect. C: Struct. Chem.* **2015**, *71* (1), 9–18.

194. Ashford, D. L.; Brennaman, M. K.; Brown, R. J.; Keinan, S.; Concepcion, J. J.; Papanikolas, J. M.; Templeton, J. L.; Meyer, T. J. Varying the Electronic Structure of Surface-Bound Ruthenium(II) Polypyridyl Complexes. *Inorg. Chem.* **2015**, *54* (2), 460–469.

195. Wiles, J. A.; Bergens, S. H.; Vanhessche, K. P. M.; Dobbs, D. A.; Rautenstrauch, V. A Versatile and High-Yield Route to Active and Well-Defined Catalysts [Ru(bisphosphane)(H)(solvent)₃](BF₄). *Angew. Chem. Int. Ed.* **2001**, *40* (5), 914–919.

196. Enachi, A.; Baabe, D.; Zaretzke, M.-K.; Schweyen, P.; Freytag, M.; Raeder, J.; Walter, M. D. [(NHC)CoR₂]: Pre-Catalysts for Homogeneous Olefin and Alkyne Hydrogenation. *Chem. Commun.* **2018**, *54* (98), 13798–13801.

197. Friedfeld, M. R.; Zhong, H.; Ruck, R. T.; Shevlin, M.; Chirik, P. J. Cobalt-Catalyzed Asymmetric Hydrogenation of Enamides Enabled by Single-Electron Reduction. *Science* **2018**, *360* (6391), 888–893.

198. Colborn, R. E.; Garbauskas, M. F.; Hejna, C. I. Synthesis and Characterization of New Adducts of Cobalt bis(2,4-pentanedionate). Molecular Structure of a *cis*-Complex: Cobalt bis(2,4-pentanedionate) *N,N,N′,N′*-tetraethyl-1,2-diaminoethane. *Inorg. Chem.* **1988**, *27* (20), 3661–3663.

199. Pasko, S.; Hubert-Pfalzgraf, L. G.; Abrutis, A.; Vaissermann, J. Synthesis and Molecular Structures of Cobalt(II) β-Diketonate Complexes as New MOCVD Precursors for Cobalt Oxide Films. *Polyhedron* **2004**, *23* (5), 735–741.

200. Andersen, R. A.; Wilkinson, G. Bis(neopentyl)-, Bis(trimethylsilylmethyl)- and Bis(2-methyl-2-phenylpropyl)- magnesium. *J. Chem. Soc., Dalton Trans.* **1977**, 809–811.

201. Sun, P.; Krishnan, A.; Yadav, A.; MacDonnell, F. M.; Armstrong, D. W. Enantioseparations of Chiral Ruthenium(II) Polypyridyl Complexes Using HPLC with Macrocyclic Glycopeptide Chiral Stationary Phases (CSPs). *J. Mol. Struct.* **2008**, *890* (1–3), 75–80.

202. Amiri, M.; Martinez Perez, O.; Endean, R. T.; Rasu, L.; Nepal, P.; Xu, S.; Bergens, S. H. Solid-Phase Synthesis and Photoactivity of Ru-Polypyridyl Visible Light Chromophores Bonded Through Carbon to Semiconductor Surfaces. *Dalton Trans.* **2020**, *49* (29), 10173–10184.

203. Kaufhold, S.; Petermann, L.; Sorsche, D.; Rau, S. "Trojan Horse" Effect in Photocatalysis–How Anionic Silver Impurities Influence Apparent Catalytic Activity. *Chem. Eur. J.* **2017**, *23* (10), 2271–2274.

Appendix

Chemical Numbering

$[Ru\text{-}(H)_2(PPh_3)_3]^- K^+$ 40

41

42

43

44

45

46

$K_2[Ru_2H_4(PPh_2)(PPh_3)] \bullet (diglyme)_2$ 47

48

49

50

$[Ru_4H_4(CO)_8(P^nBu_3)_4]$ 51

52

53

54

$[Ru(CO)_2(CH_3COO)_2(P^nBu_3)_2]$ 55

56

57

58

59

60

61

62

63

64

65

66

RuH_2L_n
$L = P(^nC_8H_{17})_3$
$n = 3$ or 4
67

68

$RuH(OMe)L_n$ 69

$RuH(OCH_2CH_2Ph)L_n$ 70

RuL_{n+1} 71

72

73

74

75

76

77

78

79

80

81

82

83

84

85

86

87

88

89

90

91

92

93

94

225

95 96 97 98 99 100 101

102 103 104 105 106 107

108 109 110 111 112 113

114 115 116 117 118 119

120 121 122 123 124 125

126 127 128 129 130 131

132 133 134 135 136

137 138 139 140 141 142

143

144

145

146

147

148

149
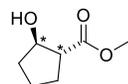
150
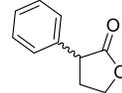
151
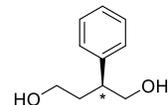
152
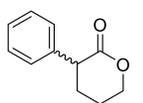
153
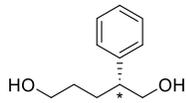
154
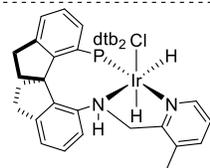
155
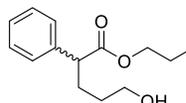
156
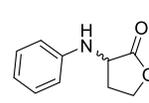
157
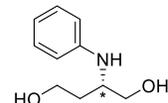
158
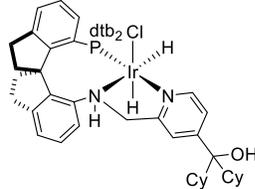
159
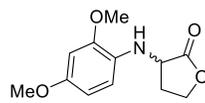
160
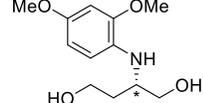
161
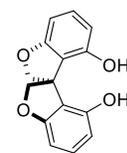
162
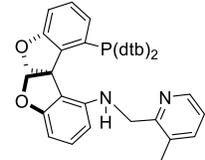
163
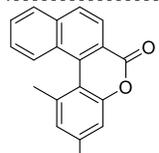
164
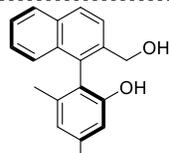
165
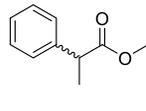
166
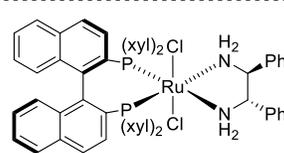
167
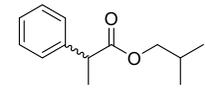
168
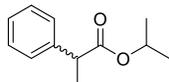
169
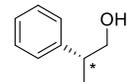
170

171

172

173

174

175
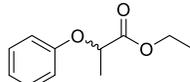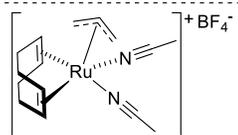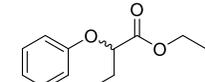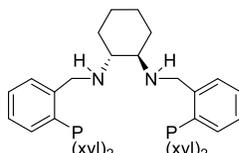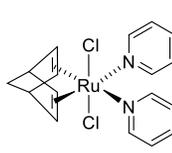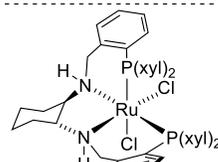
Λ-β-*cis*-**176**
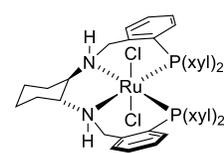
trans-**176**
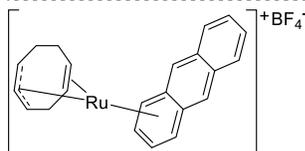
177
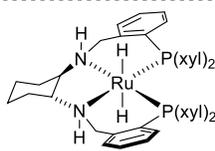
178
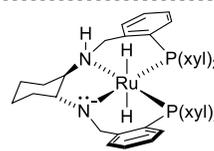
179
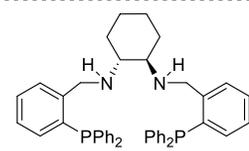
180

181

182

183

184

185

227
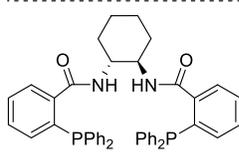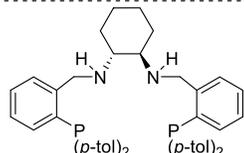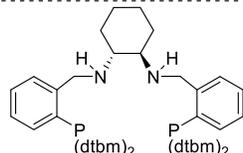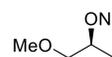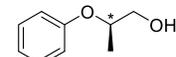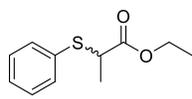
186
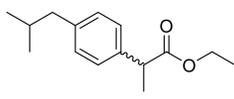
187
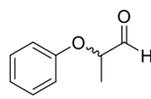
188
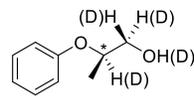
189
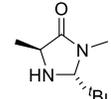
190
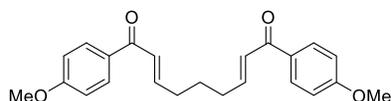
191
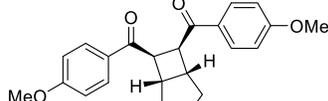
192
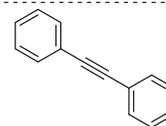
195
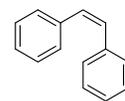
196
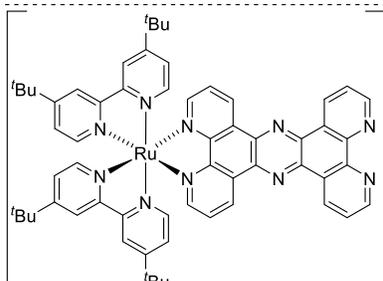
193
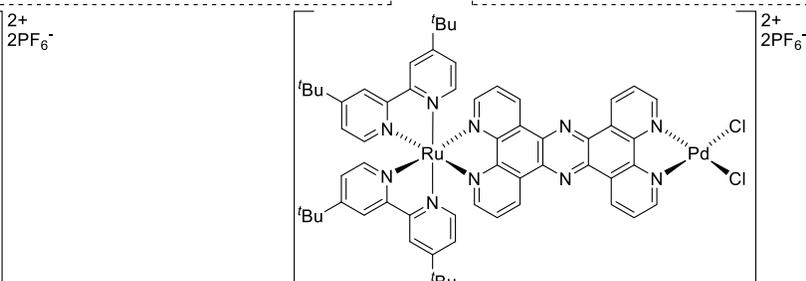
194
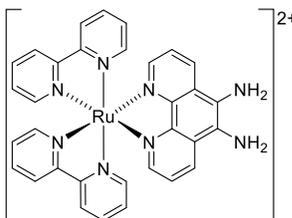
197
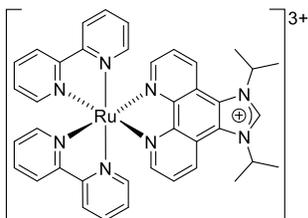
198
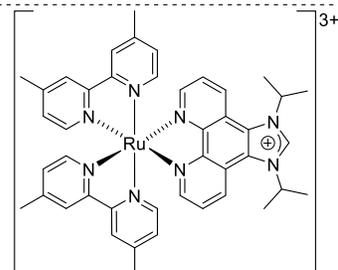
199
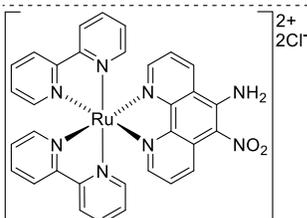
200
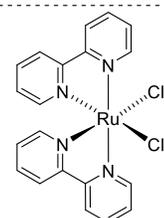
201
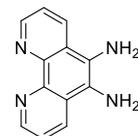
202
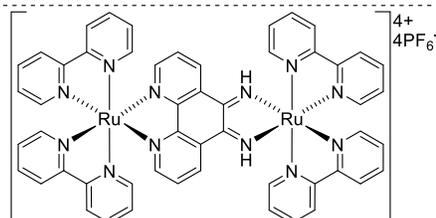
203
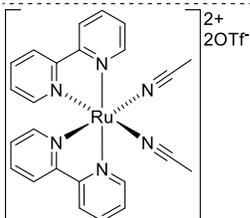
204
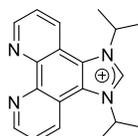
205

206

207

208

209

210

211

228

Ph₂ P, H, solv, solv, BF₄⁻, **212**

Ph₂ P, H, H₂ N, N, N, N, Ru, N, N, N, 2+ 2X⁻, **213**

ᵗBu, N, Co, SiMe₃, SiMe₃, N, ᵗBu, **214**

ᵗBu, N, Co, H, H, N, ᵗBu, **215**

ᵗBu, N, Co, N, ᵗBu, **216**

N, N, Ru, N, N, Ph, N, N, Co, SiMe₃, SiMe₃, N, 2+ 2OTf⁻, **217**

N, N, Ru, N, N, Ph, N, N, Co, SiMe₃, SiMe₃, N, 2+ 2OTf⁻, **218**

Ph₂ P, Ru, BF₄⁻, **219**

O, **220**

OH, **221**

N, N, Co, SiMe₃, SiMe₃, **222**

O, O, Co, N, N, **223**

Si, Mg, Si, **224**

225

HO, O, O, **226**

H, N, N, H, P(dtb)₂, P(dtb)₂, **227**

N, N, Ru, N, N, N, N, N, 2+ 2Cl⁻, **228**

N, N, Ru, N, N, N, N, N, 2+ 2Cl⁻, **229**

Ph₂ P, Cl, H₂ N, N, N, N, Ru, N, N, N, 2+ 2X⁻, **230**

Ph₂ P, Cl, N, Ru, Cl, N, **231**

N, N, Ru, N, N, Ph, N, N, AgCl, N, 2+ 2Cl⁻, **232**

N, N, Ru, N, N, Ph, N, N, AgCl, N, 2+ 2Cl⁻, **233**

229